Universidade de Aveiro Departamento de Química
2017

André Manuel Moreira Palma

Métodos Preditivos para os Parâmetros de Associação de Moléculas Multifuncionais com a CPA EoS.

Predictive Methods for the Association Parameters of Multifunctional Molecules with the CPA EoS.

Universidade de Aveiro Departamento de Química
2017

André Manuel Moreira Palma

Métodos Preditivos para os Parâmetros de Associação de Moléculas Multifuncionais com a CPA EoS.

Predictive Methods for the Association Parameters of Multifunctional Molecules with the CPA EoS.

Tese apresentada à Universidade de Aveiro para cumprimento dos requisitos necessários à obtenção do grau de Doutor em Engenharia Química, realizada sob a orientação científica do Professor Doutor João Manuel da Costa e Araújo Pereira Coutinho, Professor catedrático do Departamento de Química da Universidade de Aveiro, do Doutor António José do Nascimento Queimada, Technical consultant na empresa KBC Advanced Technologies Limited (A Yokogawa Company) e da Doutora Mariana Belo Oliveira, Técnica de vigilância tecnológica no RAIZ – Instituto de Investigação da Floresta e Papel.

o júri

presidente

Prof. Doutor Fernando Joaquim Fernandes Tavares Rocha
Professor Catedrático da Universidade de Aveiro

Prof. Doutor Georgios Kontogeorgis
Full Professor, Technical University of Denmark, Dinamarca

Prof. Doutor Javier Vijande Lopez
Professor Titular, da Universidade de Vigo, Espanha

Prof. Doutor Eduardo Jorge Morilla Filipe
Professor Auxiliar da Universidade de Lisboa

Doutor Pedro Jorge Marques Carvalho
Equiparado a Investigador Auxiliar da Universidade de Aveiro

Doutor António José do Nascimento Queimada
Technical Consultant na empresa KBC Advanced Technologies Limited (A Yokogawa Company)
(orientador)

agradecimentos

Before thanking my supervisors, friends and family, I would like to acknowledge Infochem-KBC for supporting this project and financing this thesis.

Em seguida, começo os agradecimentos gerais:

Em primeiro lugar ao prof. João Pereira Araújo Coutinho,
por todos os desafios que me levaram a este caminho.
Em seguida ao António José do Nascimento Queimada
Por todo o apoio e paciência quando a tese parecia parada.
Para finalizar agradeço à Mariana Belo Oliveira,
Todo o know-how e ideias para a tese, desde a fase primeira.

Quero também agradecer ao meus amigos e colegas do laboratório,
Que me perdoavam quando eu não vestia a bata para as limpezas.
Neste grupo que nunca se esqueceu de colocar alegria no inventário.
Foram muitos os sorrisos e tristezas as partidas e surpresas.
E mesmo sendo eu o elemento menos participativo, fixado no meu canto.
quero referir a importância da PAThmilly e todo o seu encanto.

Mas desçamos o País e voltemos a Lisboa, Sintra e outros mais,
Para agradecer aos meus amigos a paciência para me aturar.
Quando as coisas corriam menos bem e eu os ia maçar
ou quando, iam bem eu os inundava de piadas secas e banais.
Agradeço também a todos os amigos espalhados pelo Mundo.
E aos professores que fizeram do meu conhecimento mais profundo.

Quero agradecer também à minha família, Avó, tios e primos.
Por todo o apoio nos momentos felizes e também nos que o são menos.
Ao meu afilhado pela energia e "façanhas" de que tanto nos rimos.
E aos meus "compadres" pelas belas figuras que por vezes fazemos.

Por fim quero agradecer aos meus pais, pelo ambiente em que fui criado.
Por todo o carinho e apoio na minha vida e por todos os ensinamentos dados.
E agora, como pouco mais tenho a dizer e já não me sinto inspirado.
Agradeço também ao leitor desta tese, pelo interesse nestes resultados.

palavras-chave

CPA, equações de estado, equilibrio de fases, funções alfa, métodos de contribuição de grupos, pontos críticos, propriedades derivadas.

resumo

O projeto e otimização de processos envolvendo moléculas associativas multifuncionais é de elevada importância para as indústrias química, petroquímica, farmacêutica, alimentar, energética e de cosméticos.

A equação de estado (EoS) Cubic –Plus-Association (CPA) tem demonstrado ser um modelo termodinâmico adequado para a descrição de diversas moléculas associativas. Este modelo é utilizado frequentemente na indústria de gás e petróleo para a descrição, entre outros, de sistemas de água com hidrocarbonetos e de formação e inibição de hidratos de gás. Os seus parâmetros são geralmente obtidos através de um ajuste à pressão de saturação e de densidade do liquido de um composto puro. Contudo, a falta/impossibilidade de medição deste tipo de dados (visto alguns destes compostos não existirem como líquidos puros) dificulta a sua utilização. Desta forma, o uso da CPA em simuladores de processos é limitado, visto não termos acesso a parâmetros para um largo grupo de compostos. Além disto, os engenheiros de processo não têm disponibilidade para parametrizar cada composto não disponível na literatura. Como tal, são necessários métodos preditivos para estes parâmetros para um uso eficaz da CPA em simuladores de processo.

O principal objetivo deste trabalho é generalizar o uso da CPA para moléculas multifuncionais. A contribuição do termo associativo foi generalizada para aceitar qualquer número de grupos associativos em cada molécula, com número e carácter (eletrófilo, nucleófilo ou hibrido) dos sítios definidos pelo utilizador. Foram desenvolvidas ferramentas para gerar automaticamente parâmetros da CPA, contudo, em vez de um ajuste geral de todos os parâmetros a dados de pressões de vapor e densidades do líquido, os parâmetros do termo associativo são passiveis de ser transferidos entre grupos similares e/ou de serem calculados por métodos de contribuição de grupo. Após isto, os restantes parâmetros (do termo cubico) podem ser obtidos através do ajuste a correlações de propriedades dos compostos puros. A utilização de outras propriedades que não pressões de vapor e densidades da fase líquida é analisada, especialmente no caso das capacidades calorificas.

Uma função alfa, diferente da de Soave, foi aplicada nesta versão da CPA, sendo feita uma análise sobre as implicações desta mudança.

A nova versão da CPA incorporando as alterações propostas nesta tese é extensivamente comparada com versões do modelo previamento reportadas na literatura.

keywords Alpha functions, critical points, CPA, derivative properties, group contribution methods, phase equilibria.

abstract

Design and optimization of processes dealing with streams containing multifunctional associating molecules is of great importance to the chemical, petrochemical, pharmaceutical, cosmetics, food and energy industries. The Cubic-Plus-Association (CPA) equation of state (EoS) has been shown to be a general and accurate thermodynamic model to deal with a variety of associating molecules. It is widely used in the oil and gas industry to simulate, among others, systems with water and hydrocarbons, and hydrate formation and inhibition.

Currently, CPA parameters are obtained by simultaneously fitting pure component vapour pressure and liquid density data. But the lack of such data, or the impossibility to measure them (as some of these compounds do not exist as pure liquids) hampers its use. As a result, its application in process simulators is limited, as there are no pure component parameters for every component we might be interested in. Also, process engineers who want to use the model do not want to have the trouble of fitting a set of CPA parameters for each new component. Thus, predictive methods to generate CPA parameters are needed.

The main goal of this work is to generalize the use of the CPA EoS to any associating molecule. The association contribution of the model is generalized to consider any number of associating groups in each molecule with user-defined number of sites and corresponding nature (electrophile, nucleophile or hybrid). Tools are developed to automatically generate CPA parameters, but instead of simultaneously fitting all parameters from pure component vapour pressure and liquid density data, the associating parameters are transferable between similar groups and/or can be generated from a group-contribution approach. Then, the remaining (cubic) parameters can be obtained from pure component property correlations. The use of properties other than vapour pressures and liquid densities, mainly liquid heat capacities is also analysed.

An alpha funtion, different from that of Soave, is employed in this version of CPA and an analysis is conducted on the implications of this change. An extensive comparison between the new model and previously reported of CPA is also carried and discussed.

Table of Contents

Figure index

Table Index

List of symbols and abbreviations

General terms

A – Helmholtz energy

AAD – Average absolute deviation - $\%AAD = \frac{|\Omega_i^{exp} - \Omega_i^{calc}|}{\Omega_i^{exp}} \times 100\%$

APACT – Associated-Perturbed-Anisotopic-Chain-Theory

Cp – Isobaric heat capacity

Cv – Isochoric heat capacity

CPA – Cubic Plus Association

ESD – Elliott-Suresh-Donohue

EoS – Equation of State

FOG – First order groups

GC – Group contribution

GCA – Group contribution with association

k and k_b – Boltzmann constant

k_{ij} – Binary interaction parameter related to the energy of the physical term

k_T – Isothermal compressibility

l_{ij} - Binary interaction parameter related to the volume of the physical term

NC – Number of components

NG – Number of groups

n – number of moles

P – Pressure

P_c – Critical pressure

PR – Peng Robinson

SAFT – Statistical Associating Fluid Theory

s-CPA – Simplified CPA

PC-SAFT – Perturbed chain SAFT

SAFT-VR – SAFT variable range

SOG – Second order groups

SW – Square well

R – Universal gas constant

SRK – Soave Redlich Kwong

T – Temperature

T_c – Critical temperature

u – Speed of sound

V – Volume

v_0, v_t - volume before and after translation, respectively

WCA – Weeks-Chandler-Anderson

x - mole fraction

X^{Ai} – Fraction of molecules i not bonded at site A

Z – Compressibility

α_p - Coefficient of thermal expansion at constant pressure

α_V – Coefficient of thermal expansion at constant volume

Δ – Association strength

μ_{JT} – Joule-Thomson coefficient

ρ - Molar density

%Dev. - percentage of deviation

Compound name abbreviations

1,3-Pr$(OH)_2$ - 1,3-propanediol

1,4-Bu$(OH)_2$ - 1,4-buanediol

1,5-Pe$(OH)_2$ - 1,5-pentanediol

1,6-He$(OH)_2$ - 1,6-hexanediol

2-PrOH - 2-propanol

2-BuOH - 2-butanol

2-PeOH/3-PeOH - 2-pentanol/3-pentanol

MeSH – Methanethiol

EtSH – Ethanethiol

1-PrSH – 1-propanethiol

1-BuSH – 1-butanethiol

2-PrSH – 2-propanethiol

2-BuSH – 2-butanethiol

HC - hydrocarbon

MEG - monoethylene glycol

THF – tetrahydrofuran

MTBE – methyl tert-butyl ether

tert-BuOH = tert-butanol

Upper and lower scripts

Attr. – Attractive

assoc, phys - association and physical terms

c - critical

Chem – Chemical

Disp – dispersive

exp., calc. - experimental, calculated

FV – Free volume

HS – hard-sphere

i, j = pure component indexes

ig = ideal gas

np = number of points

npo = number of phases to optimize

Pert – perturbation

Phys – Physical

Rep – Repulsive

res. = residual

Sat. – Saturation

Seg – Segment

GCA terminology

d_i – hard sphere diameter of component i

NGA – Number of associating groups

n_i^* - Total number of moles of associating group *i*

M_i – Number of associating sites

$\kappa^{k,i,l,j}$ – Volume of association

$\varepsilon^{k,i,l,j}$ – Energy of association

$\tilde{q}$ – Number of surface segments

g_{mix} – Characteristic dispersive energy per total segments.

θ_k – Surface fraction of group *k*

g_{ij} – Dispersive energy between groups *i* and *j*

α_{ij} – Non-randomness parameter.

q_i – Group surface

g_{ii} –Dispersive energy between like groups

T_i^* - Reference temperature of group *i*

SAFT terminology:

g – Radial distribution function

d – Temperature dependent segment diameter

κ– Volume of association

ε– Energy of association

σ – Temperature independent diameter

m – Chain length parameter

v^{00} – Temperature dependent volume

n_i – number of groups of type *i*

R_i – Contribution of group *i* to the chain length

λ_s - Diameter softness

π_i^* - Perturbed coefficient

$\Delta\pi_i$- Total perturbation felt by groups of type *i*

$\mu_{\pi,i-j}$ – Perturbation on $\Delta\pi_i$ by any adjacent group of kind *j*

$p_{i_k-j_l}$ – Relative position of group *k* to group *l*

$v_{k,i}$ – Number of segments of type *k* in component *i*

S_k – Proportion at which each segment contributes to the properties of the molecule

ζ_{kl}^{eff} - Effective packing fraction

ε_{kl} – well depth of square-well interaction of range λ_{kl}

K_T^{HS} – Isothermal compressibility of the reference hard-sphere mixture

$z_{k,i}$ – Fraction of group *k* in component *i*

ΔV_i – UNIFAC group contribution for liquid molar volumes

δ – Solubility parameter

CPA terminology:

A, a - energy parameter of CPA.

a_0 - value of the energy parameter at the critical point.

A_i - site A in molecule i

B, b - co-volume

$c_1 – c_5$ - alpha function parameters

c_{vs} - volume shift

m_i - the mole number of sites of type *i*

X_{A_i} - mole fraction of component *i* not bonded to site A

δ – Cubic equation selection parameters

β – Volume of association

Δ - association strength

ε – Energy of association

1 Introduction

1.1 Scope and objectives

Multifunctional molecules are present in a wide range of processes and applications. Thermal controlled systems use this kind of molecules for thermostating and refrigeration purposes, presenting also some applications as cryoprotectants. In separation processes they present various relevant roles, as for example gas dehydration and liquid-liquid extractors for refined oil products. In the petrochemical industry they present some important uses, especially ethylene glycol which is used as a hydrate inhibitor. They are also the basis of most polymer formulations and present diverse uses in the pharmaceutical industry be it as drug or additives. Some other relevant uses include their applications in the cosmetic, pesticide, and aerosol industries. Table 1.1 presents some examples of multifunctional components and applications of these compounds.

Table 1.1 Examples of multifunctional components and their applications

Compound name	***Structure***		
triethylene glycol	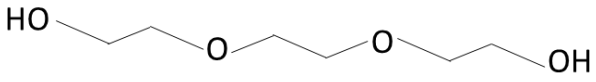		
diethanolamine	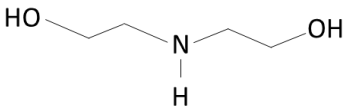		
ferulic acid	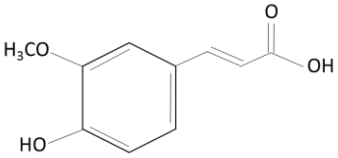		
cysteamine	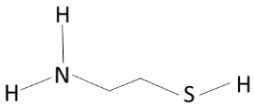		
glycerol	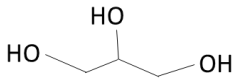		
1,2-ethanethiol	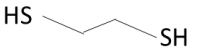		
adipic acid	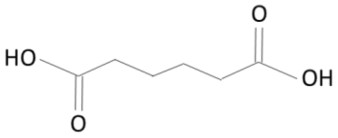		
L-cysteine	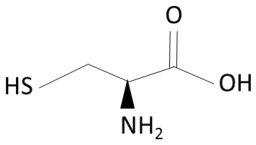		
	Formula	Boiling T (K)	Examples of applications
triethylene glycol	$C_6H_{14}O_4$	561.0	The most applied absorvent in natural gas dehydration [1]
diethanolamine	$C_4H_{11}NO_2$	541.5 (decomposes)	Important component for the cosmetics industry
ferulic acid	$C_{10}H_{10}O_4$	Unknown/decomposes	Precursor for the manufacture of other aromatic compounds
cysteamine	C_2H_7NS	decomposes	Drug applied for the treatment of cystinosis.
glycerol	$C_3H_8O_3$	561 (decomposes)	Solvent and sweetening agent
1,2-ethanethiol	$C_2H_6S_2$	419.2	A common building block for organic chemistry
adipic acid	$C_6H_{10}O_4$	610.7	Used in the production of nylon
L-cysteine	C_2H_7NS	Unknown/decomposes	Used in the treatment of asthmatics

The correct description and optimization of these processes requires access to accurate thermodynamic data over large ranges of temperature and pressure. However the high complexity and polar/associative nature of these molecules, allied to the difficulty, or impossibility, to measure some of their properties results in the lack of adequate information to develop adequate models of to carry its simulation. This lack of data presents an opportunity as well an important challenge for the improvement of existing/development of new thermodynamic models.

Whenever such molecules are present in a process, it has been common practice to define the entire process or a sub-flowsheet of the process with an empirical g^E model, such as NRTL[2] or UNIQUAC[3], as classical cubic equations of state, such as Peng-Robinson, are well known to fail to accurately describe mixtures with those components. These g^E models provide enough accuracy for process simulation purposes, but require some caution whenever extrapolated outside of the conditions used for the parameter fitting or when new components need to be involved. This somehow hampers accurate design simulations, as in these exploratory studies the simulator is used to understand which components (such as a solvent for extraction) or optimal conditions shall be used. Thus the use of these g^E models, has been decreasing in the last few years due to their lack of predictive capacities (except for particular cases like UNIFAC, which incorporates predictive capacities).

EoS g^E mixing rules are successful in obtaining results for associative compounds while describing correctly larger temperature and pressure ranges, nevertheless most of these models incorrectly describe highly asymmetric systems and present weaker performances than those of more recent association models. [4]

SAFT-like EoS, explicitly take into account hydrogen bonding, presenting advantages over the classical approaches on the modelling of associative compounds. The CPA EoS[5], is one such approach, which allies the simplicity of a cubic EoS, its predictive nature and accuracy,[6] with an association term that allows its use for polar and associative compounds turning this EoS into an asset that can be easily integrated in process simulators. One of the major advantages of the CPA model is that it reduces to a cubic equation of state for every non-associating component, what makes it a powerful replacement for cubic equations of state in process simulation, as only associating components will require a special treatment. For example in the oil and gas industry, all pseudo component properties used by the cubic equations of state can be used by CPA as well.

There is today a need for models able to describe multiple thermodynamic and transport properties, as well as the phase equilibria with a single set of pure parameters.[7] Most models are nowadays unable to do this, and those with that capacity use a very high number of parameters decreasing their predictive ability. There is also a need for more predictive methods for multifunctional molecules, as in many cases their liquid densities and vapour pressures are not available or are impossible to measure due to thermal degradation.[8] Thus more accurate sets of parameters are needed for multifunctional molecules. According to de Villiers et al.[9] these should be obtained using more properties and pressure conditions during the parameter fitting.

With this work we pretend to upgrade the current CPA model while also making it more generalized and easier to use for non-thermodynamic experts, such as chemical engineers running a process simulator. We will be looking at how the current model can be improved by:

- Analysing how the *b* parameter (and volume) is treated in the cubic term (fitted co-volume or standard co-volume with a volume shift)
- Defining an explicit multifunctional associative approach with user defined groups, number of sites in each group and site types (electrophilic, nucleophilic, hybrid)
- Creating a group-contribution scheme for the associative parameters of different associating groups.
- Estimate the remaining CPA parameters by using the critical properties and some temperature dependent correlations for properties such as vapour pressure, liquid density and liquid heat capacities.
- Analysing other possible alpha functions in the cubic term.

A study on the behaviour of associative groups is proposed in this work, with a primary focus on the hydroxyl group in diverse families of compounds. To improve the quality of CPA parameters a new property is to be studied as an alternative for the parameterization process. Previous studies with soft-SAFT from our group suggested the heat capacity to be the property with best prospects,[10] thus we opted to start with the introduction of Cp, while the prediction of other derivative properties will also be analysed.

This work is divided in seven main sections **1. Introduction**, **2. A modified CPA and first applications, 3. Secondary alcohols, diols and glycerol, 4. Water and aqueous systems, 5. Thiols and amines, 6. Critical points of mixtures, 7. A tentative group contribution method for multifunctional molecules.**

The first part of this thesis, **1. Introduction,** provides a brief context on equations of state and g^E models, as well as a review on the applications of group contribution methods when used in conjunction with advanced equations of state.

The second part of the document, **2. A modified CPA and first applications,** starts by highlighting the differences between the version developped in this work and one of the most used versions of CPA, the simplified CPA (s-CPA). The chapter also presents the first set of results, for primary alcohols, including an analysis of both the pure properties and the description of binary VLE and LLE. Here the transferability approach is applied for the associative parameters, which will be kept in most of the other chapters. In this chapter as in subsequent ones, the various versions of CPA are compared on the description of pure properties and phase equilibria. This chapter is based on the manuscript Palma, A. M.; Oliveira, M. B.; Queimada, A. J.; Coutinho, J. A. P. Re-evaluating the CPA EoS for improving critical points and derivative properties description. Fluid Phase Equilib. 2017, 436,85−97.

The third section here presented, **3. Secondary alcohols, diols and glycerol** studies the changes introduced by steric hindrance and the number of hydrogen groups have in the associative parameters. This chapter starts the analysis on the advantages and issues of using liquid heat capacity as an alternative property for the parameterization. Beside binary VLE and LLE, this chapter introduces analyses on the description of gas solubility and multicomponent phase equilibria, which includes analysis on the description of ethylene glycol + petroleum condensates. This chapter is based on the manuscript: Palma, A. M.; Oliveira, M. B.; Queimada, A. J.; Coutinho, J. A. P. Evaluating Cubic Plus Association Equation of State Predictive Capacities: A Study on the Transferability of the Hydroxyl Group Associative Parameters. *Ind. Eng. Chem. Res.* **2017**, *56* (24), 7086–7099.

As suggest by the title, the fourth chapter, **4. Water and aqueous systems,** addresses the description of the pure properties of water and its mixtures. This chapter includes an important study on the use of restrictions for alpha functions. A discussion on the differences between the LLE description using the various CPA versions, mainly in the temperature dependencies of the non-aqueous phases, is also presented.

The transferability approach is expanded to secondary amines and thiols in chapter **5. Thiols and amines,** expanding the study on the description of pure properties and phase equilibria for two new types of compounds.

The following section, **6. Critical points of mixtures,** introduces a different topic. The version of CPA here applied forces the correct description of pure compound critical temperatures and pressures, thus it is of interest to verify if these properties are accurately described for mixtures. The systems here reported, containing compounds studied in all of the previous sections, are analyzed and, when available, the previously applied binary interaction parameters used.

7. A tentative group contribution method for multifunctional molecules, presents the first version of a group contribution method and reports its first results for hydroxyl group containing compounds.

To finish the document a general section of **Conclusions and Perspectives** is presented. The Perspectives section includes a brief analysis of the different functions, rules and methodologies available for CPA, and a summary of what has been tested and learned about these during this work, as well, as what still needs to be analysed.

1.2 Classic Thermodynamic Models

Models capable of accurately describing phase equilibria for a large range of conditions are essential tools for the industry. Diverse models have been proposed and used in the selection and optimization of processes and equipment.

The development of cubic equations of state started long before the appearance of personal computers, nevertheless it was only with the development of apparatus with large computational power that they become widely used, were subject of an intensive development and became of great utility to the industry. Cubic EoS present a simple mathematical formulation, using parameters that are usually calculated from critical properties of the pure compounds, enabling fast calculations and ease of use. The capacity of this equations to provide a good description of the phase equilibria in wide ranges of pressure and temperature of non-polar compounds makes them a very powerful tool. The most used cubic equations of state are the Peng-Robinson (PR)[11] and the Soave-Redlich-Kwong (SRK)[11], largely applied in both the chemical and petrochemical industries simulators. As most of the other cubic EoS, these equations are generally used with terms based on critical properties, but also include an attractive term dependent on the acentric factor to improve the description of the vapour pressure far from the critical point.

Despite these advantages, cubic equations are unable to describe systems containing polar and associative compounds. Being conventional models they are also unable to describe conditions near the critical point and at very low temperatures. To improve results near the critical point two methodologies have been proposed, the first suggesting a recursive approach.[12],[13] This method is nevertheless highly demanding in terms of computational capacity.[14] The second approach, usually named crossover equations, is based on Chen and Tang work.[15],[16] This method uses the correct asymptotical description of the critical point, while transforming the space of the variables to enable a progressive increase of the influences of critical fluctuations. Despite a number of works concerning cross-over equations, as the models are always being changed there are scarce versions tested for large groups of systems or compounds.[14] Some cross-over models have also been used for more modern equations of state like SAFT.[17],[18] More information about the advantages and issues of cubic equations and most specifically SRK will be discussed below in chapter 3.1. An analysis of group contribution methods for both cubic and more complex equations of state are proposed as a review and will be introduced in the final version of this document.

Systems of polar compounds have been described for a long time using activity models based on the local composition concept. Contrary to cubic EoS these models can cope with the description of polar compounds while also providing a good description of non-polar molecules, nevertheless their range of applicability is restricted to low pressures and small temperature ranges. Some of the better known local composition models are NRTL[2] and UNIQUAC.[3] These models do not present predictive capacities, thus some models were proposed based on group contribution methods, from which the most famous is UNIFAC.[19]

To achieve both good results for mixtures containing polar compounds and satisfactory results for high pressures, models mixing equations of state and Gibbs free energy models were proposed. Firstly introduced by Huron and Vidal,[20],[21] the EoS g^E mixing rules create many possibilities through the combination of EoS and g^E and different rules for their mixing. Two of the most important mixing rules were introduced by Michelsen et al.[22] the MHV1 and MHV2 rules. Despite their success in describing systems with polar compounds, most of these approaches are unable to describe large asymmetric systems. Also for more complex systems with more than two components, this models are unable to perform as well as some more recent approaches based on association theory and requiring a smaller number of parameters.[4]

1.3 EoS based on perturbation theory and their applications in tandem with GC methods.

Process simulators are important tools for the design, optimization and decision making of industrial processes. Providing them with a reliable thermodynamic description while ensuring small processing times is a major challenge currently faced by process simulators.

Cubic equations of state, g^E models and their combination are the preferred methods to describe phase equilibria and thermodynamic properties. However, the simplicity of these methods is unable to cope with the description of complex compounds, their mixtures and a broader set of operating conditions.

Association equations of state are the most powerful tool to describe the thermodynamic behaviour currently available. Nevertheless, their use is, in many cases, hindered by the need to parameterize every new compound in study. This problem could be overcome by introducing group-contribution methods for parameter estimation, allowing for automatic parameter generation. Below we will describe the state of art on the application of group-contribution methods for association EoS, based on perturbation theory. The advantages of these approaches, as well as their shortcomings, are considered, providing a comprehensive analysis of the recent developments in this field.

1.3.1 Introduction

One of the main concerns of a process engineer are the separation steps of any process. The correct choice and optimization of a separation process, operation conditions and solvents are needed to reduce the high costs of separation as well as increasing security while reducing health and environmental risks.

Knowledge of the thermodynamic properties of the systems involved in the separation step is of outmost importance to create an efficient and safe process. Nevertheless, testing every system experimentally is not possible and despite the high number of binary systems already studied, there is still a lack of data on multicomponent/multiphase systems in the open literature. To deal with this issue, accurate thermodynamic models are needed to predict the properties of these systems.

The most widespread models to address these issues are the cubic equations of state (the most widely used being Peng-Robinson and Soave Redlich Kwong), excess Gibbs energy

models, and the combination of the two previous methods. Despite their strength and simplicity, these are not able to describe systems containing highly associative, highly asymmetric and most multiphasic systems.

Since the last decade of the previous century, models which explicitly take into account the effect of hydrogen bonding have been object of significant developments[8]. These association models are able to describe phase equilibria and physical properties of compounds capable of hydrogen bonding, be it with other molecules of the same component (self-association) or with different components (cross-association). Some important examples are the group contribution with association equation of state (GCA)[23], the Statistical Associating Fluid Theory (SAFT)[24], the Associated-Perturbed-Anisotopic-Chain-Theory (APACT)[25], the Cubic Plus Association equation of state (CPA)[5] and the Elliott-Suresh-Donohue EoS. These have proven to be a huge improvement over the classical models when dealing with polar/associative molecules.

However, to date, many simulations in the industry involving processes containing associative molecules and multiphase systems still use a cubic EoS in their property packages. This is in part due to the predictive capacities of the cubic equations of state, which only need data for the critical properties to describe many pure compounds, while, in most cases, for more complex equations of state a fitting of one or more parameters are required, usually to saturation data. Many compounds already have their parameters established for an association equation of state, however with diverse versions of each equation and the increasing number of molecules of interest, fitting all compounds is simply not feasible.

Group contribution methods are important tools in the prediction of thermodynamic properties. These have been previously applied in combination with excess Gibbs energy models, as well as in EoS-g^E approaches to improve the predictive capacities of these models. Allying the predictive capacities of these methods and the accuracy of association equations of state is an attractive prospect. This work focuses on the combination of group contribution methods and association equations of state, which is expected to help widespread the use of these models. This study concerns specifically those based on perturbation theories, mainly the SAFT family of equations, where GCA and CPA are considered special cases and will receive specific mention. The ESD (Elliott−Suresh−Donohue) is a special case of a predictive EoS which accounts for association, this EoS has one group contribution method for polymers, however, the EoS will not be analysed in detail as the method was later expanded to SAFT and the general description is presented in the SAFT section.

SAFT type EoS[8] are models based on Wertheim's first order thermodynamic perturbation theory (TPT1) for associating fluids.[8] SAFT and its variations have been successfully applied to diverse systems, both with non-associating compounds with large asymmetries (e.g. CO_2 with alkanes with the original SAFT; mixtures of methane, H_2, CO, ethane with alkanes using PC-SAFT [26]),[8] and associative compounds, which is the area where this theory is most relevant. One area where SAFT proved to be an extremely important tool was the description of polymers and their mixtures.[8] Some recent applications of SAFT equations of state include the description of ionic liquids and deep eutectic solvents. [27,28]

A large array of SAFT versions have been proposed since its original publication in 1990, with various approaches being conducted for group contribution methods for both the physical parameters of the pure compounds and the binary interaction parameters [29–35]. Constant values, or more rarely, group contribution methods for the association parameters have also been employed with good results [34–36].

The Cubic Plus Association (CPA) equation of state combines an association term based on Wertheim's theory with the simplicity of a cubic EoS (e.g. SRK, PR), enabling good predictions for associative/polar compounds, while for hydrocarbons it simplifies into an accurate but also, simple cubic equation.

CPA was firstly introduced in 1996 by Kontogeorgis et al. [5] with the objective of describing multicomponent and multiphase equilibria of diverse mixtures of hydrocarbons and polar/associative compounds, like water, alcohols, glycols, esters and organic acids [8]. CPA has proved its worth in the description of associative and polar systems, while for hydrocarbons the use of SRK or other cubic equations have long been established as adequate choices. Thus CPA is seen as a good compromise between accuracy and simplicity, being considered the best choice for modelling associative systems which do not need the more elaborate SAFT equation, such as polymers and other more complex molecules.[8]

The group contribution with association (GCA) equation of state uses, as the name implies, a group contribution method to describe the dispersive term of the model, being a particular case of a perturbation theory EoS already coupled with a group contribution method.

GCA was proposed by Gros et al. [23] as a combination of Wertheim's perturbation theory and the group contribution (GC) EoS, with the main objective of describing multicomponent systems containing associating compounds. GCA, as the first association equation of state with an incorporated group contribution method. It has been compared with previous EoS + GC

models and has shown relevant advantages with the explicit introduction of the associative term.

1.3.2 Group contribution methods and equations of state

The equations of state analysed in this work explicitly separate the physical from the chemical dependencies to compressibility. This can be observed in equation 1.2.

$$Z = Z^{phys} + Z^{assoc} = Z^{phys} + Z^{chem} - 1 = Z^{attr.} + Z^{rep.} + \frac{n_T}{n_0} - 1 \quad (1.2)$$

Where $n_T/n_0 - 1$ corresponds to the association term, n_T is the true number of moles existing after association and n_0 is the apparent number of moles without considering association.

GCA

GCA is a special case of an EoS, where a group contribution method is introduced directly into the EoS attractive term. This term is a group contribution version of a density dependent local composition expression (NRTL). The repulsive term (free-volume) is a hard sphere term based on the Carnahan-Starling equation, being usually described, in terms of the Helmholtz energy, as follows:

$$\frac{A^{fv}}{RT} = \frac{3\lambda_1\lambda_2}{\lambda_3}(Y-1) + \frac{\lambda_2^3}{\lambda_3^2}(Y^2 - Y - \ln Y) + n\ln Y \quad (1.3)$$

where:

$$Y = \left(1 - \frac{\pi\lambda_3}{6V}\right)^{-1} \quad (1.4)$$

$$\lambda_k = \sum_{i=1}^{NC} n_i d_i^k \quad (1.5)$$

T is temperature, R is the universal gas constant, V is the total volume, NC is the number of components and n_i is the number of moles of component i. The hard sphere diameter d_i is obtained from:

$$d_i = 1.065655\, d_{ci}\left[1 - 0.12exp\left(-\frac{2T_{ci}}{3T}\right)\right] \quad (1.6)$$

With T_{ci} being the critical temperature of compound i and d_{ci} is the value of d_i at this temperature.

The association term is a modified form of the expression used within SAFT, which is expressed as:

$$\frac{A^{assoc}}{RT} = \sum_{i=1}^{NGA} n_i^* \left[\sum_{k=1}^{M_i} \left(\ln X^{(k,i)} - \frac{X^{(k,i)}}{2} \right) + \frac{M_i}{2} \right] \quad (1.7)$$

Where *NGA* is the number of associating groups n_i^* is the total number of moles of associating group *i, M_i* is the number of associating sites and *X* is the fraction of group *i* not bonded to site *k*, given by:

$$X^{(k,i)} = \left[1 + \sum_{j=1}^{NGA} \sum_{l=1}^{M_j} \rho_j^* X^{(l,j)} \Delta^{(k,i,l,j)} \right]^{-1} \quad (1.8)$$

The molar density is here presented as ρ_j^*, while the association strength is:

$$\Delta^{(k,i,l,j)} = \kappa^{k,i,l,j} \left[exp\left(\frac{\varepsilon^{k,i,l,j}}{RT} \right) - 1 \right] \quad (1.9)$$

With $\kappa^{k,i,l,j}$ and $\varepsilon^{k,i,l,j}$ being the parameters representing the volume of association and the energy of association, respectively.

The attractive term, as mentioned above, is based on NRTL and can be described by:

$$\frac{A^{att}}{RT} = -\frac{(z/2)\tilde{q}^2 g_{mix}(T,V)}{RTV} \quad (1.10)$$

Where *z* is the coordination number, which is set to 10. $\tilde{q}$ is the number of surface segments and g_{mix} is the characteristic dispersive energy per total segments.

These are calculated from:

$$g_{mix} = \sum_{j=1}^{NG} \theta_j \sum_{k=1}^{NG} \frac{\theta_k g_{kj} \tau_{kj}}{\sum_{l=1}^{NG} \theta_l \tau_{lj}} \quad (1.11)$$

$$\tilde{q} = \sum_{i=1}^{NC} \sum_{j=1}^{NG} n_i v_{ji} q_j \quad (1.12)$$

θ_k is the surface fraction of group *k*, *NG* is the number of groups and v_{ij} is the number of groups of type *j* in molecule *i*. With:

$$\theta_j = \frac{1}{\tilde{q}} \sum_{i=1}^{NC} n_i v_{ji} q_j \quad (1.13)$$

$$\tau_{ij} = exp\left(\alpha_{ij} \frac{\tilde{q} \Delta g_{ij}}{RTV} \right) \quad (1.14)$$

$$\Delta g_{ij} = g_{ij} - g_{jj} \quad (1.15)$$

Where g_{ij} is the dispersive energy between groups *i* and *j* and α_{ij} is the non-randomness parameter.

The five pure group specific parameters of GCA are the group surface q_i, and four parameters applied in the calculation of the dispersive energy between like groups g_{ii}:

$$g_{ii} = g^*_{ii}\left(1 + g'_{ii}\left(\frac{T}{T_i^*} - 1\right) + g''_{ii}\ln\left(\frac{T}{T_i^*}\right)\right) \quad (1.16)$$

Where T_i^* is a reference temperature specific to each group.

Up to four binary interaction parameters can be applied. The first two are the non-randomness parameters (α_{ij} and α_{ji}), while the remaining two present the dispersive energy between unlike groups, as is presented in equations 1.17 and 1.18.

$$g_{ij} = k_{ij}\sqrt{g_{ii}g_{jj}} \quad (1.17)$$

$$k_{ij} = k_{ji} = k^*_{ij}\left(1 + k'_{ii}\ln\left(\frac{T}{T^*_{ij}}\right)\right) \quad (1.18)$$

Where T_{ij}^* is an arithmetic mean between the reference temperatures of groups i and j.

When considering association, GCA authors have used constant parameters for each associating group, independently of the structure of the molecule. Nevertheless, it is important to note that some of the differences in association behaviour may be accounted for in the physical term. Different groups are employed for smaller molecules (ex. no physical parameters are introduced for the OH group, but are introduced instead for methanol [CH3-OH] and ethanol [CH3-CH2-OH], while the remaining compounds with a primary hydroxyl group use the group [CH2-OH]). It is important to note that the associative scheme used for water with this EoS is a 2B scheme, instead of the 3B and, 4C schemes usually applied with CPA and SAFT. Cross-association is accounted for, using a set of constant parameters fitted to each pair of associating groups.

GCA was the first association EoS to be built specifically as a group contribution methodology. It could be located between SAFT and CPA in terms of processing speed and complexity, being able of accurate descriptions with lower processing times than SAFT. Its pure component parameters are usually correlated from vapour pressure data, with binary phase equilibria (from diverse types of equilibria) being used for the parameterization of the group contributions for binary interaction parameters. In the literature concerning this equation, no pure properties, except P^{sat}, were calculated.

In 2009, to improve results for the description of systems containing water, Pereda et al. [37] proposed to use a modified version of equation 1.6, only for this compound:

$$d_w = d_{wc} = \left\{0.554\left[exp\left(-2\frac{T_c}{3T}\right)\right]^2 - 0.543\left[exp\left(-2\frac{T_c}{3T}\right)\right] + 1.097\right\} \quad (1.19)$$

This approach enabled to improve the description of the mutual solubility of hydrocarbons and water.

GCA is thus, able to describe a large diversity of phase equilibria, while retaining much simplicity, when compared to other GC methods discussed below. Nevertheless, the uses of this method are mostly for phase equilibria calculations, with other properties not studied with this equation.

General SAFT concepts

A large number of SAFT variants have been proposed during the last decades. This section will focus on the variants applied in tandem with a group contribution method. Some relevance will be given to SAFT-γ and variants, as these equations were built with a group contribution feature in mind, as was the case for GCA.

The contributions to the residual Helmholtz energy, in SAFT equations, are usually divided into a segment term, a chain term and an association term. The differences between most of the SAFT variations are due to changes in the segment term. The chain term can, in most versions, be written as:

$$\frac{a_{chain}}{RT} = \sum_i x_i (1 - m_i) \ln\left(g_{ii}(d_{ii})^{hs}\right) \quad (1.20)$$

With g_{ii} being a radial distribution function, itself dependent on a temperature dependent segment diameter d_{ii}.

The association term is also common among the diverse versions of SAFT:

$$\frac{a_{assoc}}{RT} = \sum_i x_i \left[\sum_{A_i}\left(\ln X^{A_i} - \frac{X^{A_i}}{2}\right) + \frac{1}{2}M_i\right] \quad (1.21)$$

with M_i being the number of association sites on molecule *i* and X^{A_i} the fraction of molecules *i* non-bonded at site A. It should be noted that this expression will be changed in approaches that use a non-average group-contribution method for the associative parameters (ex. SAFT-γ) as the association sites will be linked to a specific group instead of the whole molecule. X^{A_i} is given by:

$$X^{A^i} = \left[1 + \sum_j \sum_{B_j} \rho_j X^{B_j} \Delta^{A_i B_j}\right]^{-1} \quad (1.22)$$

where ρ_j is the molar density of component *j* and $\Delta^{A_iB_j}$ is the association strength between site A and B of molecules *i* and *j* respectively, which is calculated from:

$$\Delta^{A_iB_j} = d_{ij}^3 g_{ij}(d_{ij})^{seg} \kappa^{A_iB_j} \left[exp\left(\varepsilon^{A_iB_j}/kT\right) - 1\right] \quad (1.23)$$

where *k* is the Boltzmann factor, *T* is the temperature and *ε* and *κ* are the association energy and volume, respectively.

It is important to note that most versions of SAFT use, in approximation, a temperature independent diameter (*σ*) instead of d_{ij}, in the original SAFT (SAFT-0) these two parameters can be correlated from:

$$\frac{d}{\sigma} = \frac{1+0.2977kT/\varepsilon}{1+\frac{0.33163kT}{\varepsilon}+f(m)\left(\frac{kT}{\varepsilon}\right)^2} \quad (1.24)$$

With:

$$f(m) = 0.0010477 + 0.025337\frac{m-1}{m} \quad (1.25)$$

Where *m* is the number of segments.

As presented above the segment term is where most differences are visible. This term can generally be presented as:

$$a^{seg} = a_0^{seg} \sum_i x_i m_i \quad (1.26)$$

where m_i is a parameter linked to the chain-length of molecule *i*.

$$a_0^{seg} = a_0^{hs} + a_0^{disp.} \quad (1.27)$$

Different hard-sphere expressions are used in the various versions of SAFT. One of the better - known is the Carnahan-Starling (used in SAFT-VR, PC-SAFT and SAFT-γ, the remaining versions use a simplified version of the C-S equation). Tables are presented in annex showing some of the variations on the contributions for most of the versions of SAFT here discussed, for SAFT-γ/GC-SAFT-VR and variants, this is discussed/shown in their respective sections, while their base equation, SAFT-VR, is presented in the annex. Most differences arise from the dispersive term, which for SAFT-0 can be written as:

$$a_0^{disp} = \frac{\varepsilon R}{k}\left(a_{01}^{disp} + \frac{a_{02}^{disp}}{T_R}\right) \quad (1.28)$$

where:

$$a_{01}^{disp} = \rho_R[-0.85959 - 4.5424\rho_R - 2.1268\rho_R^2 + 10.285\rho_R^3] \quad (1.29)$$

$$a_{02}^{disp} = \rho_R[-1.9075 - 9.9724\rho_R - 22.216\rho_R^2 + 15.904\rho_R^3] \quad (1.30)$$

$$T_R = \frac{kT}{\varepsilon} \quad (1.31)$$

and:

$$\rho_R = [6/(2^{0.5}\pi)]\eta = [6/(2^{0.5}\pi)]\zeta_3 \quad (1.32)$$

where:

$$\zeta_m = \frac{\pi\rho_s}{6}\sum_{k=1}^{NS} x_{s,k}\sigma_{kk}^m \quad (1.33)$$

The subscript *s* means that these are segment, and not molecular, properties.

For both the original and simplified PC-SAFT, the dispersive terms are the same and can be obtained from:

$$\frac{a^{disp}}{kTN} = \frac{A_1}{kTN} + \frac{A_2}{kTN} \quad (1.34)$$

with:

$$\frac{A_1}{kTN} = -2\pi\rho m^2\left(\frac{\varepsilon}{kT}\right)\sigma^3\int_1^\infty \tilde{u}(x)g^{hc}(m, x\sigma/d)x^2dx \quad (1.35)$$

$$\frac{A_2}{kTN} = -\pi\rho m\left(1 + Z^{hc} + \rho\frac{\partial Z^{hc}}{\partial\rho}\right)^{-1} m^2\left(\frac{\varepsilon}{kT}\right)^2\sigma^3\frac{\partial}{\partial\rho}\left[\rho\int_1^\infty \tilde{u}(x)^2 g^{hc}(m, x\sigma/d)x^2dx\right] \quad (1.36)$$

In these expressions $\tilde{u}(x) = u(x)/\varepsilon$ is the reduced potential function and $x = r/\sigma$ is the reduced radial distance around a segment. It is important to note that here the radial distribution function is related to the chain instead of the segments. Expressions are given to calculate the integrals and $\left(1 + Z^{hc} + \rho\frac{\partial Z^{hc}}{\partial\rho}\right)$. Naming the integrals I_1 and I_2 in order of appearance, the expressions for these three terms can then be written as:

$$\left(1 + Z^{hc} + \rho\frac{\partial Z^{hc}}{\partial\rho}\right) = \left(1 + m\frac{8\eta - 2\eta^2}{(1-\eta)^4} + (1-m)\frac{20\eta - 27\eta^2 + 12\eta^3 - 2\eta^4}{\left((1-\eta)(2-\eta)\right)^2}\right) \quad (1.37)$$

With $\eta = \zeta_3$.

$$I_1 = \sum_{i=0}^{6} a_i\eta^i \quad (1.38)$$

$$I_2 = \sum_{i=0}^{6} b_i\eta^i \quad (1.39)$$

Where:

$$a_i = a_{0i} + \frac{m-1}{m} a_{1i} + \frac{(m-1)(m-2)}{m} a_{2i} \quad (1.40)$$

$$b_i = b_{0i} + \frac{m-1}{m} b_{1i} + \frac{(m-1)(m-2)}{m} b_{2i} \quad (1.41)$$

These expressions for the integrals are based on the Lennard-Jones potential and the radial distribution function of O'Lenick et al. [38]. 42 constants are necessary for these calculations (*a'*s and *b'*s) and these were fitted to the pure component properties of *n*-alkanes.

SAFT-γ is a variation of SAFT-VR built specifically with a group contribution methodology in mind. The dispersive term of this variation is explained during the presentation of the group contribution method on SAFT-γ section, the SAFT-VR description is similar to this approach except for the GC methodology.

In this section the focus will be on the group contribution methods and in some cases, specifically for some of the SAFT-γ variants the reader is forwarded to the original articles if further information is deemed necessary, as these variants have very specific differences, not concerning, directly, the group contribution.

Figure 1.1 presents a scheme of the molecular methods applied in the following group contribution methods. Most of these methods employ an average of the group parameters for the whole molecule and create thus an effective homonuclear approach. SAFT-γ, its variants and GC-SAFT-VR use a fused heteronuclear group approach, which enables the interaction between specific groups, instead of considering only interactions between molecules as a whole:

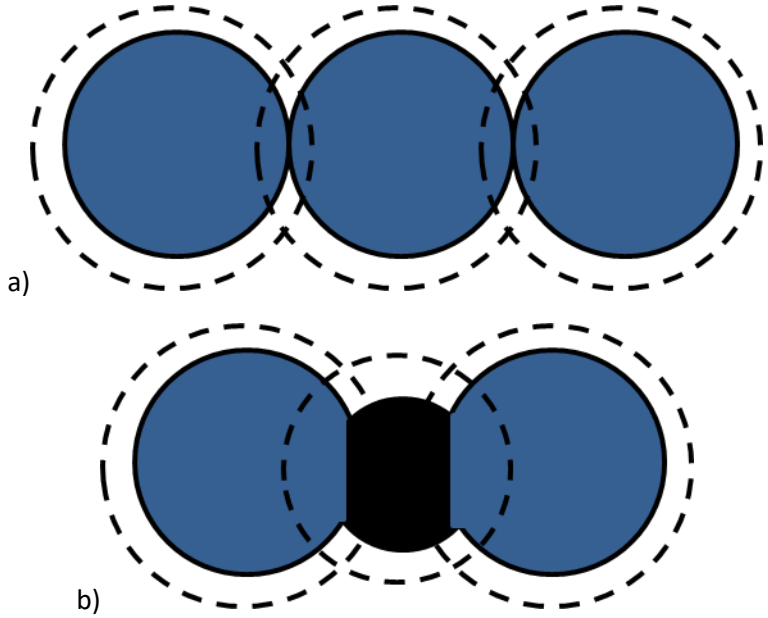

Figure 1.1 Representation of the molecular methods applied with the group contribution methods for propane. a) Homonuclear-chain of united atom segments, b) fused heteronuclear united-atoms.

A pseudo group-contribution method for SAFT-0

In 1999 a pseudo group-contribution method was proposed with SAFT-0. In this approach, only the parameter for the segment diameter and chain length are calculated from a group contribution method. The value for m_{CH_2} is obtained directly from the slope of the parameter for *n*-alkanes, then m_{CH_3} is also obtained from the m of *n*-alkanes when removing the values for the CH_2 and dividing the resulting value by the two CH_3 groups. A similar approach is employed when different groups are to be parametrized, being the final *m* value a sum of the group contributions.

The temperature independent volume v^{00} is obtained through a similar group-contribution, while only considering that instead of v^{00} the calculation is made for $m.v^{00}$. This methodology will be applied in other group-contribution methods with SAFT.

Tamouza et al. GC-SAFT approach

In 2004 Tamouza et al. [29] proposed a group contribution method for SAFT and SAFT-VR, inspired on the Lorentz-Berthelot combining rules. In this method, the adjustable parameters of the physical term, on both equations, were considered to be averages of those obtained from the constituent groups. The averages for size parameters are considered to be arithmetic, while that for the energy parameter is geometric, as is presented in the following equations:

$$\varepsilon_{molecule} = \sqrt[\sum_{i=1}^{n_{groups}} n_i]{\prod_{i=1}^{n_{groups}} \varepsilon_i^{n_i}} \quad (1.42)$$

$$\sigma_{molecule} = \frac{\sum_{i=1}^{n_{groups}} n_i \sigma_i}{\sum_{i=1}^{n_{groups}} n_i} \quad (1.43)$$

$$\lambda_{molecule} = \frac{\sum_{i=1}^{n_{groups}} n_i \lambda_i}{\sum_{i=1}^{n_{groups}} n_i} \quad (1.44)$$

where n_i is the number of groups of type *i*.

The chain parameter is considered to be a sum of the contributions to chain length (R_i) from each group.

$$m_{molecule} = \sum_{i=1}^{n_{groups}} n_i R_i \quad (1.45)$$

In 2005 the same authors [39] expanded this approach to associating compounds. In the same year Thi et al. [40] applied the method to PC-SAFT. Despite the group contribution methodology for the pure compounds, for mixtures the binary interaction parameters must still to be adjusted.

Hemptinne and co-workers [41–43], while expanding this approach to the version of PC-SAFT for polar compounds (PPC-SAFT), proposed correlations based on London's theory for the binary interaction parameter corresponding to the energy of the dispersion term (interaction parameters for the associative term are also used and are considered constant between associative groups). Using PPC-SAFT, Kontogeorgis and co-workers [44,45] have analyzed the descriptions of both the VLE and LLE of a large range of mixtures and proposed a different predictive approach for the binary interaction parameters. In this case, no k_{ij} is applied and instead the l_{ij} is studied. These parameters were adjusted to the mutual solubility of oxygenated compounds in water, using constant parameters for each family of oxygenated compounds (ex: $l_{ketones,water}$=-0.01099), thus creating a predictive method for the compounds on each family. It is important to note that both binary interaction parameters for association parameters are also calculated and applied in the same manner.

In 2016, Ahmed et al. [46] proposed a modification to the description of the temperature dependent diameter of water:

$$d(T) = \sigma_T \left[1 - \lambda_s exp\left(-3\frac{\varepsilon}{kT}\right)\right] \quad (1.46)$$

Where λ_s is the diameter softness. In the original PC-SAFT this value is 0.12. It is also important to note that σ is now temperature dependent for water. This approach was tested for water

mixtures, using both a method for the prediction of k_{ij}'s and the method of Kontogeorgis and co-workers [9].

In 2016 Trinh et al. [47] have proposed a predictive method for the calculation of l_{ij} based on the non-additive term of the square-well equation of state. This also conforms to a group contribution method, which is based on the work of Thi et al. [48]:

$$l_{ij} = \frac{1}{n_i^{group} n_j^{group}} \sum_k \sum_l n_i^{group\ k} n_j^{group\ l} L^{kl} \quad (1.47)$$

n_i^{group} is the number of groups in molecule *I*, $n_i^{group\ k}$ is the number of groups *k* in molecule *i* and L^{kl} is the non-addictive parameter between groups *k* and *l*.

This methodology was applied for the calculation of Henry constants, concerning the solubility of hydrogen in oxygenated compounds, presenting very reasonable results and a better predictive capacity than the proposed methods for the prediction of k_{ij}.

Vijande et al. approach for PC-SAFT

In 2004 Vijande et al. [30] have proposed a group-contribution method for non-associative compounds using PC-SAFT, which was further expanded in 2010 [49]. In the original work, the authors proposed an additive group, in which the parameters are a sum over all types of functional groups present on a given molecule:

$$m_{molecule} = \sum_i n_i m_i \quad (1.48)$$

$$(m\varepsilon)_{molecule} = \sum_i n_i m_i \varepsilon_i \quad (1.49)$$

$$(m\sigma^3)_{molecule} = \sum_i n_i m_i \sigma_i^3 \quad (1.50)$$

With n_i being the number of groups of type *i*.

In this first version, the authors considered that a functional group does not affect the properties of another functional group. However, this leads to the need of creating diverse versions of each group, depending on their position on a specific molecule. In the second version of this approach, the mutual effect of two functional groups on each other contributions was introduced. Considering a generic molecular coefficient π, the perturbed coefficient for a specific group can be written as:

$$\pi_i^* = \pi_i + \Delta\pi_i \quad (1.51)$$

Where π_i^* is the perturbed coefficient and $\Delta\pi_i$ is the total perturbation felt by groups of type *i*.

The perturbation felt by a specific group of type *i*, depends on its position in the chain, thus, the value of $\Delta\pi_i$ is not constant. Thus, it is necessary to distinguish groups of the same type in different positions of the chain. Considering *i* and *j* as two types of group and *k*, *l* two groups of the respective type, $\Delta\pi_{i_k}$ becomes the perturbation felt by group *k* of type *i*. Having $\Delta\pi_{i_k-j_l}$ as the perturbation on group k of type *i* due to the presence of group *l* of type *j*, it is possible to write the total perturbation as:

$$\sum_i n_i \Delta\pi_i = \sum_i \sum_{k=1}^{n_i} \Delta\pi_{i_k} = \sum_i \sum_j \sum_{k=1}^{n_i} \sum_{l=1}^{n_l} \Delta\pi_{i_k-j_l} \tag{1.52}$$

$\Delta\pi_{i_k-j_l}$ can then be calculated from the perturbation on $\Delta\pi_i$ by any adjacent group of kind *j* ($\mu_{\pi,i-j}$) and the relative position of group *k* of type *i* to group *l* of type *j* ($p_{i_k-j_l}$). This second parameter is defined as the number of bonds between each group, and the final relation is given by:

$$\Delta\pi_{i_k-j_l} = \frac{\mu_{\pi,i-j}}{p_{i_k-j_l}} \tag{1.53}$$

Thus, the sums presented on equation 1.52 are only dependent on the distance between each group. Knowing that each group does not affect itself, but affects other groups of the same type ($\mu_{\pi,i-i}$ can have a non-zero value), it is possible to introduce S_{i-j}as:

$$S_{i-j} = S_{j-i} = \left(\sum_{k=1}^{n_i} \sum_{l=1}^{n_j} \frac{1}{p_{i_k-j_l}}\right)_{i_k \neq j_l} \tag{1.54}$$

With this information and knowing that the relevant value is the sum of $\mu_{\pi,i-j}$ and $\mu_{\pi,j-i}$, and not each of them individually, these parameters can also be considered symmetric.

When transposing from the generic π to the general parameters of PC-SAFT we need to calculate the expressions for both ε and σ:

$$\mu_{m\varepsilon,i-j} = \frac{m_i+m_j}{2}\mu_{\varepsilon,i-j} \Leftrightarrow \mu_{\varepsilon,i-j} = \frac{2\mu_{m\varepsilon,i-j}}{m_i+m_j} \tag{1.55}$$

$$\mu_{m\sigma^3,i-j} = \frac{m_i+m_j}{2}{\mu_{\sigma,i-j}}^3 \Leftrightarrow \mu_{\sigma,i-j} = \left(\frac{2\mu_{m\sigma^3,i-j}}{m_i+m_j}\right)^{1/3} \tag{1.56}$$

And thus the final expressions for the molecular parameters can be written as:

$$m_{molecule} = \sum_i n_i m_i + \sum_i \sum_j \mu_{m,i-j} S_{i-j} \tag{1.57}$$

$$(m\varepsilon)_{molecule} = \sum_i n_i m_i \varepsilon_i + \frac{1}{2}\sum_i \sum_j (m_i + m_j)\mu_{\varepsilon,i-j} S_{i-j} \tag{1.58}$$

$$(m\sigma^3)_{molecule} = \sum_i n_i m_i \sigma_i^3 + \frac{1}{2}\sum_i \sum_j (m_i + m_j){\mu_{\sigma,i-j}}^3 S_{i-j} \tag{1.59}$$

It is important to note that the reference groups for this method are those linked to an infinite chain of methylene (CH_2) and thus the perturbation caused by these groups over another

group is always 0 ($\mu_{\pi,i-CH_2} = 0$). Nevertheless, in this specific case $\mu_{\pi,i-CH_2} \neq \mu_{CH_2-\pi,i}$, thus, the perturbation felt by the CH_2 chain due to other groups in the molecule is not 0.

In 2014 Vijande et al. [36] expanded this methodology for compounds with a single associating group. The expression for the association parameters is given by:

$$\pi^{AB}_{molecule} = \pi^{AB}_{\gamma} + \sum_j \mu_{\pi^{AB},\gamma-j} S_{\gamma-j} \tag{1.60}$$

Where *γ* is an associating group and π^{AB} is a general association parameter. It is important not to forget that the associative group also contribute to the parameters of the physical term. Also, when *j* is a non-associating group, $\mu_{\pi^{AB},j-\gamma} = 0$. However, the associative parameters are affected by the presence of other groups and so $\mu_{\pi^{AB},\gamma-i}$ can have a non-zero value. Also of note is that, for the compounds of interest on the paper (primary alcohols and amines), the relative mutual position of CH_3 and the associating group are given by:

$$S_{CH_3-\gamma} = S_{\gamma-CH_3} = \frac{1}{1+n_{CH_2}} \tag{1.61}$$

And thus the association parameters will present an asymptotic behaviour.

SAFT-γ

In 2007 a different approach was introduced by Lymperiadis et al. [35], based on SAFT-VR. In this approach, a fluid is created based on hetero-segmented monomers, which are then fused to form a chain. Thus, in this case, instead of an average value for all groups, the contributions of each group towards the Helmholtz energy are calculated individually and the interactions between two different molecules are calculated from the interactions between each segment, and not from an average set of parameters for the whole molecule. The Helmholtz energy of the monomer (segment) term is calculated from a second order high temperature expansion applied to the reference, which is a hard sphere mixture:

$$\frac{A^{mono}}{Nk_BT} = \frac{A^{hs}}{Nk_BT} + \frac{A_1}{Nk_BT} + \frac{A_2}{Nk_BT} \tag{1.62}$$

The equation for the Helmholtz energy concerning the hard sphere term is:

$$\frac{A^{hs}}{Nk_BT} = \left(\sum_{i=1}^{n_{components}} x_i \sum_{k=1}^{n_{segments}} v_{k,i} S_k\right)\left(a^{hs}\right) \tag{1.63}$$

Where a^{hs} is the hard-sphere contribution of a segment. $v_{k,i}$ represents the number of segments of type *k* in component *i* and, as the segments in this method present different sizes, S_k introduces the proportion at which each segment contributes to the properties of the molecule.

$$a^{hs} = \frac{6}{\pi\rho_\omega}\left[\left(\frac{\zeta_2^3}{\zeta_3^2} - \zeta_0\right)\ln(1-\zeta_3) + 3\frac{\zeta_1\zeta_2}{1-\zeta_3} + \frac{\zeta_2^3}{\zeta_3(1-\zeta_3)^2}\right] \quad (1.64)$$

The group number density of the mixture (ρ_s) is related to the molecular density by:

$$\rho_\omega = \rho\left(\sum_{i=1}^{NC} x_i \sum_{k=1}^{NS} v_{k,i} S_k\right) \quad (1.65)$$

Where $x_{\omega,k}$ is the number of groups of type *k* in the mixture ω.

$$x_{\omega,k} = \frac{\sum_{i=1}^{NC} x_i v_{k,i} S_k}{\sum_{i=1}^{NC} x_i \sum_{j=1}^{NS} v_{j,i} S_j} \quad (1.66)$$

A similar approach is applied for the remaining terms of the monomer contribution. Thus, the original values for the parameters of a segment are kept intact and when concerning mixtures of different compounds, the interactions can be accounted for with higher accuracy and without the need of binary interaction parameters.

For the mean-attractive energy per molecule [35,50,51].

$$\frac{A_1}{Nk_BT} = \frac{1}{Nk_BT}\left(\sum_{i=1}^{NC} x_i \sum_{k=1}^{NS} v_{k,i} S_k\right) a_1 \quad (1.67)$$

a_1 is calculated from the pair-attractive contributions between two different groups *k* and *l*:

$$a_1 = \sum_{k=1}^{NS}\sum_{l=1}^{NS} x_{\omega,k} x_{s,l} a_1^{kl} \quad (1.68)$$

which are obtained from:

$$a_1^{kl} = -\rho_s a_{kl}^{vdw} g_{0,kl}^{HS} \quad (1.69)$$

Considering an hypothetical pure fluid of diameter σ_x at contact and at an effective packing fraction ζ_{kl}^{eff}, $g_{0,kl}^{HS}\left(\sigma_x, \zeta_{kl}^{eff}\right)$ is the pair correlation of said fluid. In the first applications a square-well potential was applied and, in this case, the value for the van der Waals attractive parameter is given by:

$$a_{kl}^{vdw} = \frac{2\pi}{3}\varepsilon_{kl}\sigma_{kl}^3\left(\lambda_{kl}^3 - 1\right) \quad (1.70)$$

With ε_{kl} being the well depth of square-well interaction of range λ_{kl} and σ_{kl} the contact distance of segments *k* and *l*.

In these conditions the radial distribution function is calculated from [52]:

$$g_{0,kl}^{HS} = \frac{1-0.5\zeta_{kl}^{eff}}{\left(1-\zeta_{kl}^{eff}\right)^3} \quad (1.71)$$

The value of ζ_{kl}^{eff} is here calculated from:

$$\zeta_{kl}^{eff} = c_{1,kl}\zeta_x + c_{2,kl}\zeta_x^2 + c_{3,kl}\zeta_x^3 \quad (1.72)$$

$$\begin{pmatrix} c_{1,kl} \\ c_{2,kl} \\ c_{3,kl} \end{pmatrix} = \begin{pmatrix} 2.25855 & -1.50349 & 0.249434 \\ -0.669270 & 1.40049 & -0.827739 \\ 10.1576 & -15.0427 & 5.30827 \end{pmatrix} \begin{pmatrix} 1 \\ \lambda_{kl} \\ \lambda_{kl}^2 \end{pmatrix} \tag{1.73}$$

With:

$$\zeta_x = \frac{\pi}{6} \rho_\omega \sigma_x^3 \tag{1.74}$$

Using the following mixing rule:

$$\sigma_x^3 = \sum_{k=1}^{NS} x_{\omega,k} \sigma_{kk}^3 \tag{1.75}$$

Having calculated A_1 it is now of interest to look at the calculation of A_2:

$$\frac{A_2}{N k_B T} = \left(\frac{1}{N k_B T}\right)^2 \left(\sum_{i=1}^{NC} x_i \sum_{k=1}^{NS} v_{k,i} S_k\right) a_2 \tag{1.76}$$

Where:

$$a_2 = \sum_{k=1}^{NS} \sum_{l=1}^{NS} x_{\omega,k} x_{\omega,l} a_2^{kl} \tag{1.77}$$

The pair contributions are given by:

$$a_2^{kl} = \frac{1}{2} K^{HS} \varepsilon_{kl} \rho_\omega \frac{\delta a_1^{kl}}{\delta \rho_\omega} \tag{1.78}$$

Where K^{HS} is the isothermal compressibility of the reference hard-sphere mixture, which for the sake of consistency with the mean-attractive term, the authors calculated from the Carnahan and Starling [52] expression, obtaining:

$$K^{HS} = \frac{(1-\zeta_3)^4}{(1+4\zeta_3+4\zeta_3^2-4\zeta_3^3+4\zeta_3^4)} \tag{1.79}$$

In this version, to obtain a compact equation for the chain term, effective molecular parameters are applied. These are related to the segment parameters in the following manner:

$$\bar{\sigma}_{ii}^3 = \frac{\sum_{k=1}^{NS} v_{k,i} S_k \sigma_{kk}^3}{\sum_{k=1}^{NS} v_{k,i} S_k} \tag{1.80}$$

$$\bar{\varepsilon}_{ii} = \sum_{k=1}^{NS} \sum_{l=1}^{NS} z_{k,i} z_{l,i} \varepsilon_{lk} \tag{1.81}$$

$$\bar{\lambda}_{ii} = \sum_{k=1}^{NS} \sum_{l=1}^{NS} z_{k,i} z_{l,i} \lambda_{lk} \tag{1.82}$$

$z_{k,i}$ is the fraction of group k in component i, which is given by:

$$z_{k,i} = \frac{v_{k,i} S_k}{\sum_{k=1}^{NS} v_{k,i} S_k} \tag{1.83}$$

When considering a square-well potential, the chain term is described as:

$$\frac{A_{chain}}{N k_B T} = -\sum_{i=1}^{NC} x_i \left(\sum_{k=1}^{NS} v_{k,i} S_k - 1\right) \ln\left(g_{ii}^{SW}(\bar{\sigma}_{ii}; \zeta_3)\right) \tag{1.84}$$

Other variants have been tested with different potentials.

This version also presents differences in the calculation of the associative parameters. The volume available for bonding of sites *a* and *b* on groups *k* and *l* of components *i* and *j* can be obtained from:

$$K_{ijklab} = \frac{4\pi\bar{\sigma}^{ij^2}}{72r_d^2}\left[\ln\left(\frac{r^c_{klab}+2r_d}{\bar{\sigma}^{ij}}\right)\left(6r^{c^3}_{klab} + 18r^{c^2}_{klab} - 24r_d^3\right) + \left(r^c_{klab} + 2r_d - \bar{\sigma}^{ij}\right)\left(22r_d^2 - 5r_d r^c_{klab} - 7r_d\bar{\sigma}^{ij} - 8r^{c^2}_{klab} + r^c_{klab}\bar{\sigma}^{ij} + \bar{\sigma}^{ij^2}\right)\right] \quad (1.85)$$

Where $\bar{\sigma}_{ij}$ is obtained from an arithmetic mean of $\bar{\sigma}_{ii}$ and $\bar{\sigma}_{jj}$, $r_d/\bar{\sigma}_{ij}$ is the reduced distance between the association site and the centre of the interaction sphere (set to the value of 0.25) and r^c_{klab} is the cutoff distance. Thus, as in the case of the methodology of Vijande et al. [30], the association parameters will depend on the structure of the molecule and not only on the nature of the associating group (in SAFT-γ this is only true for the volume of association interactions).

In 2008 Lymperiadis et al. [53] extended the approach for groups with multiple spherical segments, where $S_k=v_k'S_k'$, with v_k' being the number of segments in group *k* and S_k' is a modified segment size to accommodate the previous parameter.

This EoS has been linked with developments, using various force fields, which have improved the link between experimental data and Coarse-Grained (CG) models. Some newer variants, which modify not only the force field, but introduce other modifications to SAFT-γ, have been proposed and are analysed further in this review. The better-known of these versions is SAFT-γ Mie introduced by Papaioannou in 2014 [54].

Extension of the ESD group contribution to SAFT and PC-SAFT

Another group contribution method was proposed by Emami et al. [31] in 2008. This approach was an extension to the methodology presented for ESD by Elliott and Natarajan [55] to SAFT and PC-SAFT, creating a different group contribution method than that of Tamouza et al. [29]. To adapt this methodology, a correspondence between the different EoS was needed. A relation was then introduced between the molecular volume and the equation parameters. For SAFT equations this comes as:

$$b = \pi m\sigma^3/6 \quad (1.86)$$

In this methodology the association volume is correlated from the physical term parameters:

$$K^{AD} = 0.035\, b/m \quad (1.87)$$

The energy of association is the average of all associating groups in the molecule, with constant values for each type of associating group. Nevertheless, it is important to note that only groups with 2 associating sites were considered in the original version of the method. Restrictions are then introduced to the remaining parameters. For calculating the *b* parameter the extended Hoy [56] correlation is applied:

$$Z_L^{298} = \frac{0.1 V_L^{298}}{298R} \tag{1.88}$$

The 0.1 in equation 1.88 is the pressure of application of the equation in MPa. The liquid molar volume at 298 K (V_L^{298}) is given by:

$$V_L^{298} = 12.1 + \sum v_i \Delta V_i \tag{1.89}$$

With ΔV_i being the group contribution for liquid molar volumes as introduced by Hoy [56].

The authors then use the internal energy from liquid molar volume and heat of vaporization as obtained from the Costantinou and Gani GC method [57] to restrict the internal energy departure functions and obtain the value for the energy parameter. This is presented in the following equation:

$$\frac{\delta^2 V_L^{298}}{298R} = -\frac{U}{298R} \tag{1.90}$$

Where δ is the solubility parameter given by $\delta = \left[\left(H_{vap}^{298} - 298R\right)/V_L^{298}\right]^{1/2}$.

The segment number is then obtained from

$$m = 1 + \sum v_i \Delta m_i \tag{1.91}$$

With Δm_i being the group contribution for the shape factor.

One of the main advantages of this method is that all the pure data necessary for the calculation of the pure compound parameters are obtained through other group contribution methods and thus, no experimental data is needed in order to use this methodology.

GC approach with first and second order groups for sPC-SAFT

Tihic et al. [32] proposed yet another GC approach, using the simplified PC-SAFT for systems containing polymers. The methodology is based on Constantinou and Gani group contribution method [57] and introduces two levels of group contributions: First order groups (FOG), which only give information on the groups present in the molecule, but which are not capable to distinguish between two isomers (eg. 2-pentanol and 3-pentanol, both have 2 CH_3, 1 CH, 2 CH_2

and 1 OH groups) and second order groups (SOG) which introduce information on the structure of the molecule. The parameters for a molecule are then obtained from:

$$m_{molecule} = \sum_i (n_i m_i)_{FOG} + \sum_j \left(n_j m_j\right)_{SOG} \tag{1.92}$$

$$(m\sigma^3)_{molecule} = \sum_i \left(n_i m_i \sigma_i^3\right)_{FOG} + \sum_j \left(n_j m_j \sigma_j^3\right)_{SOG} \tag{1.93}$$

$$(m\epsilon/k)_{molecule} = \sum_i (n_i m_i \epsilon_i/k)_{FOG} + \sum_j \left(n_j m_j \sigma_j^3 \epsilon_j/k\right)_{SOG} \tag{1.94}$$

GC-SAFT-VR

In 2009 Peng et al. [34] proposed a different group contribution method based on the hetero-segmented version of SAFT-VR. Being based on the same version of SAFT, the GC approach here applied presents some similarities to SAFT-γ. Nevertheless, in this version, the fraction of groups/segments are related to a pure component instead of the whole mixture, as is the case with SAFT-γ as can be seen when comparing equations 1.65 and 1.94.

$$x_{s,ki} = \frac{x_k m_{ki}}{\sum_{i=1}^{NC} x_i \sum_{k'=1}^{n'_k} x_k m_{ki}} \tag{1.95}$$

where n'_k is the number of group types on component *k*.

This leads to applying the interactions between groups of each molecule as can be seen in the example below:

$$a_1 = \sum_{l=1}^{n} \sum_{j=1}^{n'_l} \sum_{k=1}^{n} \sum_{i=1}^{n'_k} x_{s,ki} x_{s,lj} a_1^{ki,lj} \tag{1.96}$$

And thus eliminates the need to create a set of effective parameters when considering the chain term.

Some other notorious differences include the use of a different effective packing fraction expression based on the works of Patel et al. [58].

$$\zeta_{kl}^{eff} = \frac{C_{1,kl}\zeta_x + C_{2,kl}\zeta_x^2}{(1 + C_{3,kl}\zeta_x)^3} \tag{1.97}$$

$$\begin{pmatrix} C_{1,kl} \\ C_{2,kl} \\ C_{3,kl} \end{pmatrix} = \begin{pmatrix} -3.16492 & 13.35007 & -14.80567 & 5.70286 \\ 43.00422 & -191.66232 & 273.89683 & -128.93337 \\ 65.04194 & -266.46273 & 361.04309 & -162.69963 \end{pmatrix} \begin{pmatrix} \frac{1}{\lambda_{ki,lj}} \\ \frac{1}{\lambda_{ki,lj}^2} \\ \frac{1}{\lambda_{ki,lj}^3} \\ \frac{1}{\lambda_{ki,lj}^4} \end{pmatrix} \tag{1.98}$$

Another important difference is in the K^{HS} function applied, which in this version is the Percus-Yevick expression:

$$K^{HS} = \frac{\zeta_0(1-\zeta_3)^4}{\zeta_0(1-\zeta_3)^2+6\zeta_1\zeta_2(1-\zeta_3)+9\zeta_3^2} \quad (1.99)$$

In this method the chain contribution is given by:

$$\frac{A_{chain}}{Nk_BT} = -\sum_{k=1}^{n}\sum_{ij} x_k \ln\left(y_{ki,kj}^{SW}(\bar{\sigma}_{ii})\right) \quad (1.100)$$

The first sum is over all components, while the second takes into account the chain formation and connectivity of the segments. Here *SW* stand for square-well and:

$$y_{ki,kj}^{SW} = exp\left(-\beta\varepsilon_{ki,kj}\right) g_{ki,kj}^{SW}(\bar{\sigma}_{ii}) \quad (1.101)$$

with $\beta = 1/k_BT$

The association term is calculated in a similar manner to SAFT-γ.

GC method for polymers with PC-SAFT

In 2012 Peters et al. [33] presented a GC method for the parameters of polymers and their mixtures using PC-SAFT. This method uses the same approach as the one from Tamouza et al. [29]. Nevertheless, the authors have shown that parameters calculated previously for groups, do not transfer well to polymers. Thus, different sets of group parameters need to be used for polymeric molecules.

The same authors proposed in 2013 [59] a GC method for the binary interaction parameters between polymers and solvents.

$$\left(1-k_{ij}\right) = \frac{\left[\sum_{p=1}^{NG_i} n_{p,i} \sum_{s=1}^{NG_j} n_{s,j}\right]}{\sqrt{\prod_{p=1}^{NG_i}\prod_{s=1}^{NG_j}\left(1-k_{ps}\right)^{n_{p,i}n_{s,j}}}} \quad (1.102)$$

Here k_{ps} is the contribution to the binary interaction parameter from each pair of polymer-solvent groups and $n_{p,I}$ is the number of groups of type *p* in polymer *i* and the same for the solvent. It is important to note that the authors only use the groups for solvents in the binary interaction parameters. For the pure solvent parameters the authors use optimized sets.

This methodology enables the reduction of SAFT parameters to fit systems containing polymers and co-polymers, while providing accurate results for the analysed systems, in some cases with better results for mixtures than those presented previously using the conventional parameterization.

SAFT-γ WCA

In 2013 a SAFT-γ based approach was developed by Ghobadi and Elliot [60] with the objective of creating a consistent model for the description of interfacial properties, without the need of

a full molecular simulation. This version is based on Weeks-Chandler-Anderson potential. In this version the Helmholtz energy contributions are divided in:

$$a = a^{id} + a^{WCA} + a^{chain} + a^{pert} + a^{assoc.} \tag{1.103}$$

The Helmholtz free energy is, in this version, directly compared to the corresponding terms in molecular simulation.

The perturbation contribution in equation 1.103 is based on a third order Zwanzig high temperature expansion [61,62]:

$$a^{pert} = \frac{A_1}{T} + \frac{A_2}{T^2} + \frac{A_3}{T^3} \tag{1.104}$$

Where:

$$A_1 = \frac{1}{Nk_B^1}\langle U' \rangle_0 \tag{1.105}$$

$$A_2 = \frac{-1}{2!Nk_B^2}\left(\langle U'^2 \rangle_0 - \langle U' \rangle_0^2\right) \tag{1.106}$$

$$A_3 = \frac{-1}{3!Nk_B^3}\left(\langle U'^3 \rangle_0 - 3\langle U' \rangle_0 \langle U'^2 \rangle_0 + 2\langle U' \rangle_0^3\right) \tag{1.107}$$

$\langle U' \rangle_0$ is an average over the configurations of the reference system for the total potential of the system.

The Helmholtz energy of WCA spheres is given by:

$$a^{WCA} = \frac{1}{\rho}\left(-n_0 ln(1-n_3) + \frac{n_1 n_2 \gamma_1}{(1-n_3)} + f_3 n_2^3\right) \tag{1.108}$$

With:

$$f_3 = \frac{(3\gamma_2 - 2\gamma_3)n_3 - 1.5(\gamma_2 - \gamma_3)[2n_3 - n_3^2] + \gamma_3(1-n_3)^2 ln(1-n_3)}{36\pi n_3^2 (1-n_3)^2} \tag{1.109}$$

γ_i are adjustable parameters fitted to simulation data of WCA spheres, $n_\omega = \rho \sum_i^{NC} x_i M_i^\omega$. The description of M_i^ω is presented in the annexes.

The chain term is also different in this version. The authors have shown that for some molecules, as is the case of some two-site molecules, the chain contribution can easily present a value of 0. To solve this issue, this version uses:

$$a^{chain} = -\sum_{i=1}^{NC} x_i \left(\frac{1}{2}\sum_{k=1}^{NS} v_{k,i} S_k NB_k\right) lng_{ii}^{WCA} \tag{1.110}$$

Where NB_k stands for the number of chain links for a site of type k. More information on the specifics of this equation can be found in the original article [60].

In 2014 Ghobadi and Elliot [63] expanded this version to associative compounds. The approach for this term is similar to what was presented when applying SAFT-γ for bulk fluids. For inhomogeneous systems a more complex approach is applied based on the works of Segura et al. [64] and Bymaster et al. [65]. It is important to note that such an approach comes with a high cost in terms of number of parameters. Twelve adjustable parameters are used per non-associating group, with six extra parameters for associating groups, two of those concerning the number of sites. In the first work with this equation of state, very reasonable results are presented for liquid density and derivative properties of alkanes up to dodecane. Vapour pressure presents higher deviations, which are, however, still in the range of magnitude of other group contribution methods with SAFT. As in most of these methods, the critical temperatures and pressures are not correctly described. In the second and third works with this version of SAFT, the authors present very reasonable results for interfacial properties and expand these to molecules with groups capable of hydrogen bonding.

This model was based on the TraPPE force field, nevertheless as shown by the authors its parameter transferability is inferior to that of TraPPE. Further information on this approach can be found in the articles discussed above.

SAFT-γ Mie

A new version of SAFT-γ employing a Mie potential force field was presented in 2014 by Pappaioanou et al. [54]. This version uses a higher order temperature expansion for the monomer term, which can be described as:

$$\frac{A^{mono}}{Nk_BT} = \frac{A^{hs}}{Nk_BT} + \frac{A_1}{Nk_BT} + \frac{A_2}{Nk_BT} + \frac{A_3}{Nk_BT} \tag{1.111}$$

However, instead of the dependence with *σ,* the effective hard-sphere diameter d_{kk} is applied:

$$d_{kk} = \int_0^{\sigma_{kk}} \left[1 - exp\left\{-\frac{\Phi_{kk}^{Mie}(r_{kk})}{k_BT}\right\}\right] dr \tag{1.112}$$

Where the interaction energy between two segments is given by:

$$\Phi_{kl}^{Mie}(r_{kl}) = C_{kl}\varepsilon_{kl}\left[\left(\frac{\sigma_{kl}}{r_{kl}}\right)^{\lambda_{kl}^r} - \left(\frac{\sigma_{kl}}{r_{kl}}\right)^{\lambda_{kl}^a}\right] \tag{1.113}$$

Here λ_{kl}^r and λ_{kl}^a are the repulsive and attractive exponents of the intersegment interaction. To ensure that at the minimum of these interactions the value obtained is $-\varepsilon_{kl}$, C_{kl} comes as:

$$C_{kl} = \frac{\lambda_{kl}^r}{\lambda_{kl}^r - \lambda_{kl}^a}\left(\frac{\lambda_{kl}^r}{\lambda_{kl}^a}\right)^{\frac{\lambda_{kl}^a}{\lambda_{kl}^r - \lambda_{kl}^a}} \quad (1.114)$$

The hard-sphere term of the monomer part of the equation is mainly the same as that of SAFT-γ. In the A_1 contribution the value of $a_{1,kl}$ is now obtained from:

$$a_{1,kl} = C_{kl}\left[x_{0,kl}^{\lambda_{kl}^a}\left(a_{1,kl}^s(\rho_s, \lambda_{kl}^a) + B_{kl}(\rho_s, \lambda_{kl}^a)\right) - x_{0,kl}^{\lambda_{kl}^r}\left(a_{1,kl}^s(\rho_s, \lambda_{kl}^r) + B_{kl}(\rho_s, \lambda_{kl}^r)\right)\right] \quad (1.115)$$

where $x_{0,kl} = \sigma_{kl}/d_{kl}$ and:

$$B_{kl}(\rho_s, \lambda_{kl}) = 2\pi\rho_s d_{kl}^3 \varepsilon_{kl}\left[\frac{1-\zeta_x/2}{(1-\zeta_x)^3} I(\lambda_{kl}) - \frac{9\zeta_x(1+\zeta_x)}{2(1-\zeta_x)^3} J(\lambda_{kl})\right] \quad (1.116)$$

To simplify the integration of the potential, $I(\lambda_{kl})$ and $J(\lambda_{kl})$ are introduced, their use is explained in detail by Lafitte et al. [66]. Similar modifications are needed to the term $a_{2,kl}$ as well as the introduction of equations for A_3. Six pure parameters are needed in this method to describe a non-associating group plus five parameters for association compounds, it is important however, that three of these parameters correspond to the number of bonding sites and number of hydrogen bond receptors and acceptors. On the first work with this version of SAFT the authors show relevant advantages in the description of derivative properties, being able, for many compounds, to present correct descriptions for vapour pressure and liquid density, while presenting reasonable results for derivative properties, including speed of sound. The predictive capacity for phase equilibria has also been shown, and for many binary systems this model is able to produce a completely predictive description, where, most other methods of the same type need binary interaction parameters. For a complete explanation of these modifications as well as other changes concerning the use of the Mie-potential the reader is forwarded to the original SAFT-γ Mie paper [54].

In this version the association strength uses a more complex function:

$$\Delta_{ij,kl,}^{ab} = \sigma_{ij}^3 I_{kl}^{ab}\left[exp\left(\varepsilon_{kl}^{HB,ab}/k_b T\right) - 1\right] \quad (1.117)$$

with $I_{kl,ab}$ as a dimensionless integral. The evaluation of this integral is discussed by Lafitte et al. [66] and Dufal et al. [67]. One of these evaluation methods consists in an approximation based on a Barker-Henderson zeroth-order perturbation approach, in which $g^{mie}(r) \cong g_d^{HS}(r)$. Assuming $r^2 g_d^{HS}(r) \cong d^2 g_d^{HS}(d)$ an expression close to that of other SAFT variants:

$$I_{kl,ab} \approx g_d^{HS}(\bar{d}_{ij}) K_{ijkl}^{ab} \quad (1.118)$$

CPA

CPA allies the simplicity of a cubic equation of state with the rigour of an associative term based on Wertheim's theory. This approach creates a simple, fast, yet efficient equation of state for associating compounds. These are desirable characteristics for the industry, as an increase in processing time, even if small, might have a relevant impact in the simulation of an industrial process.

In terms of pressure, the physical term (cubic term) of CPA can be written as:

$$P_{cubic} = \frac{RT}{v-b} - \frac{a}{(v+\delta_1 b)(v+\delta_2 b)} \tag{1.119}$$

Where δ_1 and δ_2 are parameters specific to a cubic EoS. Usually the cubic term applied with CPA is the Soave-Redlich-Kwong (SRK), for which, $\delta_1 = 1$ and $\delta_2 = 0$. The term a is $a(T) = a_c\left(1 + c_1\left(1 - \sqrt{T_r}\right)\right)^2$.

Binary interaction parameters in the cubic term are used to correct the cross-energy parameters:

$$a_{ij} = \sqrt{a_i a_j}\left(1 - k_{ij}\right) \tag{1.120}$$

The association term is similar to the ones presented before and can be written as:

$$P_{assoc} = -\frac{RT\rho}{2}\left(1 + \rho\frac{\partial lng}{\partial \rho}\right)\sum_i n_i \sum_{A_i}\left(1 - X_{A_i}\right) \tag{1.121}$$

with:

$$X_{A_i} = \frac{1}{1+\rho\sum_j x_j \sum_{B_j} X_{B_j}\Delta^{A_iB_j}} \tag{1.122}$$

where:

$$\Delta^{A_iB_j} = gb^{ij}\beta^{A_iB_j}\left(e^{\frac{\varepsilon^{A_iB_j}}{RT}} - 1\right) \tag{1.123}$$

CPA usually presents tendencies within a specific family of compounds for both the energy parameter at the critical temperature (a_c) and the co-volume of the cubic term (b). However, the alpha function parameter (c_1) presents a high variability and should be regarded with concern if a group contribution method for the whole equation is needed. The association parameters do not present the same flexibility as in SAFT or GCA. In most cases considering them constant within a specific family of compounds is not possible, unless a modified version of the model is employed [68,69]. Oliveira et al. [70] and Queimada et al. [71,72] have tried to obtain correlations based on the van der Waals volume, for the pure parameters. Nevertheless, even within the same family of compounds, in most cases, the tendency of the

alpha function parameter was irregular and was not possible to develop predictive correlations for this parameter.

Successful group contribution methods applied to CPA have mainly addressed the correct description of mixture phase equilibria. These have been conducted using the PR-CPA version, where the SRK cubic term of the Simplified CPA [73] model is replaced by Peng-Robinson. In equation 1.119 this corresponds to having δ_1 = 1+√2 and δ_2 = 1-√2.

Mahabadian et al. [74] and Hajiew et al. [75,76] incorporated the GC-method developed by Jaubert and co-workers [77] for the PR EoS, PPR78 (eq. 1.124 and 1.125), with CPA. The former used the original version while the latter introduced some modifications.

$$k_{ij}(T) = \frac{-\frac{1}{2}\times Sum - \left(\frac{\sqrt{a_i(T)}}{b_i} - \frac{\sqrt{a_j(T)}}{b_j}\right)^2}{2\frac{\sqrt{a_i(T)a_j(T)}}{b_i b_j}} \tag{1.124}$$

$$Sum_{PPR78} = \sum_{k=1}^{Ng}\sum_{l=1}^{Ng}(\alpha_{ik} - \alpha_{jk})(\alpha_{il} - \alpha_{jl})A_{kl}\left(\frac{298.15}{T}\right)^{\left(\frac{B_{kl}}{A_{lk}}-1\right)} \tag{1.125}$$

N_g being the number of groups, *k* and *l* are indexes representing the groups, *A* and *B* are symmetric group interaction parameters (A_{kl}=A_{lk}) and α_{ik} is the fraction of groups *k* in molecule *i*, given by:

$$\alpha_{ik} = \frac{number\ of\ k\ groups\ in\ molecule\ i}{total\ number\ of\ groups\ in\ molecule\ i} \tag{1.126}$$

The modification, mentioned above, was based on the description of binary interaction parameters for water + hydrocarbons, which were not correctly described with the original PPR78. Hajiw et al. [75] introduced modifications to equation 124 for the specific case of interactions with associating groups. Three group parameters were introduced for these interactions:

$$Sum_{asso} = \sum_{k=1}^{n_{groups}}\sum_{l=1}^{n_{groups}}(\alpha_{ik} - \alpha_{jk})(\alpha_{il} - \alpha_{jl})(C_{kl}T^2 + D_{kl}T + E_{kl}) \tag{1.127}$$

Applying this modified method, the same authors showed the capacities of GC-PR-CPA to describe the minima of LLE solubility in systems containing water and heavy hydrocarbons, using a temperature dependent k_{ij}. Accurate results are obtained for gas-liquid equilibria of liquid alkanes with water, while the aqueous solubility of heavier alkanes present a correct behaviour.

Hajiw et al. [76] have tested the same approach for the analysis of methanol content in natural gas. GC-PR-CPA is able to represent the azeotropic compositions and to accurately describe partition coefficients, both in a wide range of temperatures.

One of the better-known applications of CPA is for the description of systems with hydrate formation/inhibition. Using the original PPR78 group contribution with PR-CPA, Mahabadian et al. [74] applied CPA to a multiphase flash in the presence of hydrates. Accurate predictions are obtained for the hydrate stability, using this approach, obtaining good estimations of the hydrate dissociation conditions.

These analysis were only applied to systems containing a single associating compound (water or methanol), thus no study was ever made on the need to correlate association binary interaction parameters or on the use of PPR78, with or without modifications, between two associating molecules.

1.3.3 Results and comparison of these methods

In this section, a brief analysis of results, using the different methods for some well-studied compounds/mixtures is presented.

For pure components properties it is not fair to include CPA, as its pure component parameters are optimized from fitting vapour pressure and liquid density data. For GCA, the authors only present the results for saturation pressure, and thus this will be the only property in analysis for this model. For most of the SAFT GC approaches presented, the deviations on the vapor pressure and liquid density are on the same order of magnitude as those of their optimized counterparts.

Emami et al. [31] presented a comparison between the results of their GC method and that of Tihic et al. [32], for vapor pressures. For the twelve families of compounds used in the study the method of Emami et al. [31] showed superior results. Nevertheless, it is notorious that for compounds with a lower molecular weight the predicted vapor pressures are not accurate. However, this method also adds the advantage of not requiring a previous optimization to pure component data. The data needed for the optimization is obtained through other group contribution methodologies and the authors report an average deviation of less than 30% for the vapor pressure data of the 666 compounds used in the study.

The most studied GC methodology for SAFT and PC-SAFT is that based on the work of Tamouza et al. [29] and its extension to polar compounds known as GC-PPC-SAFT [41]. Some results, obtained using GC-PPC-SAFT for the pure vapor pressures and liquid densities of alkanes and alkanols were analyzed and are compared with the results using the work of Vijande et al. [30,49] expanded for associative compounds [36]. The predictions are compared to Multiflash [78] correlations (ethanol up to 1-butanol) and to correlations obtained from the data in the DIPPR [79] and TRC [80] databases for the remaining compounds. For most compounds, there are some similarities between the deviations from both methods. Nevertheless for these compounds, the approach of Vijande et al. seems more consistent in the deviations for vapor pressure and presents a better description of liquid densities. These results are presented in table 1.2.

For heavy alkanols like eicosanol, the deviations obtained for vapor pressures are high. However, the volatility of these compounds is low, and the uncertainties in their measurements are considerable, and it is to be expected that these models, especially using group contribution methods will present difficulties in the description of vapor pressure. Interestingly enough using the method of Vijande et al. [36] for associating compounds, the results for liquid density are still quite accurate when compared to the DIPPR correlation. For this compound, the deviations of the method of Tamouza et al. [29] are still close to the average deviation of the method of Emami et al. [31].

Table 1.2 Deviations for vapor pressure and liquid densities of ten *n*-alkanols.

		%AAD			
		Vijande et al.		Tamouza et al.	
Compound	*Trange* (K)	P^{sat}	*ρliq*	P^{sat}	*ρliq*
ethanol	260-400	4.62	0.96	5.86	2.88
1-propanol	260-400	4.89	1.31	4.49	1.23
1-butanol	260-410	1.03	0.75	7.84	2.24
1-pentanol	315-455	2.50	0.05	1.72	2.06
1-hexanol	275-455	3.37	0.31	5.45	2.50
1-heptanol	285-445	6.78	0.53	10.75	1.89
1-octanol	300-460	7.77	0.70	7.20	1.66
1-nonanol	300-470	7.26	0.51	4.22	1.86
1-decanol	330-490	11.10	1.04	3.36	1.16
1-eicosanol	404-574	40.24	3.31	31.08	14.39

It is important to remember that the calculation of the method of Vijande et al. [36] does not take into account a polar contribution, which is expected to decrease the accuracy for specific compounds/systems, which depend greatly on these contributions.

GCA authors have shown good results for the vapor pressure of pure compounds. Some examples include Sanchéz et al. [81] which presented deviations below 7% for a large group of aromatic compounds in temperature ranges of 0.52-0.95 *Tc*. A second example are the results that Soria et al. [82] presented for both branched alkanols and branched alkanes with deviations below 5%. However, the method of calculation of the critical diameter had to be changed as the authors pointed out, and this will affect the description of the critical point. Another example is the accuracy of the description of alkanes up to 36 carbons studied by Prieto et al. [83] and which yields deviation in most cases inferior to 5%.

The more complex methods on this list are the SAFT-γ variants and GC-SAFT-VR, both based on SAFT-VR. These models require more information on the structure of the molecules. However, when these models were first presented by Lymperiades et al. [35] and Peng et al. [34], they showed to be able to predict the properties of heavy compounds within reasonable accuracy. The reported results for the average deviations of vapor pressure of the *n*-alkanols between ethanol and 1-decanol with SAFT-γ [84] never exceed 4%, while those for liquid density are mostly within 1% of deviation. These methods have been applied to a large range of complex compounds and mixtures and a short list of works is reported in the annexes.

The following paragraphs present a brief comparison for systems that have been analyzed by more than one of these methods or have been calculated in this work.

Most SAFT variants are known to present higher deviations, than CPA and GCA, when describing systems of water and alkanes. This is verified in the results by Hajiew et al. [75] when the authors compare their results to those of GCA and GC-PPC-SAFT. This is also emphasized in the work of Sánchez et al. [81] where the authors compare the results of GCA with those of sPC-SAFT and s-CPA, being the results of those two equations, which use an optimization approach instead of a group contribution, comparable. However, SAFT-γ already presents a high accuracy for these systems, as presented by Papaioanou et al. [84] with results that are comparable to GCA for the LLE, while in most cases being able to present a better description of the VLE. Figure 1.2 presents the results for the VLLE of water + 1-pentanol and water + 1-hexanol using both SAFT-γ and the approach of Vijande et al. with PC-SAFT. For water + 1-pentanol the results for GCA from Soria et al. [85] are also presented. GCA is able to

provide a very good description of this system for both its VLE and LLE. The description with SAFT-γ is also satisfactory, but while keeping a good description of the LLE, a decrease in the quality of the VLE is observed.

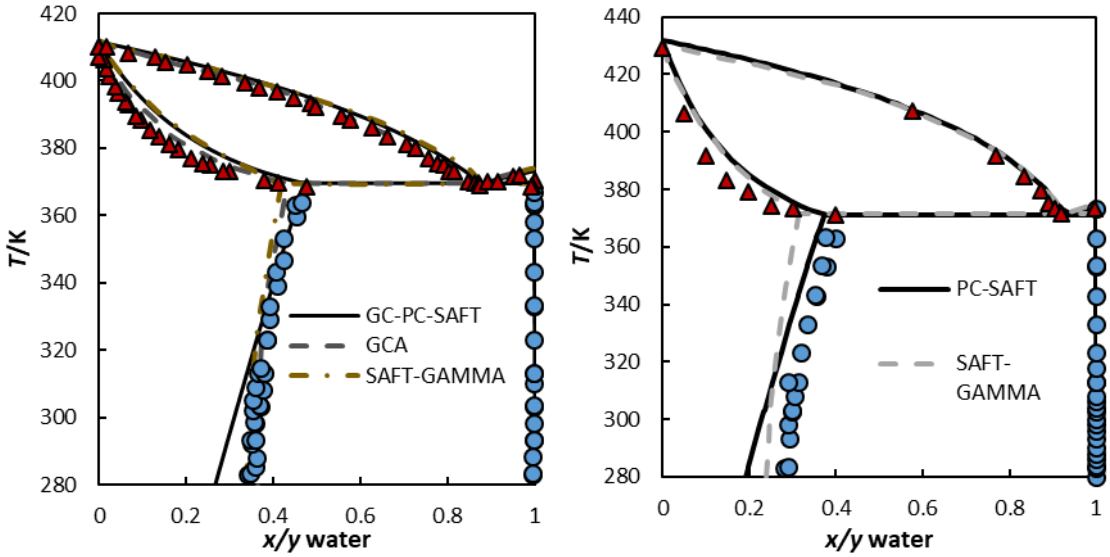

Figure 1.2 Results for the description of the systems water + 1-pentanol (left) and water + 1-hexanol (right) at 1 atm. Experimental data values are from Góral et al. [86], Cho et al. [87] and Tunik et al. [88]. The k_{ij} applied for GC-PC-SAFT was optimized in this work (k_{ij}=0.02 and 0.04 respectively).

A similar accuracy for the VLE of water with ethanol is reported with GC-PPC-SAFT [89] and SAFT-γ [90]. Similar results are also obtained using the approach of Vijande et al. with a single k_{ij} that was obtained in this work and are presented in figure 1.3, where these are compared with those of GC-PPC-SAFT using only a k_{ij} (the best sets from Pereira et al. [89] use two other binary interaction parameters). Both GC-PPC-SAFT and SAFT-γ tend to overestimate the pure saturation pressure when compared to these experimental data, while the calculations with GC-PC-SAFT present an underestimation of these values.

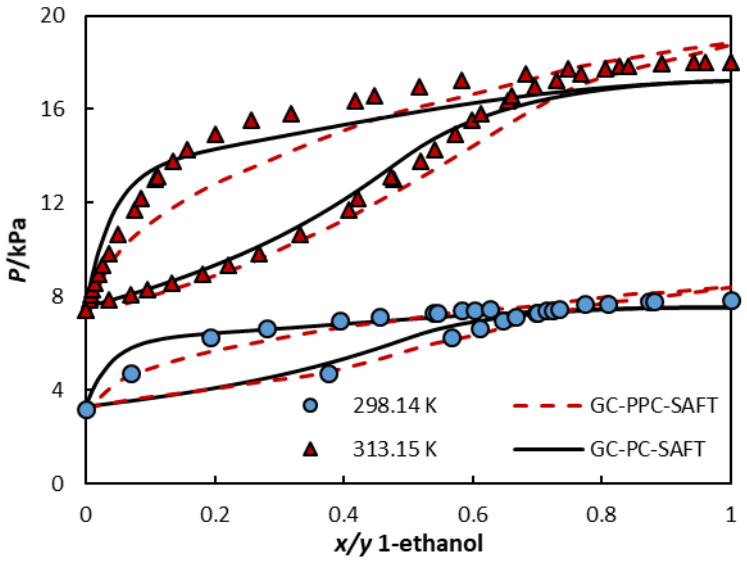

Figure 1.3 Results for the VLE description of water + ethanol with GC-PC-SAFT and GC-PPC-SAFT. Experimental data values are from Phutela et al. [91] and Vu et al. [92]. The k_{ij} applied for GC-PC-SAFT was optimized in this work (k_{ij}=-0.025).

Figure 1.4 compares the results of PC-SAFT and GC-PR-CPA for the description of the VLE of methanol with small alkanes. The results for CPA are in very good agreement with the literature data, while both SAFT models present higher deviations, especially when using the GC method from Vijande et al. However, GC-PPC-SAFT predicts a LLE immiscibility in both systems, which is not shown in the experimental data.

The results for systems containing phenol/anisole and other hydrocarbons were calculated with both GC-PPC-SAFT [93] and GCA [94]. These results are mostly equivalent, however, GCA is still able to outperform GC-PPC-SAFT in the description of most of these systems.

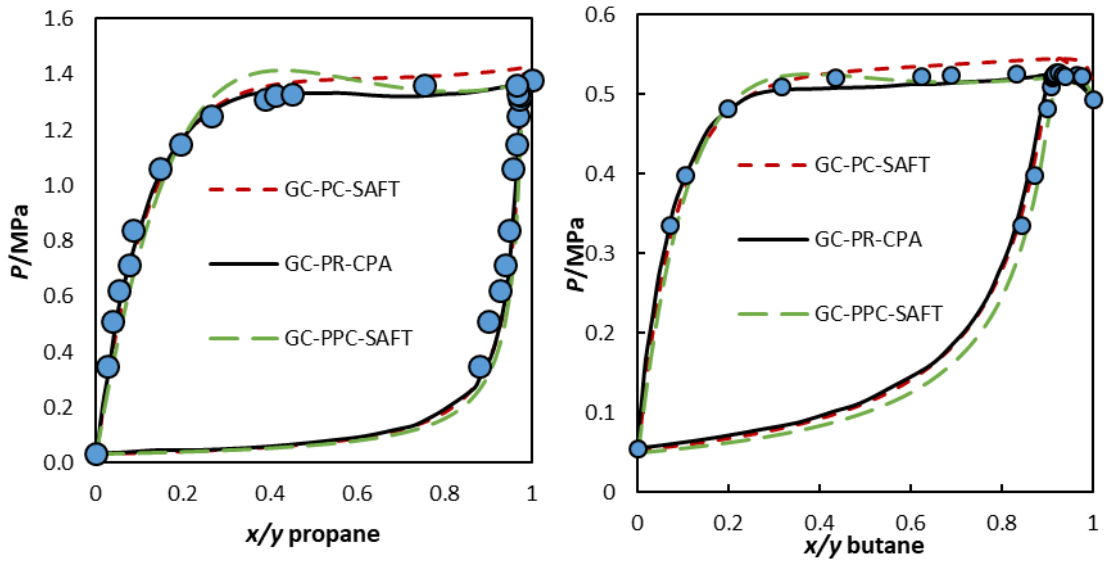

Figure 1.4 Results for the description of methanol + propane at 313 K [95] (left) and methanol + butane at 323 K [96] (right) with GC-PC-SAFT, GC-PPC-SAFT and GC-PR-CPA. The k_{ij}'s applied for GC-PC-SAFT and GC-PPC-SAFT were calculated in this work (GC-PC-SAFT kij=0.045 for both systems /GC-PPC-SAFT k_{ij}=0.030 and 0.014 respectively).

Both GC-sPC-SAFT [32,97] and GC-SAFT-VR [98] have been applied to the description of a large number of polymer containing systems. While both equations present interesting results it is of note that for most systems a binary interaction parameter obtained through non-predictive methods is needed for GC-sPC-SAFT, while for GC-SAFT-VR this is not observed. This is one of the main advantages of GC-SAFT-VR and SAFT-γ not only in this case, but also in the general case of systems for which there is a lack of experimental data. In the description of many systems, these versions present a more predictive behavior and do not require the use of binary interaction parameters. Nevertheless, this is not universal and there are diverse situations where these versions need binary interaction parameters. Examples of this are description of gas solubility. Lobanova et al. [99] with SAFT-γ-Mie, that reported the need to use this type of parameters to fit the data for mixtures in analysis, showing interesting results for these systems, while also exploring the capacities of these SAFT variants to link experimental data and molecular models. In the description of gas solubility in ionic liquids, Ashrafmansouri and Raeissi [100] also reported this need, while achieving an accurate description of the pure liquid density of these compounds and deviations below 5% in the pressures obtained for the binary systems.

The phase equilibria of CO_2/other gases with alkanes/water/alkanols have been one of the topics of interest for calculations using group contribution methods. Other studies with SAFT-γ, and variants include a study dedicated to fluids of relevance to the gas and oil industry [101].

In this work, the authors present some results for systems of methane/ethane/CO_2 + alkanes/water with deviations below 5%. Another example is the implementation of SAFT-γ in molecular design of CO_2 solvents [102], leading to the design/discovery of new solvents for these processes. With GC-SAFT-VR, Haley and McCabe [103] have studied the description of fatty acid methyl ester + CO_2 systems with very reasonable results.

Beside SAFT-γ and GC-SAFT-VR, GCA has also been used for the description of systems containing gases. One of the examples of the quality of these predictions is presented by Prieto et al. [83] where the phase equilibria of CO_2 with hydrocarbons with up to 36 carbons is predicted by GCA. The predictions for VLE are within 10% of AAD. While for the LLE the composition of hydrocarbon phases is predicted mostly within 10%, the CO_2 rich phase is far more challenging and the model usually presents deviations above 30%. In a similar effort, Huynh et al. [42,43], using GC-PPC-SAFT, have obtained results for the description of VLE containing CO_2/methane/ethane/H_2S/N_2 with a large range of hydrocarbons. The authors created a binary interaction correlation for the binary interaction parameters, thus eliminating the need to optimize every set of binary interaction parameters for these systems. Using this methodology, the authors reported deviations below 10% for most systems. Huyhn et al. [104] have conducted a similar study for the VLE of CO_2 with linear and branched *n*-alkanols, presenting similar results. Various results for other systems containing gases, mainly CO_2, with these methods were obtained in the literature. The tables in annex reference which works analyzed this type of data/results.

Some results have been reported for multifunctional compounds. Rozmus et al. [105] have studied the performance of GC-PPC-SAFT in the description of alkanolamines and alkanediols. For the latter the results for liquid density up to 1,6-hexanediol present deviations below 1%. The 3 heavier alkanols being studied present average deviations in pressure below 4%. However, it is important to note that it was necessary to change the association and chain contributions from the OH group for compounds with two of these groups. For an heavier alkanediol, 1,10-alkanediol, and alkanolamines the authors report deviations mostly above 8% for the saturation pressures.

Chremos et al. [90] presented results using SAFT-γ for systems of alkanolamines + water/CO_2. The results are accurate when a second-order group methodology [106] is introduced.

Most of these methods present advantages for specific applications. While SAFT-γ and GC-SAFT-VR are in many cases the most accurate models, the need of higher processing times in

many situations does not compensate for the increase in accuracy, especially in long processes with a large number of compounds. The remaining GC SAFT variants, while not as accurate for many systems, are not to be discarded, especially the GC-PPC-SAFT, which is able to describe very reasonably diverse polar systems. GCA and CPA being simpler equations present the advantage of lower processing times, while in some systems, like the solubility of hydrocarbons/alkanols in water, their results are equivalent to those of SAFT-γ.

SAFT-γ and its variants have the advantage that their new applications improve the link between coarse-grained models and experimental data.

Hendriks et al.[7] stated that the industry is looking for models capable not only of multicomponent and multiphase equilibria, but also able to describe a large range of properties, be it for the pure compounds or for mixtures. The derivative properties of pure compounds are one of these groups of properties of interest. However, with GC methods, not much has been presented in the literature, except for SAFT-γ.

Vijande et al.[36,49] have studied the description of the heat of vaporization at 298.15 K for a large number of alkanes, primary alcohols, methyl esters and primary amines, using PC-SAFT, with largely accurate results. The same authors have studied the dependency of H_{vap} with temperature for dodecane, 2-methyl-pentane, 2,2-dimethyl propane and ethyl propanoate with similarly accurate results. Pereira et al.[89] have presented results for the heat of vaporization using GC-PPC-SAFT for selected esters related to biodiesel systems and glycerol. The average deviations for these predictions are inferior to 5% in all compounds, while only for two ethyl esters (ethyl laureate and ethyl myristate) average deviations above 2.2% in the selected temperature range are observed.

Lubarsky et al. [107] have also analysed with GC-PPC-SAFT the description of speed of sound, *Cp*, isothermal compressibility, isobaric expansivity and adiabatic compressibilites, for some selected alkanols, ethers, esters and ketones. were obtained with this method were then compared with those of the non-GC CP-PC-SAFT. Between these models, GC-PC-SAFT has advantages in the description of vapour pressure and isobaric heat expansivity coefficients. However, for the compounds analysed, this model presents low accuracy for most of the other properties in analysis, including liquid density. With the same approach, Rozmus et al.[105] analysed the description of properties for alkanediols and alkanolamines. These multifunctional molecules present an important challenge to the model and start showing its

limitations by presenting difficulties in the description of the heat of vaporization of alkanediols.

Using the parameters from Vijande et al.[36,49] the isobaric heat capacity and speed of sound of some selected alkanes and alcohols were calculated in this work. For alkanes these are compared to those applying the group contribution of Tamouza et al. [29] when extended to PC-SAFT, as presented by Thi et al.[40].

The deviations for the *Cp* of alkanols are presented in Tables 1.3 and 1.4. The description of *Cp* for alkanols and speed of sound for 1-heptanol are presented in figure 1.5 and 1.6.

Table 1.3 Deviations for the analyzed properties of the first 10 primary alkanols, using the method of Vijande et al.[36,49]

		%AAD
Compound	*Trange* (K)	*Cp*
methanol	260-400	16.95
ethanol	260-400	4.01
1-propanol	260-400	6.83
1-butanol	260-410	6.57
1-pentanol	315-455	4.59
1-hexanol	275-455	5.61
1-heptanol	285-445	4.66
1-octanol	300-460	4.85
1-nonanol	300-470	5.31
1-decanol	330-490	4.58

With GC-SAFT-VR Silva et al.[108] have reported a good description for the heat of vaporization of four fluorinated alcohols at near room temperature. The same authors have estimated the thermal expansion coefficient at 298.15 K for these compounds, within the expected temperature trend.

Table 1.4 Deviations for the analyzed properties of five n-alkanes.

		%AAD Vijande et al.**[49]**			%AAD Tamouza et al.**[29,40]**		
Compound	*Trange* (K)	*P*	*ρliq*	*Cp*	*P*	*ρliq*	*Cp*
butane	200-410	2.93	1.73	1.40	1.64	1.31	0.58
pentane	260-410	2.33	1.80	1.69	0.15	1.94	1.47
hexane	260-450	1.62	2.15	0.63	0.74	2.09	0.50
Heptane	260-520	1.12	2.58	0.65	1.03	2.21	0.55
octane	260-520	2.11	2.89	0.65	2.25	2.26	0.65

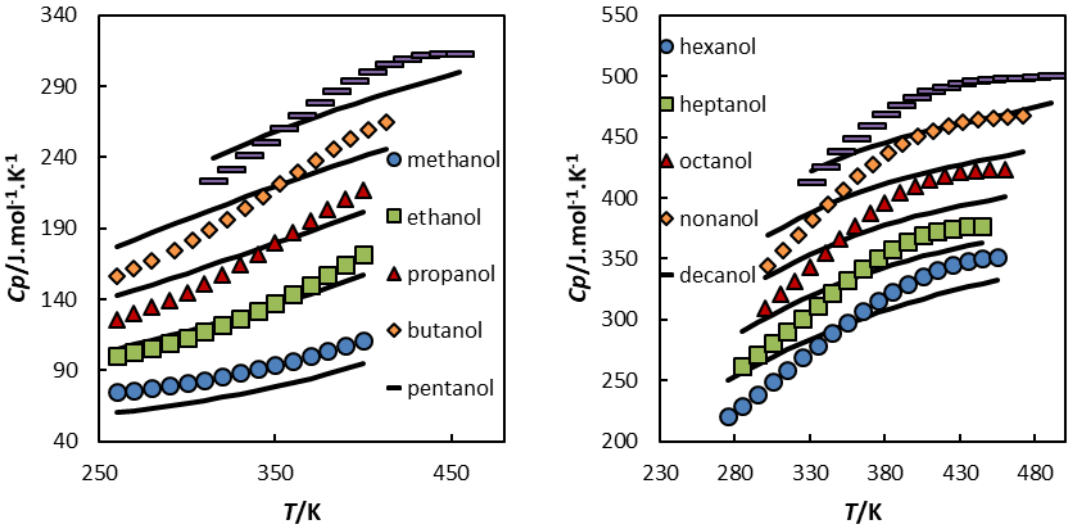

Figure 1.5 Results for the description of 1-alkanols *Cp*, using the method of Vijande et al.[36,49] The *Cp* data values were obtained from various sources[79,80,109–111].

Papaioanou et al.[54] showed the difference in prediction accuracy using different potentials (Mie or SW) with SAFT-γ. The Mie variant is shown to outperform the SW variant in this regard. The authors have presented average errors below 2% for the *Cp, Cv* and speed of sound of alkanes, with higher deviations for the isothermal compressibility k_T (<4%) and the thermal expansion coefficient α_V (<6%). For alkyl esters the deviations are higher, nevertheless, most of these properties are still described within 6% of deviation. Accurate predictions were also presented for the *Cv* of butane and heptane by Ghobadi et al.[60], using SAFT-γ WCA variant.

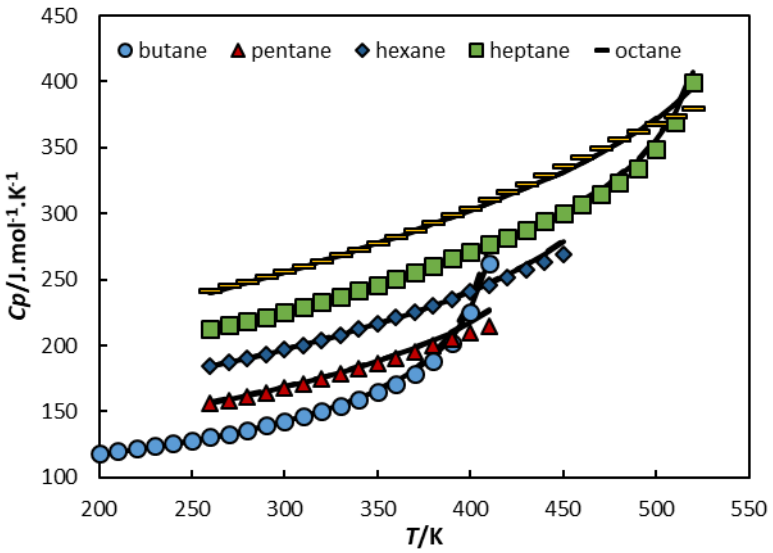

Figure 1.6 Results for the description of *n*-alkanes *Cp*, using both methods. The *Cp* data values were taken from Multiflash™ [78].

As discussed above, the results for derivative properties of alkanes were calculated using PC-SAFT and can be compared with those using the SAFT-γ variants in figures 1.7 to 1.9. The results present a similar behaviour using both base methodologies for PC-SAFT (Vijande et al. [36,49] and Tamouza et al. [29]) and thus in these figures only the results obtained using the method of Vijande et al.[36,49] are presented.

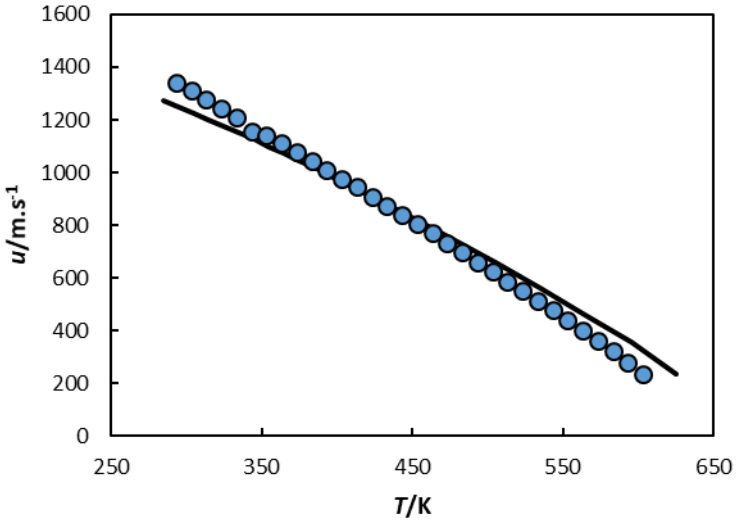

Figure 1.7 Results for the description of 1-heptanol speed of sound, using the method of Vijande et al.[36,49], data values are from the TRC database[80].

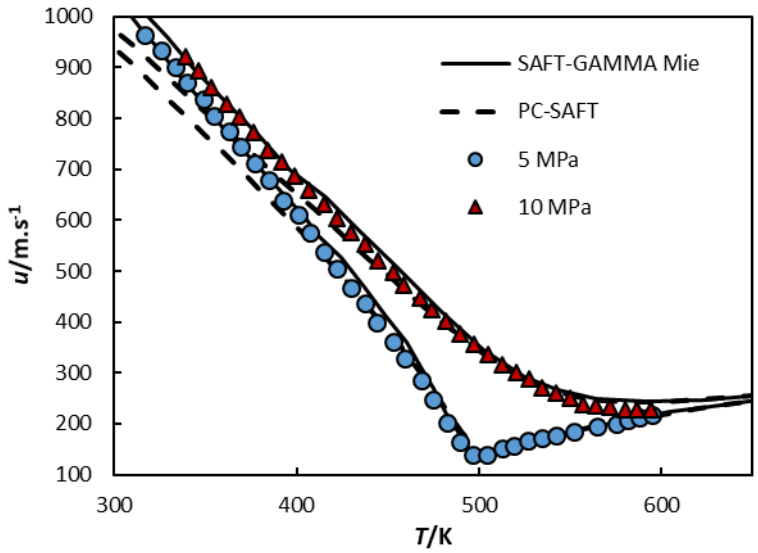

Figure 1.8 Speed of sound, of *n*-pentane using PC-SAFT (dashed lines) and SAFT-γ Mie (full lines), data values are from the REFPROP [112] database.

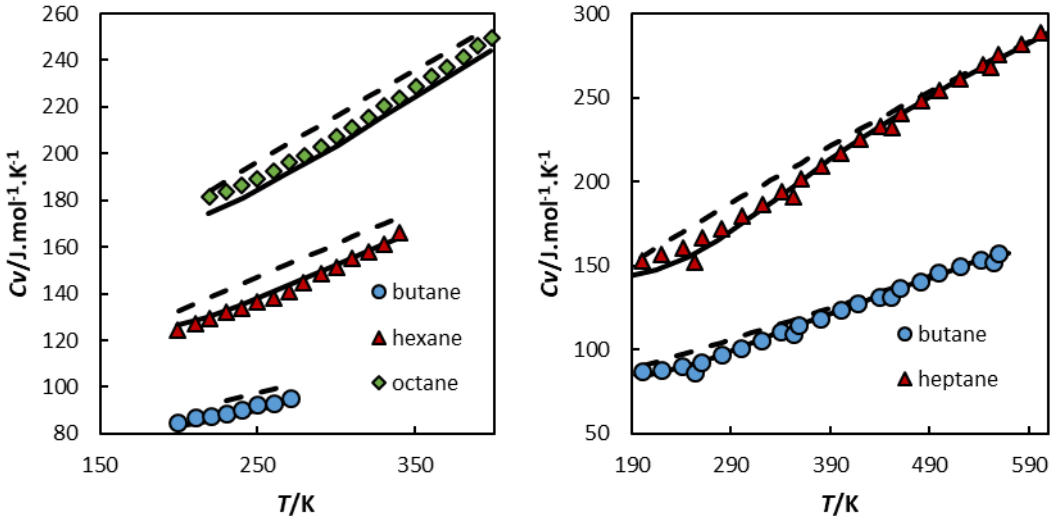

Figure 1.9 Results for the *Cv* of *n*-alkanes. Comparison between PC-SAFT (dashed lines) and SAFT-γ Mie (full lines) at 0.1 MPa (left). Comparison between PC-SAFT (dashed lines) and SAFT-γ WCA at 20 MPa (right).

SAFT-γ variants present consistently better results for the derivative properties. However, PC-SAFT is able to reasonably capture the temperature dependency of *Cv*. For the temperature dependency of the speed of sound, this version is able to describe the property at temperatures close to the critical point, but shows discrepancies at lower temperatures.

Dufal et al.[113] predicted the *Cp* for alkenes within a reasonable deviation. For carboxylic acids the same authors studied the description of the speed of sound, which is reasonably

predicted at higher temperatures, presenting, however, an incorrect tendency with temperature when compared with literature data.

For acetone, also with SAFT-γ Mie, but employing association sites that only interact with specific groups/compounds, Sadeqzadeh et al.[114] obtained an acceptable prediction of both the speed of sound and *Cp*. Using the same approach the authors predicted the heat of vaporization for carboxylic acids (from butanoic to octanoic acid), these predictions present some overestimation when compared to those of the literature, but their behaviour with temperature is correct for most of this family.

Avendaño et al.[115], studied the description of speed of sound, *Cp, Cv,* k_T, Joule-Thomson coefficient (μ_{JT}) and coefficient of thermal expansion (α_p) for carbon tetrafluoride (CF_4) and sulfur hexafluoride (SF_6), using SAFT- γ Mie. This approach presents very reasonable results in the near critical and supercritical region for all studied properties. On a similar study with CO_2, Avendaño et al.[116] found SAFT-γ Mie able to describe the same group of derivative properties in near critical and supercritical conditions, showing a correct description of the properties on these conditions. Papaioanou et al. [101] studied the *Cp* of CO_2 with SAFT-γ Mie achieving an accurate description for this property in the near critical and supercritical region.

Lobanova et al.[117] tested CG force fields associated with SAFT-γ to represent water. These methodologies improve the description of thermodynamic properties from CG models, but is unable to capture the description of most derivative properties.

1.3.4 Conclusions

In general, the group contribution methods are able to describe the analysed properties without a glaring reduction in accuracy from the original parameters.

Both SAFT, its variants and GCA have shown very promising results with group contribution methods. However, there is an increasing interest of the industry in models able to describe, simultaneously, thermophysical properties and multiphase equilibria and in the case of the former there is a severe lack of tests concerning properties other than density and pressure when using the GC methodologies combined with association equations of state.

CPA presents very interesting results. Nevertheless, despite its processing speed advantages, group contribution methods for this equation so far only contemplate binary interaction parameters. Thus this equation is still lagging behind on the predictive capacity methodologies

achieved nowadays with SAFT or GCA. It is also important to note that despite the group contribution methods applied for the pure components, in some cases SAFT approaches still need to fit, instead of predict through GC methods, binary interaction parameters, to obtain more accurate results for mixtures.

SAFT-γ and its variants opened the way for applications linked to the use of coarse grained models with the support of an EoS to create a bridge between the experimental data and these models. The characteristics of these methodologies also enabled their application to the calculations of interfacial properties.

The studies available for the calculation of derivative properties with these type of methods, include those using SAFT-γ Mie, for alkanes, alkyl acetates and CO_2 and with GC-PC-SAFT with some hydrocarbons. These predictions showed to be reasonably accurate.

Improvements on these predictive methods are expected to increase the number of industrial applications taking advantage of these models. However, the competition from cubic EoS and g^E models does not only come from their predictive capacities, but also from their simplicity, ease of implementation and processing times. In these last two aspects, CPA is a strong contender, nevertheless as discussed above, its group contribution methodologies are currently at a stage of development well behind those of other EoS. The powerful capacities of these equations have an important role in solving present and future problems, which the classical methods are unable to describe. However, it is not likely that the classical methods, especially the cubic EoS, will lose their position as the main thermodynamic property estimators in the industry. The use of these equations, despite their less accurate results, not relevant for many processes and application, since their processing speed and simplicity would be lost by introducing an advanced equation of state.

2 A modified CPA and first applications

2.1 Abstract

Although the CPA EoS was initially developed 20 years ago to meet industrial solicitations, namely the need to describe mixtures of hydrocarbons and water, including the formation and dissociation of hydrates, it has only recently received a widespread use in mid-stream and downstream oil and gas processing, or in the petrochemical and chemical industries. One of the reasons for such limited use of the model in the industry is the necessity to parameterize every associating component from saturation data. This involves access to pure component databases and some advanced knowledge in thermodynamics and numerical methods, which are often behind the scope of process design engineers.

This work revisits the CPA model, evaluating its strengths and weaknesses and attempting at identifying some opportunities for improvement. Using *n*-alkanols from C1 to C10 and their mixtures with other *n*-alkanols and *n*-alkanes, it investigates the description of the pure component critical points, saturated liquid densities as a function of temperature and some second-order derivative properties. It also explores new methodologies to regress the CPA parameters in a more systematic way, making it easier to generate parameters with less intervention from the user.

2.2 Introduction

Design and optimization of processes using multifunctional molecules is of great importance to the chemical, petrochemical, pharmaceutical, cosmetics, food and energy industries. There is a need for simple, yet accurate, models able to cope with the requirements of the industry. Before the mid of the 1990's there were few reliable equation of state based approaches for the description of mixtures including strongly polar and associative molecules in broad ranges of temperature and pressure. The development of excess Gibbs energy mixing rules for equations of state provided some opportunities for modelling mixtures with polar compounds, but at the expense of having to use more parameters and in some cases having to re-estimate them. A good review on the use of excess Gibbs energy models in equations of state has been reported by Kontogeorgis and Coutsikos [118].

Based on Wertheim's ideas on association [119–122] the Statistical Associating Fluid Theory (SAFT) [123,124] EoS was developed and on its trail the CPA [5] model appeared as an alternative to model associating mixtures while keeping all the advantages, simplicity, and well

known behaviour of cubic equations of state. The CPA can thus be seen as a special case of a cubic equation of state where associating components are involved. The CPA relevance as a simple, yet accurate, model for associative compounds has been growing since then, both in the academia and in the industry, although its use in the industry is still essentially limited to upstream oil and gas applications, where mixtures of water and hydrocarbons during production and the formation of hydrates in transportation are the most well-known applications of the model [8,125].

Although CPA would be the right option to replace cubic equations of state in process simulators, up to until recently, not many commercial simulators implemented the model. This model can be found for example, in the physical properties package Multiflash™ and in the SPECS software from CERE at the Technical University of Denmark. So its use in process simulation was until recently limited to what could be achieved by using the CAPE-OPEN interface with these two packages. Nowadays, CPA is a well-established model in the literature and has been expanded to other fields of applications, as is the case of biodiesel [6,126–128]. It is also gaining ground in the field of industrial simulators, being now available in the Petro-SIM™ and Hysys simulators, as well as in many in house simulators.

The *n*-alkanols are a well-studied family with CPA. Various studies have been reported on their mixtures with other alkanols [129,130], water [73,131], amines [132] and hydrocarbons [73,130,131,133–136], as well as on other relevant properties of the pure compounds such as surface tension using a combined EoS/gradient theory approach [70]. Villiers et al. [9] have also studied the description of derivative properties for both *n*-alkanes and *n*-alcohols. Other CPA applications include the description of glycols with water and hydrocarbons [137–141], mixtures with organic acids [142], description of fluorocarbons [143] and the extension to some multifunctional compounds, as alkanolamines [144] and phenolic compounds [71,72].

As for other association equations of state, the CPA model needs to be parameterized for every new associating component that has not previously been studied. The right balance between the attractive and repulsive terms in the equation of state can only be achieved if all parameters are regressed simultaneously from equilibrium data, usually from vapour pressure and saturated liquid densities. Although one can now find in the open literature sets of CPA parameters for the most common compounds, their number and variety is still quite limited. There is also not much reflexion on how to systematically parameterize molecules with multiple associating groups such as alkanolamines or oxygenated compounds relevant for biorefinery applications such as polyols, and phenolics, many of them solid at room

temperature or for which no saturation pressures and densities are available, or even measurable. These are some of the actual model drawbacks hampering its success and more widespread use in commercial simulators, since the common end user of a process simulator is understandably reluctant in regressing the CPA parameters for all new associating components present on his process.

One of the main objectives of this work is to generate accurate CPA parameters with little or no user intervention. Ideally this should be done using a small set of data already available from the simulator pure component database and fitting as few parameters as possible, so that the model parameters are transferable or predictive. For that purpose, it is necessary to understand the balance between the cubic and associative terms and evaluate all known weaknesses of the current CPA model.

This work started from the standard version of the CPA model [73] and investigated its known weaknesses: 1) not meeting the defined critical temperature, 2) missing the temperature dependence of pure component saturated liquid densities, 3) using an α function in the cubic term that can provide unreliable results for a few properties in some extreme conditions (as discussed by Le Guennec et al. [145]), and 4) having an incorrect description of the molar volume pressure dependence, which lead to a poor description second derivative properties. For this analysis the *n*-alkanols will be used as case study, as this family should also allow us to look into the associative parameters for the –OH group, trying to establish some "rules" or tendencies for their change with chain length.

The focus of this work will then be an evaluation of the advantages and disadvantages of a modified CPA model that will try to overcome the identified limitations of the model. The properties in study are the vapour pressure, liquid density, liquid isobaric heat capacity and heat of vaporization. It is important to note that a correct description of pure compound properties does not guarantee accurate results for mixture phase equilibria. So, the VLE of binary systems containing *n*-alkanols with alkanes or two *n*-alkanols will also be studied to insure that the new sets of parameters are transferrable for mixtures. LLE equilibria is also studied for mixtures of alcohols and alkanes.

2.3 The modified CPA model

To obtain the modified CPA here used, the starting point was the simplified CPA (s-CPA) as currently available from the literature.[73] CPA models account for physical interactions using

a term based on a cubic EoS. In the case of s-CPA this is the SRK EoS.[146] Using a single sum over sites, as proposed by Michelsen et al.[147], CPA can be written in terms of compressibility factor, as:

$$Z = Z^{phys} + Z^{assoc} = \frac{1}{1-B\rho} - \frac{A(T)\rho}{RT(1+B\rho)} - \frac{1}{2}\left(1 + \rho\frac{\delta lng}{\delta\rho}\right)\sum_i m_i(1 - X_i) \quad (2.1)$$

Where A represents the energy parameter ($A(T) = n^2\,a(T)$), B the covolume parameter ($B = nb$), ρ is the density, g is a simplified hard-sphere radial distribution function,[73] X_{A_i} is the mole fraction of component *i* not bonded at site A and m_i is the mole number of sites of type *i*. The mixing rules for *a* and *b* are presented in equations 2.2 and 2.3:

$$a = \sum_i \sum_j x_i x_j a_{ij} \quad (2.2)$$

$$b = \sum_i x_i b_i \quad (2.3)$$

where:

$$a_{ij} = \sqrt{a_i a_j}\left(1 - k_{ij}\right) \quad (2.4)$$

and k_{ij} are binary interaction parameters.

Presently, the alpha function used with the modified CPA is a modified Mathias-Copeman function[148], that can use up to 5 parameters:

$$a(T) = a_c(1 + STR \times c_1 + STR^2 \times c_2 + STR^3 \times c_3 + STR^4 \times c_4 + STR^5 \times c_5)^2 \quad (2.5)$$

where *STR* is $(1 - \sqrt{T_r})$ and C_1 to C_5 (C_x) are the alpha function parameters. The use of a high order polynomial introduces inconsistencies when extrapolating the results above the critical point. Thus, it is necessary to introduce a correction in the form of the following conditions:

$$\begin{cases} T < T_c \ \alpha = eq.1 \\ T = T_c \ \alpha = 0 \\ T_c < T \leq 1.05T_c \ \alpha = \frac{S_1 - MC_1}{2}\frac{T_r - 1.0}{0.05^2} + MC_1 \\ 1.05 < T_r \leq 1.10 \ \ \alpha = \frac{MC_1 - S_1}{2}\frac{T_r - 1.1}{0.05^2} + S_1 \\ T_r > 1.1 \ \alpha = \alpha_{API} = 1 + S_1\left(1 - \sqrt{T_r}\right) \end{cases} \quad (2.6)$$

where alpha API is the soave type alpha function proposed by Graboski and Daubert.[149], MC_1 is the same parameter as c_1 from equation 2.5 and AK_2 is the parameter from the API alpha function.

Equation 2.7 introduces the calculation of X_i.

$$X_i = \frac{1}{1 + g\rho \sum_j m_j X_j \Delta^{ij}} \quad (2.7)$$

with the association strength (Δ^{ij}) given by:

$$\Delta^{ij} = gb^{ij}\beta^{ij}\left(e^{\frac{\varepsilon^{ij}}{RT}} - 1\right) \quad (2.8)$$

where ε^{ij} and β^{ij} are the association energy and volume for interactions between sites *i* and *j*.

The s-CPA uses a simplified radial distribution function, which is given by equation 2.9.[73,150]

$$g(\rho) = \frac{1}{1 - 0.475b\rho} \quad (2.9)$$

The difference of this new version of CPA lies in the restrictions used in the pure component parameterisation process. This version forces a_c and *b* to obey the critical temperature and critical pressure. In this way, part of the parameters have a direct relation to the critical point, enhancing the predictive capacity of the model.

$$P_{CPA}\left(Tc^{exp}, Vc^{calc}\right) = Pc^{exp} \quad (2.10)$$

$$\left(\frac{\partial P}{\partial v}\right)_T \Big|_{\substack{T=T_c \\ v=v_{calc}}} = 0 \quad (2.11)$$

$$\left(\frac{\partial^2 P}{\partial v^2}\right)_T \Big|_{\substack{T=T_c \\ v=v_{calc}}} = 0 \tag{2.12}$$

The objective function used in the parameterisation is also different from s-CPA. The molar volume is not optimized directly being instead obtained through a Peneloux type volume shift:[151]

$$v_t = v_0 - c_{vs} \tag{2.13}$$

where c_{vs} is the volume shift. Using this type of volume-shift does not affect the calculations of vapour pressure, heat of vaporization and heat capacities as is discussed by Jaubert et al.[152]

Also relevant to this process is the separation of the optimization of associative and cubic terms. Given a starting point for the associative parameters, the cubic term is generated, with the alpha function being parameterized directly to the vapour pressure curve. The whole group of parameters can be then optimized by adjusting the associative parameters, as the cubic term is automatically generated from the critical data and vapour pressure curve.

The following equations were considered to optimize the values of k_{ij}.

$$OF = \sum_i^{np} \left(\frac{T_{bub}^{exp.} - T_{bub}^{calc.}}{T_{bub}^{exp.}}\right)^2 \tag{2.14}$$

$$OF = \sum_i^{np} \left(\frac{P_{bub}^{exp.} - P_{bub}^{calc.}}{P_{bub}^{exp.}}\right)^2 \tag{2.15}$$

$$OF = \sum_k^{npo} \sum_i^{np} \left(\frac{x_{i,k}^{exp.} - x_{i,k}^{calc.}}{x_{i,k}^{exp.}}\right)^2 \tag{2.16}$$

where *npo* is the number of phases to optimize.

When two or more associative compounds are present in a mixture, CPA needs combining rules for the cross-associative parameters. CR-2[130] was here applied, as proposed by Kontogeorgis et al.:[129]

$$\beta^{ij} = \sqrt{\beta^i \beta^j} \tag{2.17}$$

$$\varepsilon^{ij} = \frac{(\varepsilon^i + \varepsilon^j)}{2} \tag{2.18}$$

Contrary to what is usually done with CPA, in this work association schemes are linked to each group and not to each molecule. In this way, considering the 2B[123] scheme for the hydroxyl group, diols will have a 2x2B association scheme. This is not much relevant when considering compounds with similar associative groups, as is the case in 1,ω-alkanediols, but for more complex molecules with varying types of groups, and or, affected by steric hindrance, this will enable implementing group dependent parameters, which are expected to improve the predictive capacities of CPA.

Kontogeorgis et al.[153], have compared the schemes for the hydroxyl group, fitting binary phase equilibria with both the 2B and the more accurate (and complex) 3B[123] scheme. Their results show that the 3B scheme does not improve the results when comparing to the 2B scheme. Each of these schemes holds advantages in the description of specific properties as discussed by de Villiers et al.[9].

In the case of water the selected scheme was 4C. This scheme is considered better than the 3B scheme for application on equations of state and is also suggested as the preferential scheme by a group of molecular simulation results. [153]

These association schemes are presented in table 2.1

Table 2.1 Association schemes used and referenced in this work.

Association Scheme Designation	Example
2B	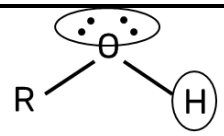
3B	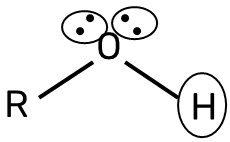
4C	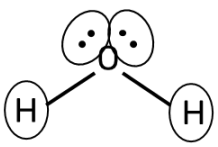

Further specifics on how this modified version was obtained is presented in the next subsection.

2.4 First applications results

2.4.1 Adjusting the critical point

The use of CPA usually involves the regression of cubic and associative parameters to saturated liquid density and vapour pressure data away from the critical point. Due to this procedure, both the critical temperature and critical pressure tend to be overestimated. This can be observed for methanol in Figure 2.1, calculated using the parameters from Oliveira et al [70].

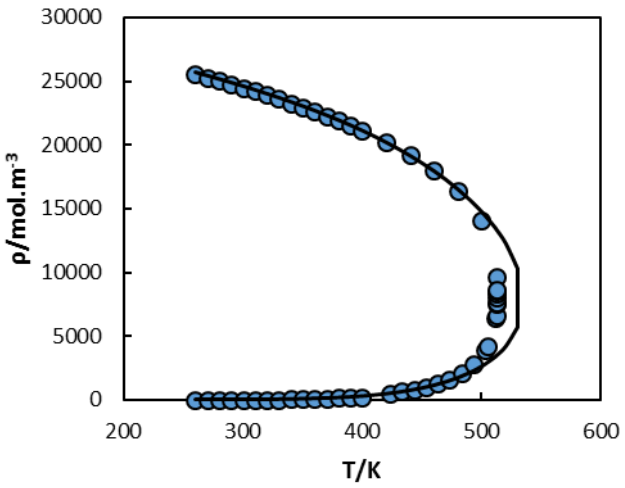

Figure 2.1 methanol saturated densities with s-CPA.

This creates an inconsistency in the model, where the critical temperature set to be used in the calculation of the *a* parameter is not obeyed by the model. It was then investigated how the CPA model and the parameters regression could be improved, to eliminate this inconsistency.

As stated in the model section, it was opted to introduce modifications into an s-CPA model to force both a_c and *b* to obey the critical temperature and pressure conditions. This is expected to enhance the predictive capacity of the model, as part of the parameters are now anchored to the critical point. An analysis, and subsequent modifications, with similar objectives was

proposed by Polishuk for SAFT + cubic [154] and PC-SAFT [155]. With CPA, Vinhal et al. [156] have presented a work with a similar objective, but a different approach.

This approach was first tested on the methanol data. To obtain the first estimates for the association term it was taken into account the relations presented by Kontogeorgis et al. [8] where the association parameters are related to the enthalpies and entropies of hydrogen bonding:

$$\varepsilon \propto -\Delta H \tag{2.19}$$

$$\beta \propto e^{\frac{\Delta S}{R}} \tag{2.20}$$

The same authors shown similarities between the results of the CPA associative parameters and the association contribution to the heat of vaporization (H_a). Based on this idea two sets were tested, the first used the value of $|H_a|$ presented by Nath et al. [157] as the energy parameter, while for β we used a value close to that proposed by Kontogeorgis et al. [73] The second set, used a similar approach for ε, but instead recalculated H_a with data from the DIPPR database [79] while for β the value obtained was $RT_{boil}e^{\frac{\Delta S^v}{R}}$. After adjusting the a_c and b values, the Soave alpha function was adjusted to vapour pressure data. The parameters and deviations for the vapour pressure and of liquid densities are presented in Table 2.2. As can be observed from Table 2.2 and Figure 2.2, while set 1 provides better estimates of vapour pressures, liquid densities and liquid heat capacities for methanol, the results are much worse than those obtained using the best parameter set from the literature [70].

Table 2.2 Parameters and %AAD between 0.5-0.78 T_r, for the first tests with methanol.

Set	a_c (Pa.m^6.mol^{-2})	b (10^5.m^3.mol^{-1})	c_1	β.10^2	ε (J.mol^{-1})	% AAD P^{sat}	ρ_{liq}
1	0.59	4.34	0.780	1.46	21866	4.63	25.7
2	0.77	4.78	0.847	1.03	19816	8.40	33.3
Oliveira et al. [70]	0.43	3.22	0.747	3.41	20859	0.45	0.34

The first estimates were the results of simple assumptions and, as expected, present large deviations. Using theoretical estimates for the association parameters and with values of a_c and b being fitted to the critical point, the only parameter left to be optimized is c_1. However, there are other interesting remarks before further improvements. Results for other properties present qualitatively correct descriptions despite the deviations, as shown in Figure 2.2 for the isobaric liquid heat capacity. A possible way to improve these results is to replace the simple Soave-type alpha function with a 3-parameter Mathias-Copeman function. Indeed, if the

Mathias-Copeman function is used instead of the Soave function, by fitting only the vapour pressure data, the results become quite accurate for vapour pressure, heat of vaporization and liquid *Cp*, as reported in Table 2.3.

Still, the estimates of liquid densities are not yet as accurate as required. The use of a temperature independent volume shift in cubic equations of state, as well as a linear combining rule have been studied by Jaubert and co-workers [152,158]. It was shown, that with this approach it is possible to improve the description of the liquid volume without decreasing the accuracy of phase equilibria and without affecting most other properties, such as *Cp* or heat of vaporization.

In this manner, to improve the volume description, a Peneloux type volume shift [151] was introduced in CPA. This volume shift is constant and is obtained by matching the liquid density at a reduced temperature of 0.7 *Tc*. The results are shown in Table 2.3 for the first set of associative parameters. The description of liquid density obtained, Figure 2.3, is less accurate than what was observed with the parameters by Oliveira et al. [70] This is probably due to the higher value of the co-volume parameter, which will affect the general behaviour of the density curve, despite the volume shift. The results for vapour pressure are improved. Without adjusting the range of temperatures between 400 K and the critical point, the present value of %AAD for vapour pressure is below 0.8%. The results for liquid *Cp*, Figure 2.2, and heat of vaporization present similar accuracy to those from the literature. It should be noted that these are preliminary results, using an approximate approach for the associative parameters. The capacities of this approach to improve the presented derivative properties will be further explored below in the next sub-section.

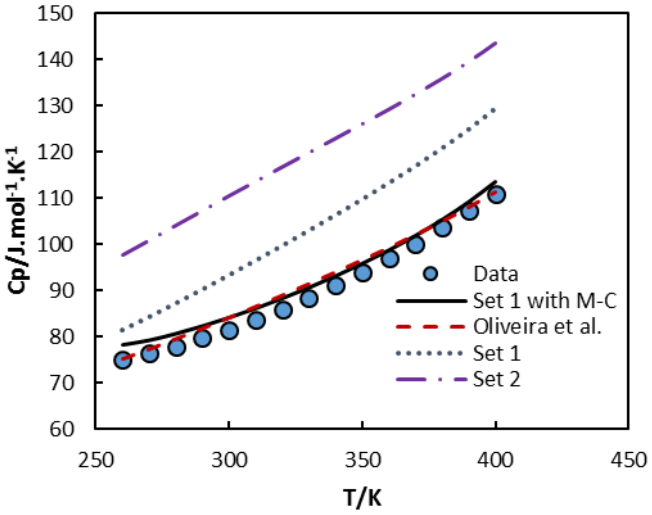

Figure 2.2 Results for the liquid *Cp* of methanol using sets 1 using both alpha functions, [146,148] set 2 and the results from Oliveira et al. [70]

Table 2.3 Mathias-Copeman parameters using the first set of associative parameters (Table 2.2), with a constant volume shift, and respective %AAD between 0.5-0.78 T_r.

					%AAD			
Set	*c1*	*c2*	*c3*	*Vshift*/dm^3.mol^{-1}	P^{sat}	*Cp*	ΔH^{vap}	ρ_{liq}
Set 1 using the M-C alfa function	1.05	-1.61	2.01	0.0226	0.30	2.56	1.12	2.26

Given the results with the Mathias-Copeman alpha function it was interesting to investigate if the description of liquid density near the critical point could still be improved. For that purpose a more flexible alpha function, based on the Mathias-Copeman function [148] but with up to 5 parameters was used (equation 2.5).

It was found that by increasing the values for the associative strength (Δ) the value of the co-volume will be reduced. With this approach it was possible to greatly improve the liquid density results in both methanol and ethanol. However, for these smaller compounds, there is an important degradation of the description of the vapour phase density at higher temperatures, as well as of the *Cp* (with average absolute deviations larger than 13% between 260 and 400 K) and the heat of vaporization (with an average absolute deviation close to 30% in the same temperature range). Vapour pressure accuracy is slightly decreased for the analysed compounds, especially in the case of butanol. Figure 2.3 presents the results for the saturated densities of methanol. The results for all the alcohols analysed are presented in Table 2.4. The experimental critical point data of the first ten *n*-alkanols is presented in Table 2.5.

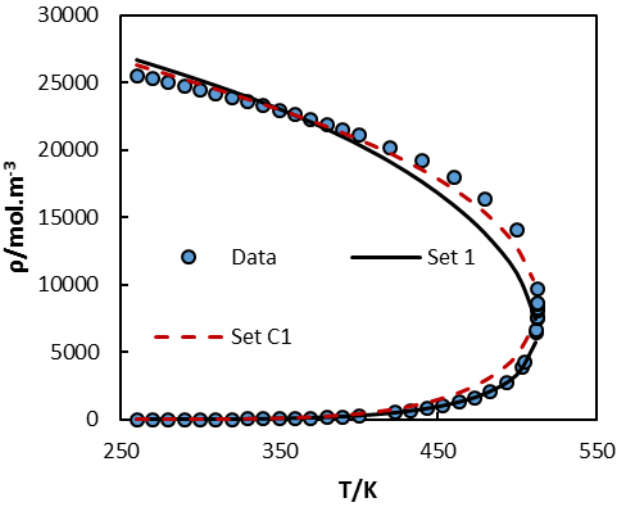

Figure 2.3 Density results for methanol with a 3 parameter Mathias-Copeman function [148] (set 1, Table 2.3) and with a 5-parameter alpha function after optimization of the association parameters (Table 2.4).

For heavier alcohols, from heptanol to nonanol, it is possible to compromise and decrease only slightly the accuracy of the density description while also predicting the results for *Cp*. The description of heat of vaporization is also improved, presenting a %AAD of 3.06% between 285 and 445 K in the case of 1-heptanol.

Results for the liquid densities from ethanol to 1-nonanol are presented in Figure 2.4. Figure 2.5 presents results for *Cp* for the studied compounds. For 1-heptanol it was possible to achieve a better compromise between liquid density and second derivative properties than for the other alcohols. This has to do with using higher values for the association parameters, which increases the accuracy of the density description near the critical point, but if not high enough, tend to decrease the accuracy for the temperatures below 0.7 *Tc*, as is presented in Figure 2.6. The fact that a higher association strength works well for 1-heptanol but less so for higher alkanols might be explained by the change in liquid density curvature above 1-heptanol. As can be seen in Figure 2.6, using the 1-heptanol association parameters for 1-octanol and 1-nonanol, the curvatures obtained are far more accentuated, this is also more severe for 1-nonanol than for 1-octanol.

This kind of compromise was not achieved for 1-propanol up to 1-pentanol, and the results present similarities to those of methanol and ethanol. In a first approach, the values of the association energy parameter were set as constant to test the predictive capacities of the model. Nevertheless, despite the high variability of the β parameter, no relevant improvements were observed by varying the two parameters simultaneously.

Table 2.4 Parameters and results for the alcohol optimization (set C-1).

alcohol carbon N°	1	2	3	4	5	7	8	9
a_c (Pa.m^6.mol^{-2})	0.20	0.27	0.35	0.52	0.90	2.31	4.35	5.14
b (10^5.m^3.mol^{-1})	2.29	3.08	3.80	5.17	7.59	13.90	17.60	19.66
c_1	0.35	0.72	0.32	0.45	0.98	0.89	1.64	1.56
c_2	-0.04	-3.38	2.05	1.44	-6.91	-4.29	-8.95	-5.77
c_3	1.85	23.48	2.12	3.78	49.21	36.54	42.40	23.87
c_4	0.00	-39.98	0.00	0	-93.35	-79.95	-83.21	-40.93
c_5	0.00	21.75	0.00	0	53.49	56.82	60.25	24.97
β.10^2	3.76	3.63	4.85	4.94	5.04	1.56	0.15	0.11
ε (J.mol^{-1})	26913	26913	26913	26913	26913	26913	26913	26913
Vshift/ dm^3.mol^{-1}	-0.007	-0.015	-0.023	-0.024	-0.024	0.019	0.037	0.043
%AAD ρ_{liq}	2.90	2.02	2.10	2.74	3.72	2.90	3.42	4.81
%AAD P^{sat}	2.96	2.85	1.39	3.49	0.11	0.03	0.57	0.74
T *range* (K)	260-512.64	260-513.92	260-536.78	280-563.10	310-588.1	320-632.30	330-652.30	330-670.90
Tc calc. (K)	512.6	513.9	536.8	563.1	588.1	632.3	652.3	670.9
Pc calc. (MPa)	8.09	6.13	5.17	4.42	3.90	3.09	2.78	2.53
%Dev. *Vc calc.*	-3.31	-4.28	-7.23	-3.027	-2.42	14.07	18.86	16.76

Table 2.5 Literature critical points for the first 10 *n*-alkanols [78,79].

alcohol carbon N°	1	2	3	4	5	6	7	8	9	10
$Tc^{exp.}$ (K)	512.6	513.9	536.8	563.1	588.1	610.3	632.3	652.3	670.9	688.0
$Pc^{exp.}$ (MPa)	8.09	6.14	5.17	4.42	3.90	3.42	3.09	2.78	2.53	2.31
$Vc^{exp.}$ (dm^3.mol^{-1})	0.118	0.167	0.219	0.275	0.326	0.387	0.444	0.509	0.576	0.645

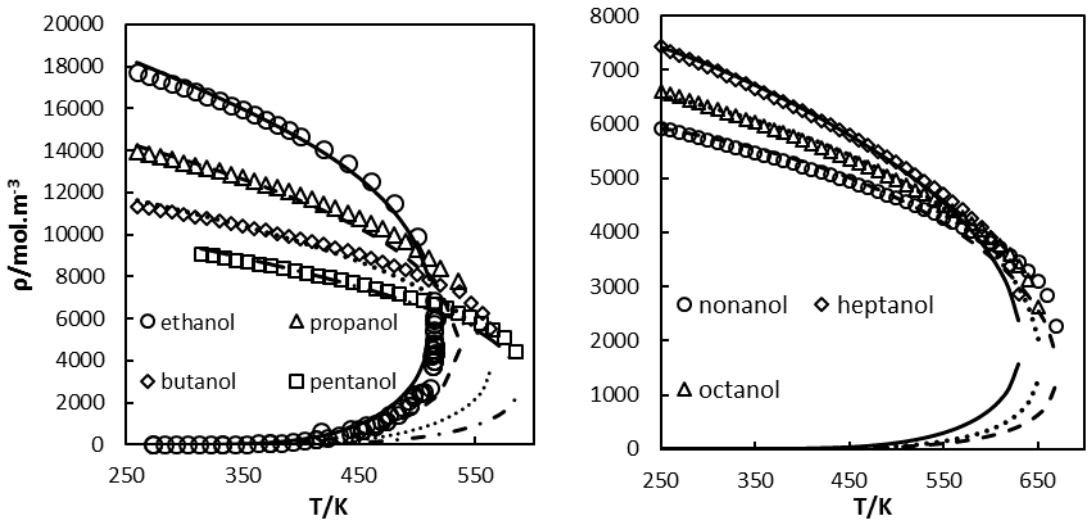

Figure 2.4 Liquid density results from ethanol to 1-pentanol (left) and from 1-heptanol to 1-nonanol (right), with a 5-parameter alpha function and optimized association parameters.

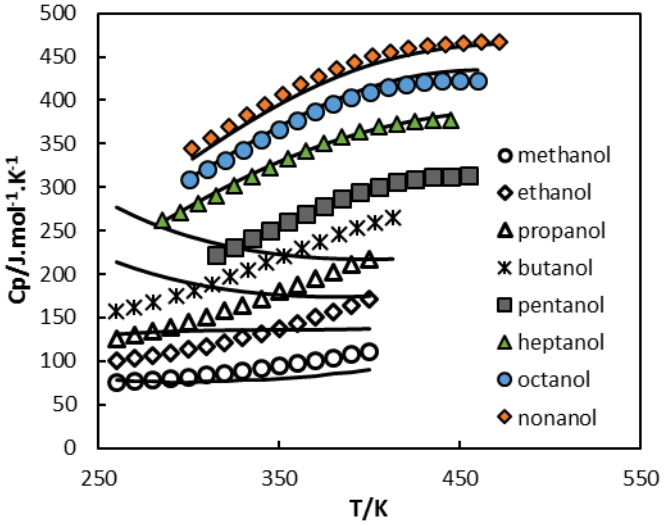

Figure 2.5 *Cp* results for the studied compounds with optimized association parameters (results are from the sets of Table 2.4).

The values obtained for the critical volume present an average deviation below 5% for methanol, ethanol, 1-butanol and 1-pentanol. For 1-propanol and the heavier alcohols these deviations are higher, with a value of 18.86% for 1-octanol being the highest deviation. It is important to note that from 1-heptanol to 1-nonanol a compromise between the description of liquid density and of the derivative properties was tested, and thus, the critical volume is expected to be less well estimated. For these compounds, if volumes at 0.9 *Tc* are considered only for 1-nonanol an error above 5% is observed.

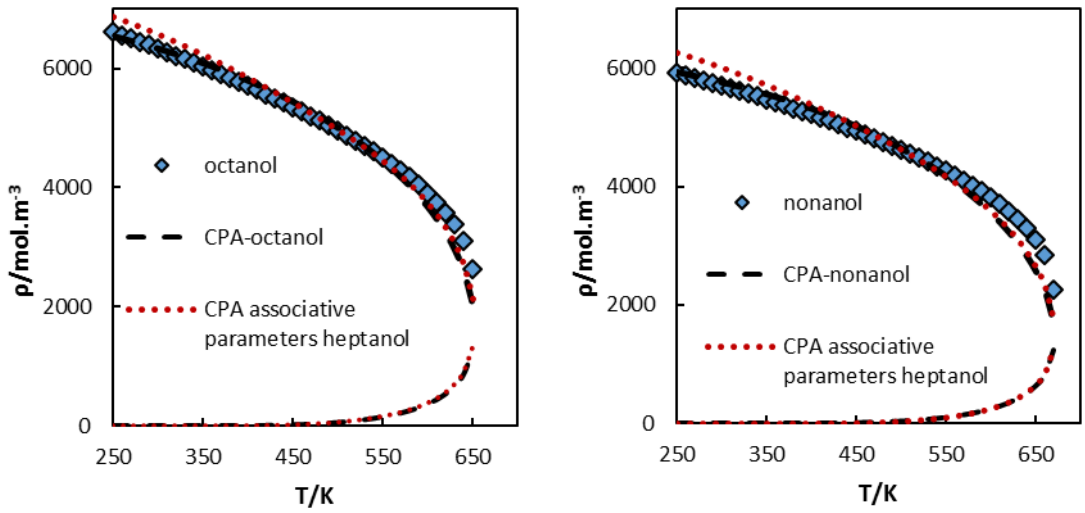

Figure 2.6 Comparison between the liquid density results for 1-octanol and 1-nonanol, using the cubic term parameters presented in Table 2.4 (left) and using 1-heptanol associative parameters (right).

The description of *Cp* presents an inaccurate behaviour for some of the lighter alkanols. This can be linked to the higher values of the associative volume, but also to some extent to the

alpha function, which, being highly flexible, if not restricted may provide some incorrect behaviour for derivative properties. In this case, the most relevant contribution should be the former. The temperature range used in the vapour pressure optimization was larger than the presented range in Figure 2.5, which should decrease the influence of the alpha function flexibility.

This analysis shows that by fitting the critical point, it is possible to obtain a correct description of liquid density on a larger range of temperatures with CPA, without using a cross-over method [15,16] or an approach based on the renormalization group theory [12,13]. However, by using this approach, the accuracy of the results for the vapour phase is decreased. This analysis will be continued when discussing results for binary mixtures.

The final parameter set obtained in this section will be hereafter referred as Critical-1 (*C1*).

2.4.2 Improving derivative properties

After the analysis of the performance of a modified CPA model to reproduce the liquid density curve while providing an accurate description of the critical point, it is important to look into its predictive behaviour. In this study we will be looking simultaneously at the liquid density, heat of vaporization, liquid *Cp* and vapour pressure from methanol to 1-decanol. As before, the values for the association energy parameter were considered constant and only the volume parameter was optimized. The alpha function used in this analysis is the modified Mathias-Copeman function with up to 5 parameters (equation 2.5).

These results are compared with those for the simplified CPA, without any modifications, after an optimization considering vapour pressure, liquid density and heat capacity with the weights for each property being 1, 1 and 0.1 respectively. This re-parameterization is required to compare the two versions of the model, with both optimized against the same datasets.

For the n-alcohols between propanol and 1-decanol it was observed that the modified version could describe the target properties using a constant value for the association volume, while keeping the constant value for the association energy. A similar approach was tested in s-CPA, however, the results presented much higher deviations and were thus not considered. Tables 2.6 and 2.7 present the parameters obtained for CPA before and after modifications, respectively, and the deviations obtained for each set.

Table 2.6 Parameter sets and results for the optimization of the s-CPA version (with no modifications)

alcohol carbon N°	1	2	3	4	5	6	7	8	9	10
a_c (Pa.m^6.mol^{-2})	0.42	0.78	1.15	1.68	2.31	2.83	3.46	4.09	4.66	5.46
b (10^5.m^3.mol^{-1})	3.21	4.8	6.38	8.03	9.73	11.3	12.98	14.69	16.34	18.12
c_1	0.72	0.62	0.88	0.85	0.81	0.93	0.88	0.97	1.06	1.07
β.10^2	3.3	0.6	0.77	0.34	0.15	0.14	0.06	0.05	0.04	0.02
ε (J.mol^{-1})	21294	24335	21913	23162	24582	23848	27151	27413	27532	28415
%AAD P^{sat}	0.28	0.46	0.62	0.36	0.27	0.54	0.88	0.33	0.95	0.77
%AAD $\rho_{liq.}$	0.18	0.43	0.43	0.59	0.59	0.81	1.16	1.22	0.94	1.25
%AAD $Cp_{liq.}$	1.13	2.00	5.31	3.95	2.93	3.31	0.66	1.22	1.81	1.03
%AAD H^{vap}	0.69	1.15	0.35	1.29	0.81	0.27	1.68	0.28	1.75	0.58
%AAD $Cp_{res.}$	2.38	4.37	12.6	9.46	7.04	8.65	1.79	3.36	5.18	3.03
T_{range} (K)	260-400	260-400	260-400	260-410	315-455	275-455	285-445	300-460	300-470	330-490
$Tc^{calc.}$ (K)	529.47	532.02	550.83	576.50	605.65	626.70	653.00	672.10	697.05	711.95
$Pc^{calc.}$ (MPa)	9.75	7.83	6.53	5.47	4.61	4.11	3.66	3.30	3.05	2.80
%Dev. *Vc calc.*	-16.80	-14.56	1.03	3.12	-3.03	5.76	-3.83	-4.85	-6.64	-8.57

Although the values for the energy and co-volume parameters from the cubic term are being directly calculated from the critical point, it is still important to look at their tendencies, as they are affected by the parameters from the associative term. In Figure 2.7 it is possible to compare these tendencies before and after the modifications to CPA.

Table 2.7 Parameter sets for the optimization of the modified CPA (set C2).

alcohol carbon N°	1	2	3	4	5	6	7	8	9	10
a_c (Pa.m^6.mol^{-2})	0.68	1.13	1.60	2.07	2.58	3.18	3.78	4.48	5.21	6.01
b (10^5.m^3.mol^{-1})	4.61	6.40	7.75	9.45	11.14	13.13	15.01	17.17	19.37	21.75
c_1	0.90	1.04	1.12	1.13	1.31	1.49	1.06	1.63	1.59	1.69
c_2	-2.47	-1.46	-0.89	-1.38	-3.72	-5.73	0.66	-6.76	-4.88	-6.10
c_3	3.26	-0.79	1.49	8.04	20.54	29.81	-0.76	35.77	22.93	30.13
c_4	0	3.76	-13.85	-31.50	-56.54	-70.72	-4.99	-81.78	-46.11	-63.28
c_5	0	0	22.67	37.84	55.71	60.07	7.32	67.68	32.33	48.54
β.10^2	0.46	0.16	0.06	0.06	0.06	0.06	0.06	0.06	0.06	0.06
ε (J.mol^{-1})	24913	24913	24913	24913	24913	24913	24913	24913	24913	24913
%AAD P^{sat}	0.34	0.32	0.12	0.27	0.44	0.21	0.26	0.05	0.79	0.27
%AAD $\rho_{liq.}$	1.94	0.93	0.48	0.64	0.59	0.68	0.47	0.39	0.69	0.34
%AAD $Cp_{liq.}$	0.91	2.20	2.25	1.38	1.37	1.77	1.25	1.14	1.57	0.83
%AAD H^{vap}	1.57	0.50	0.71	1.40	0.42	0.85	1.89	0.48	1.91	0.77
%AAD $Cp_{res.}$	1.79	4.93	5.52	3.50	3.32	4.60	3.36	3.18	4.43	2.77
T_{range} (K)	260-400	260-400	260-400	260-410	315-455	275-455	285-445	300-460	300-470	330-490
Vshift (dm^3.kmol^{-1})	18.6	19.1	15.5	17.1	17.5	21.7	23.7	29.0	37.2	42.2
$Tc^{calc.}$ (K)	512.6	513.9	536.8	563.1	588.1	610.3	632.3	652.3	670.9	688.1
$Pc^{calc.}$ (MPa)	8.09	6.14	5.17	4.42	3.90	3.42	3.09	2.78	2.53	2.31
%Dev. *Vc calc.*	29.81	27.99	24.42	22.18	22.75	21.84	22.13	21.40	21.01	21.22

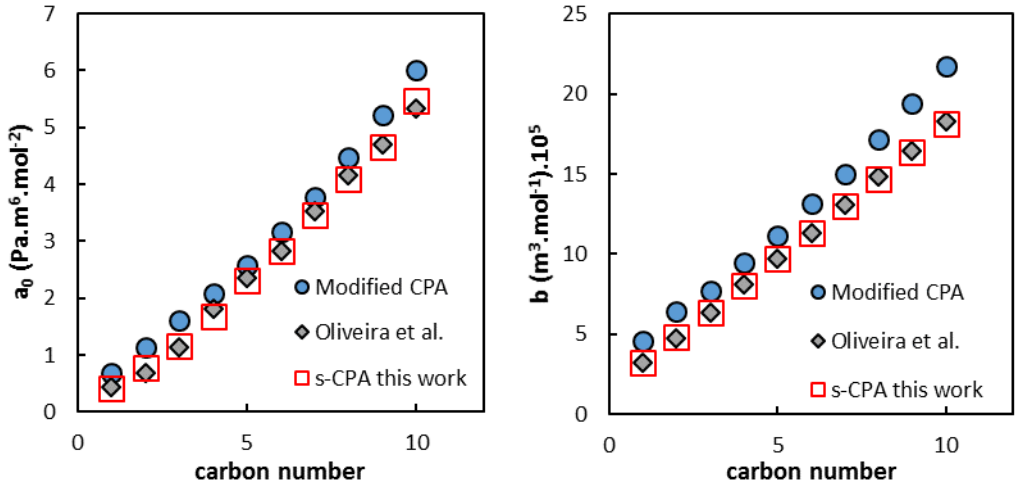

Figure 2.7 tendencies of the energy (left) and co-volume parameters (right) of the cubic term for primary alkanols, respectively (parameters from Tables 2.6 and 2.7 and Oliveira et al. [70]).

It is also important to look at the tendencies for the volume shift, to verify if these still follow a seemingly quadratic trend with the carbon number of the *n*-alcohols. This is shown in Figure 2.8.

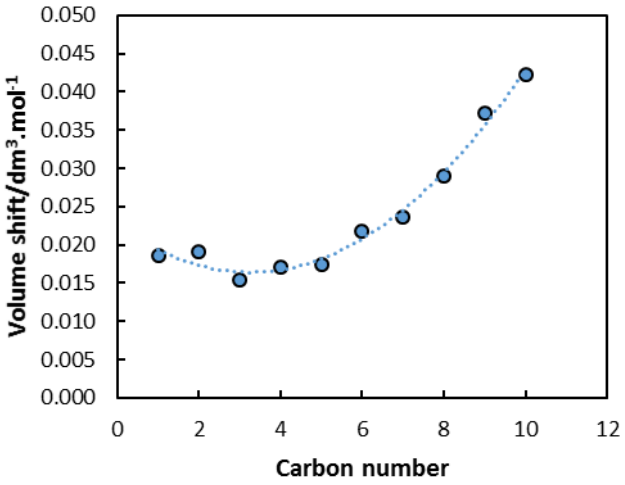

Figure 2.8 Volume shift values for the studied alcohols (from Table 2.7).

Due to the use of a highly flexible α function with multiple adjustable parameters, the results for heat capacity and heat of vaporization presented anomalous tendencies at the lower temperatures. By extending the lower temperature range, used for vapour pressure optimization, between 50 and 100 K the description of both properties, in the original temperature range, is improved. This is not, however, a consistent method, being highly affected by the quality of the vapour pressure data, and should be improved by using a better and more restricted alpha function as proposed by Jaubert and co-workers [145].

The obtained volume shifts show a different trend for the first two alcohols. As for the trend from propanol to 1-decanol, these results might be changed by using a group contribution method instead of a constant value for the β parameter, nevertheless despite some outliers, tendencies can be observed.

Due to the new optimization procedure here proposed, and the use of a more flexible alpha function, the modified version presents a higher accuracy for the vapour pressure in most cases. It is also able to describe well the liquid densities in the studied temperature ranges, and the results are, in most cases, similar to those of s-CPA if not better. As for the description of liquid *Cp*, in both cases it is possible to describe the property for heavier alcohols within *Tr* ranges between 0.5 and 0.7, nevertheless after the modifications (set C-2) the results seem to be more consistent for this property in the whole range of compounds studied. Heat of vaporization despite not being fitted in neither of the tests is well described in both cases. In general, the results from the modified version compare well with those from the calculated s-CPA set. Figures 2.9 and 2.10 present the results for heat capacity and liquid density for these compounds.

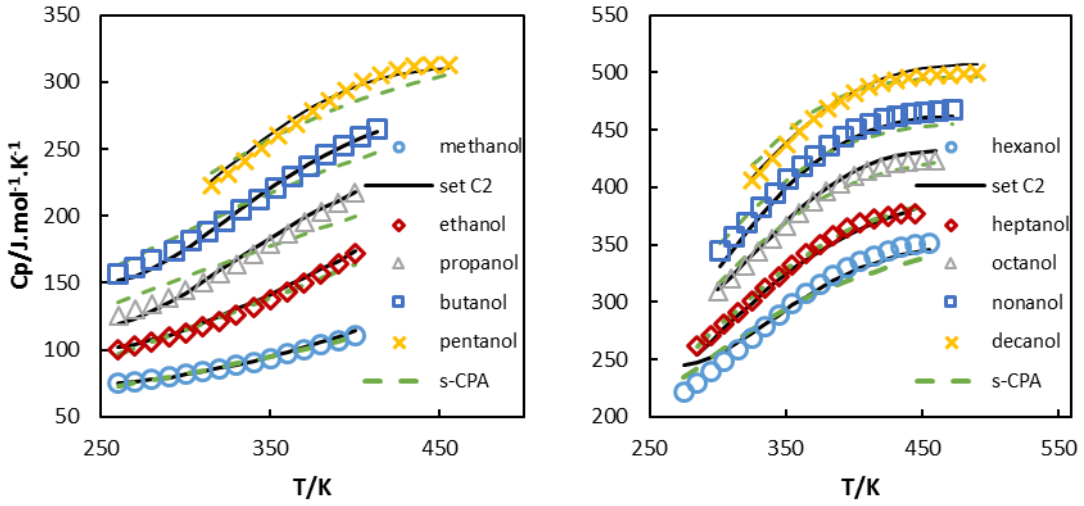

Figure 2.9 Liquid heat capacity description with the modified CPA for the analysed alkanols.

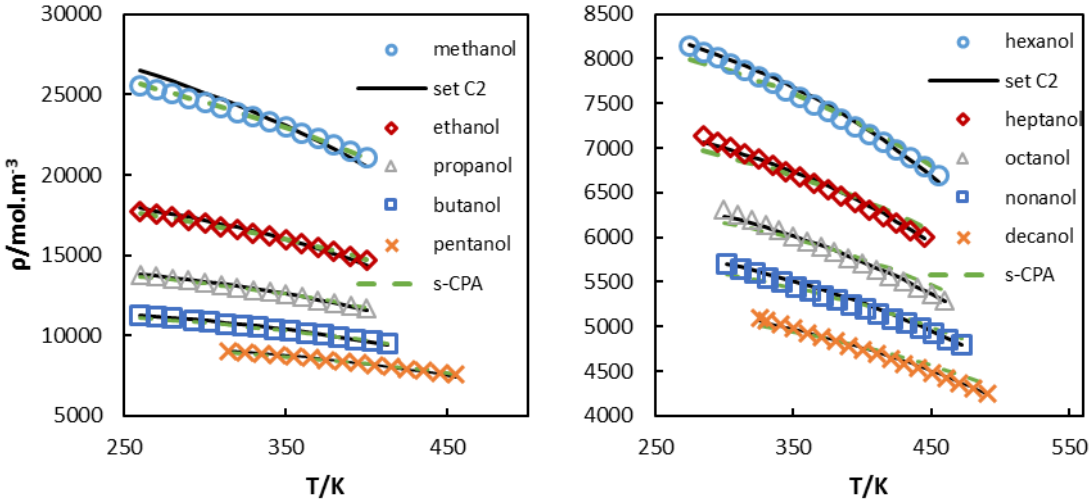

Figure 2.10 Liquid density description with the modified CPA for the analysed alkanols.

After the study of saturation properties, it is important to look at the description of some single phase properties, the results for this section are presented in Figure 2.11 and in annex. Looking at single phase densities it is possible to obtain a fair description between pressure and liquid density, however, due to the wrong temperature dependency of the saturation liquid density these results are not very accurate. Usually with SRK a temperature dependent volume shift is used in order to describe these properties. Baleed et al. [159] made a very relevant study on this, showing diverse volume shifts and their description of single phase properties. In a similar way, we tried using the following equation for the volume shift with CPA, optimized at two different temperatures:

$$v_t = v_0 - c_{vs}^0 - c_{vs}^1 T \tag{2.21}$$

Using a temperature-dependent volume shift it is possible to obtain a very reasonable estimation of the single phase liquid density up to 60 MPa, from 1-propanol to 1-decanol, in normal operation temperatures. The use of a lower association volume enables this, as for ethanol and methanol the results are only able to describe up to describe high pressure densities up to 20, 10 MPa respectively. With this approach it is also possible to obtain an accurate description for the isochoric heat capacity at atmospheric pressure, however as can be seen in the results (in annex), this comes from a compensation of the errors on the isobaric expansivity and isothermal compressibility. These incorrect descriptions also lead to an incorrect prediction of the speed of sound. This incorrect description of the volume dependency with pressure in CPA was already mentioned by de Villiers et al. [9] in their study of derivative properties in alkanes and alcohols. For heavier alcohols the modified version seems to present a more accurate description of the change of density with pressure. This is in accordance with what was suggested by Polishuk [160], as by increasing the values of the co-volume an improvement of the pressure dependency was verified. Still, for lighter alcohols s-CPA presents better results for these properties, than the modified version with a constant volume shift.

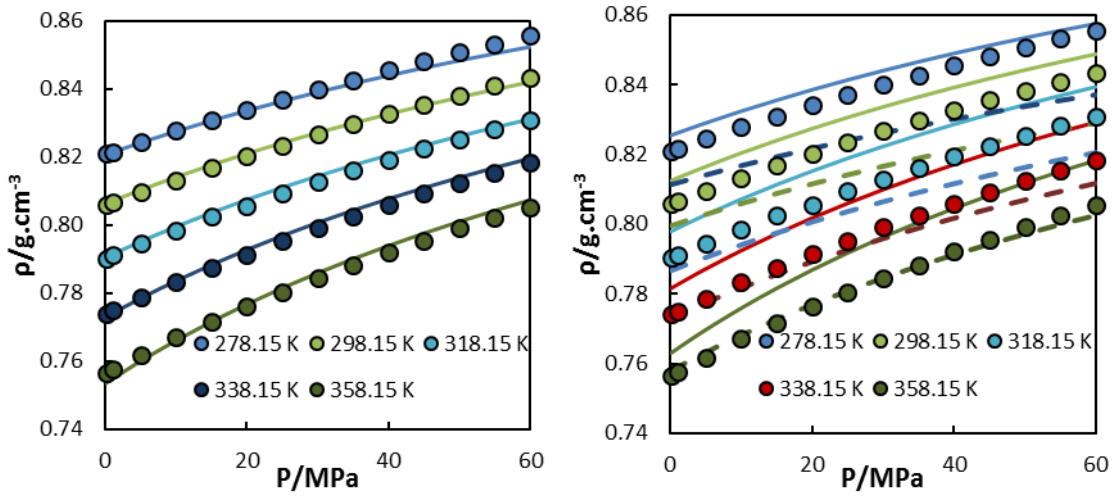

Figure 2.11 High pressure density descriptions with CPA for 1-butanol at 5 different temperatures modified CPA with a temperature dependent volume-shift (left), s-CPA (right, dashed lines), Modified CPA (right, full lines). Experimental data is from Dávila et al. [161].

2.4.3 Phase equilibria for binary mixtures containing n-alkanols

To model binary VLE systems of alcohols with alkanes, the C2 set succeeds in their description with values for the interaction parameters only slightly higher than those obtained before the modifications. The C1 set presents some difficulties in achieving a good description and despite

presenting good results for the liquid phase it displays some problems with the quality of the vapour phase description. These results are presented in Table 2.8 and Figure 2.12. The alkane parameters used with the non-modified version (s-CPA) are from Oliveira et al. [70].

Table 2.8 Results for the optimization of three binary systems with *n*-hexane

System	Alcohol Set	k_{ij}	%AAD T_{bub}
1-propanol + n-hexane [80]	s-CPA	0.024	0.30
	Set C1	-0.049	0.57
	Set C2	0.041	0.21
1-butanol + n-hexane [80]	s-CPA	0.012	0.22
	Set C1	-0.066	0.17
	Set C2	0.027	0.35
1-pentanol + n-hexane [80]	s-CPA	0.022	0.17
	Set C1	-0.026	0.22
	Set C2	0.031	0.21

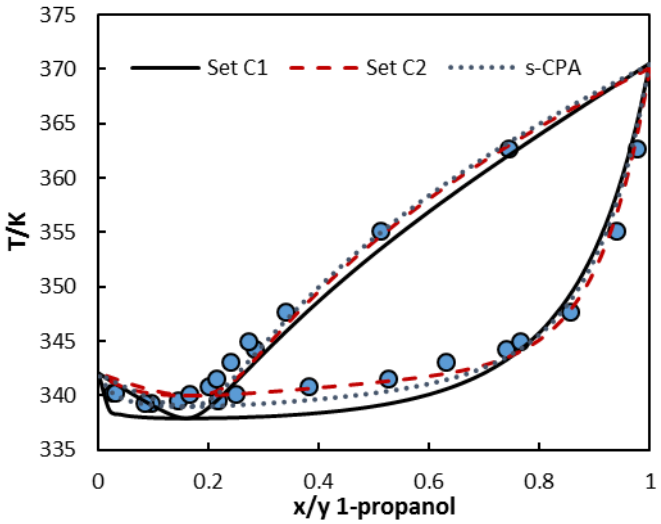

Figure 2.12 Description of the system 1-propanol + hexane, with the three sets in analysis.

Similar results were obtained for the prediction of alcohol – alcohol systems (no k_{ij}). While set C1 produces high deviations, set C2 achieves very reasonable predictions. Table 2.9 presents a comparison between the predictions of set C2 and the results with s-CPA.

Liquid-liquid modelling presents higher difficulties, however, despite the need for higher k_{ij} values in most situations, the C2 set is able to achieve very good results for this type of equilibria. For C1 these results present high deviations due to the expected excess of the associative contribution. Figures 2.13 and 2.14 present the results for the systems, methanol + hexane and ethanol + hexadecane.

Table 2.9 Predictions for the alcohol – alcohol binary systems.

System	Alcohol Set	%AAD T_{bub}
1-propanol + methanol [162]	s-CPA	0.77
	Set C1	2.06
	Set C2	0.38
1-butanol + metanol [162]	s-CPA	1.52
	Set C1	4.51
	Set C2	1.12
1-butanol + ethanol [163]	s-CPA	0.37
	Set C1	1.86
	Set C2	0.36
1-pentanol + metanol [162]	s-CPA	3.09
	Set C1	7.11
	Set C2	2.91
1-pentanol + ethanol [163]	s-CPA	1.07
	Set C1	3.47
	Set C2	1.12
1-octanol + methanol [164]	s-CPA	1.20
	Set C1	3.06
	Set C2	1.24

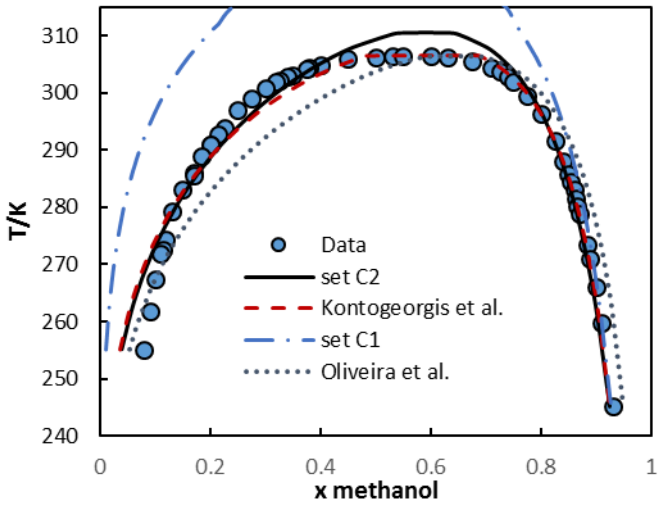

Figure 2.13 Results for the LLE equilibria of methanol + hexane (k_{ij} values are presented in Table 2.10).

As can be observed, the set C2 is able to adjust adequately the data despite of a slight overestimation of the critical point. The results for this set can be compared with those from the alcohol sets from Kontogeorgis and co-workers [73], [131], which presented the best results for both systems. Table 2.10 presents the binary interaction parameters used for these 2 systems.

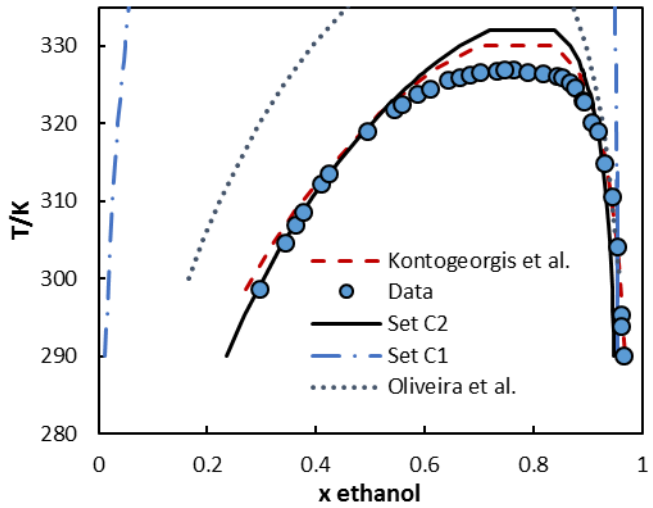

Figure 2.14 Results for the LLE equilibria of ethanol with hexadecane (k_{ij} values are presented in Table 2.10).

Table 2.10 Binary interaction parameters for the presented LLE binary systems.

	K_{ij}	
Set	MeOH – Hexane [165]	EtOH – Hexadecane [166]
C1	-0.02	-0.100
C2	0.036	-0.026
Kontogeorgis et al. [73,131]	0.007	-0.035
Oliveira et al. [70]	-0.007	-0.027

The description of the VLE equilibria for the systems above is in high agreement with the results of s-CPA. Using the binary interaction parameter from the LLE optimization in both cases, yields very similar results. A higher k_{ij} (0.052) is needed if an accurate description of the VLE is wanted with set C2. The results from set C1 are rather accurate for the liquid phase with the presented k_{ij}, nevertheless present some relevant deviations in the vapour phase. This results are presented in Figure 2.15.

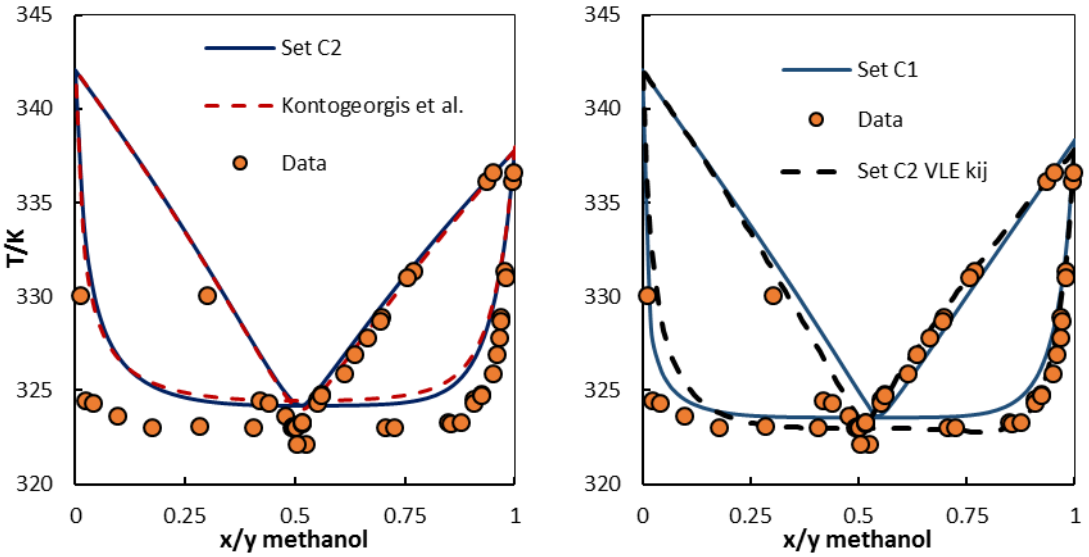

Figure 2.15 VLE results for the system methanol + hexane, using some of the k_{ij} presented in Table 2.10 and an optimized value (0.052) for VLE with set C2.

2.5 Conclusions

In this study some of CPA's weaknesses were reanalysed and efforts were made to improve them. In a first step it was shown how the critical point can be introduced in the parameterization. Using this approach, and a more flexible alpha function along with a constant volume shift to improve liquid densities, it was possible to describe the liquid density curve in a larger range of temperatures than before, including the region near the critical point. However, by doing so, the quality of the vapour pressure dependency with both liquid density and temperature is decreased, and thus derivative properties linked to these dependencies are not correctly predicted, as is the case of the heat of vaporization. This also tends to affect negatively the description of both VLE and LLE systems.

A second approach was then adopted, retaining the description of the critical pressure and temperature, but relaxing the description of the liquid density curve for higher temperatures. Using this approach, it was possible to consider the association energy a constant between the *n*-alkanols with 1 and 10 carbons and from propanol to decanol it was also possible to consider the association volume constant. With this constraints, and considering a temperature range used in most applications, this version of CPA was able to predict *Cp* and heat of vaporization, while providing an accurate description of the vapour pressure and of the liquid density after introducing the volume-shift. These results compare well with those from s-CPA with a fitting in the parameterization to density, vapour pressure and liquid *Cp*.

Considering the binary phase equilibria description, the results of this second test are in good agreement with those from the literature, despite requiring binary interaction parameters with a somewhat higher positive values.

Using only pure component vapour pressure data on the optimization routine is a relevant drawback, as the parameterization becomes largely dependent on the quality of the available data for this property. Also for some compounds this property is very difficult or even impossible to measure due to decomposition of the compounds, thus future studies must address the use of a different optimization property, or more than one property simultaneously. One alternative is to analyse if the alpha parameters should be optimized simultaneously with the associative term.

Other relevant issue is the alpha function used. Due to the high number of parameters, the optimization of the vapour pressure had to be extended to larger ranges of temperature so that relevant derivative properties presented a correct behaviour. This is further addressed in the remaining chapters of this document.

To summarise, a first set of modifications was evaluated and is able to describe the critical point and the density curve in a large range of temperatures, nevertheless leading to high inaccuracies in the description of derivative properties. The second set of modifications provides a CPA parameterization with a high predictive potential, which can be more consistent in the description of isobaric heat capacity than the original s-CPA.

3 Secondary alcohols, diols and glycerol

3.1 Abstract

To create a predictive method for an associative equation of state, the parameters of a specific associative group should be transferrable among molecules. The hydroxyl group, one of the most common associative groups, is a good starting point for this development. Based on a previous study, where a modified version of CPA was shown to present accurate results for alkanols with almost constant association parameters, this work addresses branched, secondary alcohols, 1,ω-alkanediols and glycerol to evaluate how CPA can handle steric hindrances and the presence of more than one hydroxyl group.

The pure component properties here studied are vapour pressure, saturated liquid density, saturated liquid isobaric heat capacity and heat of vaporization. Some VLE, LLE, and GLE of binary systems are also analysed, showing how the modifications affect the description of binary/multicomponent systems. Some systems containing petroleum fluids are also analysed.

3.2 Introduction

Isomerism introduces relevant changes to the properties of the compounds and, due to the increase in steric hindrance, a hydroxyl group present in a branched alkanol is expected to behave differently from one in a primary alkanol with a similar carbon number. Besides their use as solvents, the alcohols studied in this work are applied in diverse industries: both 2-propanol and tert-butanol are used in the production of fuel additives, with the first being also used as a sanitization agent and 2-butanol has applications in the perfume and food industries. These compounds are also applied as precursors for the production of diverse compounds of interest in the chemical industry.

The 1,ω-alkanediols are among the multifunctional compounds those with the simplest structure, presenting two hydroxyl groups at the ends of a linear hydrocarbon chain. The properties and three dimensional orientation of these molecules are mainly caused by the effect of hydrogen bonds, which makes these molecules interesting subjects to analyse as model molecules for hydrogen bonding, either in self-associating systems as well as to describe solute-solvent interactions for dilute solutions. They present diverse fields of applications in the industry: mono-ethylene glycol (1,2-ethanediol) is one of the most important hydrate formation inhibitors, while various of the smaller diols can be used in refrigerating and thermostating systems, as well as cryoprotectants. Diols are also used in the production of polymers such as polyurethanes and polyethers, as well as drug additives in the

pharmaceutical industry and for cosmetics formulations. Despite their importance, for most alkanediols, the experimental data on their thermophysical properties are scarce and often of questionable quality. Rowley et al.[167] have recently carried a systematic study of the existing properties for six of these compounds. Their study created sets of recommended equations for vapour pressure and heat of vaporization, while also providing some insight into the choice of experimental values for other properties, such as the isobaric heat capacity.

Due to their high associative nature, some diols present intramolecular association. This is the case of 1,3-propanediol and 1,4-butanediol, which bend to form a ring resulting from the hydrogen bonding between the hydroxyl groups at their extremities.[168]

Glycerol, due to its non-toxic nature and chemical properties, is widely known in the food and pharmaceutical industries, with diverse applications such as humectant, sweetener, lubricant and solvent. Similarly to what was presented before for some diols, glycerol also presents important qualities as an anti-freezing agent for automotive applications. This molecule is also an intermediate for a large group of chemical reactions. Other applications of glycerol include uses for botanical extraction, being a component of liquids for electronic cigarettes and being used in ultrasonic testing.

Alcohols have long been studied with the CPA EoS, both for the description of their pure properties or in systems with water, hydrocarbons, or several other compounds.[70,129,153] Various sets of parameters have been proposed to describe the *n*-alcohols family, revealing important tendencies when considering only the optimization of vapour pressure and liquid density. There is, however, a dearth of studies concerning the influence of the position of the hydroxyl group in these molecules.

Models able to describe a variety of phase equilibria, while providing a good description of both transport and thermodynamic properties are in great demand.[7] In the case of multifunctional molecules, the situation is even more dire as many of the properties are very difficult to measure or even impossible due to the thermal degradation of the compounds.[8] To improve the sets of parameters, increasing their accuracy for more properties, de Villiers et al.[9] proposed that the optimizations should be conducted using more properties and a larger range of pressure conditions. Oliveira et al.[169] have studied the use of derivative properties in the parameterization of SAFT and have shown relevant improvements with this approach.

In this study, parameter sets were obtained for a group of five secondary/branched alcohols (2-propanol, 2-butanol, 2-pentanol, 3-pentanol and tert-butanol) and for five α,ω-alkanediols

between MEG and 1,6-hexanediol, using the modified CPA version that is proposed in this thesis. The results for vapour pressure, liquid density, liquid heat capacity and heat of vaporization were then analysed, as well as, some selected binary systems from the literature.

3.3 Results and discussion

3.3.1 Pure component analysis

Continuing our studies on the hydroxyl group parameterization, from the previous chapter, the constant association energy parameter of 24913 J.mol^{-1} was here used, while the associative volume was considered constant within each family of compounds, except for MEG, in which case the ethanol associative parameters proved more accurate. The parameters obtained with ethanol were also applied to glycerol. For mono-alcohols (with a single OH group), the liquid heat capacity was used in the fitting of the associative volume parameter for secondary alcohols, while for diols and tert-butanol this parameter was only fitted to vapour pressure data.

The vapour pressure data used for the diols were obtained from Rowley et al. [167], which enables the use of this version of CPA due to the large temperature range of vapour pressure data that can be estimated. For the remaining compounds the vapour pressure curves were obtained from the DIPPR [79] and TRC [80] databases. For liquid density the curves from Multiflash [78] and DIPPR [79] were applied, except for 1,6-hexanediol, for which data by Bleazard et al. [170] were used. For the heat of vaporization the data were taken from the DIPPR [79] and TRC [80] databases as well as from the Multiflash [78] correlations, while for heat capacity most data comes from Góralski and Tkaczyk [171]. Critical data were taken from Rowley et al. [167], the TRC [80] and DIPPR [79] databases.

The parameter sets and results for liquid density, vapour pressure and heat of vaporization, as well as the critical data used in the parameterization, are presented in Tables 3.1 and 3.2. Figure 3.1 presents the tendencies, against the van der Waals volume, for both the cubic term energy at the critical temperature (a_c) and co-volume parameters, and a comparison to those for the primary alkanols. [69]

The critical data presented in Tables 3.1 and 3.2 corresponds to both the experimental and calculated values as within the presented tolerance there are no differences between these two values.

Table 3.1 Parameters and results for the studied diols and glycerol.

Compound	MEG	1,3-Pr(OH)$_2$	1,4-Bu(OH)$_2$	1,5-Pe(OH)$_2$	1,6-He(OH)$_2$	glycerol
a_c (Pa.m^6.mol^{-2})	1.72	2.25	2.72	3.22	3.82	2.59
b. 10^5 (m^3.mol^{-1})	6.87	8.27	9.88	11.56	13.57	9.11
c_1	1.10	1.37	1.30	1.33	1.32	0.45
c_2	-3.64	-2.50	-1.23	-1.25	-0.52	4.16
c_3	12.16	6.27	3.32	4.04	2.26	-19.32
c_4	-37.1	-23.1	-18.0	-20.0	-16.1	19.9
c_5	42.5	28.4	24.4	25.2	22.2	0.0
ε (J.mol^{-1})	24913	24913	24913	24913	24913	24913
β.10^2	0.162	0.075	0.075	0.075	0.075	0.162
%AAD P^{sat}	0.50	0.63	0.71	0.77	0.94	0.53
%AAD $\rho_{liq.}$	0.70	1.07	0.51	0.44	0.79	1.02
%AAD H^{vap}	0.34	1.84	3.00	0.67	0.22	0.51
T_{range} (K)	330-490	293-533	293-533	293-533	318-438	330-530
vshift (m^3.kmol^{-1})	0.020	0.019	0.017	0.019	0.022	0.025
Tc (K)	719.0	718.2	723.8	730.0	737.0	850.0
Pc (MPa)	8.20	6.55	5.52	4.75	4.08	7.50

Table 3.2 Parameters and results for the studied alkanols.

Compound	2-PrOH	2-BuOH	2-PeOH	3-PeOH	tert-BuOH
a_c (Pa.m^6.mol^{-2})	1.57	2.00	2.50	2.46	1.87
b. 10^5 (m^3.mol^{-1})	7.90	9.44	11.18	11.05	9.42
c_1	1.20	1.15	1.02	0.95	1.12
c_2	-0.69	-2.01	0.54	-0.01	-0.95
c_3	1.20	13.82	-0.81	2.81	2.30
c_4	-21.5	-50.2	-9.6	-16.4	-13.0
c_5	40.2	58.0	17.5	21.3	25.0
ε (J.mol^{-1})	24913	24913	24913	24913	24913
β.10^2	0.034	0.034	0.034	0.034	0.030
%AAD P^{sat}	0.03	0.89	1.61	0.96	0.22
%AAD $\rho_{liq.}$	1.68	0.16	0.46	0.50	0.74
%AAD H^{vap}	1.53	1.95	0.61	1.84	2.03
T_{range} (K)	293-433	254-354	251-361	275-415	254-424
vshift (m^3.kmol^{-1})	0.015	0.016	0.017	0.018	0.016
Tc (K)	508.3	536.1	560.3	559.6	506.2
Pc (MPa)	4.76	4.18	3.68	3.71	3.97

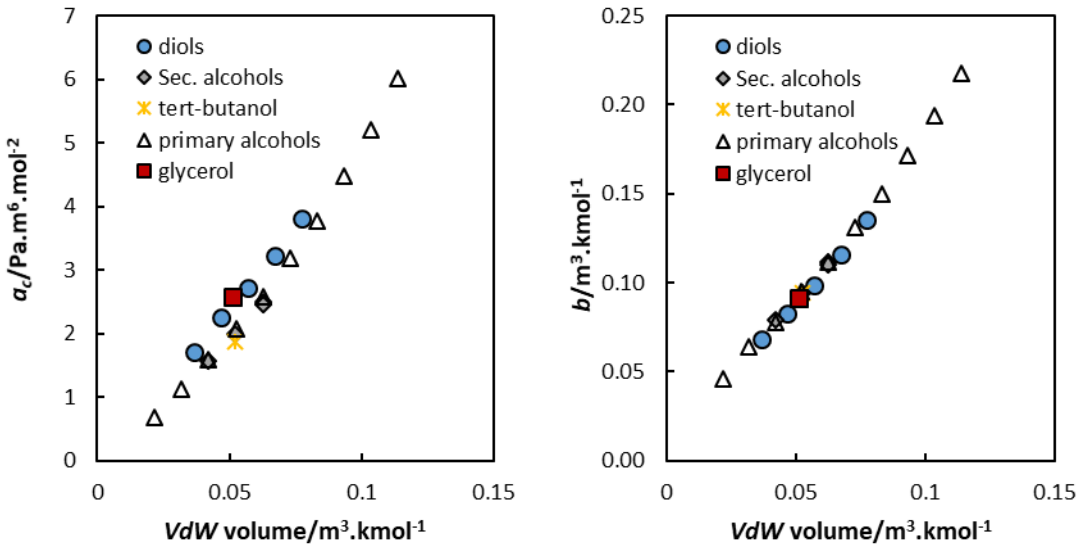

Figure 3.1 Energy and co-volume parameters of the cubic term for compounds containing hydroxyl groups and their tendencies.

As shown in figure 3.1, both the co-volume and energy parameters of the cubic term present dependencies on the van der Waals volume. It is also interesting to note that, in the case of diols, this is also true for the alpha function parameters, despite the inter-correlation between these parameters. Nevertheless, an outlier is always observed, usually 1,4-butanediol or 1,5-pentanediol. This is also patent in figure 3.2.

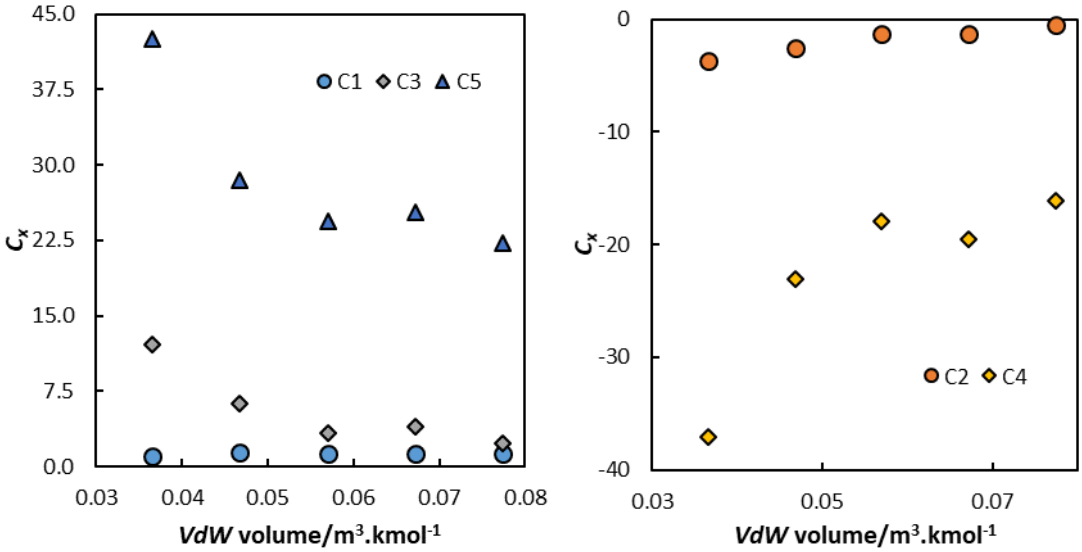

Figure 3.2 Alpha function parameters for the studied diols and their tendency with the van der Waals volume.

The values of the association volume seem to decrease for the higher steric hindrances. Similar dependencies to those previously observed for primary alcohols [69] are obtained when analysing the volume shift. For diols a similar minima, to that found between methanol and 1-

propanol, is observed at 1,4-butanediol. Glycerol presents a higher value for the volume shift, which might have to do with the higher uncertainties for its critical data. These results are reported in figure 3.3.

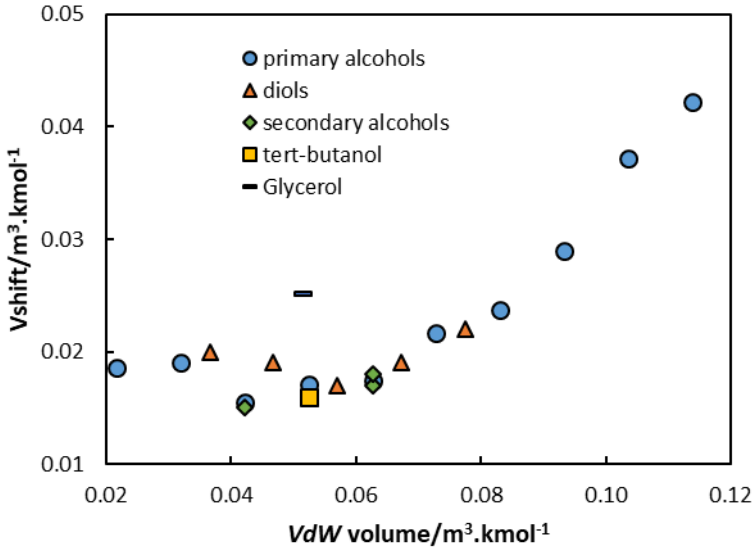

Figure 3.3 Volume shift parameters with relation to the van der Waals volume.

With this approach, liquid density, heat of vaporization and vapour pressure were all well described for MEG. For the remaining diols and glycerol, despite higher deviations, which are in part due to the higher uncertainties of the experimental data, the results are also accurate, with average deviations for each property inferior to 1% in most cases. For the other alcohols studied the results are similar. The estimation for ethylene glycol, proved to be able to describe LLE equilibria with alkanes, as will be shown in the next section. Predictions of heat of vaporization are reported in figures 3.4 and 3.5.

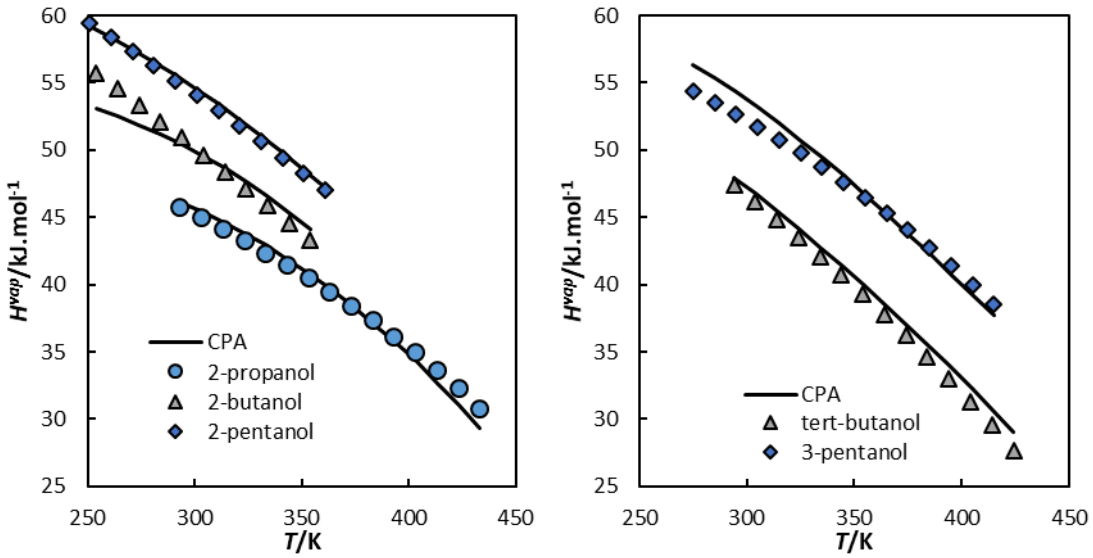

Figure 3.4 Results for the heat of vaporization of secondary/branched alkanols.

The 1,4-butanediol is the diol which presents largest deviations. This is in part due to a high degree of uncertainty in its vapour pressure curve. This is very relevant when considering the heat of vaporization, liquid *Cp* and also results for binary systems, and will be further discussed below.

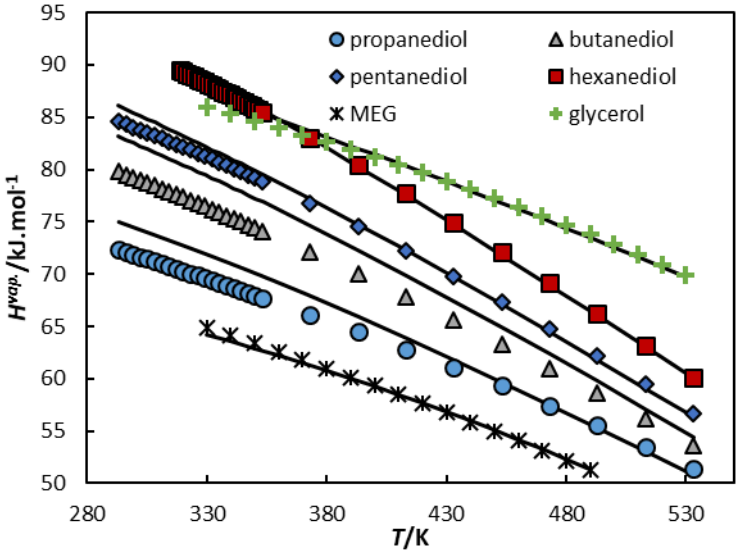

Figure 3.5 Results for the heat of vaporization of the analysed alkanediols.

The *Cp* estimates show a large dependence on the ideal gas heat capacity, as shown on Figure 3.6 using various approaches for C_p^{ideal}. Since the equation of state only provides the residual contribution to the heat capacity, an accurate ideal gas heat capacity correlation is required. Three sets of correlations for ideal gas heat capacities were analysed in the case of MEG. The

first two are available from the data on the DIPPR database [79] while the third is based on the studies of Yeh et al. [172] on the conformation of ethylene glycol.

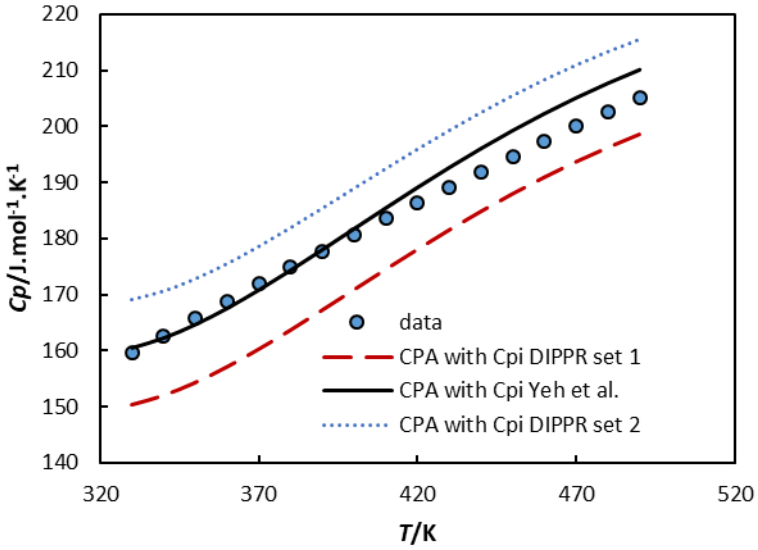

Figure 3.6 Results for the heat capacity of ethylene glycol using different sets of ideal gas heat capacity correlations.

It is important to note that some of these sets are based on group contribution methods and similar variations are obtained by using different methods of the same type. [173,174]

The results for the liquid phase *Cp* of secondary/branched alcohols are presented in figure 3.7.

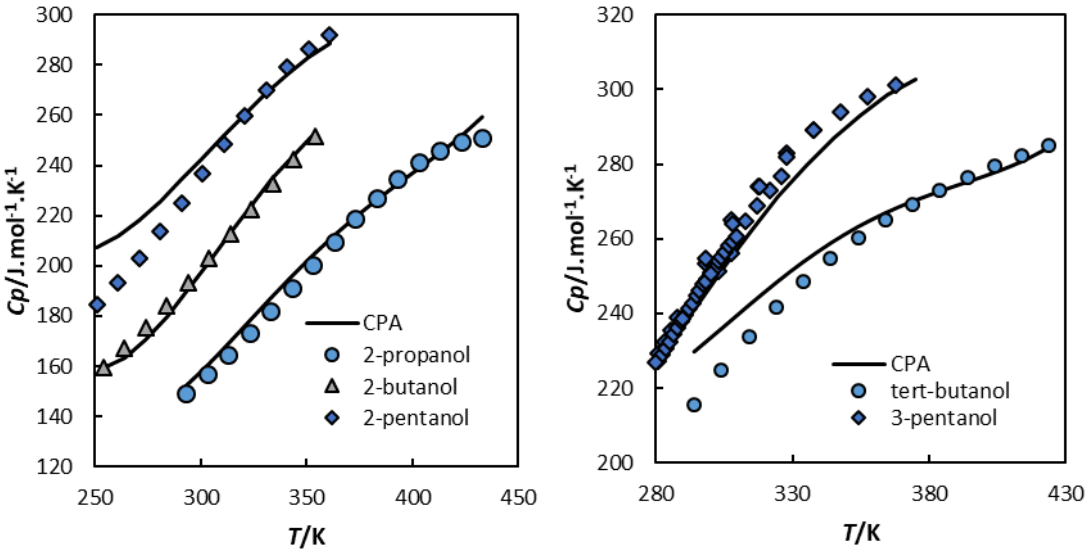

Figure 3.7 Results for the heat capacity of secondary/branched alkanols.

The results present somewhat higher deviation for *Cp* at lower temperatures, where the data have more uncertainties and the EoS presents a lower accuracy due to the unconstrained

alpha function, which having 5 available parameters is too flexible to fit to only a few properties without any constraints.

Despite the problem with the ideal gas heat capacity and the inaccuracies at lower temperatures, the *Cp* results for the remaining diols follow the expected tendencies, with an exception for 1,4-butanediol, for which the vapour pressure curve seems to present some inaccuracies, as will be discussed below when modelling binary systems. In figure 3.8 the results for *Cp* are compared with the experimental data from Góralski and Tkaczyk [171], also the results for 1,5-pentanediol are compared with the predictions of Rowley et al. [167].

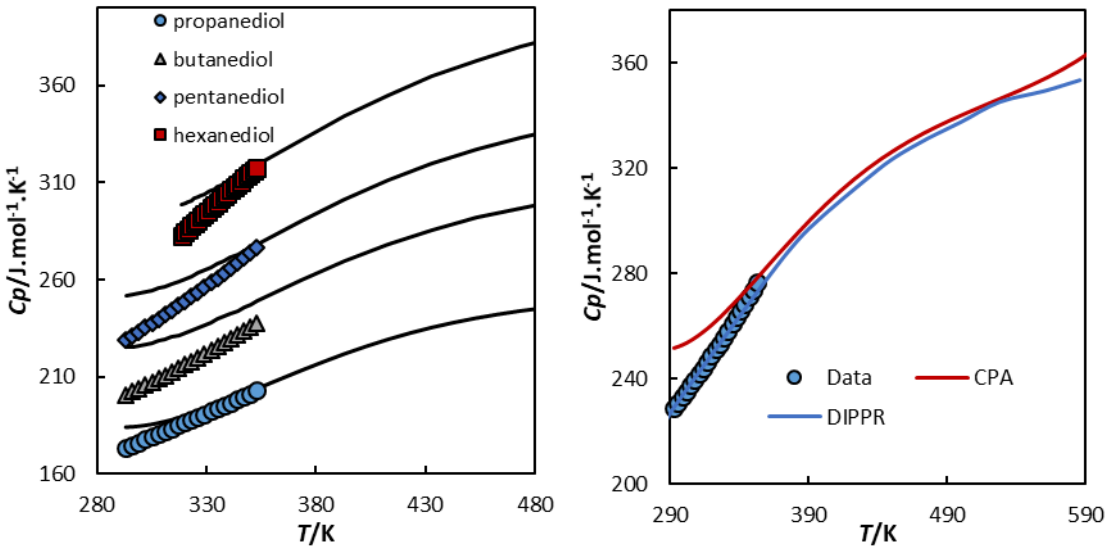

Figure 3.8 Results for the heat capacity of diols (left) and comparison with the predictions of DIPPR for the heat capacity of 1,5-pentanediol (right).

For glycerol the average deviations in *Cp* are higher than 10%.

In the presented results it is of note that the increase in the number of parameters and the parameterization process have an important influence in the predictions. As presented above, two of the parameters are obtained from the fitting of the pure compound critical temperatures and pressures, enabling the correct description of these properties. The association parameters used here are in most part constant, and thus when comparing this version to s-CPA, for most associating compounds, it has one more adjustable parameter (fitting the 5 parameters of s-CPA or fitting the 5 parameters of the modified Mathias-Copeman function plus the volume shift). It is important to note that some compounds (methanol, ethanol, MEG) present accurate results without using the whole alpha function and in future work the use of different alpha functions with less parameters should be conducted.

The accuracy of these results is in line with those obtained for the primary alkanols, thus it is now important to look at the impact of the parameterization used in the modelling of binary systems.

3.3.2 Binary systems modelling

The binary VLE systems analysed for diols with other diols and alkanols present accurate descriptions of the experimental data, which are in most cases predictive. The systems analysed were MEG + ethanol and MEG + 2-propanol, both of which are presented in figure 3.9.

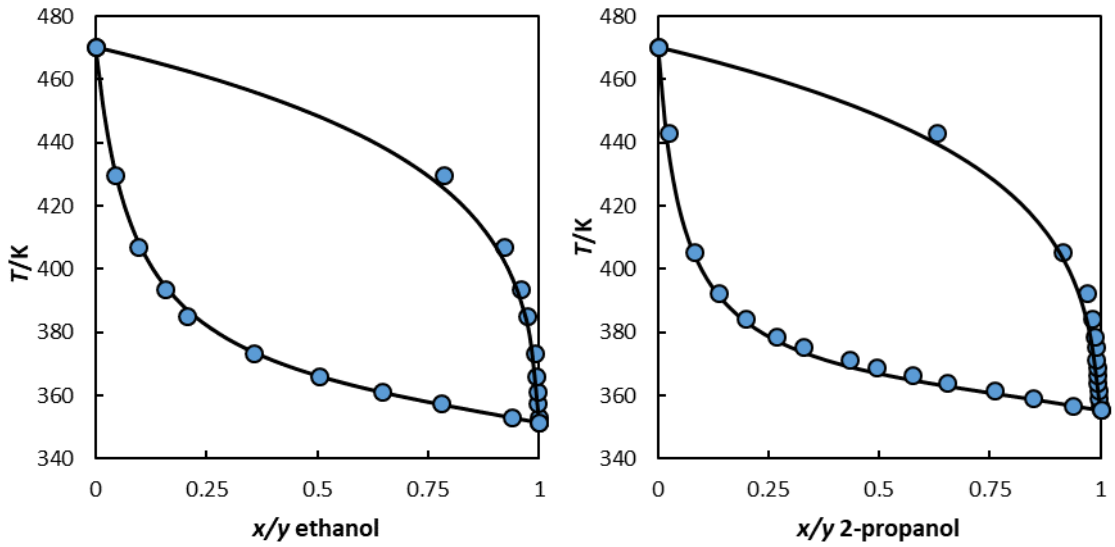

Figure 3.9 Predictions for the binary systems MEG + ethanol (left) [175] and MEG + 2-propanol (right) at 1 atm [176].

With 1,3-propanediol two systems were analysed, 1,3-propanediol + MEG and 1,3-propanediol + 2-propanol. In the second case a binary interaction parameter with the value of -0.0153 was used, while for the first systems no interaction parameter was required. The results are presented in figure 3.10.

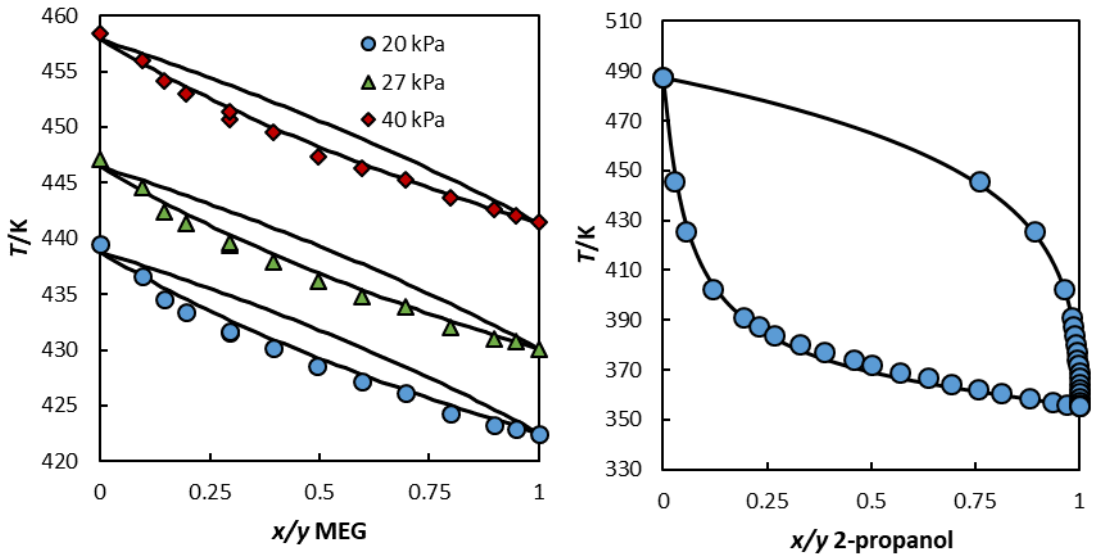

Figure 3.10 Predictions for the binary system MEG + 1,3-propanediol (left) [177] and results for the system 1,3-propanediol + 2-propanol (right) [178] at 1 atm with a k_{ij}=-0.015.

As hinted before, some deviations were observed in the vapour pressure curve of 1,4-butanediol that have now an impact upon the description of the VLE data for binary systems. In figure 3.11 the predictions for the system MEG + 1,4-butanediol are reported.

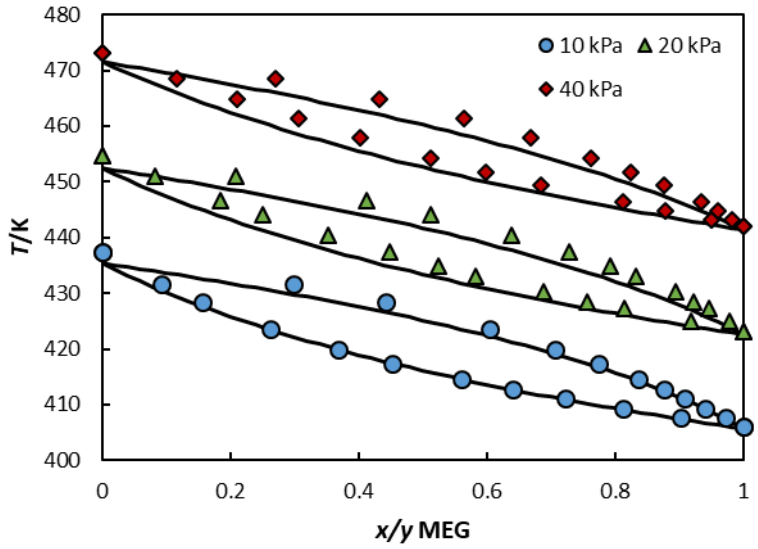

Figure 3.11 Predictions for the binary system MEG + 1,4-butanediol [179].

Differences higher than 2 K can be observed for the pure saturation temperature of 1,4-butanediol showing a slight, but relevant overestimation of the pure component vapour pressure. The deviations between CPA results for the pure 1,4-butanediol saturation pressure and the data of Yang et al. [179] are in average 7.9%, while the average for the applied vapour pressure curve was 7.2%, which is already a high uncertainty. These deviations are not very

high in terms of absolute values of temperature, but, as can be observed in figure 3.11, are detrimental for the description of the binary systems, especially at higher pressures. Combined with the higher uncertainty for the lower temperatures, it was thus expected that the derivative properties calculated would present higher deviations, as observed in the previous subsection.

The description of the VLE for binary systems of diols was mostly accurate, with only one of the systems requiring a binary interaction parameter. Results were also obtained for VLE systems with tert-butanol. In this case all systems required the use of a binary interaction parameter. The experimental data for these systems were taken from the TRC database [80]. Figure 3.12 presents the description of the system tert-butanol + ethanol using a binary interaction parameter of -0.024.

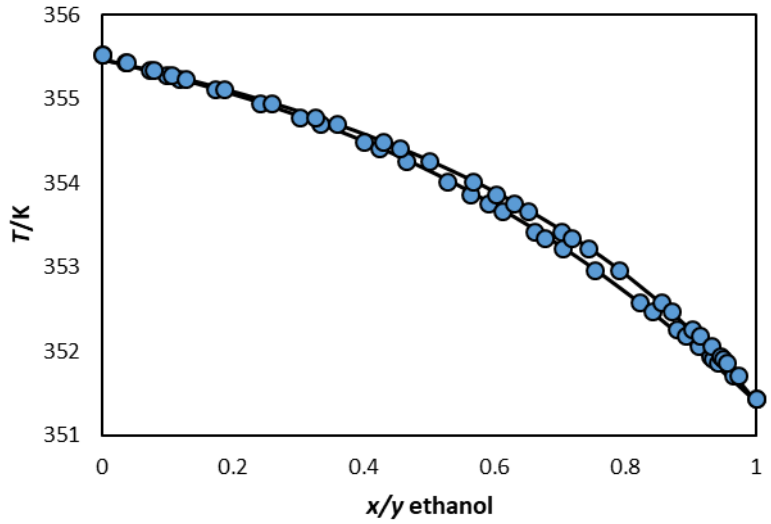

Figure 3.12 Results for the binary system tert-butanol + ethanol at 1 atm with a k_{ij}=-0.024.

The results for this system are highly accurate despite the narrow temperature difference between the boiling and dew temperatures. The results for tert-butanol + butane were also studied and are presented in figure 3.13.

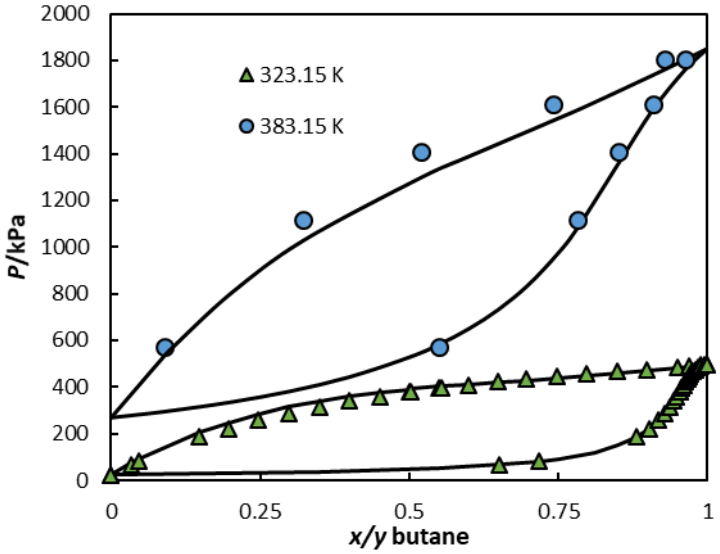

Figure 3.13 Results for the binary system tert-butanol + butane at 2 temperatures with a k_{ij}=0.0551.

To finish the analysis of the VLE description of binary systems containing tert-butanol, the system with isobutylene was also studied, which is presented in figure 3.14.

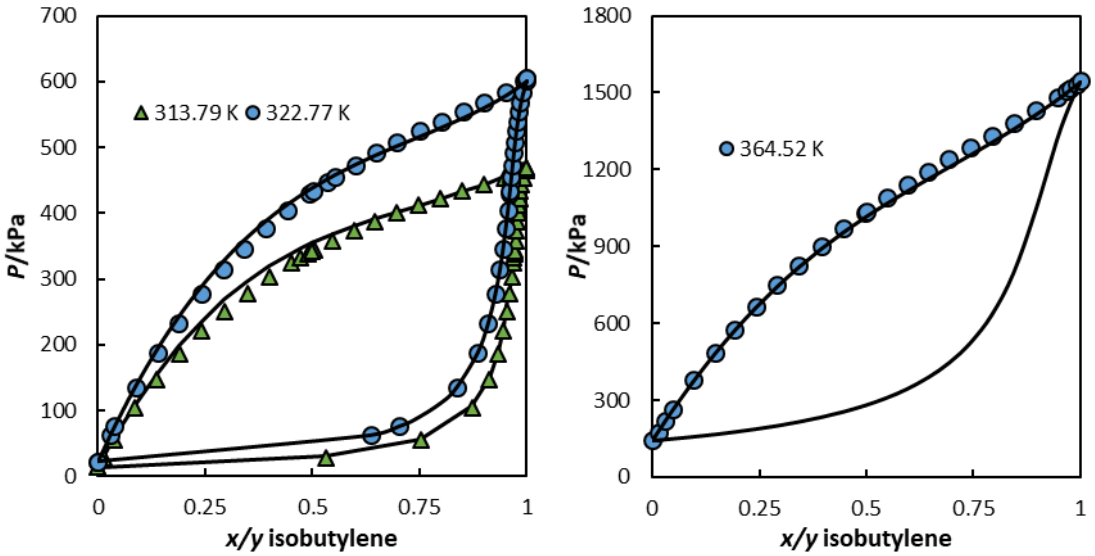

Figure 3.14 Results for the binary system tert-butanol + isobutylene at 3 temperatures with a k_{ij}=0.0370.

Binary systems with mono-alcohols/1,3-propanediol were studied to verify the quality of the glycerol parameters. These systems are well described using small interaction parameters, in most cases, as is presented in figures 3.15 and 3.16. The binary interaction parameters for these systems are presented in table 3.3.

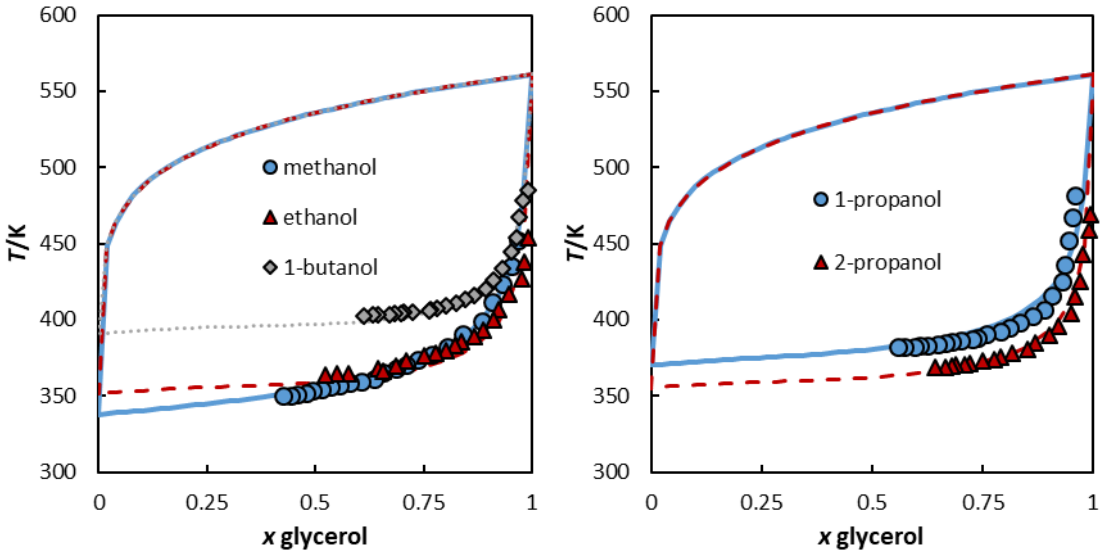

Figure 3.15 Results for the systems containing glycerol and an alcohol at 1 atm [127].

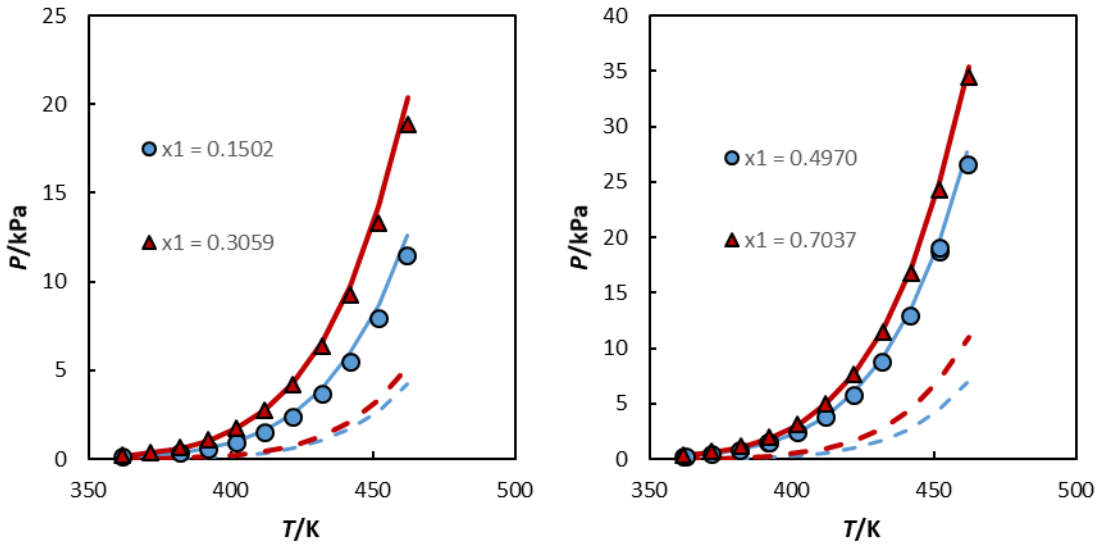

Figure 3.16 Results of the system 1,3-propanediol (1) + glycerol (2), full lines – Bubble points, dashed lines, dew points [180].

Table 3.3 Binary interaction parameters for the systems containing glycerol.

Second compound	k_{ij}
1,3-propanediol	0.015
methanol	0.008
ethanol	0.054
1-propanol	-0.009
2-propanol	0.000
1-butanol	0.018

In the last chapter, it was shown that despite the higher values of the co-volume (when compared to the original CPA model), it was possible to successfully describe LLE, with the present version, albeit with slightly higher binary interaction parameters. Thus, the description of LLE systems containing MEG was analysed, as well as the accuracy of the model to describe the solubility of gases in MEG. Comparing the results for MEG + alkanes with the data from Derawi et al. [139] and Riaz et al. [181], presented in figures 3.17 and 3.18, it is shown that the proposed parameters are able to describe these systems and despite somewhat higher deviations in the system with hexane, and the need of higher k_{ij} values, the results are comparable to those of s-CPA [140].

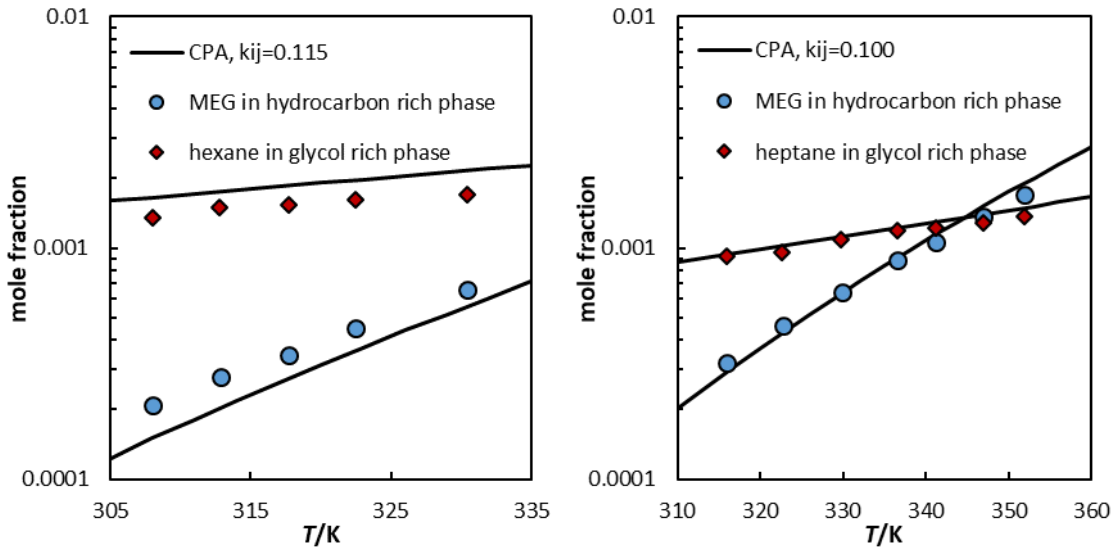

Figure 3.17 Mutual solubility results for the binary systems MEG + n-hexane (left) and MEG + n-heptane (right).

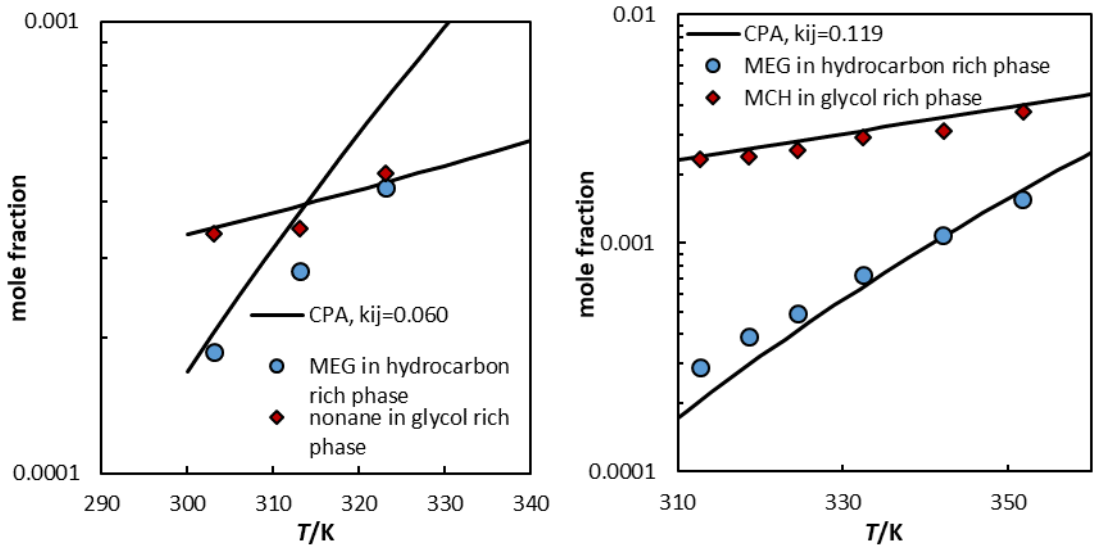

Figure 3.18 Mutual solubility results for the binary systems MEG + nonane (left) and MEG + methyl cyclohexane (right).

With these results, along with the results for the systems MEG + light alkanes, for which the modelling of the gas solubility is studied below, it is possible to correlate the binary interaction parameter values with the chain-length of the alkane. The average absolute deviations for these systems are presented in the annexes.

To evaluate the ability of the model to describe the results for gas solubility in MEG (H_2S, CO_2, COS, N_2 and methane) and MEG solubility in gas (methane and CO_2), modelling results were compared with those from the works by Jou et al. [182,183], Zheng et al. [184], Folas et al. [141] and Afzal et al. [185]. Larger binary interaction parameters were needed for all systems in study. Despite this fact, the descriptions are rather accurate and in the case of the binary systems of MEG with methane, CO_2, H_2S and COS they compare well with the results from s-CPA [8,141,185]. The CO_2, N_2, H_2S and COS were considered to be inert in this study.

Figures 3.19 to 3.22 present the results for the 5 systems investigated.

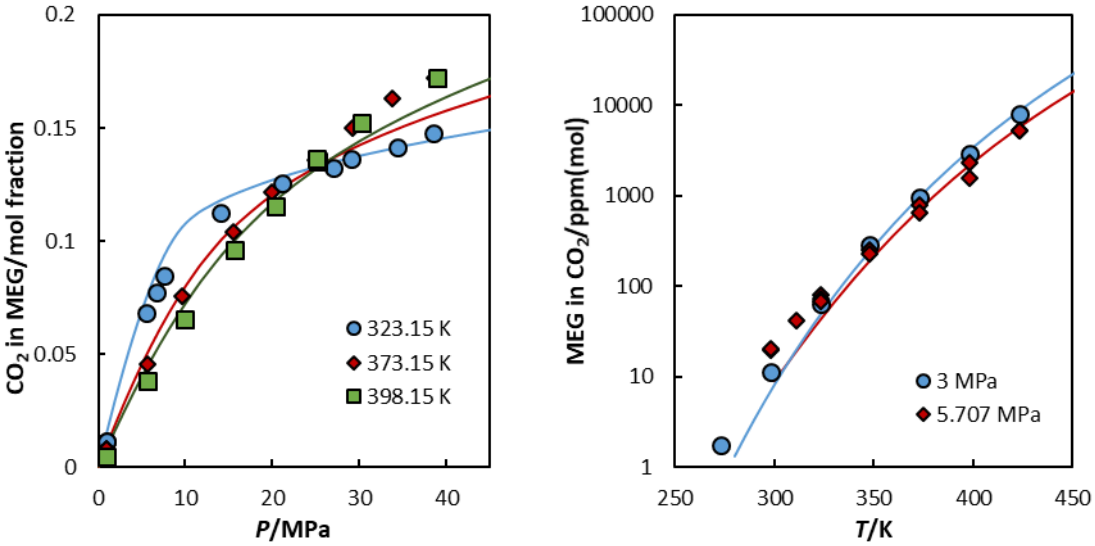

Figure 3.19 Solubility of CO_2 in MEG (left) and MEG in CO_2 (right), k_{ij}=0.147.

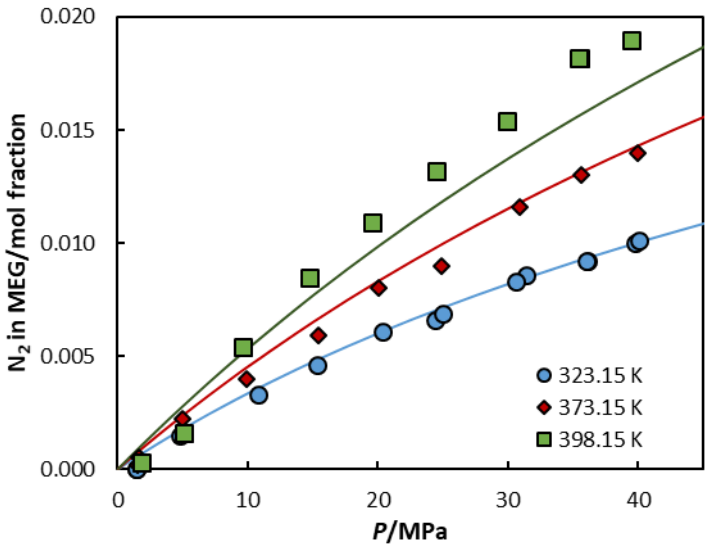

Figure 3.20 Solubility of N_2 in MEG at 3 different temperatures k_{ij}=0.590.

Despite being considered as non-associative compounds, the descriptions for the systems with CO_2 and N_2 present accurate results with CPA, figure 3.19, being equivalent to those reported by Jou et al.[183] with Peng-Robinson [11].

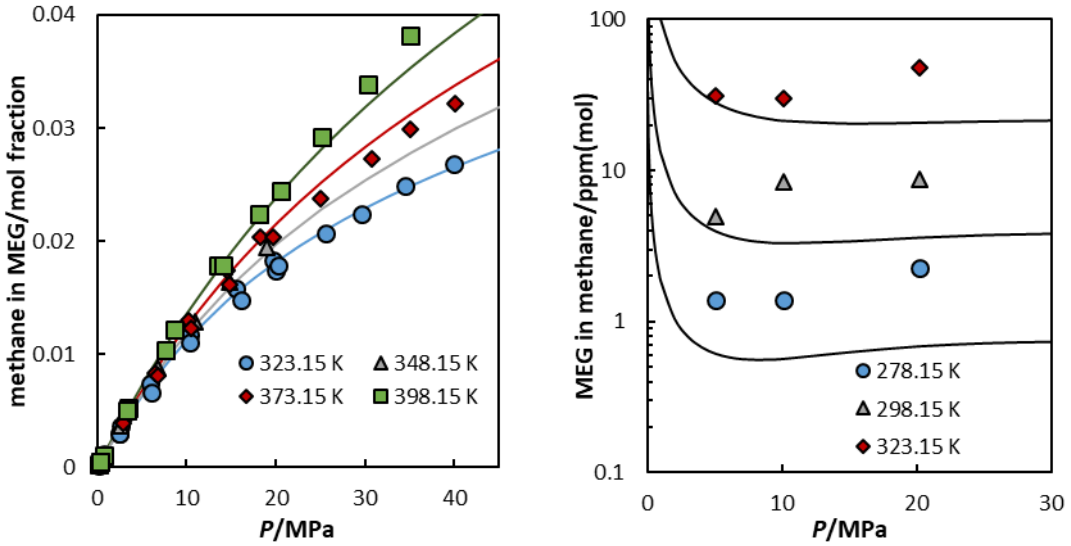

Figure 3.21 Solubility of methane in MEG (left) and solubility of MEG in methane (right) k_{ij}=0.343.

With methane, deviations are higher, as shown in figure 3.21, nevertheless the results are similar to those by Folas et al. [141] with s-CPA, and for the very low concentrations in study, are satisfactorily accurate.

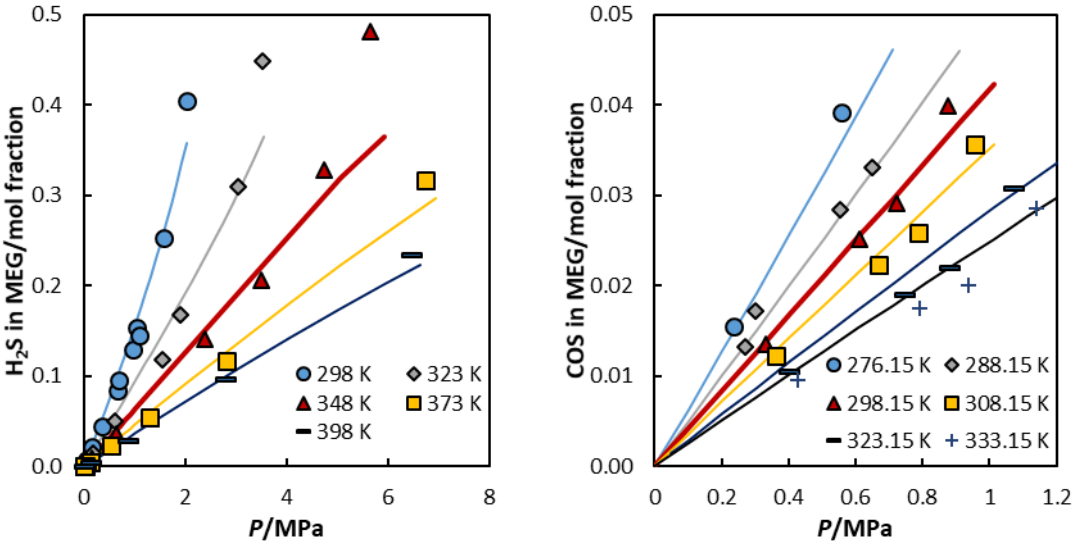

Figure 3.22 Results for the solubility of H_2S (left) and COS (right) in MEG, with binary interaction parameters of 0.039 and 0.160 respectively.

Similarly to CO_2 and N_2 the systems with H_2S and COS are accurately described despite no association sites being considered in H_2S or COS.

To complete the study on the systems of MEG + n-alkanes (for which results with methane, hexane, heptane and nonane were already analysed) the solubility of ethane and propane in MEG are presented in figure 3.23.

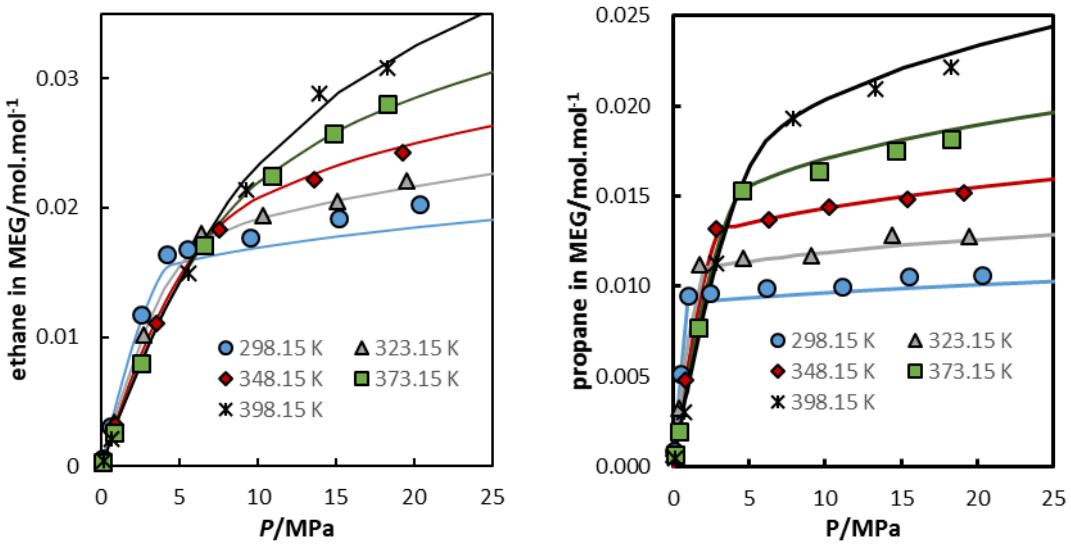

Figure 3.23 Results for the solubility of ethane in MEG[186] (left) and propane in MEG[187] (right), the binary interaction parameters are 0.237 and 0.191 respectively.

As discussed before, a dependency is observed for the binary interaction parameters of these systems with the alkane carbon number, as shown in figure 3.24. The use of the correlation enables the description of the systems in study. The %AAD for each system with the original k_{ij} and the correlated value are presented in the annexes. To further test the quality of these parameters, an analysis was carried for five systems studied by Kontogeorgis and co-workers, [181,188–191] using this binary interaction parameter correlation. The results for two other systems of the same type [192] are presented in the annexes.

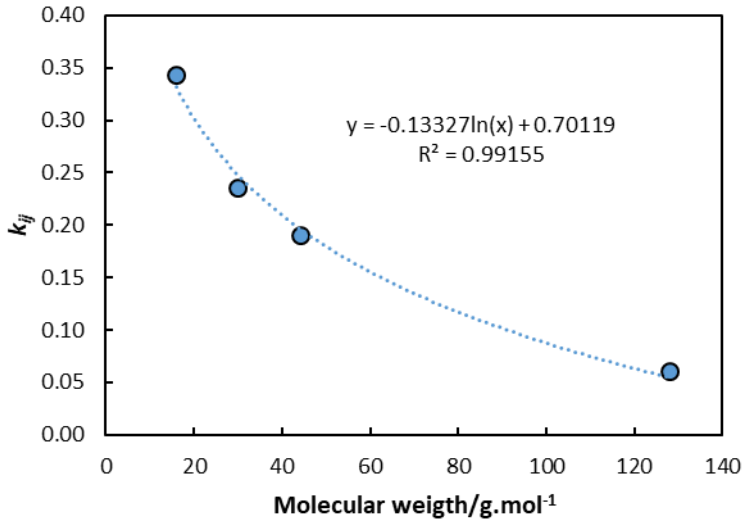

Figure 3.24 Binary interaction parameters correlation for the studied systems of MEG with alkanes and their dependency with the alkane carbon number.

The k_{ij} values for linear and branched hydrocarbons were considered to be identical.

For most analysed systems this approach is able to describe with reasonable accuracy the fraction of MEG in the hydrocarbon rich phase, or at least a correct temperature dependency is obtained. It is of note that despite the pure property description of ethylene glycol taking priority in this parameterization, with two critical properties fitted, a reasonable *Cp* temperature dependency and very satisfactory deviations for both P^{sat} and ρ_{liq}, the essential description of these systems is still captured, with light oil 1 being a particular case where the range of temperature for which the fraction of MEG in light oil is superior to that of light oil in MEG is closer to experimental data. The results for these systems as well as the comparison with the results of Kontogeorgis and co-workers [181,188–191] are presented in figures 3.25 to 3.27. The deviations obtained for these systems are presented in the annexes.

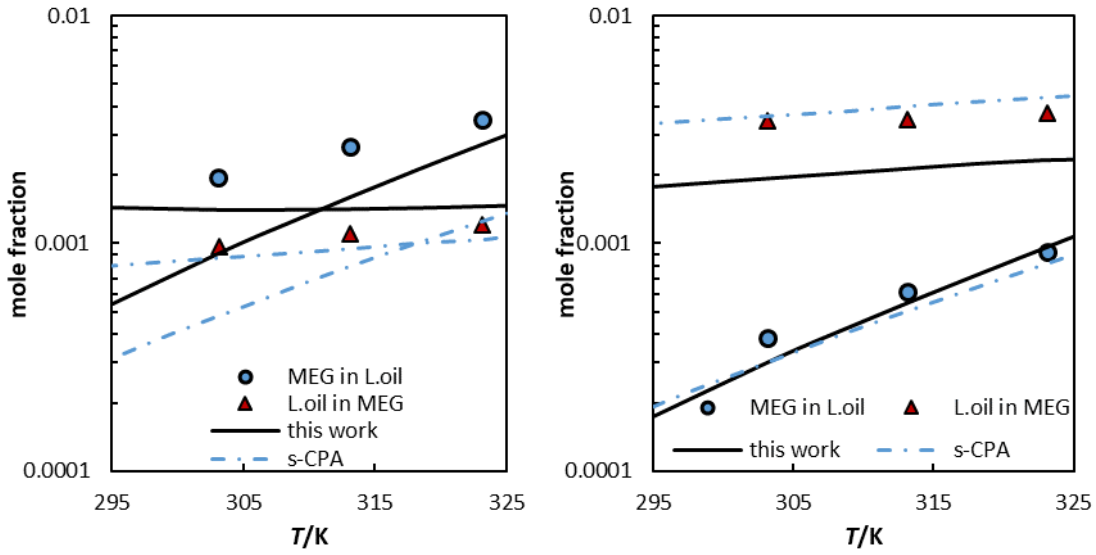

Figure 3.25 Results for the LLE descriptions of MEG with Light oil 1 (left) and MEG with Light oil 2 (right), experimental data is from Kontogeorgis and co-workers.[190]

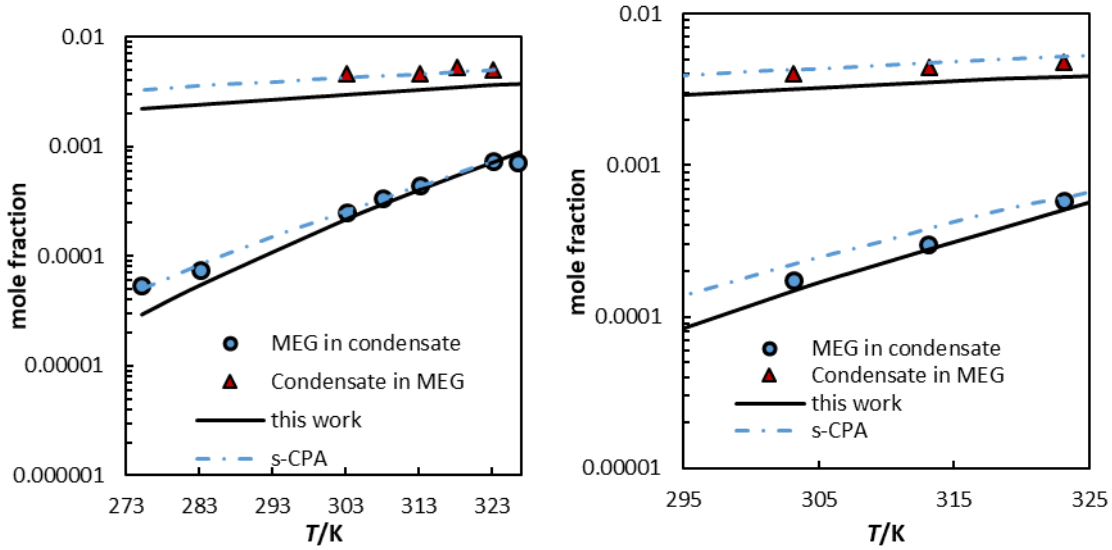

Figure 3.26 Results for the LLE descriptions of MEG with Cond-1 (left) and MEG with Cond-3 (right), experimental data is from Kontogeorgis and co-workers. [188,191]

This approach tends to overestimate the k_{ij}'s for the C10+ fractions for lighter mixtures, leading to an under prediction of the fraction of hydrocarbons in MEG phase for some of these systems. However, this also enables improvements on heavier mixtures, as is the case of light oil 1, or in some instances improving the description of the hydrocarbon rich phase.

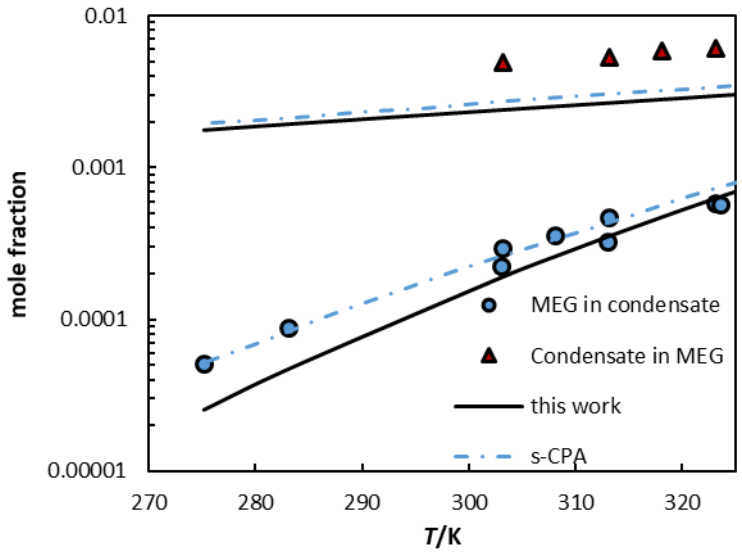

Figure 3.27 Results for the LLE descriptions of MEG with Cond-2, experimental data is from Kontogeorgis and co-workers. [188]

3.4 Conclusions

The purposed version of CPA was extended to diols and some secondary/branched alcohols. The value of the associative energy was considered constant, while the associative volume was adjusted to take into account different environments (including steric hindrance). The energy, co-volume and volume-shift parameters show tendencies with the van der Waals volume. In the case of diols the alpha function results also show tendencies for its parameters, showing promising results for the predictive capacities of this version.

Modelling results within the experimental uncertainty were obtained for most pure properties. The *Cp* presents higher deviations, however a part of these might be due to the uncertainties coming from the use of the ideal gas heat capacity correlations. However, the tendency for the property is in most cases correct, even when not using this property in the optimization, which usually is not observed with other versions of the equation. It is also of note that this version of CPA forces the correct description of both the critical pressure and critical temperature, providing a more reliable description of these properties but also of properties which depend on them, as is the case of heat of vaporization, for which, with this version, the results at the critical temperature will be 0, instead of presenting an overestimated value, while presenting mostly accurate results at normal application temperatures.

These improvements on the pure component description lead, in most cases, to the need for slightly higher binary interaction parameters. Despite this, the correlation results are of similar accuracy as those of s-CPA for most systems. Gas solubility in ethylene glycol, as well as some cases of solubility of MEG in gases were also analysed with promising results. A final test was conducted to verify the quality of multicomponent description with this new version of CPA. The results show a very reasonable description of this systems using a single correlation based on the studied systems of MEG with hydrocarbons.

To summarize, this modified version of CPA improves on the description of pure component properties, with the description of the pure component critical pressure and temperature and an increase in accuracy for the predictions of heat of vaporization and liquid *Cp*. These results were obtained using a constant and transferable value for the association energy parameter for the hydroxyl group and a very simple approach for the association volume, improving on the predictive capacity of the model. The results obtained during the binary and multicomponent system calculations are accurate and in most cases present similar quality to those from s-CPA, despite the higher k_{ij}'s.

4 Water and aqueous mixtures

4.1 Abstract

One of the major challenges of an equation of state lies in the description of water and aqueous systems. Its abundance and unique properties turn water into one of the most important molecules in the industry. However, due to these peculiar characteristics its modeling is far more complex than for any other common solvent.

In this chapter, the modified CPA model, is expanded to water and its systems. A brief analysis of the predicted water pure properties is conducted, comparing those to a previous version of the model. Results for a group of binary systems, including liquid-liquid equilibria with alkanes and alcohols, highlighting their minima in aqueous solubility, and gas solubility in water/water solubility in gas are also presented. Finally, ternary and multicomponent systems of water + hydrocarbons and water + polar compound + hydrocarbons are also modelled and discussed.

4.2 Introduction

The importance of water both in the industry and in the daily lives of the world population is undeniable, and its unique properties are an asset used in diverse ways in almost every process.

The correct description of pure water and its mixtures using an equation of state is both a necessity and a challenge. During the last decades, the development of association models brought a significant improvement to the accuracy of these systems. Some of the most well-known association models are based on perturbation theory, in most cases on Wertheim's first order thermodynamic perturbation theory (TPT1) for associating fluids.[8] CPA[5] is one of such models and combines the simplicity of a cubic equation of state with the theoretical background and accuracy expected from an association model.

The modified CPA was applied here to the description of binary and multicomponent systems containing water, while still preserving the accuracy of the pure water properties. For the latter, this study analyses the description of not only vapor pressure and liquid density, the most used properties in the parameterization of CPA, but also the estimation of derivative properties such as liquid *Cp* and heat of vaporization. A diverse group of mixtures is then analysed with a focus on the description of water + alkanes and water + alcohols/hydrate inhibitors (MEG and methanol), while also studying petroleum related fluids and their equilibria with water and these polar compounds.

As will be demonstrated, this new version of the model can reasonably describe, for the first time for CPA, the minimum in the water solubility of hydrocarbons while also matching the pure components critical temperature and pressure and better representing second derivative properties such as liquid heat capacity and enthalpy of vaporization.

4.3 Results and discussion

4.3.1 Pure water results

Our experience with the version of the CPA model[69] described above has shown that the selection of the associative parameters needs to be carried with care, especially for smaller and stronger associative compounds such as water and methanol. For methanol we found that higher values for the associative parameters could be employed, improving the description of saturated pressures, but decreasing the quality of LLE and derivative properties. The same holds true for water. Thus, the set presented here takes into account not only the description of pure water properties but also the need to correctly describe mixtures.

It is important to note that for non-associative compounds, the model is simply SRK with the fitting of vapour pressure to a different alpha function and a constant volume shift fitted to a single density point. For associative compounds, from the experience of the previous chapters, the fitting of associative parameters should be addressed by looking (or including in the parameterization) some derivative properties or binary data. For the set presented in this thesis the association parameters were fitted to C_p. Even then, more than one set was able to describe the pure properties accurately. Thus, as between VLE and LLE, the latter is harder to model, the set of parameters presenting the best description of the LLE for n-hexane + water were selected.

The description of the remaining water properties is rather accurate. A comparison between the results for this set and those using s-CPA with the set from Kontogeorgis et al.[73] is presented in Table 4.1 and Figures 4.1 and 4.2. A summary of the calculated and experimental critical properties is reported in Table 4.2. Water critical constants (T_c, P_c, V_c) and temperature dependent correlations for vapor pressure, liquid density, C_p and ideal gas heat capacities were obtained from the Infodata database in the commercial software Multiflash.[78] The vapor pressure curve applied was: $\mathrm{Ln\ P} = \mathrm{LnP_c} + \frac{-7.798(1-T_r)+1.540(1-T_r)^{3/2}-2.896(1-T_r)^3-1.038(1-T_r)^6}{T_r}$.

Table 4.1 Water CPA parameters and comparison between the set obtained in this work and the one from Kontogeorgis et al. [73] T_{range} [260 - 450 K].

Set	Parameter	value	Parameter	value	Property	%AAD
Kontogeorgis et al. [73]	a_c (Pa.m^6.mol^{-2})	0.123	*c4*	0	P^{sat}	1.17
	$b.10^5$ (m^3.mol^{-1})	1.452	*c5*	0	ρ_{liq}	1.10
	c1	0.674	ε (J.mol^{-1})	16655	Cp_{liq}	7.43
	c2	0	$\beta.10^2$	6.92	H^{vap}	1.45
	c3	0	*vshift* (m^3.kmol^{-1})	0		
This work	a_c (Pa.m^6.mol^{-2})	0.425	*c4*	1.464	P^{sat}	0.05
	$b.10^5$ (m^3.mol^{-1})	2.388	*c5*	8.628	ρ_{liq}	2.28
	c1	0.557	ε (J.mol^{-1})	22013	Cp_{liq}	0.84
	c2	-2.540	$\beta.10^2$	0.483	H^{vap}	0.42
	c3	-2.012	*vshift* (m^3.kmol^{-1})	0.012		

As can be observed in Table 4.1, the water association energy (ε) used in the new set is higher, than that used for the s-CPA. This will have a very relevant impact in the description of systems containing water as discussed below. The remaining pure associative compound parameters applied in this chapter are presented in chapters 2 and 3. The parameters for the non-associating compounds are presented in the annexes.

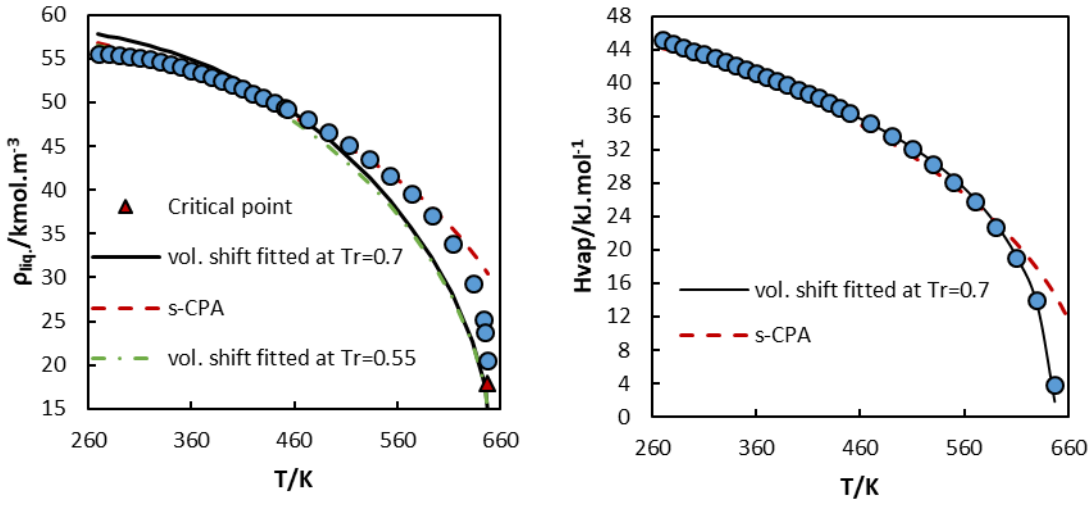

Figure 4.1 Results for the description of water saturated liquid density and heat of vaporization using the two sets of parameters and different temperatures to fit the volume shift.

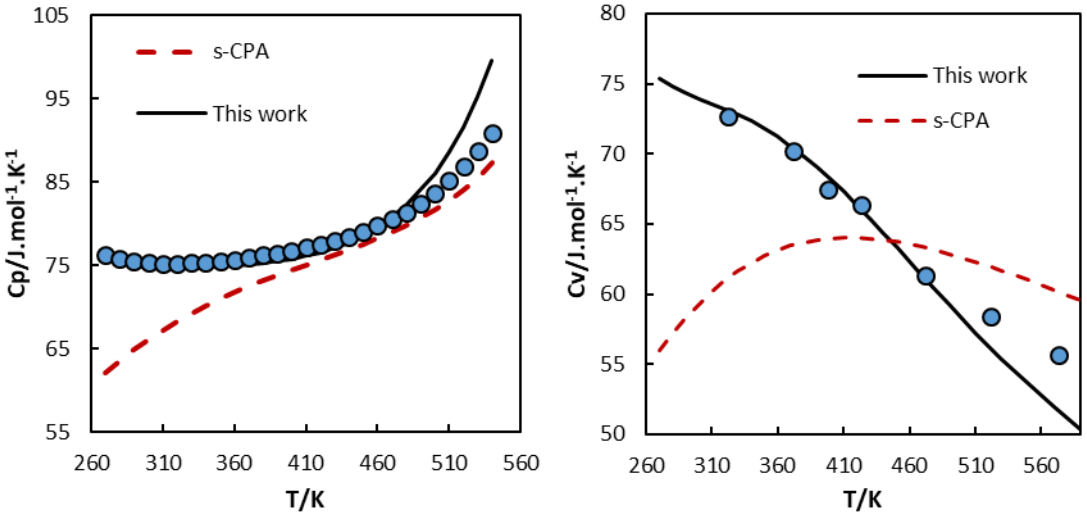

Figure 4.2 Results for the description of water heat capacity using the two parameter sets. C_v data values are from Abdulagatov et al., [193] while the values for C_p were taken from the Infodata database in MULTIFLASH.[78]

Table 4.2 Experimental critical data and results with the two parameter sets.

	Data	This work	s-CPA [73]
***Tc* (K)**	647.3	647.3	656.6
***Pc* (MPa)**	22.12	22.12	23.73
***Vc* ($m^3.kmol^{-1}$)**	0.056	0.069	0.035

In Figure 4.1, it can be seen that changing the usual reference reduced temperature for the volume shift has a significant impact on the density results, particularly at lower temperatures. This change leads to a correct description of the heat of vaporization close to the critical point and an overall better trend with temperature for this property.

As discussed in the previous chapters, the use of an unconstrained, highly flexible alpha function, can introduce some inconsistencies. However, for some specific compounds, like water, where the simple nature of CPA, and similar EoS, are unable to capture the trends of many of its unique properties, the introduction of constrictions might lead to an even worse thermophysical description. In Figure 4.3 the alpha function used in this thesis for water is plotted between reduced temperatures of 0.4 and 1 and is compared to the water set of s-CPA.[73]

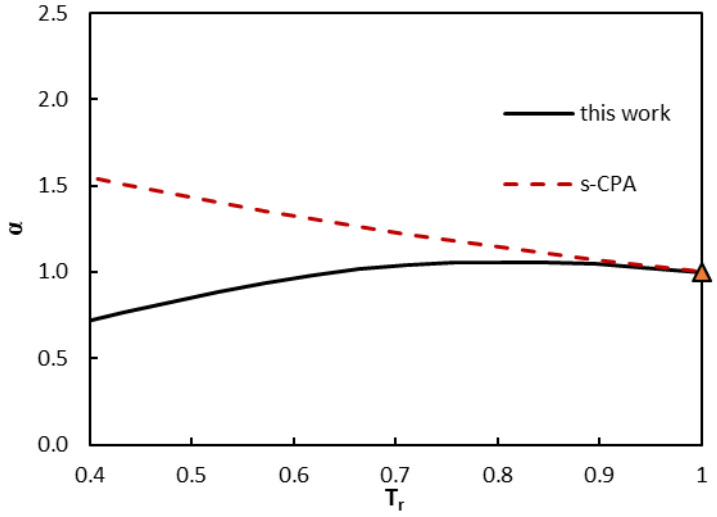

Figure 4.3 Alpha functions analyzed in this work between T_r 0.4 and 1.

As can be seen, this alpha function does not decrease in the whole range of temperatures, continuously increasing in the fitted temperature range. It is important to note that the *Cp* was used in the parameterization of this set and that C_v presents a seemingly correct physical behavior for the range of temperatures in analysis, as observed in Figure 4.2.

One important topic to address at this point is that from the experimental data available for liquid C_p and C_v, the value of these properties seems to almost cross each other between 273.15 K and 300 K, as can be observed in the work of Chen.[194]

Knowing that:

$$C_p - C_v = -T\frac{\left(\frac{\partial P}{\partial T}\right)_V^2}{\left(\frac{\partial P}{\partial V}\right)_T} \tag{4.1}$$

For C_p to have the exact same value of C_v above 0 K either the first derivative of pressure in relation to volume at constant temperature is infinite, or else, the first derivative of pressure with relation to temperature at constant volume is zero. The second hypothesis is the one of interest. It is thus important to know how this happens with CPA:

$$\left(\frac{\partial P}{\partial T}\right)_V^{cubic} = \frac{R}{V-b} - \frac{1}{V(V+b)}\frac{\partial \alpha}{\partial T} \tag{4.2}$$

In this term (cubic contribution to the derivative) the first term is always positive, while the second is positive only if the alpha function monotonically decreases with temperature.

The contribution for pressure from the association term is:

$$P^{association} = RT\tau h \tag{4.3}$$

where:

$$\tau = \frac{1}{2V}\left(V\frac{\partial \ln g}{\partial V} - 1\right) \tag{4.4}$$

$$h = \sum_i^{allsites} m_i(1 - X_i) \tag{4.5}$$

with m_i being the mole number of sites of type i.

The derivative for this term is then:

$$\left(\frac{\partial P}{\partial T}\right)_V^{association} = R\tau h - R\tau T \sum_i^{allsites} m_i \frac{\partial X_i}{\partial T} \quad (4.6)$$

h is always positive, as well as, $\sum_i^{allsites} m_i \frac{\partial X_i}{\partial T}$. The $\ln g$ decreases with increasing volume, in this way its derivative is negative above 278 K, when considering saturation or atmospheric conditions. Taking this into account, the first term of the derivative (concerning association) is negative while the second term is positive above this temperature, the opposite being true below. In the case of the Soave alpha function, one association term needs to compensate both the remaining association term and the cubic terms, for the total derivative to be zero. With the alpha function, and water parameter set proposed in this thesis, between 273 and 300 K the second term of the cubic contribution is negative and liquid densities are not used directly in the parameterization. Thus allowing $\left(\frac{\partial P}{\partial T}\right)$ to be close to zero, while retaining a correct description of vapor pressures and its derivatives.

Considering $\left(\frac{\partial P}{\partial T}\right)$ able to be zero, or close, leads to an over reliance on $\left(\frac{\partial P}{\partial V}\right)$ for the description of saturation pressures, and thus, despite presenting a better physical behavior, the values of the volume are far from correct when using a volume shift anchored to a temperature far from this region. Through this compensation of errors it is possible to increase the accuracy of predictions for pure properties of water and some LLE, while keeping a correct description of VLE.

It will also be important to analyze the Pitfalls of Soave type alpha functions presented by Segura et al.,[195] and the guidelines by Deiters [196], when looking at properties and phase equilibria where the associative compounds are near or at the critical point.

4.3.2 Modeling mixtures containing water

Binary mixtures with alkanes (C_4 to C_{10})

As was referred before, the value of the association energy is higher with the proposed set of parameters, which in turn introduces a heavier weight into the temperature dependence of the associative contribution. This change, as well as the alpha function and the volume shift, depending on the kind of system and conditions, introduce important improvements on the results, leading however to less accuracy for a few other systems. A notorious example of this is the description of water + *n*-alkane and water + *n*-alkanol systems where the increase in the association energy of water enables a better estimation of the minima in the solubility of *n*-alkanes in water and a better description of the solubility trend for the alkanols. The better

trend for these systems is associated, in some cases, with higher deviations at low temperatures. Figures 4.4 and 4.5 present the results for water + alkane between C_4 and C_{10}. Experimental data for these systems was taken from Tsonopoulos et al.,[197] Marche et al.,[198] Heidman et al.,[199] Jou et al.,[200] Pereda et al.,[37] Economou et al.,[201] Schatzberg,[202] Noda et al.[203], Góral and co-workers [204] and calculated with the expressions from Tsonopoulos.[205]

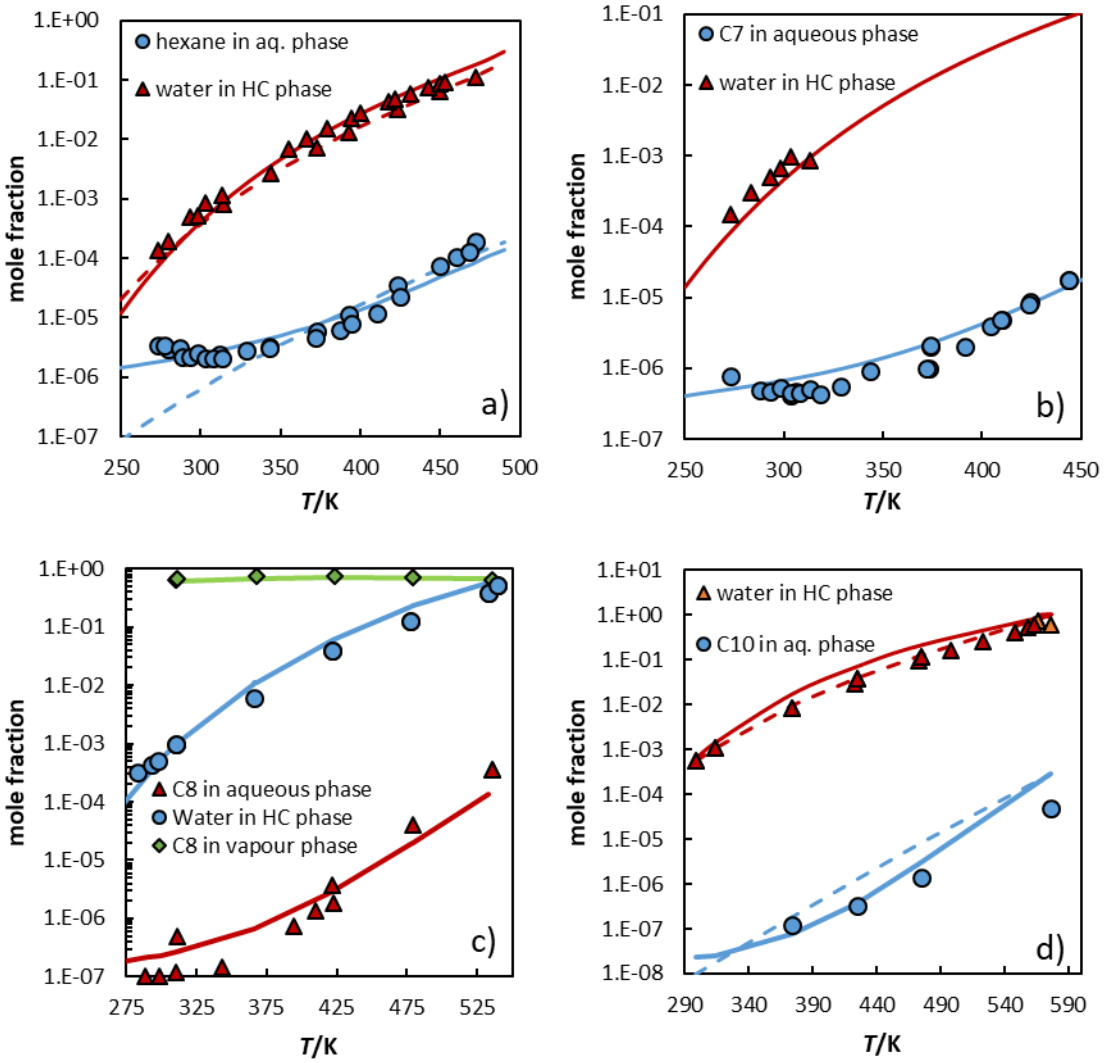

Figure 4.4 Description of the results for water + n-alkane (C_6 to C_{10}, except C_9) with both sets. Full lines are results from this work (a - k_{ij}=0.180; b - k_{ij}=0.150; c - k_{ij}=0.120; d - k_{ij}=0.065), dashed lines are results using s-CPA[125,136] (a - k_{ij}=0.044; d - k_{ij}=-0.069).

As was observed before, the binary interaction parameters are larger than those of s-CPA. Figures 4.5 and 4.6 present the results for the remaining systems used in this analysis. It is important to note that the improvements in the description of the aqueous phase, also introduce a change in the trend for the solubility in the hydrocarbon phase. Thus, if only the hydrocarbon phase was optimized, in some particular cases (mixture with decane), higher

deviations would be observed for the aqueous phase than in s-CPA. However, it is important to note that a relevant variability in the experimental data is verified (noticeable when looking at the mixtures with hexane and octane). Two figures are presented in the annexes, concerning this behavior, including the worst case, the mixture with decane.

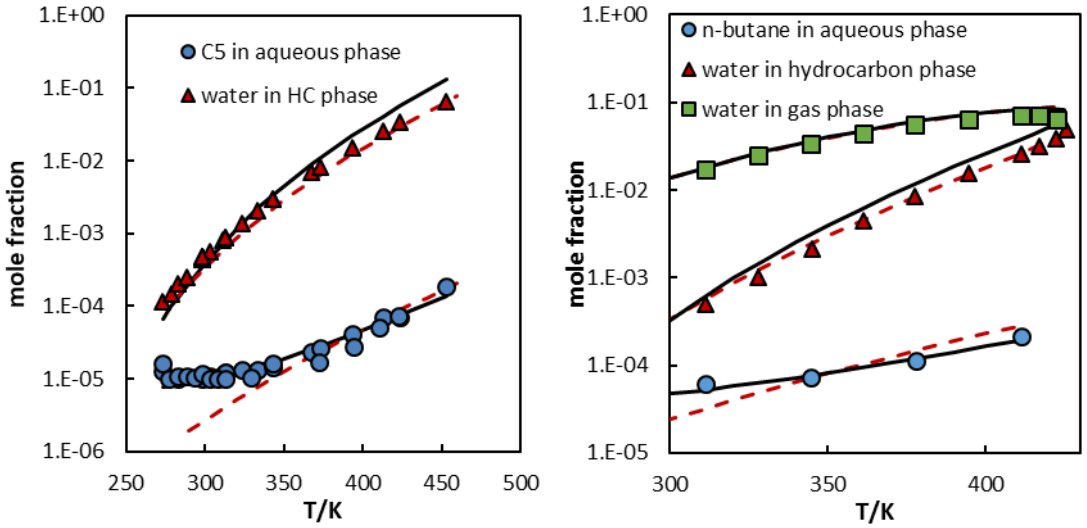

Figure 4.5 Description of the results for water + n-alkane (C_4 and C_5) with both sets. Full lines are results from this work (left - k_{ij}=0.240; right - k_{ij}=0.210), dashed lines are results using s-CPA[125,131,136] (left - k_{ij}=0.085; right - k_{ij}=0.065).

Before addressing a different class of compounds, it is important to evaluate if there is any trend for the binary interaction parameters of water + *n*-alkanes, as previously observed with s-CPA by Oliveira et al.[125] Using the results for the studied systems, it is possible to observe a good correlation for the binary interaction parameters, as can be observed from Figure 4.6.

Later in this paper, the results for some multicomponent systems will be analysed, using water, methanol/MEG and petroleum fractions. Thus, it is of importance to know how the binary interaction parameters of these two other compounds (MEG and methanol) behave for systems with alkanes. The results for methanol are presented in the annexes, while those for MEG are from chapter 3. A trend is also obtained for these systems.

Equations 4.7 to 4.9 present the correlations used between the associative compounds (water, MEG[68] and methanol) and the hydrocarbon molecular weight. Figure 4.6 shows the description of the fitting of the kij's trough these equations.

$$k_{iMEG} = -0.133\ln(MW) + 0.701 \quad (4.7)$$

$$k_{iH_2O} = -0.195\ln(MW) + 1.042 \quad (4.8)$$

$$k_{imethanol} = -2.89 \times 10^{-4} MW + 6.10 \times 10^{-2} \quad (4.9)$$

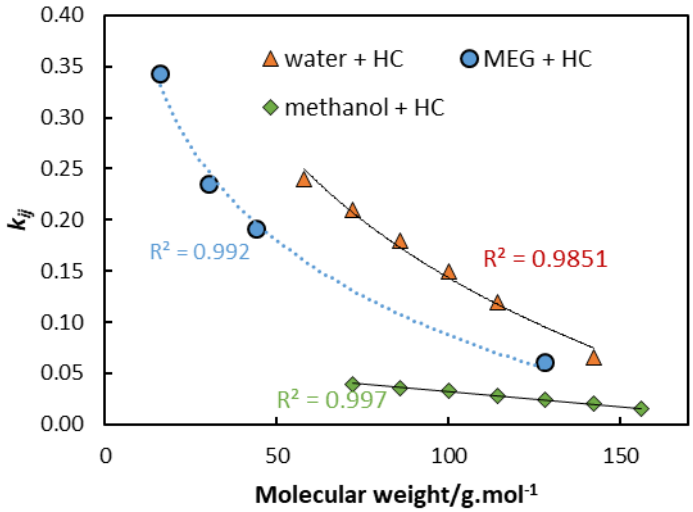

Figure 4.6 k_{ij} correlations applied in this work, for the systems of polar compounds + petroleum fluids

Binary mixtures with aromatic hydrocarbons

Using the approach of Folas et al.[136] for the description of aromatics ($\varepsilon^{ij} = \frac{\varepsilon^{assoc.}}{2}$; $\beta^{ij} = \text{fitted}$) it is possible to describe also the solubility of aromatics with this version of CPA. Figure 4.7 presents the results for water + benzene, water + toluene, water + ethylbenzene and water + o/m/p-xylene. Experimental results for these systems were taken from Góral et al.,[206] Miller and Hawthorne,[207] Jou and Mather,[208] Shen et al.[209] and Pryor and Jentoft.[210]

As in the case of alkanes, the version of CPA applied in this thesis presents a more accurate trend for the solubility of aromatics in the water phase. The results for this group of compounds are in general accurate.

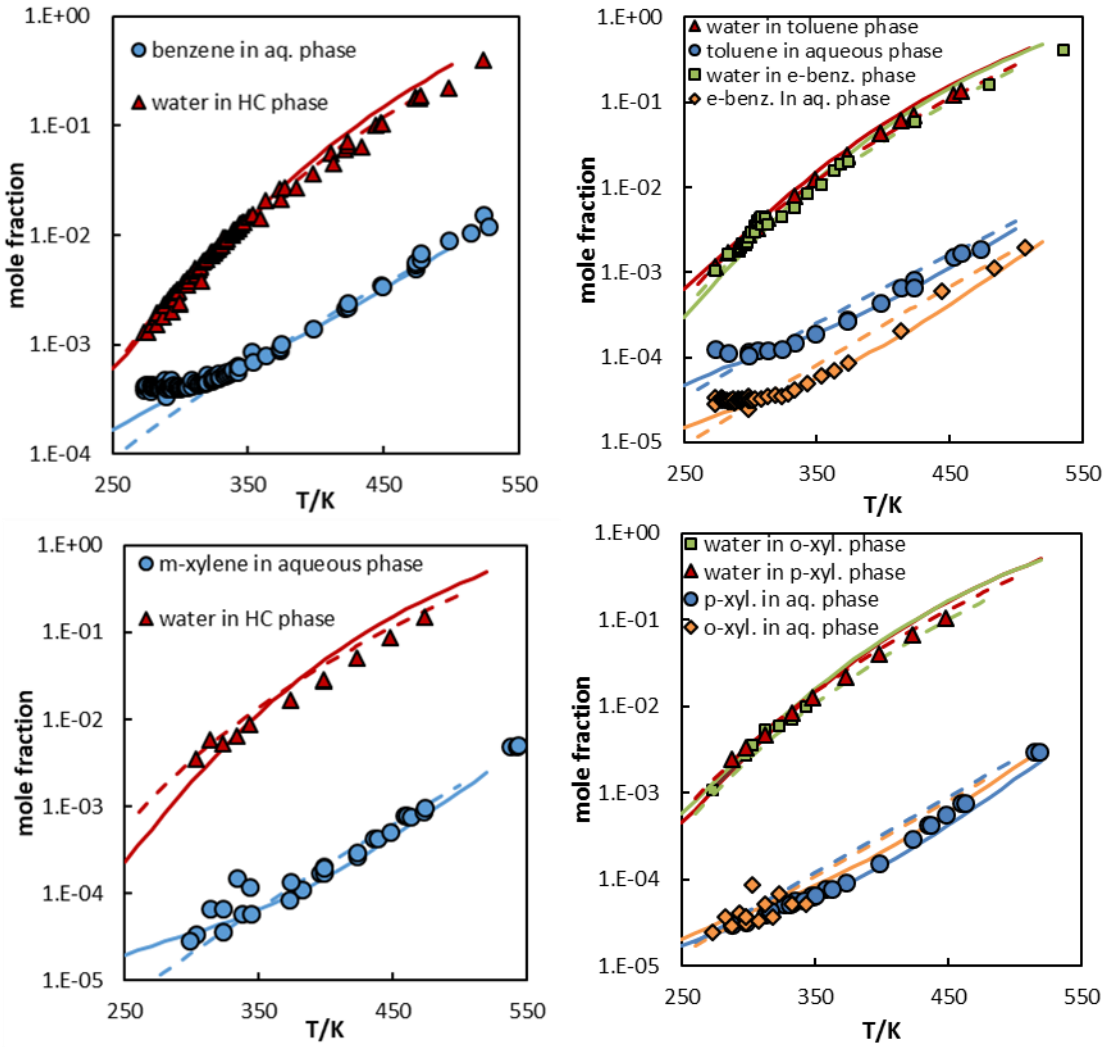

Figure 4.7 Results for water (1) + aromatic hydrocarbon (benzene (2), toluene (3), ethylbenzene (4), m-xylene (5), o-xylene (6) p-xylene (7)). Full lines are the results from this work (k_{12}=0.170, β^{12}=0.0095 ; k_{13}=0.145, β^{13}=0.0090 ; k_{14}=0.120, β^{14}=0.0060 ; k_{15}=0.102, β^{15}=0.0050 ; k_{16}=0.119, β^{16}=0.0080 ; k_{17}=0.111, β^{17}=0.0070), dashed lines are those obtained using s-CPA.[125]

Binary mixtures with alkanols

The improvement on the description of the solubility minima might be in part due to this version of CPA containing more accurate pure component information (more accurate *Cp*, corrected T_c and P_c), however, the higher value for the association energy, and different alpha function, should be the main reason for this enhanced behaviour. A similar effect is observed in systems containing water and *n*-alkanols. However, in this case, the improvement on the qualitative description of the systems does not assure an increase in their overall accuracy, as the influence on the aqueous phase is less accurate in this case. Figure 4.8 presents the results for the systems water + 1-butanol and water + 1-octanol. Experimental data are from Góral et al.[86], Lohmann et al., [211] Hessel et al. [212] and Dallos and Liszi.[213]

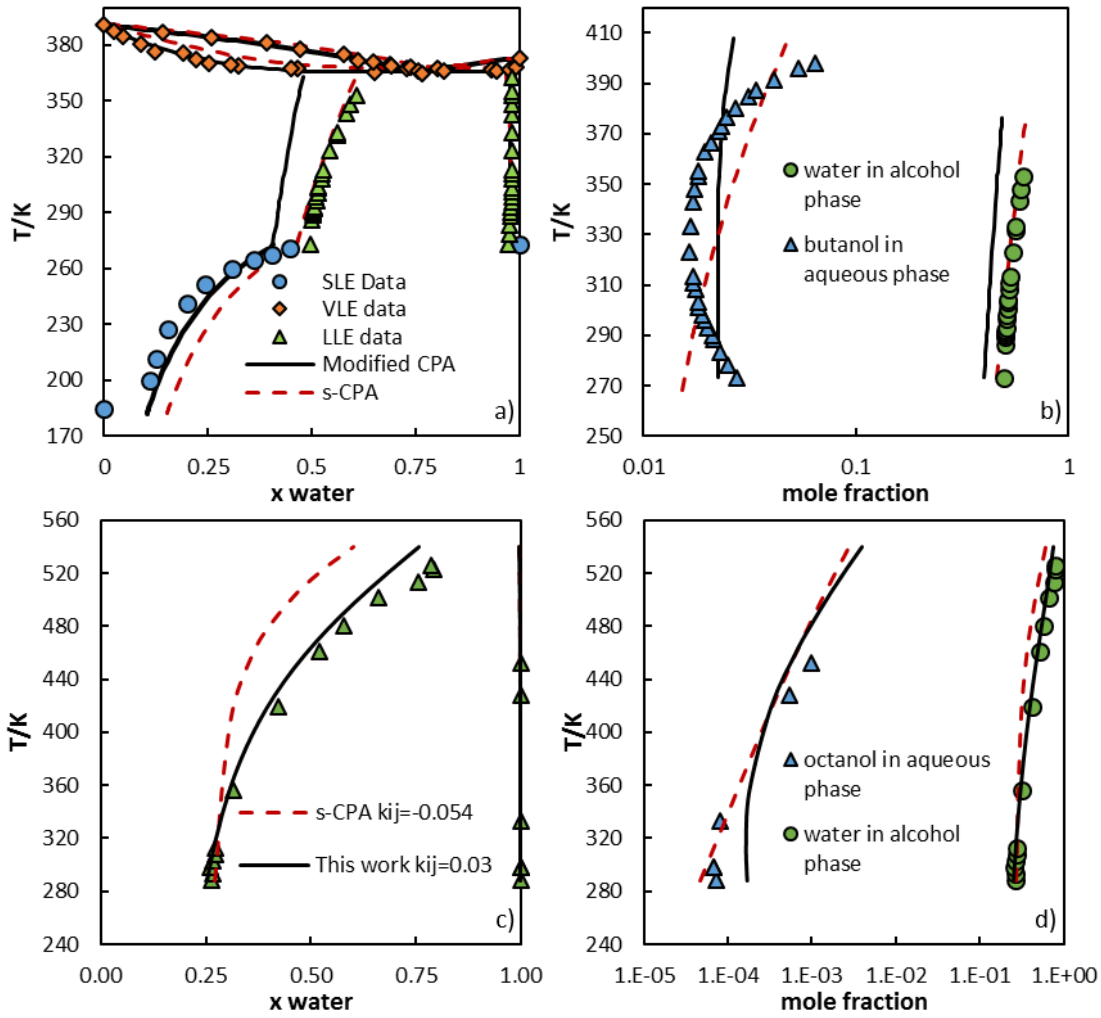

Figure 4.8 Water + 1-butanol, multiphasic results at 1 atm (a) and LLE for a larger range of temperatures (b) with the modified CPA (k_{ij}=0.032) and s-CPA (k_{ij}=-0.065) and LLE for water + 1-octanol (c and d). Using the CR-2 combining rules.

For heavier alcohols, where the association contribution becomes smaller this is less notorious. Also, the current version of the model is using the same association parameters for every OH-group in whatever alcohols,[68,69] which might affect more the LLE results of smaller chain alcohols

The VLE of water with 4 light chain alcohols (methanol, ethanol, 1-propanol and 2-propanol) were also analysed. For the mixtures with methanol and ethanol temperature independent binary interaction parameters (k_{ij}=-0.045 and k_{ij} = -0.004 respectively) were applied, while for the mixtures with 1-propanol and 2-propanol there was a need to apply a temperature dependency in these parameters (water + 1-propanol [k_{ij} = -2.93x10^{-4}T +0.125], water + 2-propanol [k_{ij} = -4.05x10^{-4}T +0.122]). A Table presenting the deviations for these systems is presented as annex. Figure 4.9 presents these binary systems, using data from Voutsas et al.,[214] Vercher et al.,[215] Soujanya et al.[216] and Bermejo et al.[217]

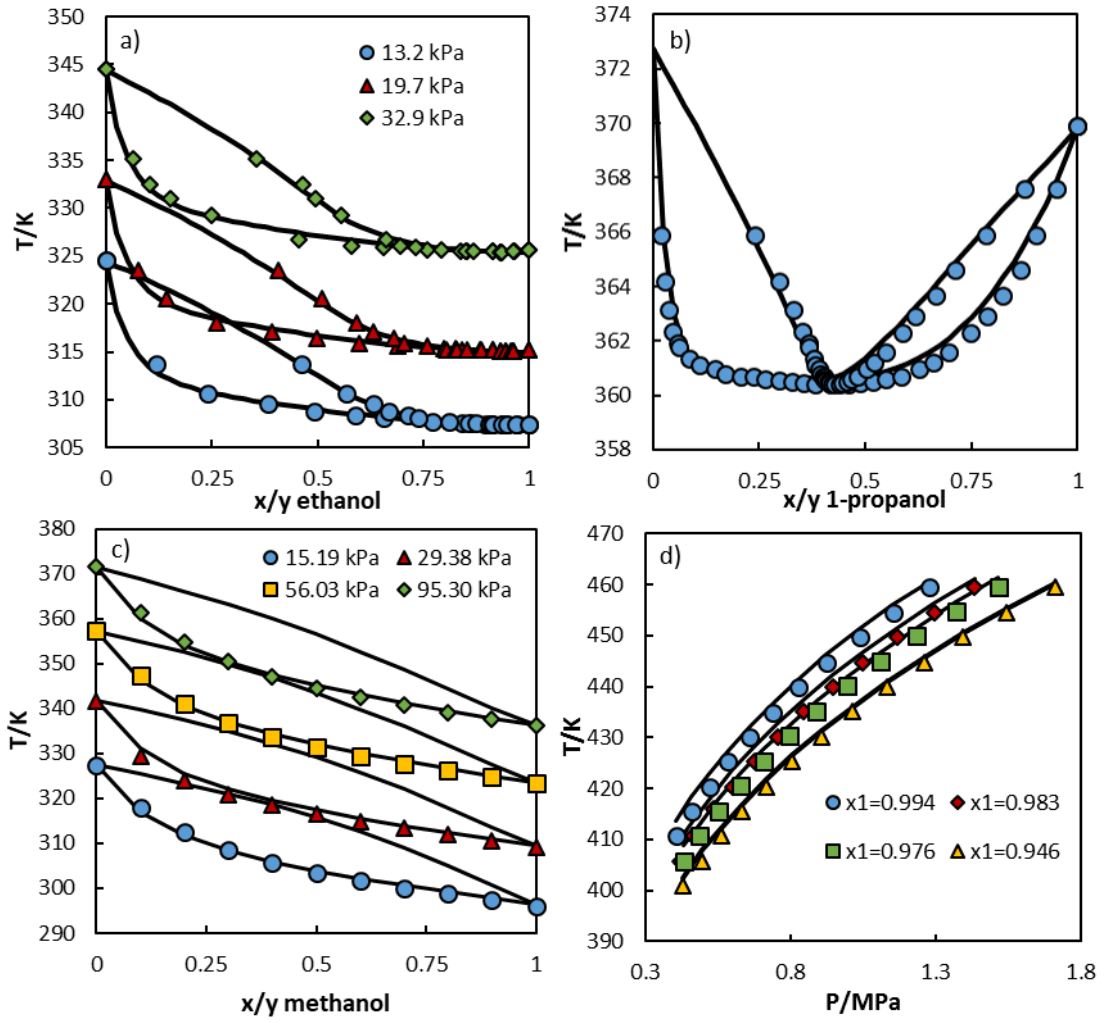

Figure 4.9 Results for water + ethanol at three different pressures (a), water + 1-propanol at 10 bar (b), water + methanol at four different pressures (c) and water + 2-propanol at 1 atm (d).

These results are very accurate and able to describe the VLE of these compounds in a wide range of conditions.

Figure 4.10 presents the results for water + ethylene glycol (using a 2 x 2B association scheme)[68] at 2 different temperatures (k_{ij} = -0.025), as well as the prediction (k_{ij} = 0) of the VLE for water + 1,3-propanediol and the correlation (k_{ij}=-0.030) for the VLE of water + glycerol. Experimental data are from Kamihama et al.,[218] Sanz et al.[219], Oliveira et al.[127] and Soujanya et al.[216]

The ternary system containing these compounds was also studied yielding 1.20% of absolute average deviation on the bubble temperatures and 4.15% on the dew temperatures, when compared to the results of Sanz et al.[219]. A Table with these results is also presented in the annexes.

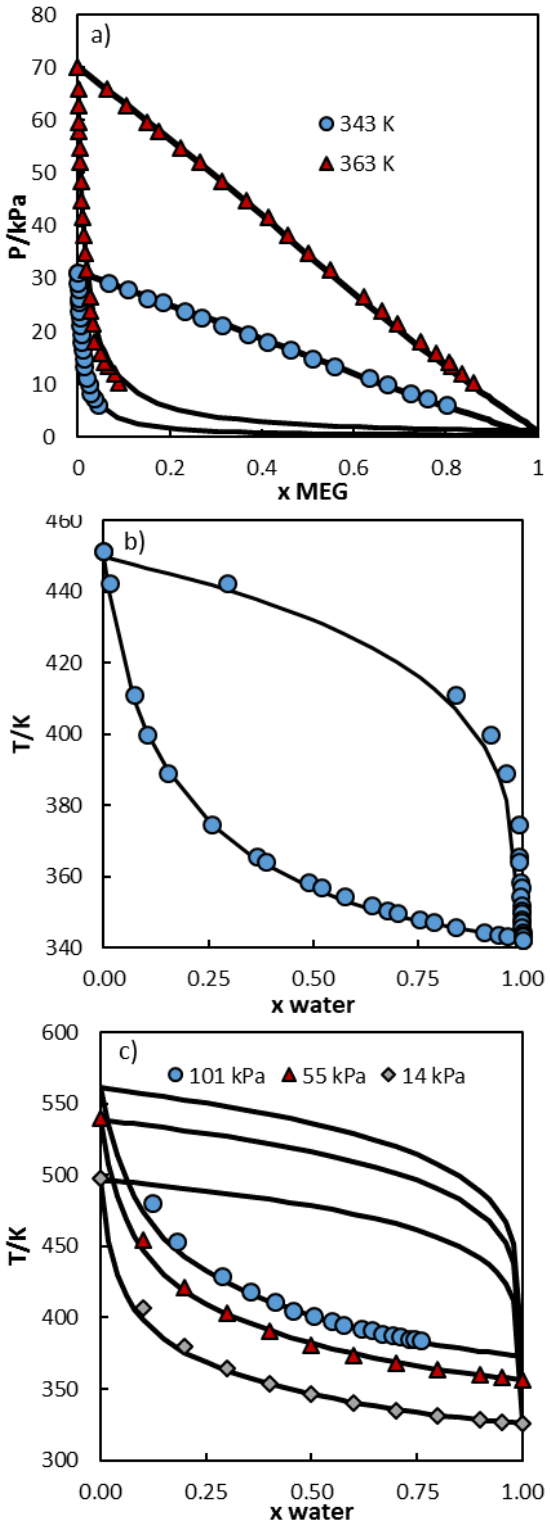

igure 4.10 Results for water + ethylene glycol at 2 different temperatures (a), water + 1,3-propanediol at 30 kPa (b) and for water + glycerol at 3 different pressures (c).

Solubility of water in gas/gas in water

Description of the solubility for binary systems containing lighter alkanes and water, despite being possible with a temperature independent binary interaction parameter, usually requires a temperature dependency for an accurate description of both phases. Figures 4.11 and 4.12 present the results for gas solubility of the three lighter alkanes with water. Experimental data values are from Kiepe et al.[220], Rigby and Prausnitz,[221] Lekvam et al.,[222] Mohammadi et al.,[223] Coan and King[224], Chapoy et al.[225] and Kobayashi et al.[226]

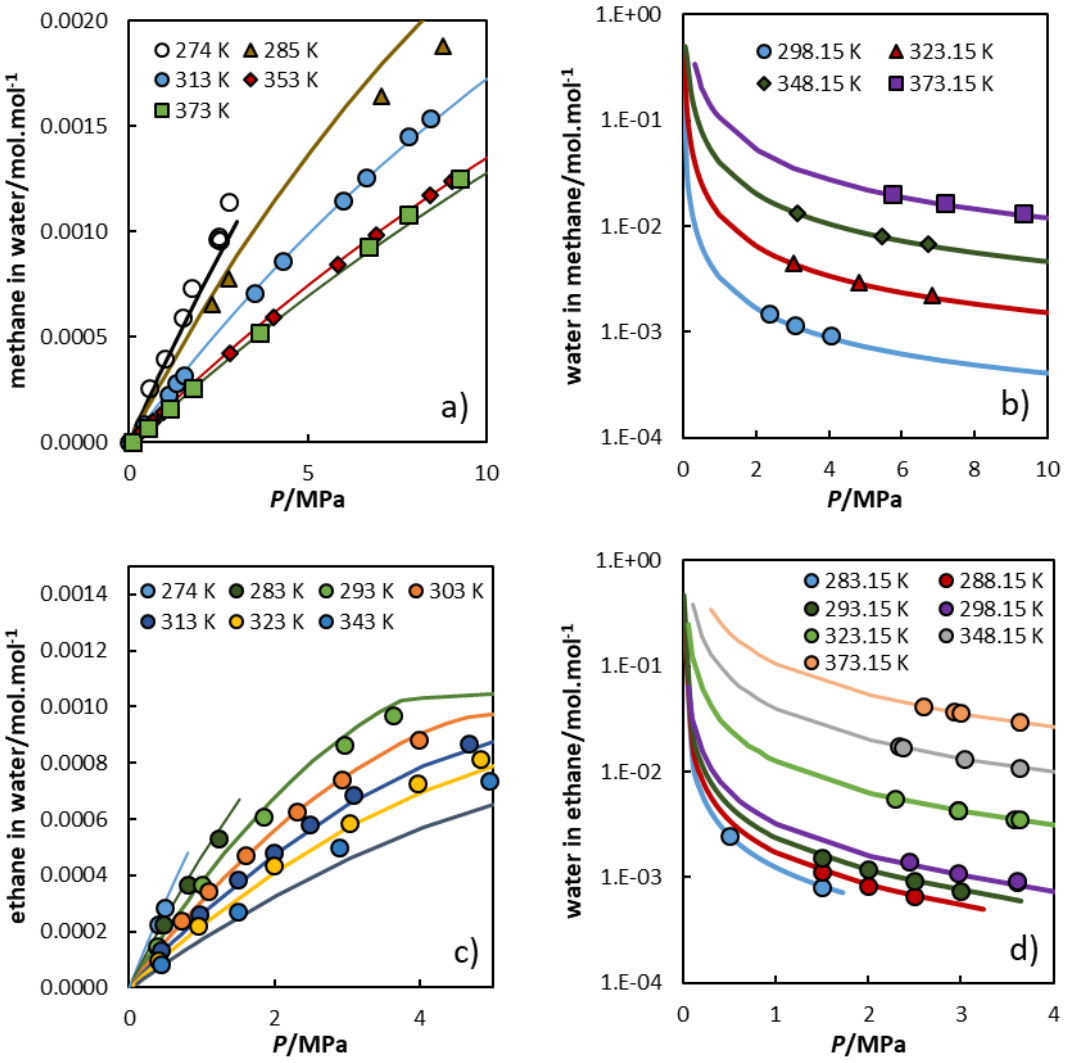

Figure 4.11 Mutual solubility for methane + water (a, b; k_{ij} = 1.48x10^{-3}*T* -0.093) and for ethane + water (c, d; k_{ij} = 9.95x10^{-4}*T*).

The results for the system water+ methane shows the model to be able to accurately describe the solubility of water in the gaseous phase while presenting good results in the liquid phase. For higher temperatures the pressure dependencies start to present deviations. Similar results are obtained for the systems containing ethane and propane.

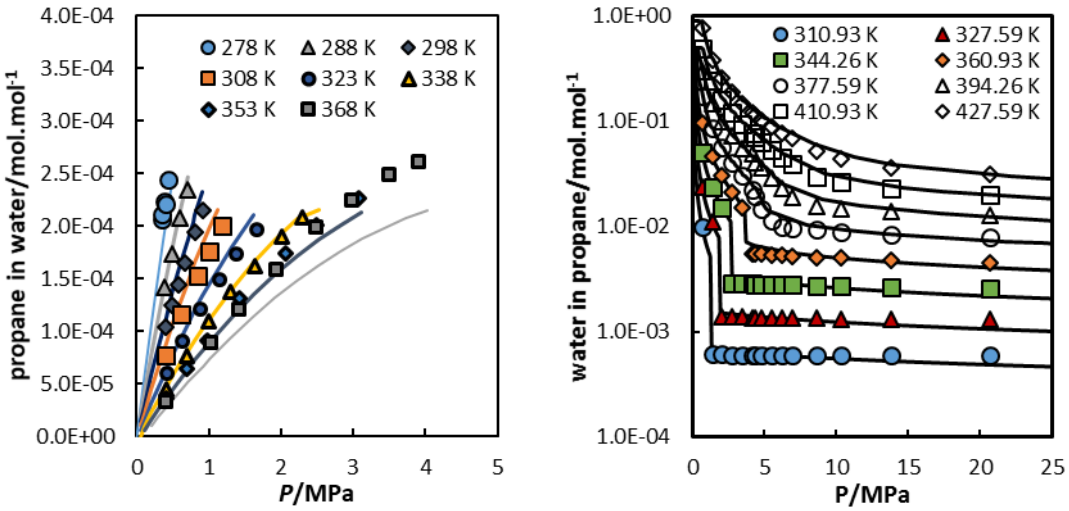

Figure 4.12 Mutual solubility for propane + water with k_{ij} = 8.90x10^{-4}T -0.01.

Aqueous mixtures containing nitrogen and carbon dioxide were also studied, while considering these compounds as non-associative. For the former, the results are accurate in both phases, using a temperature dependent k_{ij} (k_{ij} = 3.30x10^{-3}T -0.6), while for the latter the solubility in water is well described (k_{ij} = 7.20x10^{-4}T -0.07). These results are presented in Figure 4.13. Experimental data was obtained from Rigby and Prausnitz[221], King et al.[227] and Hou et al.[228].

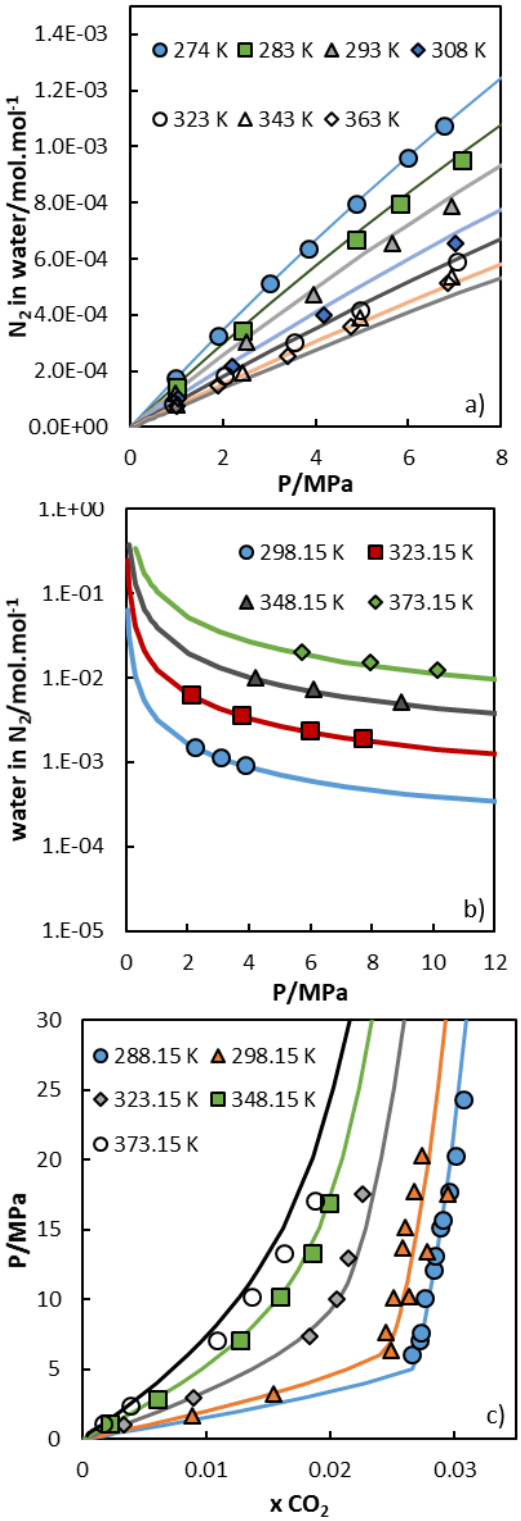

Figure 4.13 Results for the solubility of N_2 in water (a), water in N_2 (b) and CO_2 in water (c).

Multicomponent mixtures

Having established the ability of our new version of CPA to describe with accuracy binary systems with water and a range of different compounds, we turned our attention to the evaluation of its ability to describe more complex mixtures. For a start, two ternary systems

were studied: MEG + water+ methane and MEG + water + ethanol. The results for the VLLE of the first system are presented in Figure 4.14, while for the second the %AAD of the bubble temperature is 0.19 and for the dew temperatures is 0.71. The results for this second system when compared to the data of Kamihama et al.[229] are presented in the annexes. More results at different conditions, for the mixture presented in Figure 4.14 are in the annexes.

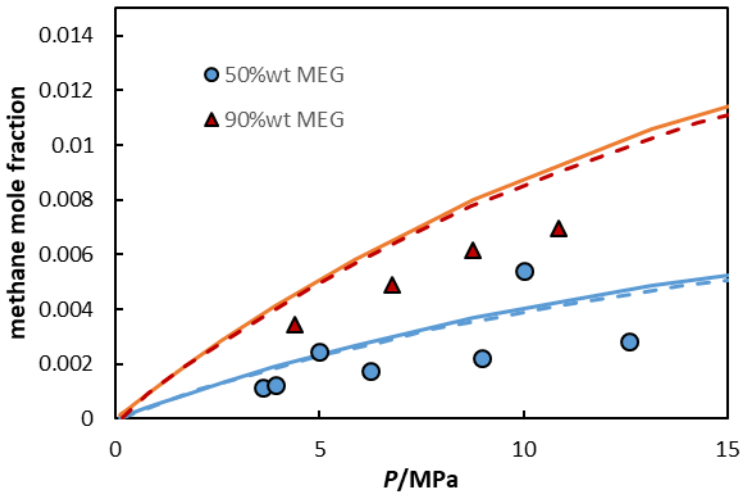

Figure 4.14 Results for the solubility of methane in water + MEG at 298.15 K (right). Full lines- modified CPA results. Dashed lines – s-CPA results. Data from Folas et al.[141] and Burgass et al.[230]

As discussed in chapter 3, this version of CPA is able to describe multicomponent systems containing ethylene glycol. These mixtures have been analysed by Kontogeorgis and co-workers,[181,188,190–192,231,232] using s-CPA, with good results. Two of these systems have not been previously studied using this version of the model and the results of these fluids when mixed with MEG are presented in the annexes.

It is important to note that the parameters used for the interactions between water/methanol and methane/ethane/propane are those previously fitted in this thesis. For many of these systems a temperature dependency was needed on the k_{ij} to correctly describe the phase equilibria. The binary interaction parameters between associative compounds are those obtained for their binary VLE description.

Figures 4.15 and 4.16 present the results for some of the systems of water + MEG + oil-based fluid studied by Kontogeorgis and co-workers[181,188,190–192,231,232] using the version of CPA proposed here. In the annexes a Table is presented comparing the average deviations of the two CPA versions for these systems. The condensate description, considered the real components up to five carbons. From six carbons up to nine carbons, four molecular lumps were considered (C6, C7, C8, C9), where all compounds in the mixture with that carbon

number were considered. Heavier molecules with ten or more carbons were considered in a single lump (C10+) with averaged properties.

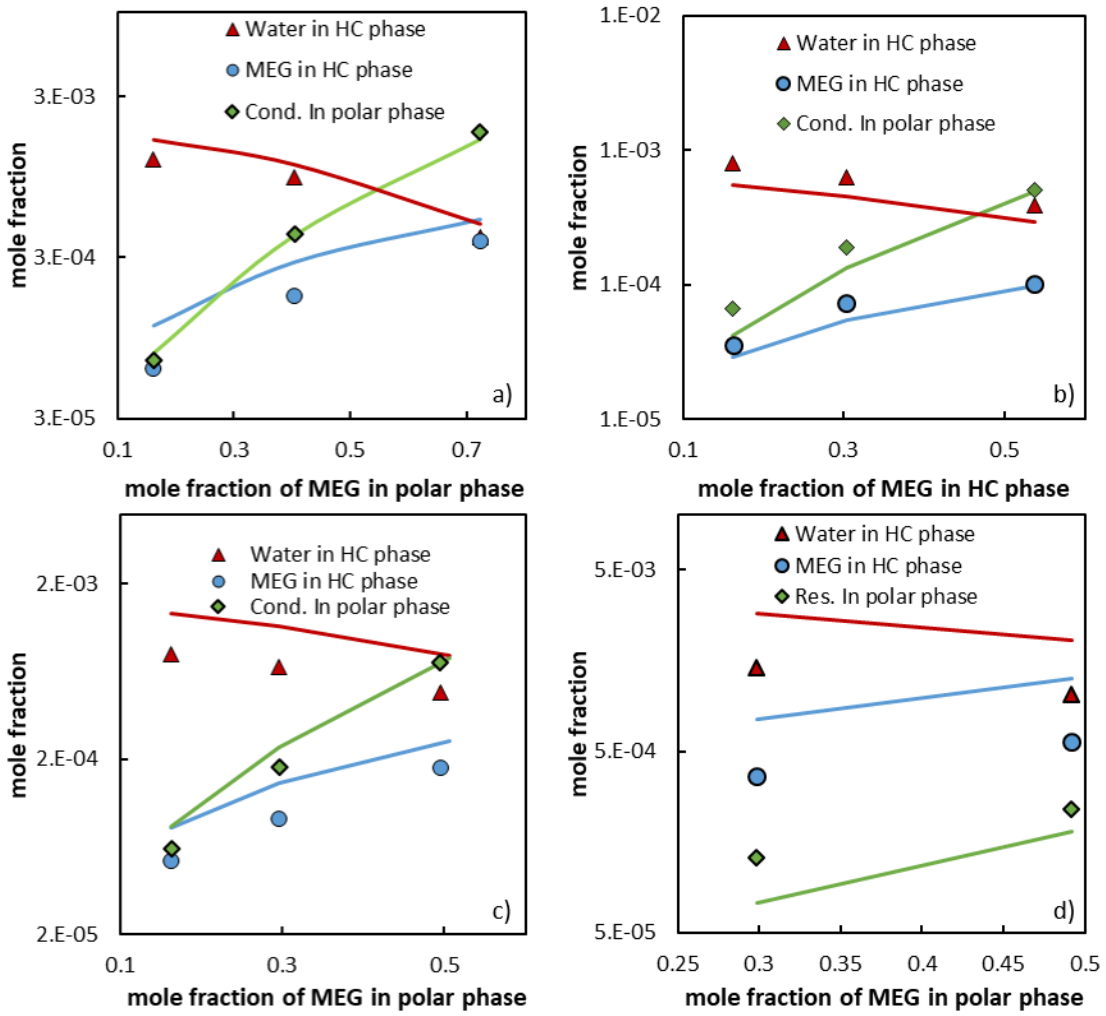

Figure 4.15 Results for the system cond-1 + water + MEG at 323 K (a), cond-2 + water + MEG at 303 K (b), cond-3 + water + MEG at 323 K (c) and for the system Light-oil 1 + water + MEG at 303 K (d). Data from Riaz et al.[188,191,231] and Frost et al.[190]

Accurate results are also obtained for the polar compounds in the hydrocarbon phase in most systems, but a higher decrease on the accuracy is verified for the heaviest system (light oil), than with s-CPA.

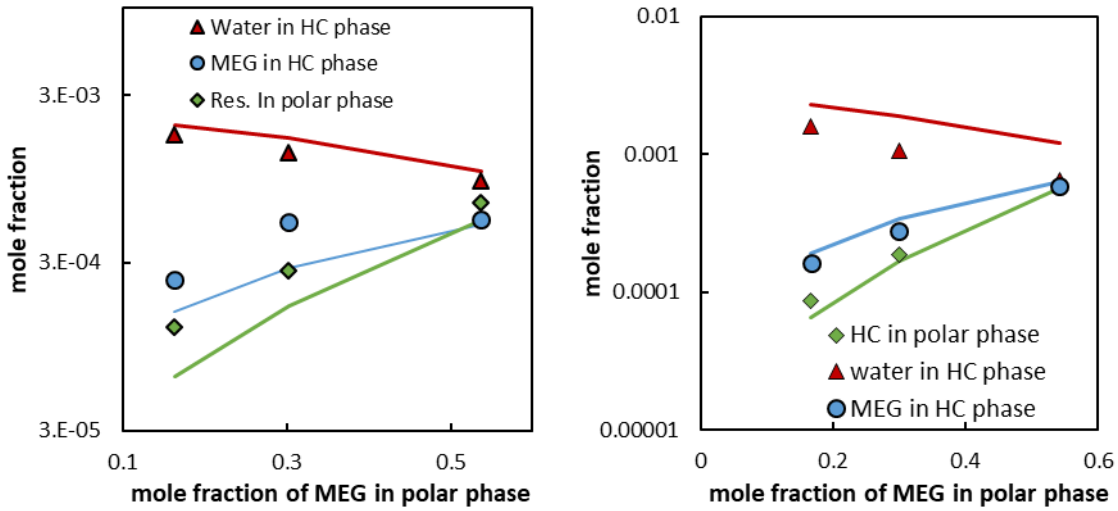

Figure 4.16 Results for the system Light-oil 2 + water + MEG at 323 K (left) and Fluid-1 + water + MEG at 323 K (right). Data from Riaz et al.[231] and Frost et al.[192]

Applying the same approach, the description of the gas condensate studied by Pedersen et al. [233] was also tested. These results are presented in Figure 4.17, as well as, those from Yan et al. using s-CPA[234]. The results obtained for these system are, in general, comparable to those of s-CPA.

Concerning results with water + methanol + HC, the mixture 2 presented by Pedersen et al.[235] and a synthetic mixture from Rossihol[236] are analysed. These results are compared to those of Yan et al.[234] on Tables in annex. It is notorious that the results obtained with the two CPA versions diverge on the accuracy for the methanol fraction in the hydrocarbon phase. The s-CPA presents significant deviations for this fraction in the synthetic mixture, while the version applied in this thesis provides a good description of the experimental data. The opposite is verified with the data from Pedersen et al.[235], while the main component in the condensate being the same as in the quaternary mixture (methane, and in similar proportions). This should in part be due to the use of diferrent combining rules, as the ratio water : methanol is rather different in these systems, and the use of different approaches for the binary interaction parameters calculation between the two versions.

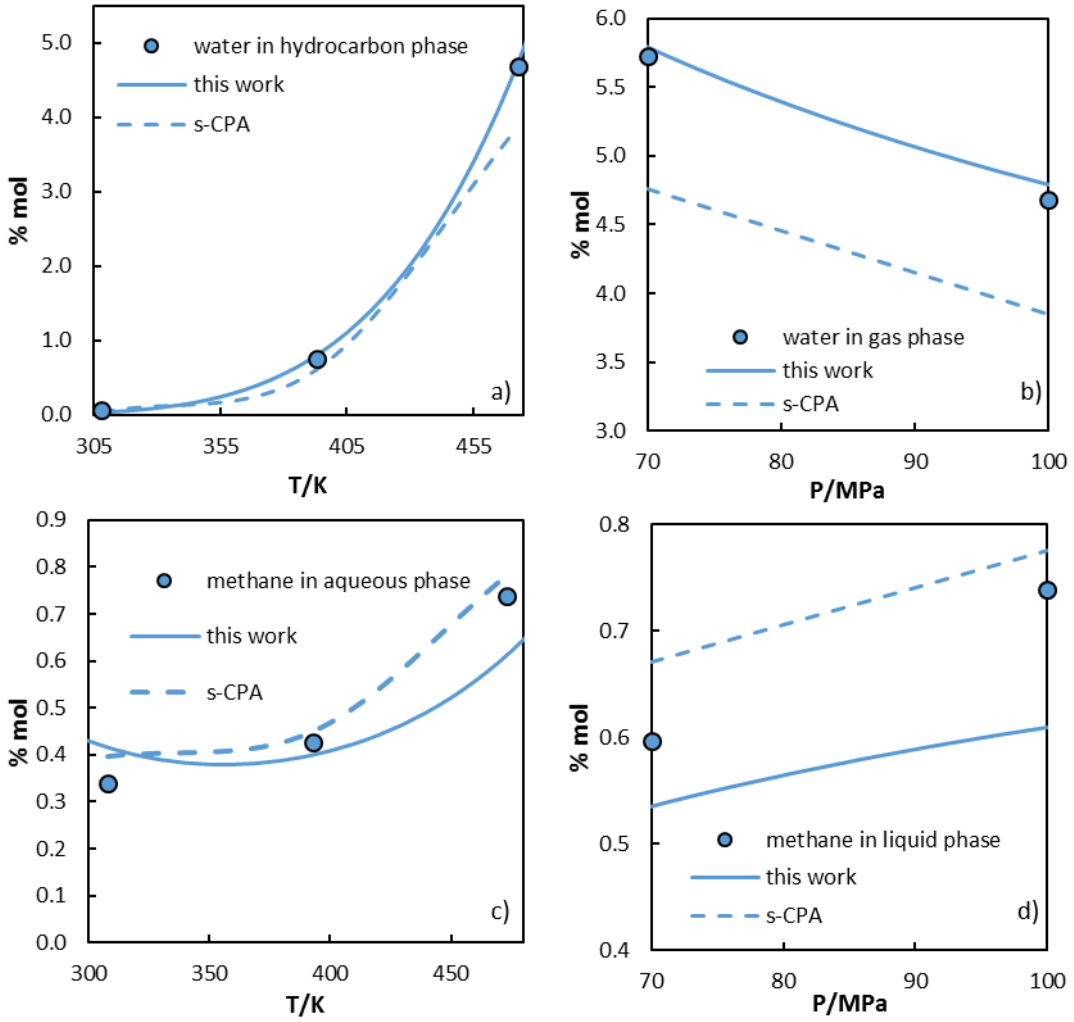

Figure 4.17 Results for the water solubility in the hydrocarbon phase at 100 MPa (a) and 473.15 K (b) and for the methane solubility in the aqueous phase at 100 MPa (c) and 473.15 K (d) (left).

4.4 Conclusions

A new version of CPA is evaluated here for the description of water containing mixtures. While its description of density for small, highly associative compounds, with a volume shift applied at 0.7 T_c, presents somewhat higher deviations, the trend with temperature is more accurate than that obtained with s-CPA. Moreover if a lower T_r is used to fit the volume shift, it is possible to obtain reasonable results for density between 0.45 and 0.85 T_r. The modifications applied in this version also lead to a better description of liquid C_p and correct values for T_c and P_c. This also enables the correct trend for the description of the heat of vaporization, as well as, a better trend with temperature for C_v. It is also important to note that for the compounds

with hydroxyl groups studied in this thesis it was possible to consider the association energy as constant.

The parameters for water on this version also lead to a higher temperature dependency on the association term, this in turn, leads to a different behavior, than previous versions, on the solubility of alkanes/alkanols in water. The solubility of the second compound, in many of these systems, now presents a trend closer to what is experimentally observed.

Accurate results are obtained for the description of the vapor liquid equilibria with alkanols and the solubility of gases in water/water in gases. It is important to remember that a single combining rule for the association parameters was applied, while some of the results from s-CPA have used different combining rules.

In the case of multicomponent systems, seven petroleum fluids were studied, using correlations for the interaction parameters between water/MEG and the petroleum compounds/fractions. These results are in most cases accurate with a decrease in accuracy for heavier fluids, which is to be expected due to the large extrapolations used in these cases. The results for multicomponent systems are comparable to those of s-CPA, while in general improving the results of binary LLE equilibria and pure properties.

This version of CPA is thus able to describe a relevant group of properties for a complex molecule like water, while presenting very promising results for VLE and LLE and an accurate representation of multicomponent systems.

5 Thiols and amines

5.1 Abstract

The predictive capacities of a modified CPA model have been analyzed in the previous chapters for compounds containing hydroxyl groups. Following that work it is now important to verify if the approaches proposed before are adequate for the description of other association groups, such as thiols and amines. This section addresses short chain thiols, (both primary and secondary), as well as three secondary amines. The analysis performed here has a focus on the pure component properties as well as on the VLE of these compounds with alkanes, aromatics, ketones, water or alkanols.

5.2 Introduction

Thiols are used or formed in a large range of industries. Some examples are the production of insecticides, petroleum refining, kraft pulping to produce paper and sewage treatment plants. These compounds are also commonly found in industrial waste streams, and, despite their concentrations in these streams being usually far below toxic levels, the strong odors of these compounds are notorious even when in small concentrations, what often requires specific treatments. [237]

Some examples of applications of secondary amines include the use of dimethylamine and dipropylamine for the production of herbicides, fungicides and disinfectants for agriculture and the use of diethylamine in the production of N,N-diethylaminoethanol. [238]

The use of s-CPA for the description of thiols has been reported for both pure properties and mixtures with alkanes [239,240]. Kaarsholm et al. [241] used s-CPA to study a large group of amines and their phase equilibria with alkanes and alkanols, presenting accurate results for these mixtures and showing relevant advantages over SRK.

Other associating models have also been applied to study amines. A large group of amines, including secondary amines, was studied by Rozmus et al. [242] with GC-PPC-SAFT, presenting a good description of phase equilibria and some mixture properties. Diverse other studies exist concerning amines with SAFT variants, [36,53,90,243,244] those are however more focused on tertiary and/or primary amines and when mixture results are presented, those are accurately described.

In this chapter, results are presented first for the description of pure properties (vapour pressure, saturated liquid densities, heat of vaporization and C_p) for both groups of compounds. The modelling of the phase behavior of secondary amines with alkanes and other

hydrocarbons is then analyzed, considering in most cases a predictive approach where no binary interaction parameters are applied. Results for the description of thiols + hydrocarbons and amines + other associative compounds are also reported and, when available, the results are compared to those of s-CPA.

5.3 Results

5.3.1 Pure component results

Similarly to the procedure previously described for the hydroxyl group, for thiols and secondary amines, the energy of association was kept constant between the same group of compounds, while the association volume was adjusted for the two lighter compounds of each family and kept constant for the remaining compounds. To be noted, these values differ for primary and secondary thiols (Table 5.1). The association scheme applied for both group of compounds was 2B. Primary amines were not studied at this time. In the future we intend to analyze which is the more adequate association scheme for primary amines with this version of CPA (either 2B or 3B). However, at the moment the code is only able to cope with groups with the same number of acceptor and donor sites. Thus, before these modifications, it is not possible to analyze the 3B scheme.

The experimental data used for the pure compounds parameterization was taken from the DIPPR [79] and TRC [80] databases, as well as from the correlations present in Multiflash [78].

The parameters obtained for each pure compound are presented in tables 5.1 and 5.2 except for the energy of association (ε), which is 13915 J.mol^{-1}.K^{-1} for thiols and 13456 J.mol^{-1}.K^{-1} for amines. Deviations on the property description are presented in the annexes, while H^{vap} , liquid densities and C_p are plotted in figures 5.1 to 5.4. The trend of the parameters, a_c and b, is also presented in figure 5.5. As in the previous chapters the cubic term parameters were fitted to saturation pressure data. Heat of vaporization data was applied in the fitting of the association parameters. These data values were taken from the DIPPR [79] and TRC [80] databases. Tables 5.3 and 5.4 present the T_c and P_c data used for the compounds studied in this chapter.

Table 5.1 Modified CPA parameters fitted for thiols using a 2B association scheme. The energy of association is 13915 J.mol^{-1}.K^{-1}

Compound	a_c (Pa.m^6.mol^{-2})	b. 10^5 (m^3.mol^{-1})	c_1	c_2	c_3	c_4	c_5	β.10^2	*vshift* (m^3.kmol^{-1})
methanethiol	0.87	4.83	1.01	-5.93	27.7	-71.4	71.7	0.50	0.007
ethanethiol	1.32	6.70	0.78	-0.83	-0.2	0.1	0.0	0.38	0.009
1-propanethiol	1.83	8.39	0.94	-1.96	9.9	-24.4	18.5	0.09	0.011
1-butanethiol	2.41	10.39	1.06	-2.30	10.1	-21.0	13.4	0.09	0.016
2-propanethiol	1.66	7.89	0.97	-2.44	11.1	-24.7	16.9	0.08	0.003
2-butanethiol	2.23	9.87	1.01	-2.08	9.5	-20.9	13.6	0.08	0.009

Table 5.2 Modified CPA parameters fitted for secondary amines using a 2B association scheme. The energy of association is 13456 J.mol^{-1}.K^{-1}

Compound	a_c (Pa.m^6.mol^{-2})	b. 10^5 (m^3.mol^{-1})	c_1	c_2	c_3	c_4	c_5	β.10^2	*vshift* (m^3.kmol^{-1})
dimethylamine	1.03	6.11	1.06	-3.49	11.9	-20.3	13.4	0.43	0.010
diethylamine	1.95	9.74	0.75	1.25	-5.2	3.4	0	0.23	0.016
dipropylamine	2.84	12.69	1.44	-3.32	13.2	-29.8	23	0.11	0.009

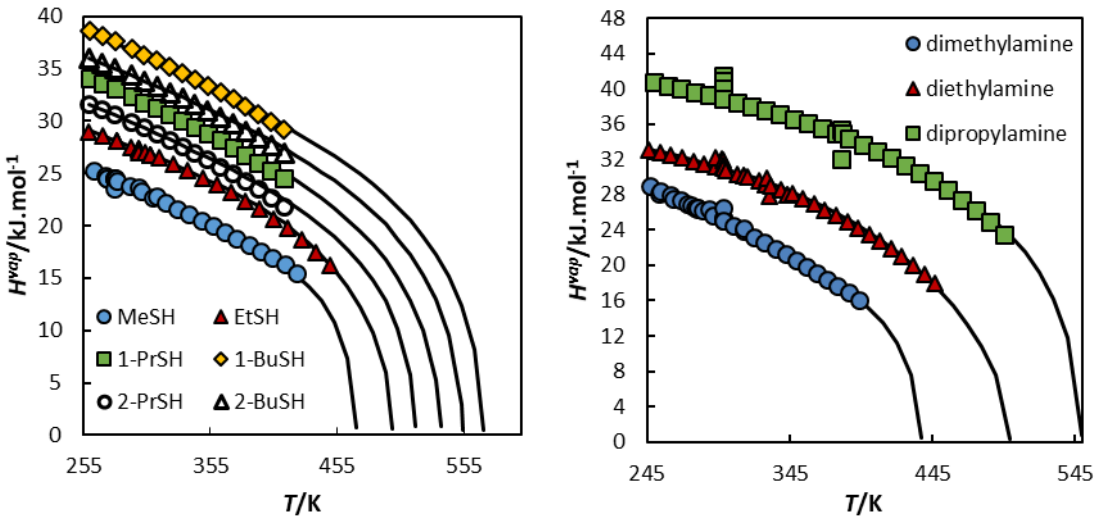

Figure 5.1 Description of the heat of vaporization for thiols (left) and amines (right)

The approach used is shown to be able to describe most of the analyzed pure component properties. For the isobaric heat capacity (C_p), the results are in some cases under/overestimated, which might be influenced by the uncertainties of the ideal gas heat capacity data (which contributes, in most cases, with more than 50% of the total C_p value). Also, for the first compound of each series the tendency observed with temperature is not obeyed. This potentially has to do with the lack of constraints in the fitting of the alpha function parameters and/or uncertainties in the vapor pressure curve. Very small changes in

the temperature range of the fitting, lead to relevant changes in the behavior of the curve. Nevertheless, this might not be the only issue present here.

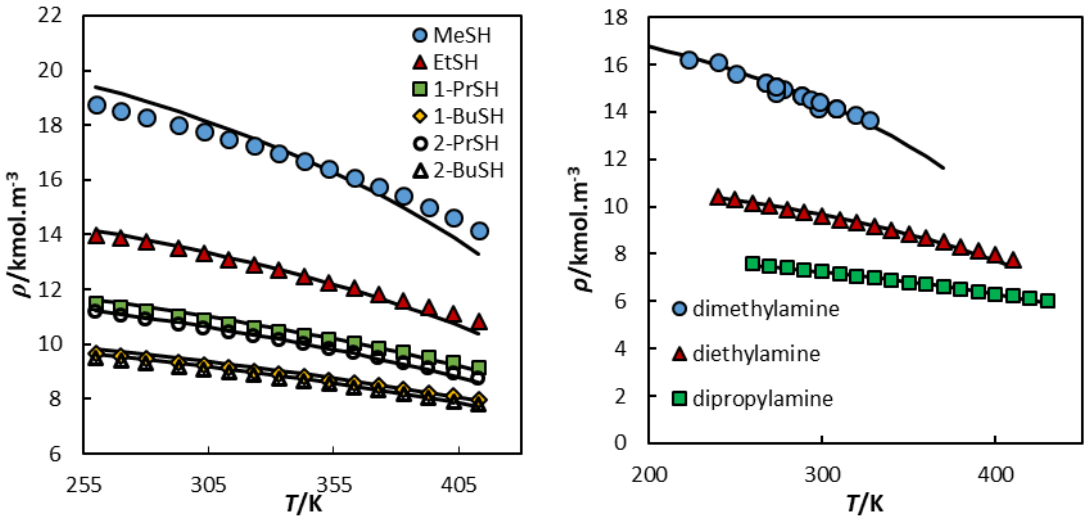

Figure 5.2 Description of liquid density for thiols (left) and amines (right)

For the remaining properties, the results are very good, with liquid densities presenting lower accuracy for the smaller associative compounds, as was the case for the alkanols in chapter 2. In figure 5.5 the trends of the co-volume and energy parameter of the cubic term are analyzed.

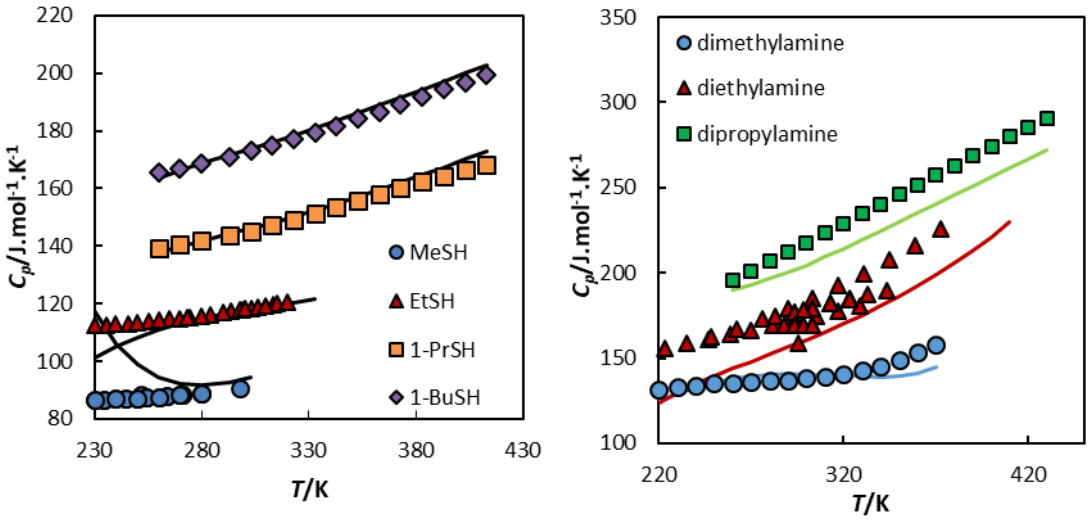

Figure 5.3 Description of liquid C_p for primary thiols (left) and amines (right)

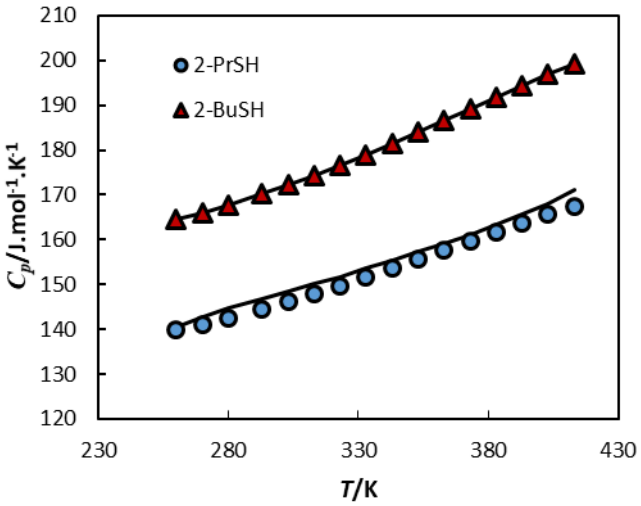

Figure 5.4 Description of liquid C_p for secondary thiols.

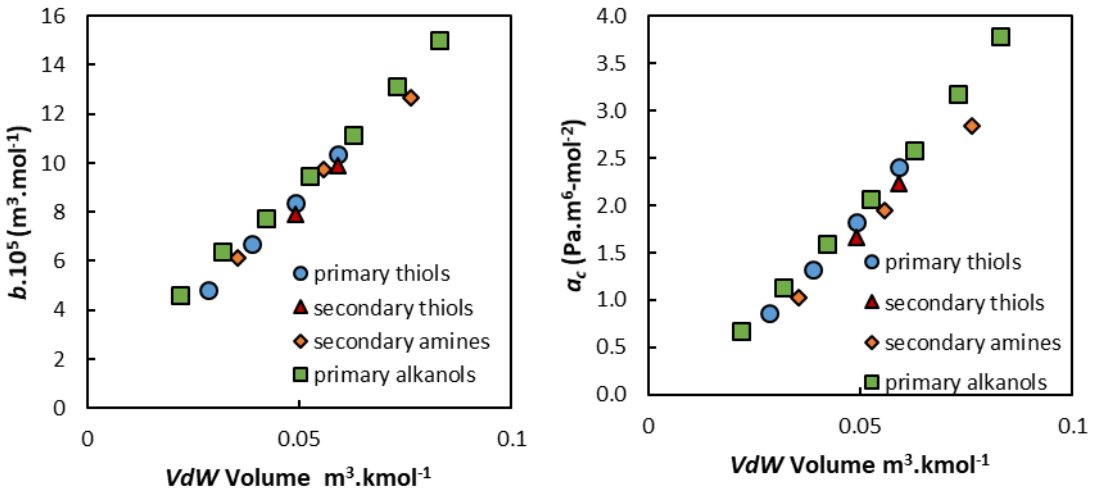

Figure 5.5 Cubic term parameters, a_c (right) and b (left), obtained for the compounds studied in this chapter and those of 1-alkanols up to 1-heptanol, obtained in chapter 2 (table 2.6).

The trends of the co-volume are very similar for the diverse compound groups studied. This is also verified with s-CPA, where Awan et al. [245] have shown a similar trend for thiols with other compounds previously studied.

Table 5.3 T_c and P_c data applied for thiols. The values are from the DIPPR [79] and TRC [80] databases.

compound	T_c/K	P_c/MPa
methanethiol	469.95	7.26
ethanethiol	498.76	5.49
1-propanethiol	536.60	4.63
1-butanethiol	570.10	3.97
2-propanethiol	517.30	4.75
2-butanethiol	554.00	4.06

Table 5.4 T_c and P_c data applied for amines. The values are from the DIPPR [79] and TRC [80]

compound	T_c/K	P_c/MPa
dimethylamine	437.20	5.34
diethylamein	499.60	3.75
dipropylamine	550.00	3.14

5.3.2 Modelling of phase diagrams of binary systems containing secondary amines

Table 5.5 presents the binary interaction parameters for the binary mixtures containing secondary amines.

Table 5.5 Binary interaction parameters applied for the mixtures containing amines.

comp. 1	comp. 2	k_{ij}	s-CPA k_{ij}	figure
n-hexane	dimethylamine	0.000	-	5.6
n-hexane	diethylamine	0.000	0.000	5.7
n-hexane	dipropylamine	0.000	-	5.8
n-heptane	diethylamine	0.000	0.000	5.7
benzene	diethylamine	0.000	0.000	5.8
benzene	diethylamine	-0.028	-0.019	5.8
acetone	diethylamine	0.020	0.011	5.9
water	dipropylamine	$-0.516 + 1.11\times10^{-3}T$	-	5.10, 5.14
water	dipropylamine	$-0.258 + 6.59\times10^{-4}T$	-	5.14
methanol	diethylamine	-0.150	-0.154	5.11
ethanol	diethylamine	-0.110	-0.113	5.12
methanol	dipropylamine	-0.095	-	5.13
ethanol	dipropylamine	-0.040	-	5.13
1-propanol	dipropylamine	-0.068	-	5.13
2-propanol	dipropylamine	-0.010	-	5.13

The ability to describe binary mixtures of amines with alkanes and other hydrocarbons was then investigated. Starting the analysis from the smaller amine in the study, dimethylamine, figure 5.6 presents the VLE predictions (k_{ij} = 0.0), for mixtures of this compound with hexane.

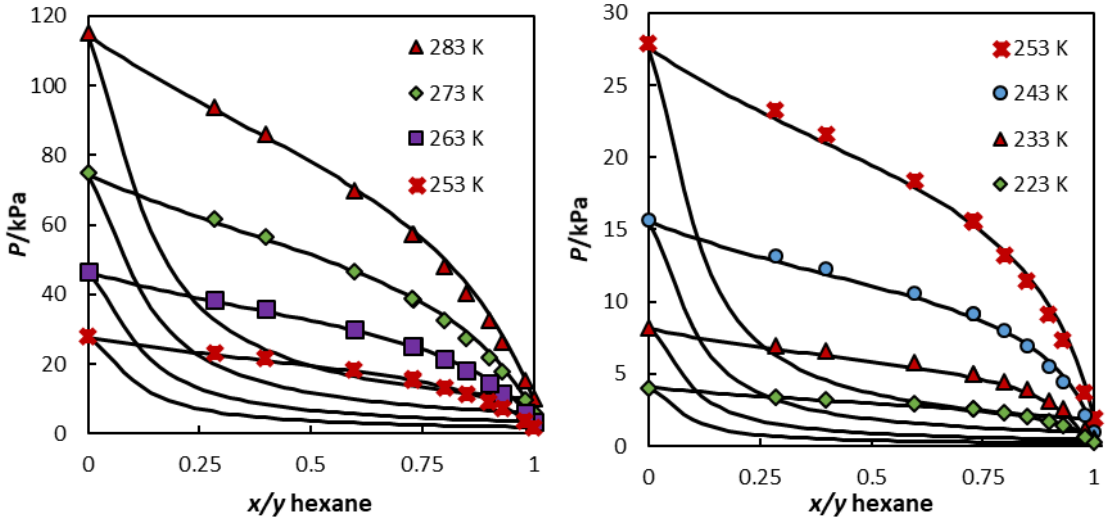

Figure 5.6 VLE of n-hexane + dimethylamine at eight different temperatures. Data from Wolff and Wuertz [246].

The predictive approach provided an accurate description of the system in the range of temperatures studied. This approach (no k_{ij}) also provides good results for the diethylamine + hexane and diethylamine + heptane systems presented in figure 5.7. Besides the modified CPA the s-CPA model was also used and shown to be able to provide an accurate descriptions of the systems studied.

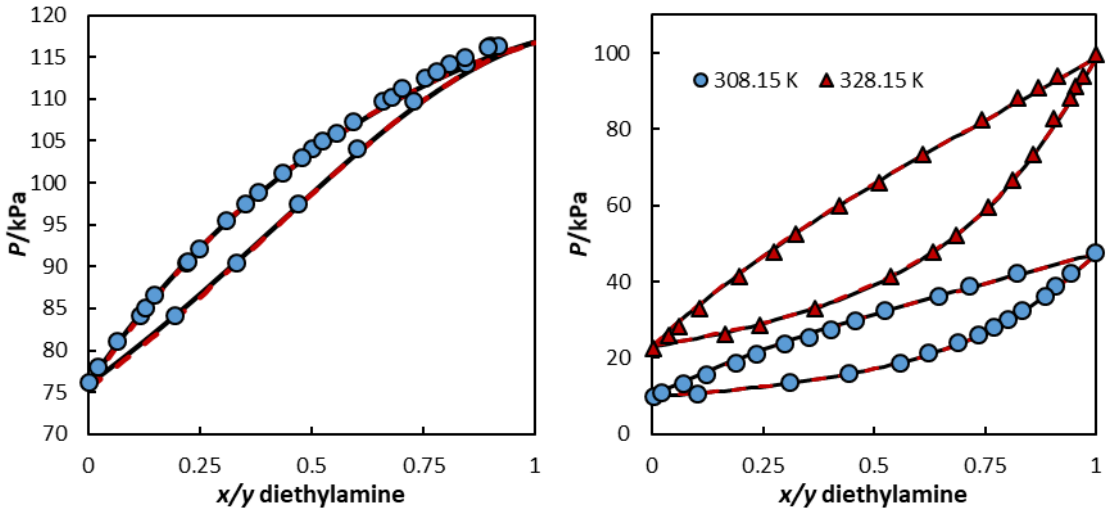

Figure 5.7 VLE of n-hexane + diethylamine at 333.15 K (left) and n-heptane + diethylamine at two different temperatures (right). Full lines – Modified CPA, Dashed lines – s-CPA. The s-CPA results on the left were previously obtained by Kaarsholm et al. [241] Data are from Humphrey and van Winkle [247] and Letcher et al. [248]

To complete the study of the ability of the modified model to describe *n*-alkanes + secondary amines, in figure 5.8 the predictions of the VLE phase diagram for dipropylamine + hexane and diethylamine + benzene are presented.

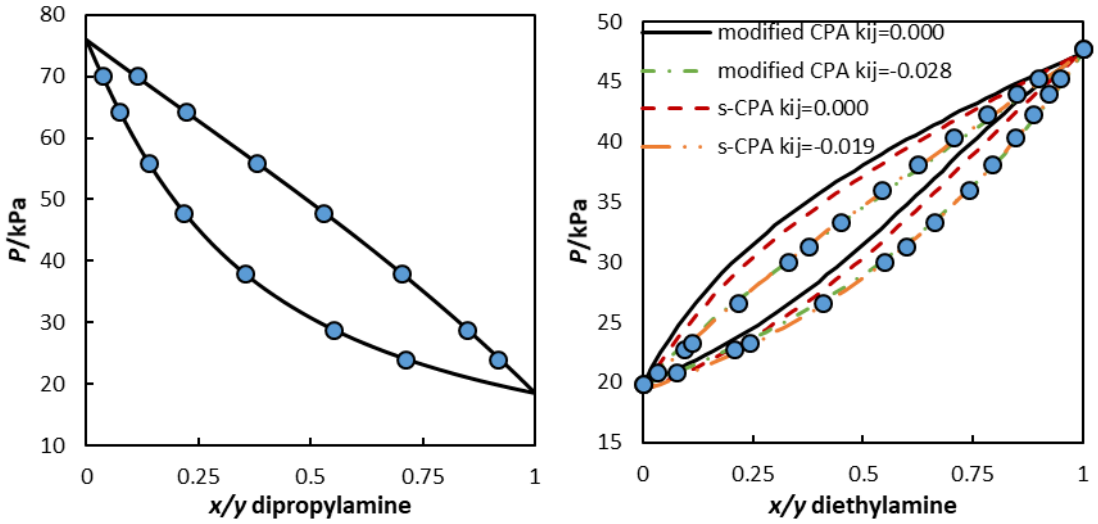

Figure 5.8 VLE prediction of n-hexane + dipropylamine at 333.15 K (left) and prediction/correlation results for benzene + diethylamine at 308.14 K (right). Data were taken from the TRC database[80] and Humphrey and van Winkle [247]

Very good results were obtained for the systems presented above, using only binary interaction parameters for the system containing benzene. This demonstrates that the modified CPA model proposed in this thesis is able to deal with mixtures containing associating compounds other than alcohols and water.

Mixtures containing alkanols, acetone and water were also studied. Figures 5.9 and 5.10 presents the results for the binaries diethylamine + acetone and dipropylamine + water.

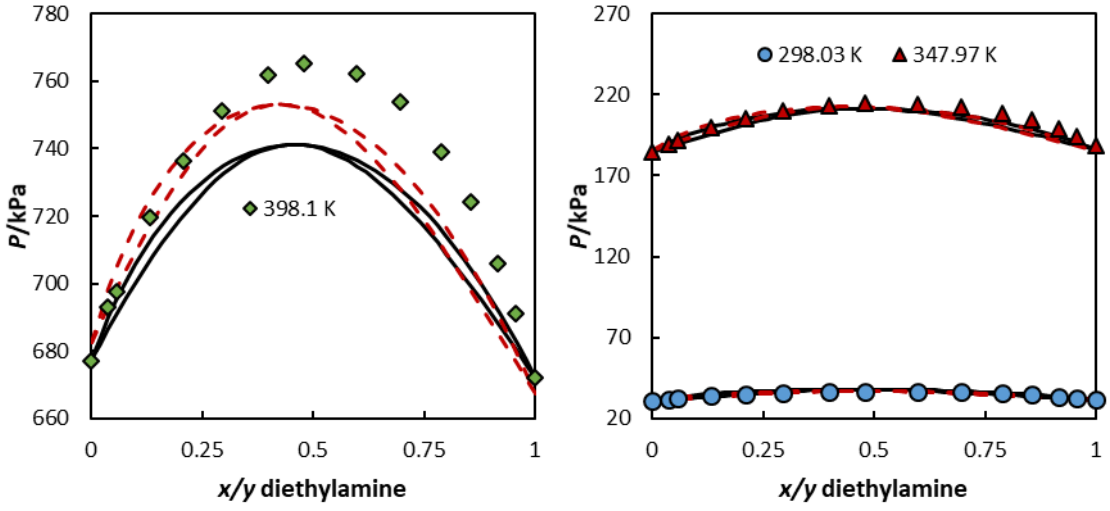

Figure 5.9 VLE results for acetone (inert) + diethylamine at three temperatures. Full lines are calculation with the Modified CPA, dashed lines are calculations with the s-CPA . Data are from Srivastava and Smith. [249]

Reasonable results are in the case of diethylamine + acetone. A similar behavior is observed for methanol + diethylamine, as presented in figure 5.11 for the case of diethylamine +

methanol with GC-PPC-SAFT. For the system with acetone, s-CPA presents a slightly better temperature trend for the overall diagram, while the modified CPA presents a better description of the "predicted" azeotrope composition for the same mixture, as seen at 398.1 K. Table 5.6 presents the deviations obtained using both versions of CPA for this mixture.

Table 5.6 Deviations obtained for the mixture acetone + diethylamine.

T/K	%AAD	
	modified CPA	s-CPA
297.97	2.07	1.19
348.09	1.17	1.48
398.10	1.25	1.23

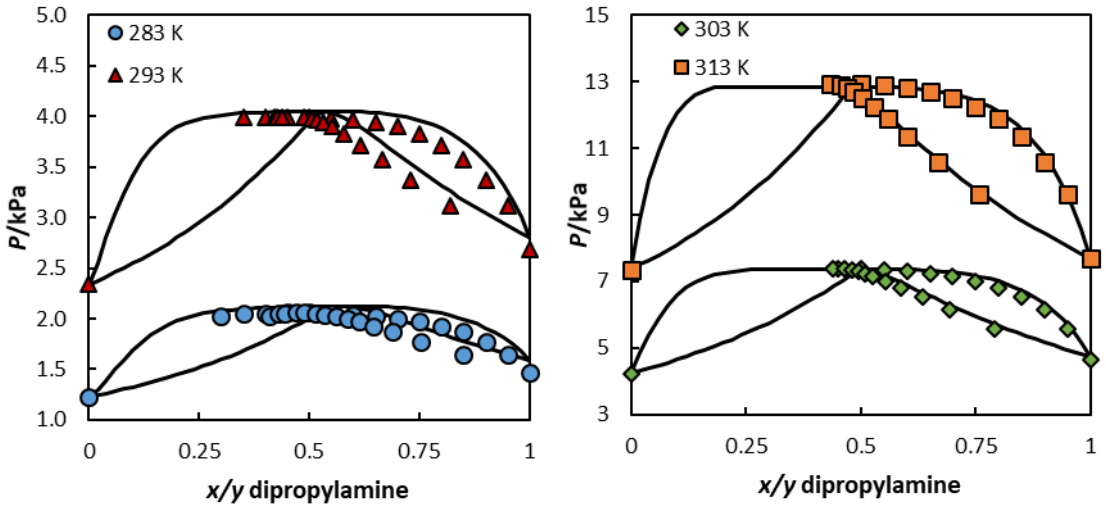

Figure 5.10 VLE results for water + dypropylamine at four temperatures. Data are from Davidson [250].

For dipropylamine + water the results present accurate trends. Nevertheless for lower temperatures the pure dipropylamine saturation pressure is not accurate, which leads to some deviations in the VLE. These are in large part due to the high variability on the saturation pressure data available for dipropylamine at low temperatures. [80]

Figure 5.11 presents results methanol + diethylamine, while figure 5.12 presents results for ethanol + diethylamine allowing, in the former case a comparison of the performance of CPA and GC-PPC-SAFT. The binary interaction parameters for both modified CPA and s-CPA for the systems with methanol were obtained in this work, being -0.150 and -0.154 respectively. For the ethanol containing system the kijs were -0.110 for the modified CPA and -0.113 for the s-CPA, this last value was taken from Kaarsholm et al. [241]

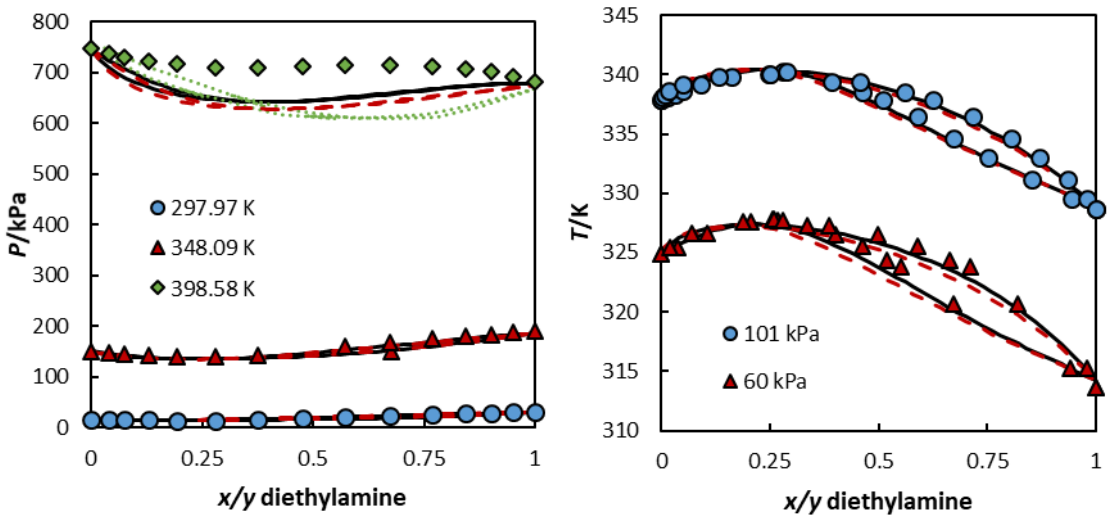

Figure 5.11 VLE description of diethylamine + methanol at three temperatures (left) and two pressures (right) full lines are results with CPA, dashed lines are results with s-CPA and dots are results with GC-PPC-SAFT [242]. Data values are from Srivastava and Smith [249] and Yang et al. [251].

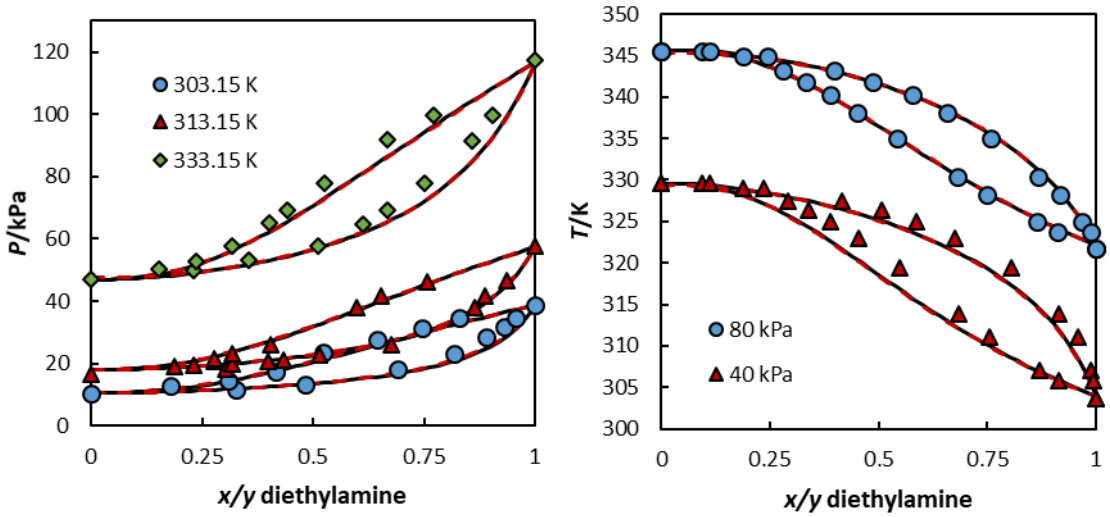

Figure 5.12 VLE ethanol (bottom) at three temperatures (left) and two pressures (right) full lines are results with CPA, dashed lines are results with s-CPA. Data values are from Yang et al. [252] and Held [253].

For these two mixtures both CPA and GC-PPC-SAFT were unable to describe the whole range of temperatures in analysis with no/or a constant k_{ij}. The results with GC-PPC-SAFT for lower temperatures are very similar to those of CPA. Resuls between s-CPA and the modified CPA for these mixtures present also similar descriptions.

Figure 5.13 presents results for the VLE phase diagrams of dipropylamine with four alkanols (methanol, ethanol, 1-propanol and isopropanol).

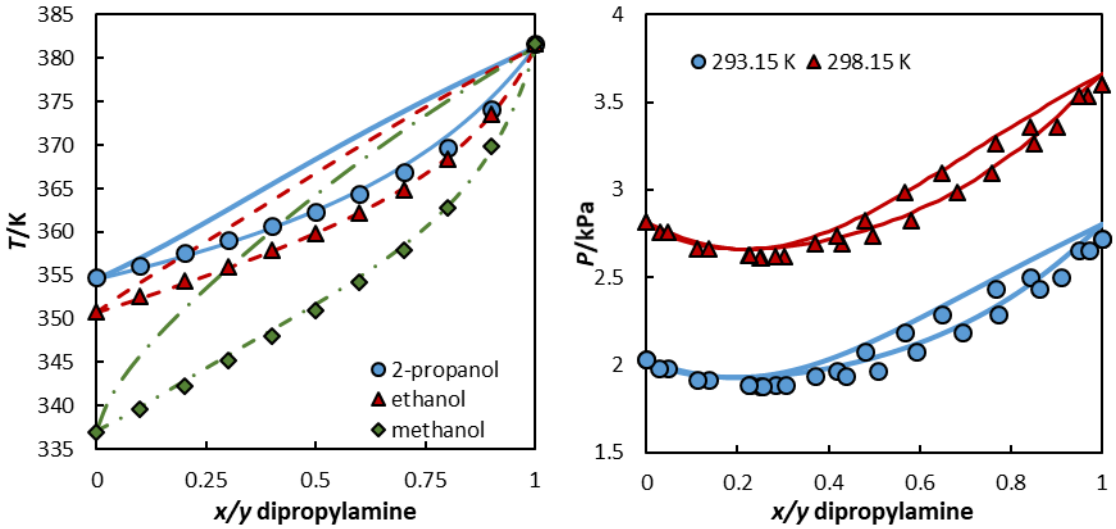

Figure 5.13 VLE description of dipropylamine + alkanol at 98.7 kPa (left) and for dipropylamine + 1-propanol at three different temperatures (right). Data are from Villa et al. [254] and Kato and Tanaka [255].

Accurate results were obtained for most of the mixtures analyzed above. Uncertainties in the vapor pressure data affect the low temperature results for dipropylamine and its mixtures. As was referred after figure 5.10. Deviations for the mixture of dipropylamine + 1-propanol at six temperatures are presented on table 5.7.

Table 5.7 Average absolute deviations obtained for the mixture 1-propanol + dipropylamine. Deviations on the pure compound pressures presented by Villa et al. [254] are also presented.

T/K	%AAD P^{BUB}	%AAD $Y_{DIPROPYLAMINE}$	%DEV. P^{SAT} DIPROPYLAMINE
293.15	5.26	29.58	2.98
298.15	3.36	26.41	1.91
303.15	1.59	23.67	0.70
308.15	0.59	21.29	0.58
313.15	1.43	1.62	0.92
318.15	1.50	18.50	1.60

In general, the modified CPA model was able to describe the VLE of mixtures containing symmetric secondary amines, with comparable results to s-CPA (for systems with diethylamine), while also introducing a correct description of the pure component critical pressure and critical temperature and keeping accurate results for vapor pressure, density and heat of vaporization.

To finish this section, the LLE for the system water + dipropylamine was analyzed, both using the binary interaction parameter from the VLE and one fitted to the LLE data (k_{ij}=-0.258 + 6.59x10^{-4}*T*). These results are presented in figure 5.14.

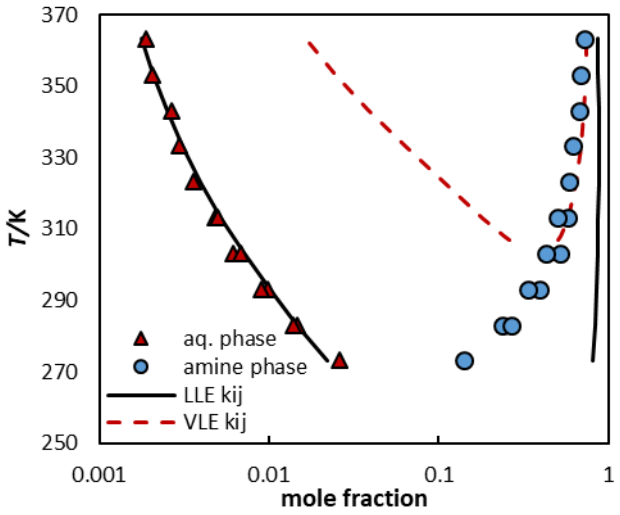

Figure 5.14 LLE for the system water + dipropylamine. Data are from Stephenson [256] and Davison. [250]

Using the VLE binary interaction parameter, the lower critical temperature of the LLE is overestimated, the amine phase is accurately represented above such temperature, but the water phase is poorly represented. On the other hand, when using a LLE fitted binary interaction parameter, the aqueous phase presents a correct trend, leading, however, to the lower critical temperature being underestimated and to some higher deviations in the amine phase. It was not possible to accurately describe both phases simultaneously, similarly to other LLE systems of water with associating compounds (as shown in chapter 4).

5.3.3 Modelling of phase diagrams of binary systems containing thiols

For systems containing thiols, the results are compared with those from s-CPA, it is however important to note that the approach used with that version of CPA does not consider association in the sulfhydryl group, while the current set of parameters with the modified version applies a 2B association scheme, as presented in table 5.1.

Table 5.8 presents the binary interaction parameters applied in this section.

Results for the system methanethiol + hexane are presented in figure 5.15.

Table 5.8 Binary interaction parameters applied for the mixtures containing thiols.

comp. 1	comp. 2	k_{ij}	s-CPA k_{ij}	figure
n-hexane	methanethiol	-0.018	0.000	5.15
n-butane	ethanethiol	0.012	0.041	5.16
n-butane	1-propanethiol	0.012	0.025	5.16
n-hexane	1-propanethiol	0.014	0.025	5.17
methylcyclopentane	1-propanethiol	0.019	-	5.17
cyclopentane	1-propanethiol	0.015	-	5.17
2-methylpentane	2-propanethiol	0.012	-	5.18

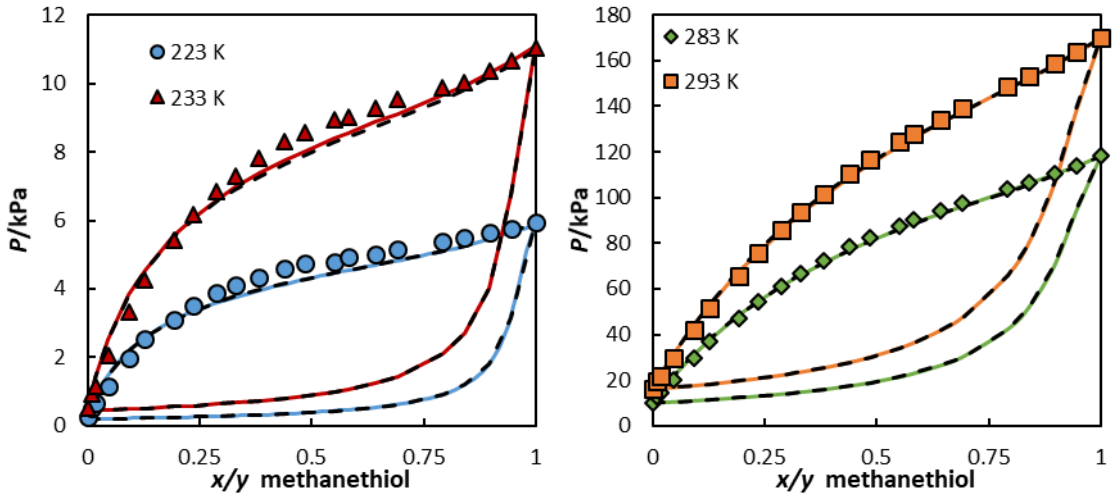

Figure 5.15 VLE description of methanethiol + hexane at four different temperatures (Full lines are results with the modified CPA, dashed lines are results using the s-CPA [245]). Data from Wolff et al. [257]

Very reasonable results are obtained using a small binary interaction parameter (k_{ij} =-0.018) for the system presented in figure 5.15. With s-CPA with was possible to describe the same mixture with no binary interaction parameter.

Decreasing the methanethiol volume of association parameter (β) leads to smaller binary interaction parameters, being possible to describe the system with no binary interaction parameter. However, the pure compound C_p description would be worse at the higher temperatures, and the volume of association would be lower than that of ethanethiol. However, as methanethiol fitting presented some issues it is important to take into account that the correct volume of association might be smaller and might be smaller than that of ethanethiol. Table 5.9 presents deviations for the two sets of parameters for methanethiol + hexane at eight different temperatures.

Table 5.9 Average absolute deviations obtained for the mixture methanethiol + hexane.

***T*/K**	**%AAD P^{bub}**	
	modified CPA	s-CPA
293.15	1.30	1.39
283.15	1.56	1.84
273.15	2.01	2.43
263.15	2.69	3.23
253.15	3.71	4.33
243.15	4.63	5.20
233.15	6.60	7.06
223.15	8.32	8.24

The modelling of the systems ethanethiol + butane and 1-propanethiol + butane was also performed and results are presented in Figure 5.16 where the modified CPA and s-CPA are compared.

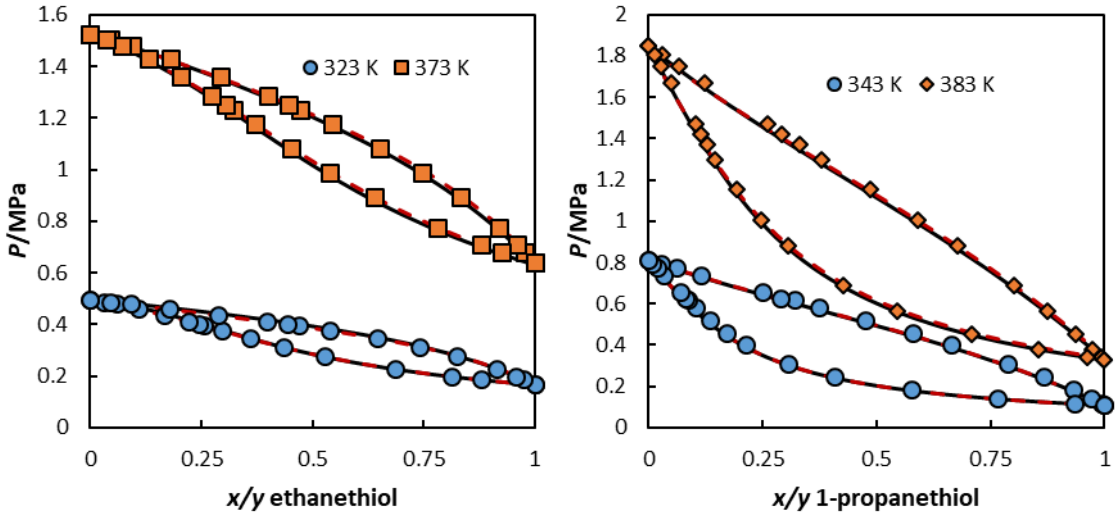

Figure 5.16 VLE description of ethanethiol + butane (left) and 1-propanethiol + butane (right). Full lines – Modified CPA, dashed lines – s-CPA [245]. Data are from Giles and Wilson [258] and Giles et al. [259]

Both approaches present accurate results for the systems in analysis, with the modified CPA requiring smaller interaction parameters, most likely due to the insertion of association on the sulfhydryl group.

The mixtures of 1-propanethiol with n-hexane, methylcyclopentane and 2 methyl-pentane, and the mixture are presented in Figure 5.17. Figure 5.18 presents the results for 2-propanethiol + cyclopentane. These mixtures are well represented, with the azeotropes being correctly described.

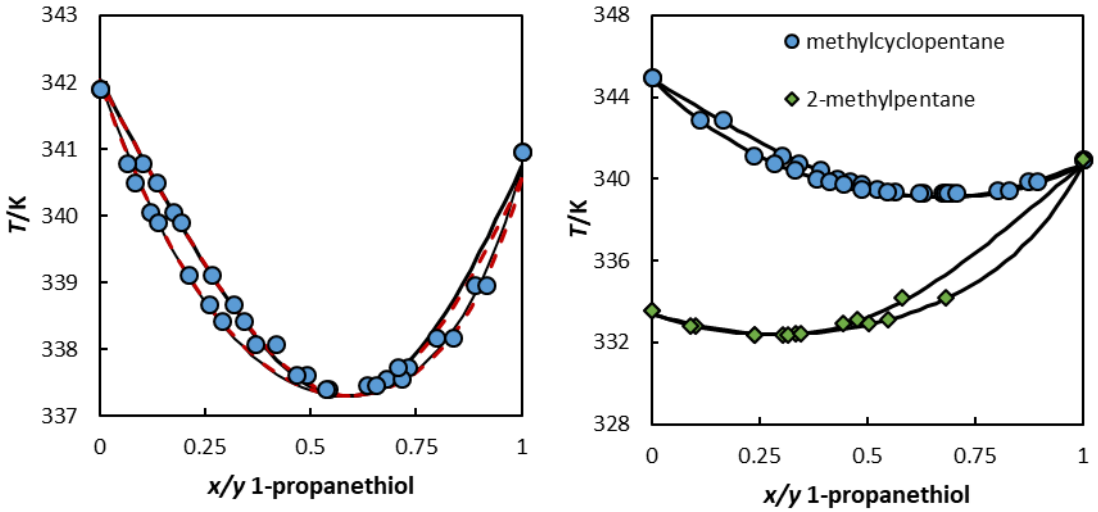

Figure 5.17 VLE description of 1-propanethiol + n-hexane (left) and of 1-propanethiol + methylcyclopentane and 1-propanethiol + 2-methylpentane (right). All mixtures at 1 atm, full lines – Modified CPA, dashed lines – s-CPA. Data are from Denyer et al. [260].

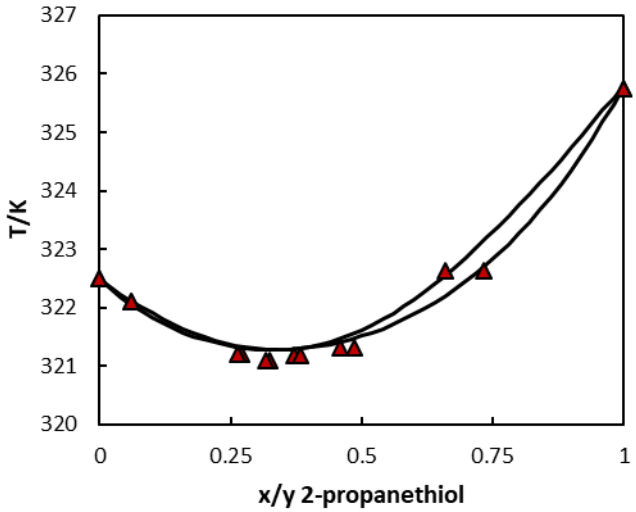

Figure 5.18 VLE description of 2-propanethiol + 2-methylpentane at 1 atm. Data are from Denyer et al. [260].

As for the mixtures with amines, this version of CPA presents accurate results for mixtures containing thiols. The approach applied with s-CPA, was not followed with the modified version, as the use of the association term improved the derivative property description. The introduction of this term lead, also, to a decrease in the values for the binary interaction parameters. The results for mixtures are similar to those obtained with s-CPA, while improving the pure component properties, mainly derivative properties (for the heavier thiols) and critical point description, as seen in section 5.3.1.

5.4 Conclusions

The description of five thiols and three secondary amines has been studied with the modified CPA model proposed in this thesis, extending the range of associative compounds for which this model has been applied. A similar transferability approach, as that of chapters 2 and 3, was employed, leading to constant association parameters for the heavier thiols. For amines only three were tested, thus it was not analyzed if the transferability approach is successful for this family of compounds, as all the compounds used different values of association volume.

The parameterization of pure compounds was very successful, with saturation pressure, liquid density and heat of vaporization presenting deviations within the uncertainties of the experimental data. Liquid heat capacity presents higher deviations, as found before for other families. Diverse factors may influence this, including the alpha function applied, the uncertainties of the ideal gas heat capacity or even the simplicity of the model.

The description of binary systems containing these mixtures is also very accurate in most cases, with some deviations observed at the lowest temperatures with amines, due to the uncertainties on the pure component saturation pressures. The single LLE analyzed presented reasonable results both when using the VLE binary interaction parameters and LLE fitted k_{ij}. However, it was not possible to simultaneously describe both phases and the lower critical temperature observed was not correct, as observed previously for the LLE of water + alkanols in chapter 4.

6 Mixture critical points

6.1 Abstract

In a phase envelope it is important to have an adequate prediction of the critical point. This point identifies the conditions where the bubble curve becomes the dew curve, and the nature of the single phase region outside the phase envelope as being “gas like”, “liquid like” or supercritical.

Hydrate formation and the condensation of gases are some of the risks that need to be understood and addressed in the oil and gas industry. The importance of applications in the near/supercritical region have also been increasing such as in the case of producing CO_2 rich reservoirs or using gas injection processes. In all of these cases the previous knowledge of the mixture critical point is relevant to avoid production problems and to optimize processes.

The version of CPA applied in this thesis, is shown to accurately describe the critical temperatures and pressures of pure compounds (chapters 2 through 5). The next natural step is to verify if this improved performance also extends to mixtures.

Binary and ternary systems containing alkanes, alkanols, amines, water, ketones, aromatics, ethers or THF are studied and compared to existing experimental data. The binary interaction parameters here applied were regressed from VLE and/or LLE systems at lower temperatures. A comparison with recent literature results using the simplified CPA and PC-SAFT is also presented.

6.2 Introduction

The use of supercritical compounds has long been an interesting option for diverse industrial processes. The use of supercritical CO_2 for the extraction of caffeine (decaffeination of coffee) is among the oldest and better known processes and a large range of applications has since been found for supercritical fluids. [261]

For these applications, it is important to have a correct knowledge of the critical properties of a mixture, for better designing and optimizing the process and avoid operational issues such as flow problems. The unique properties of supercritical fluids, being neither completely liquid like nor gas like, presenting properties pertaining usually to each of these type of fluids, are the main reason for their usefulness and versatility.

Equations of state are important tools in process simulation software, due to their ease of implementation and versatility. Cubic EoS, the most successful of these models are however, unable to completely describe the full critical data of a compound or mixture [262,263],

without the use of specific treatments as is the case of cross-over methods. [14,264,265] This is even more evident for the case of molecules capable of hydrogen bonding.

Even though the full description of the pure component critical data is not currently achievable with classical approaches in cubic equations of state, these models are built such that the pure component critical temperature and critical pressures are usually well described, as both of these are often used in the parametrization process. So, as far as the pure component critical temperatures and pressures are well described, it is reasonable to assume that mixture critical points can also be well estimated.

Apart from equations of state there are other methods to predict critical properties of binary mixtures. In the case of ternary mixtures, methods like those by Hicks and Young [266] or by Cibulka [267] can be applied. However, these are far more complex than equations of state and/or overly rely on the correlation of the experimental data, having little or no predictive capacity. For multicomponent mixtures the most widely used methods are those of Heidmann and Khalil [268], Michelsen [269] and Hoteit et al. [270]

Recently, equations of state including an association term (s-CPA [73] and PC-SAFT [26]), have been applied for the description of critical properties of binary mixtures including an association compound + hydrocarbons or CO_2 [156,271], with very good results for both the critical temperature and critical pressure. However, the correct description of critical point, even for pure compounds, using this type of EoS involves the need of specialized parameterization methods. [156] Since its creation, the version of CPA applied in this thesis has been parameterized with this purpose in mind, using an approach where the energy and co-volume parameters of the physical term are obtained directly from the pure compound critical data, similarly to what is done in a cubic EoS, but with given association parameters.

In this work, a large range of binary mixtures is studied using this approach. These include alkanols + water, alkanols + alkanols and alkanols + alkanes. Some other specific systems are analysed, such as the phase equilibria of water + n-hexane, where the capacities/limitations of the model are more evid. The binary interaction parameters applied here were not specifically fitted to the critical data, but instead to the VLE/LLE at low temperatures or gas solubility data.

To describe solvating compounds, the approach proposed by Folas et al. [136] is applied. This approach was previously tested, with this version of CPA in chapter 4, to describe the LLE of water and aromatics with promising results. A comparison of the results obtained by Vinhal et al. [156] and Gil et al. [271] is presented for the systems of methanol with alkanes and alkanols with n-hexane, respectively. Beside the description of binary data, some ternary systems of alkanols with alkanes and alkanols with MTBE are presented.

6.3 Results and Discussion

A large set of the binary interaction parameters used for the systems presented here have been obtained in previous chapters. For the other cases, the VLE results are presented in annex.

At the beginning of each subsection, a table is presented with the binary interaction parameters used for the presented mixtures, starting with table 6.1. Each table redirects the reader to the figures where each binary interaction parameter is applied. The table does not include the figures for ternary mixtures. However for those cases, the binary interaction parameter used is always the one obtained from the fitting of VLE and the less complex (if a constant and a temperature dependent k_{ij} are available the one used is the constant one)

When only data for the critical temperature is available, the predictions of critical pressure are presented in the annexes. The pure component parameters for each associative molecule are presented in the previous chapters on tables 2.6, 3.1, 3.2, 4.1 and 5.1. For non-associating compounds a table is presented in the annexes.

6.3.1 Critical points for binary mixtures of alkanols

Table 6.1 Binary interaction parameters for mixtures of alkanols

comp. 1	comp. 2	fitted to	k_{ij}	figures	notes
methanol	1-propanol	no k_{ij}		6.1, 6.2	-
methanol	1-butanol	no k_{ij}		6.1, 6.2	-
ethanol	2-propanol	VLE (2 temp.)	-0.009	6.3	VLE in annex

The systems methanol + 1-alkanol are shown next. The descriptions of binary equilibria containing these compounds, due to their similarities, are usually predictive, and thus, no binary interaction parameter was introduced. Figures 6.1 and 6.2 present the results for the systems methanol + 1-propanol and methanol + 1-butanol.

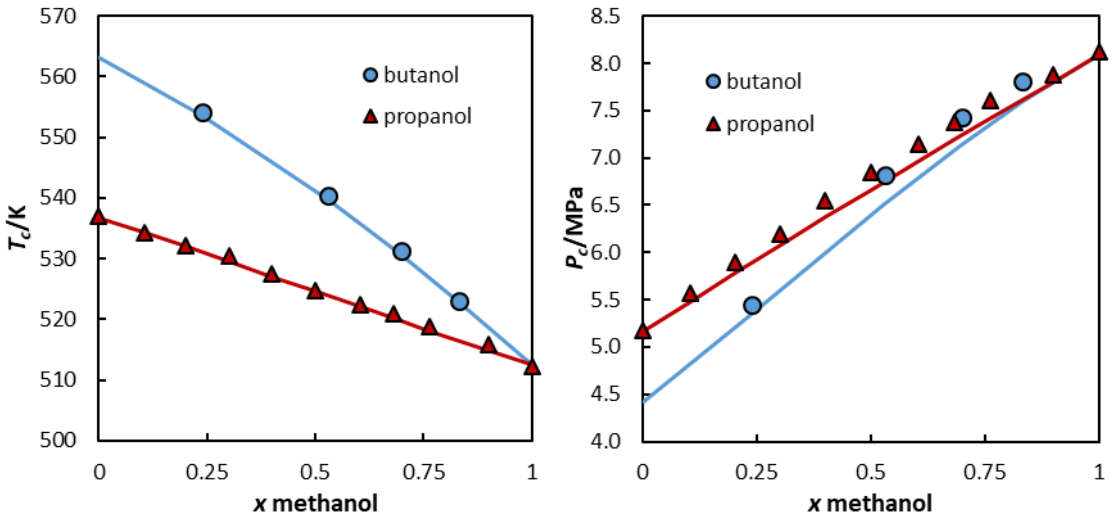

Figure 6.1 Predictions of T_c (left) and P_c (right) for the whole range of compositions on of methanol + 1-propanol and methanol + 1-butanol. Experimental data from Nazmutdinov et al. [272] and Wang et al. [273].

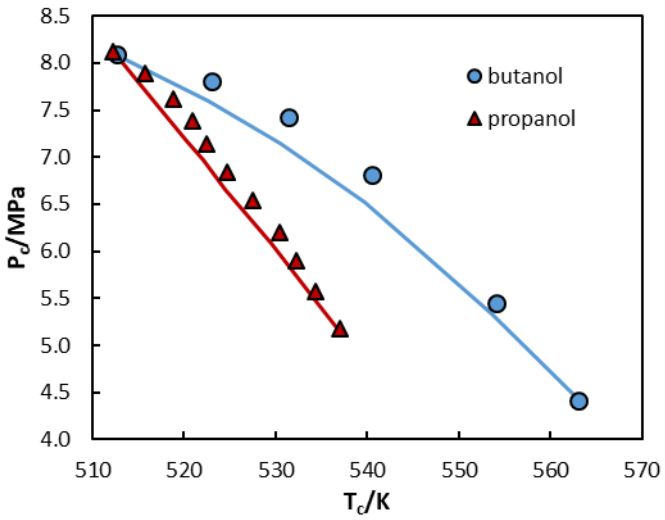

Figure 6.2 Curve of the predicted P_c in relation to predicted T_c for methanol + 1-propanol and methanol + 1-butanol mixture, compared to experimental data for both properties. Experimental data from Nazmutdinov et al. [272] and Wang et al. [273].

For these systems an accurate description of the critical temperatures were obtained. Critical pressures present higher deviations and this is partly due to the alpha function applied in this modified version, but also, due to the smaller weight of the critical term in this version .The volumes of association for the sets with this version are lower than those with s-CPA. Even if the energies of association are higher, close to the critical point the association term will be less relevant than in s-CPA, and lead to results of P_c closer to SRK.

Continuing the analysis of systems containing two alkanols figure 6.3 presents the results for the critical temperature of ethanol + 2-propanol mixtures. For this binary mixture a binary

interaction parameter was fitted to the results at the temperatures of 303.15 and 313.15 K from Zielkiewicz et al. [274]

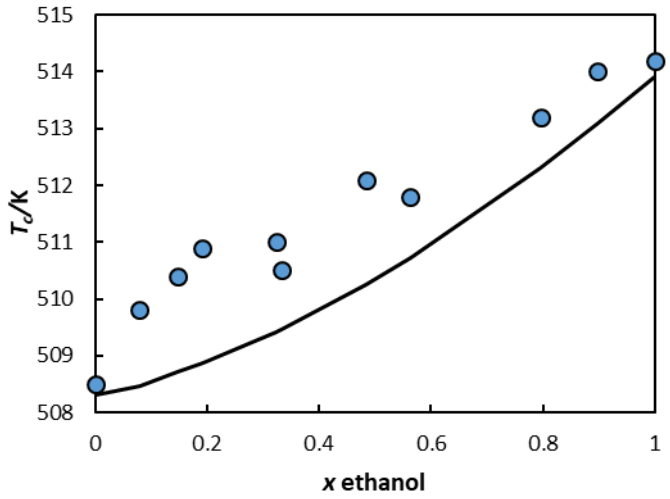

Figure 6.3 Results for the T_c of ethanol + 2-propanol mixtures as function of the ethanol composition. Experimental data from Nazmutdinov et al. [272].

The results for this system present higher deviations, likely to be due to the approach used for the association volume of alkan-2-ols, where this parameter is considered constant. The use of a group contribution method is tested in chapter 7 (figure 7.10), where the results are seemingly improved, by the use of a higher volume of association. Nevertheless it is relevant to note that the uncertainties of the critical data for this mixture appear to be high.

6.3.2 Critical points for binary mixtures of alkanol + water

The binary interaction parameters for this section are presented in table 2.

Table 6.2 Binary interaction parameters for mixtures of alkanol + water

comp. 1	comp. 2	fitted to	k_{ij}	figures	notes
water	methanol	VLE (6+ temp.)	-0.045	6.4, 6.5	VLE chapter 4
water	ethanol		-0.004	6.4, 6.5	
water	1-propanol		$0.125-2.93\times10^{-4}T$	6.4, 6.5	

Changing one of the alkanols to water, results in the description presented in figures 6.4 and 6.5. It is important to note that the binary interaction parameters for these compounds have been obtained for a large range of temperatures.

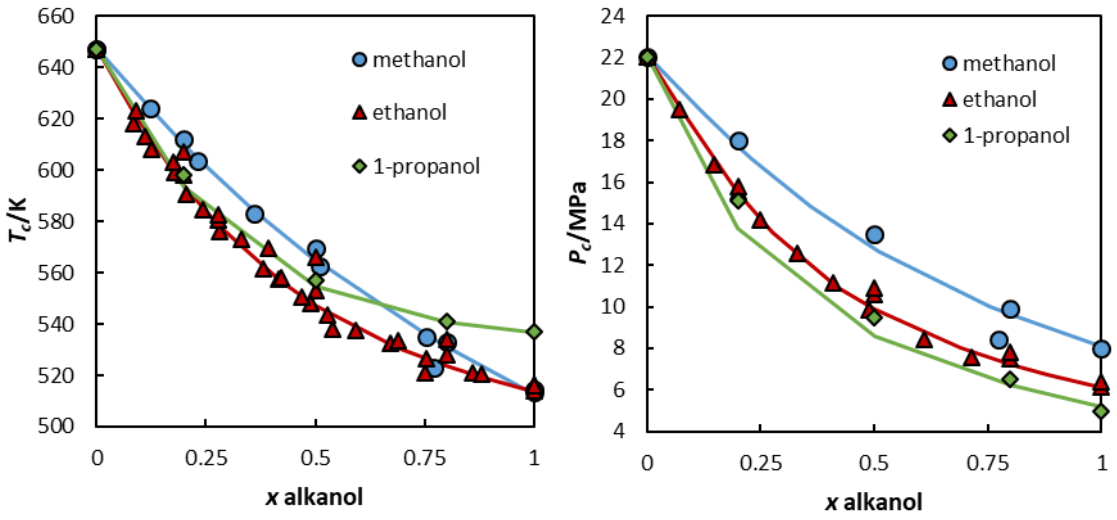

Figure 6.4 Results for T_c (left) and P_c (right) as function of the composition of water for water + methanol, water + ethanol and water + 1-propanol mixtures. Experimental data from Hicks and Young [275], Marshall and Jones [276] and Bazaev et al.

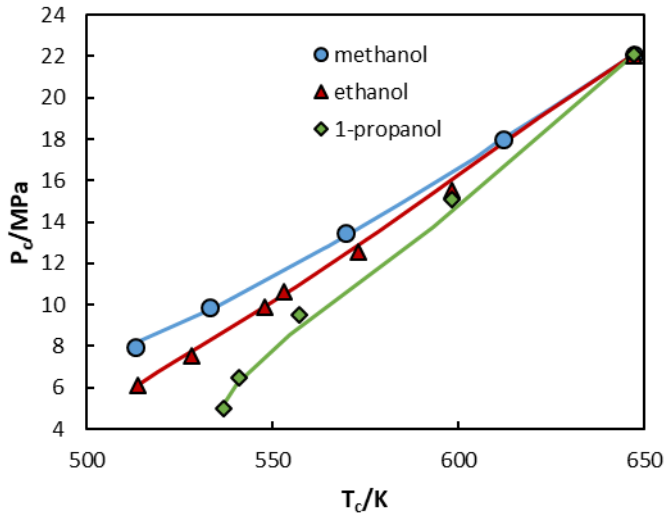

Figure 6.5 Results for P_c as function of T_c for water + methanol, water + ethanol and water + 1-propanol mixtures. Experimental data from Hicks and Young [275] and Bazaev et al. [277].

The experimental data from Marshall and Jones used in figure 6.4, presented results for T_c only. Thus, these are not used on figure 6.5.

Using binary interaction parameters, previously correlated to VLE for these systems, it is possible to achieve a very good description of the critical locus for the studied mixtures.

6.3.3 Critical points for binary and ternary mixtures of alkanols + alkanes

The binary interaction parameters for this section are divided between tables 6.3 and 6.4. With the first presenting results for mixtures containing primary alcohols and the second results with secondary alcohols. No binary interaction parameter was applied between two alkanes.

Table 6.3 Binary interaction parameters for mixtures of 1-alkanol + alkane

comp. 1	comp. 2	fitted to	k_{ij}	figures	notes
methanol	hexane	VLE (1 bar)	0.052	6.7	VLE and LLE results in chapter 2 and annex
methanol	hexane	LLE	0.036	6.6	
methanol	hexane	VLE (6 temp.)	$-0.069+4.00\times10^{-4}T$	6.7	
methanol	heptane	LLE	0.033	6.6	
methanol	octane	LLE	0.028	6.6	
ethanol	hexane	VLE (1 bar)	0.056	6.7, 6.9	
ethanol	hexane	VLE (4 temp.)	$-0.068+3.74\times10^{-4}T$	6.7	
1-propanol	hexane	VLE (1 bar)	0.041	6.7, 6.10	
1-propanol	hexane	VLE (2 temp. & 1 bar)	$0.143-2.81\times10^{-4}T$	6.7	
1-butanol	hexane	VLE (1 bar)	0.027	6.7	
1-pentanol	hexane	VLE (0.93 bar)	0.031	6.7	
ethanol	butane	VLE (293 K)	0.047	6.9	VLE in annex
ethanol	pentane	VLE (3 temp.)	0.097	6.9	
ethanol	heptane	VLE (1 bar)	0.046	6.9	
ethanol	octane	VLE (1 bar)	0.046	6.9	
ethanol	cyclohexane	VLE (4 press.)	0.071	6.9	
1-propanol	heptane	VLE (1 bar)	0.050	6.10	
1-propanol	octane	VLE (1 bar)	0.040	6.10	
1-propanol	decane	VLE (363 K)	0.015	6.10	
1-propanol	cyclohexane	VLE (1 bar)	0.072	6.10	

Having looked at systems where both compounds present association it is now important to verify if this version of the model is able to provide accurate results for systems where only one compound is associative. Vinhal et al. [156] have recently studied the description of these properties for methanol + *n*-alkanes using s-CPA with reparametrized sets (both the pure compounds and binary interaction parameters). Thus, it is of interest to compare the results using both methodologies.

The same authors have also studied how the new sets described LLE. Despite the decrease in accuracy, their results are still able to describe the LLE for this mixture. As first test, with the modified version, it is interesting to verify if the opposite is verified. The sets of binary interaction parameters obtained for the LLE of methanol + *n*-alkanes were applied and the results can be observed in figure 6.6.

Table 6.4 Binary interaction parameters for mixtures of 2-alkanol + alkane

comp. 1	comp. 2	fitted to	k_{ij}	figures	notes
2-propanol	hexane	VLE (1 bar)	0.073	6.8	VLE in annex
2-butanol	hexane	VLE (1 bar)	0.039	6.8, 6.12	
2-pentanol	hexane	VLE (1 bar)	0.030	6.8	
2-propanol	octane	VLE (1 bar)	0.055	6.11	VLE in annex
2-propanol	decane	VLE (363 K)	0.021	6.11	
2-butanol	heptane	VLE (0.95 bar)	0.045	6.12	
2-butanol	octane	VLE (1 bar)	0.043	6.12	
2-butanol	nonane	correlation	0.041	6.12	Corr. In the annex
2-butanol	decane	correlation	0.039	6.12	Corr. In the annex
2-butanol	cyclohexane	VLE (1 bar)	0.070	6.12	VLE in annex

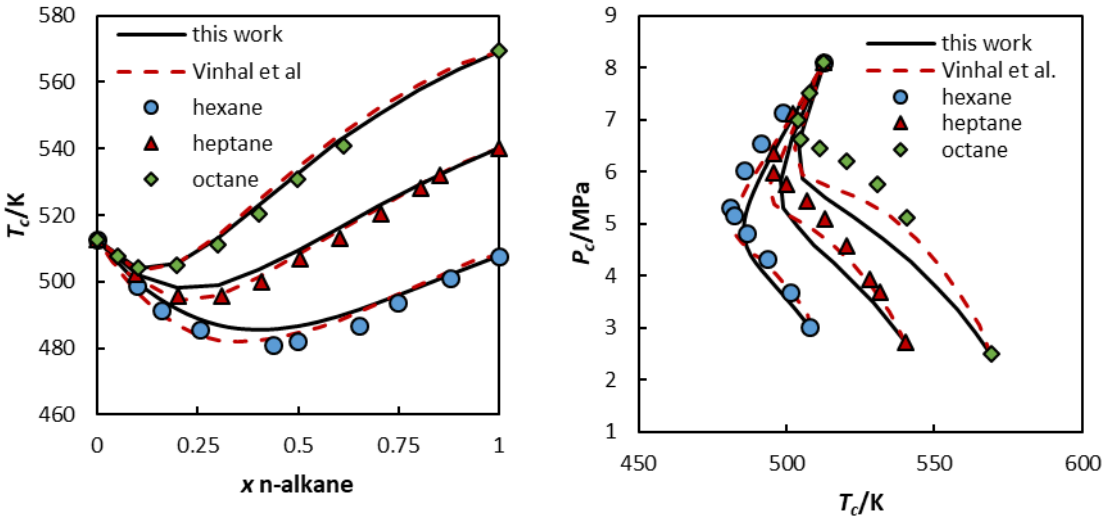

Figure 6.6 Results for T_c and P_c as function of the critical composition for methanol + hexane, methanol + heptane and methanol + octane. Experimental data from de Loos et al. [156].

The higher deviations on T_c for the first two alkanes in analysis, are mainly due to the use of the LLE k_{ij} instead of fitting these parameters from equilibria closer to the critical point. In the case of the critical pressure deviations, this is expected, as the use of a complex alpha function introduces problems near the critical point, as discussed above after figure 6.2. The current description of the model near the critical point is presented in chapter 2 at the end of "The modified CPA model" section. In this manner, despite enforcing the correct description of the critical pressure of the pure compounds, for compounds of different families it is expected that the critical pressures of mixtures will have a behaviour closer to that of SRK, especially if the critical pressures of the two pure compounds are not similar. In these cases both the alpha

function and the association volume are unable to describe accurately the vapour pressure when not at high concentrations of the associative compound.

Further description of different alkanols with n-hexane was conducted considering a temperature dependent k_{ij}. However, as observed with SAFT [271], for methanol and ethanol, those k_{ij} underestimate T_c for the smaller alkanols. In the case of 1-propanol, this is not the case and there is a large overestimation of T_c for some compositions (figure 6.7 c). The use of a group contribution for the volume of association is able to improve the results slightly for alkanols from 1-propanol onwards, mostly for 1-propanol for which the adjusted value for this parameter should be closer to that of ethanol (chapter 7, figure 7.9). For 1-butanol + hexane a constant k_{ij} was able to correctly describe the VLE of the system in a range of temperature between 283 and 393 K and thus no temperature dependency was applied. The results for these mixtures are presented In figures 6.7 and 6.8. A different approach, also used here, is to consider the k_{ij}'s calculated for systems at, or near, 1 atm, presented, as well, in figure 6.7. For 1-butanol, as well as, 1-pentanol there is no comparison as only constant binary interaction parameters were applied (Due to lack of data in the case of 1-pentanol, while for 1-butanol, this constant k_{ij} was able to describe VLE in a large range of temperatures). A comparison is also presented between the results of this work and those of Gil et al. [271] using PC-SAFT. The experimental data used for these compounds is from Gil et al. [271] and LagaLázaro [278].

There seems to be a need to use a quadratic temperature dependency, in the k_{ij}, if a correct description of VLE, for a large range of temperatures, and critical data are to be achieved. This is particularly the case for the systems with smaller alcohols and both for the results of this work and those with SAFT [271]. The physical term for the heavier alkanols gains weight and thus these compounds tend to behave closer to alkanes. Thus the behaviour of these compounds will be more similar and easier to predict. It is also interesting to look at the predictions using k_{ij}'s calculated from VLE at typical measurement conditions. These results are very good and no temperature dependency seems to be needed.

The T_c results for hexane + secondary alkanols using k_{ij}'s regressed at 1 atm, are presented in figure 6.8.

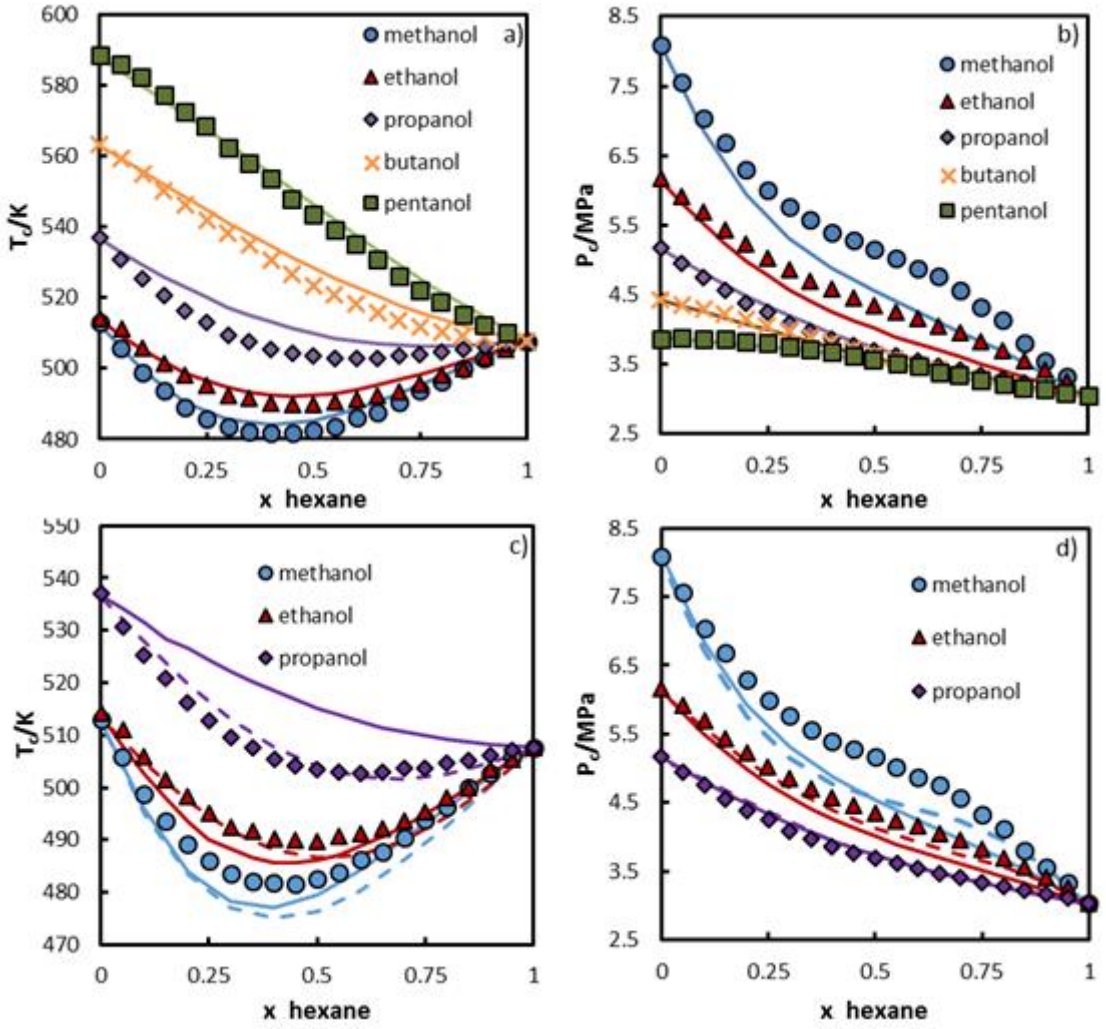

Figure 6.7 Critical points for hexane + alkanol using different k_{ij} values (a, b: obtained from VLE at 1.013 bar, 0.94 bar for 1-pentanol ; c, d: (*T* dependent [full lines], SAFT results [69] [dashed lines])

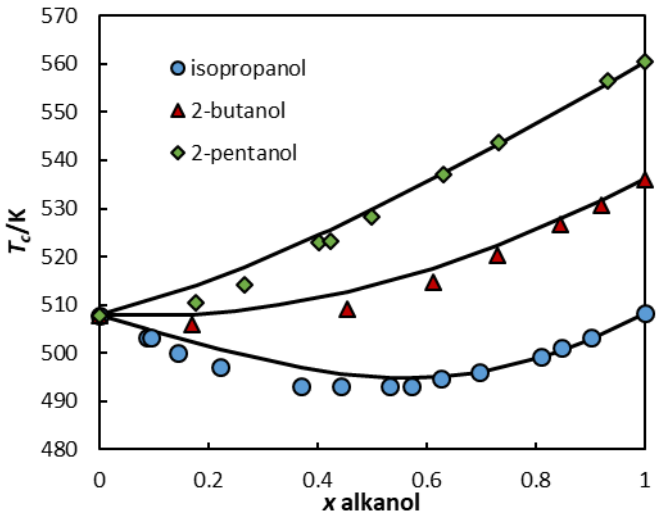

Figure 6.8 Description of *n*-hexane + secondary alkanols. Data values are from Morton et al. [279] and Hicks and Young [275].

The results for these systems are remarkable for an approach using a constant association volume. The use of a group contribution approach for this parameter should contribute to a slightly better description for the systems related with 1-propanol and 2-propanol (as with previous mixtures containing these compounds). It is also important to look at the description of ethanol and 1-propanol with different alkanes or cycloalkanes. The results for ethanol + alkanes are presented in figure 6.9.

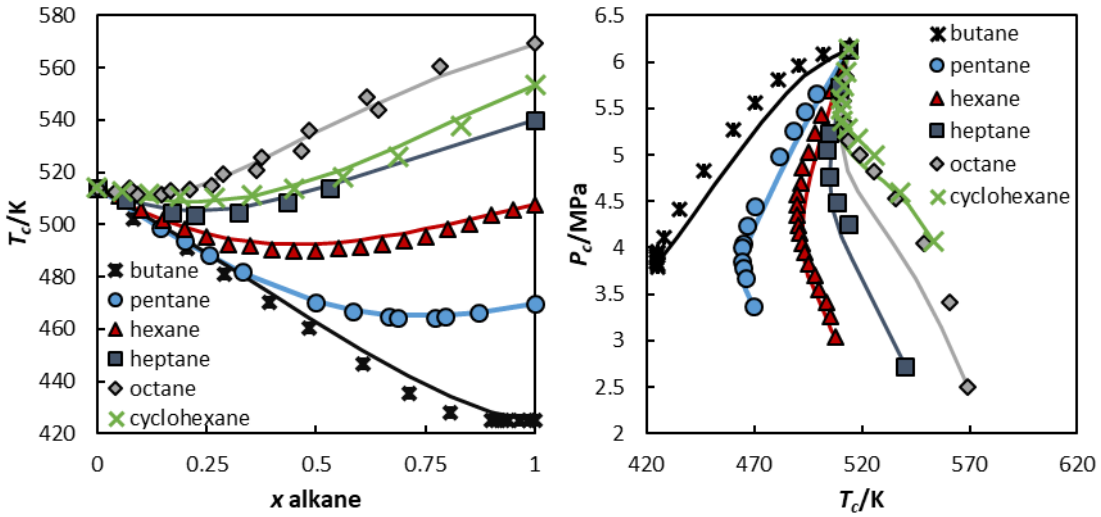

Figure 6.9 Results for systems containing ethanol + alkane. Data from He et al. [280] and Soo et al. [281].

For mixtures of 1-propanol + different alkanes the results are presented in figure 6.10.

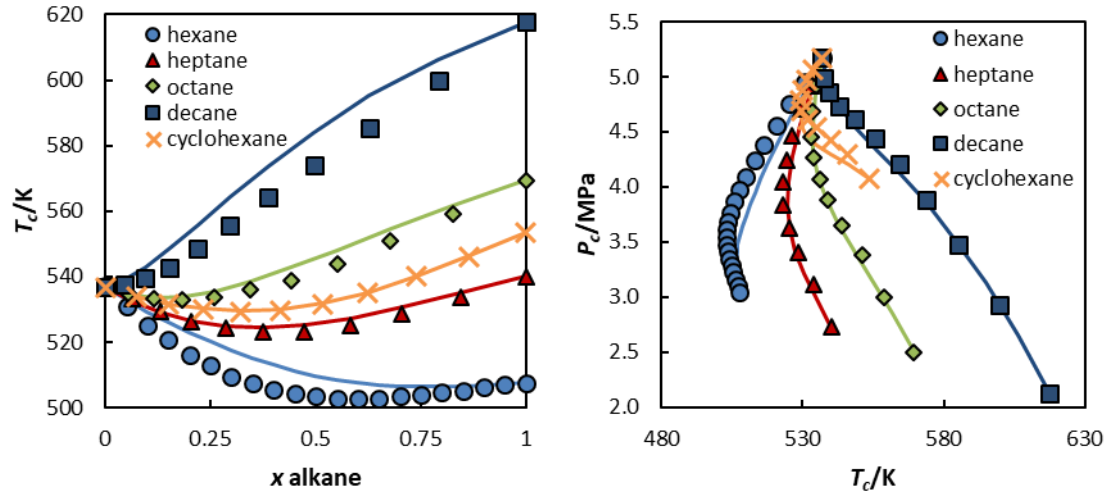

Figure 6.10 Results for systems containing 1-propanol + alkane. Data from Xin et al. [282].

The results are quite good, considering the simplified approach used. For the systems of 2-propanol + octane and 2-propanol + decane the results are presented in figure 6.11.

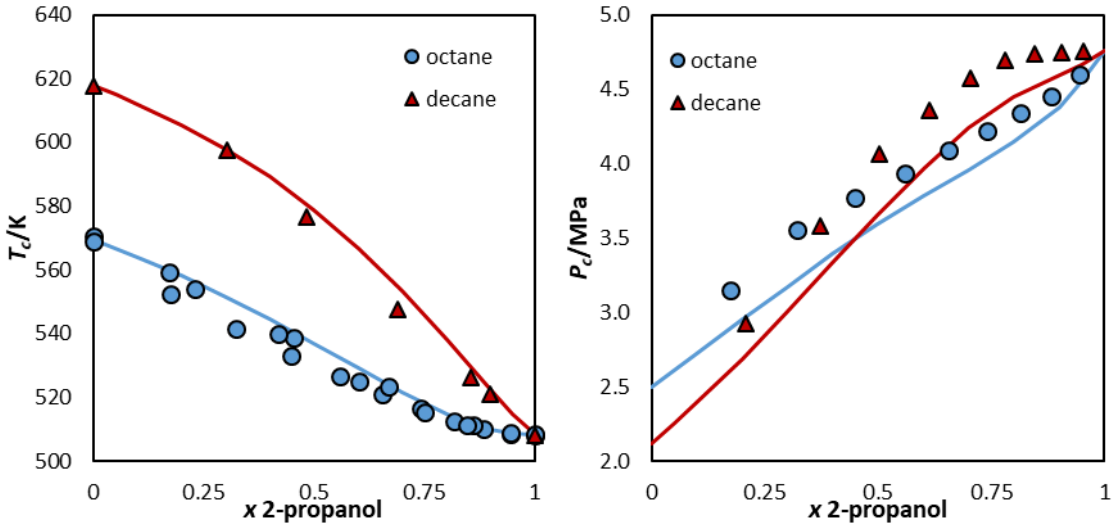

Figure 6.11 Results for systems containing 2-propanol + alkane mixtures. Data from He et al. [280] Morton et al. [279] and Nazmudtinov et al. [272].

The results for 2-propanol with alkanes are in general more accurate. For 2-butanol + alkanes the results are also analysed in figure 6.12.

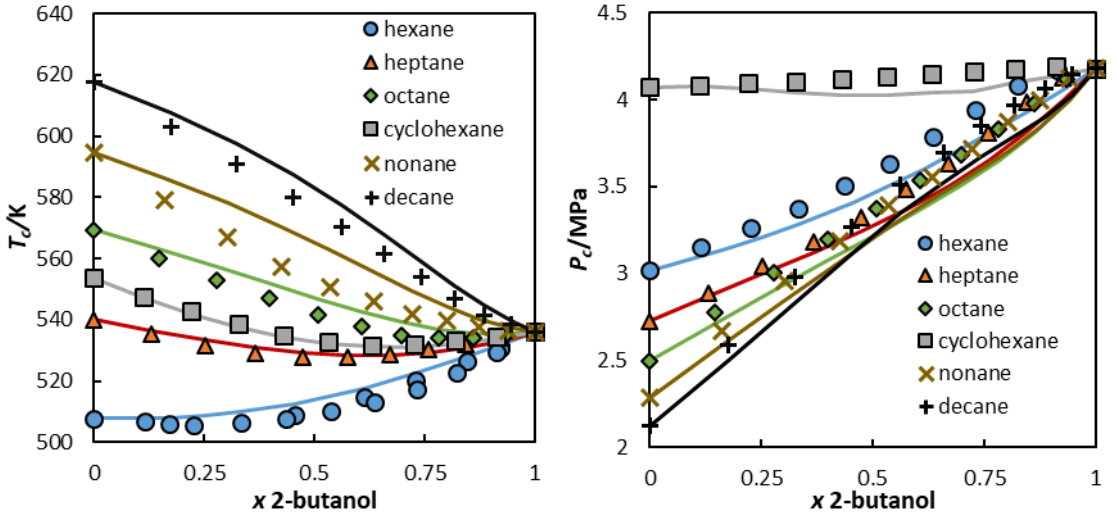

Figure 6.12 Results for mixtures containing 2-butanol + alkane. Data values for these systems are from He et al. [283] and Morton et al. [279]

After analysing these binary systems, it is important to look at the description of ternary systems containing alkanols and hydrocarbons. Figures 6.13 and 6.14 present parity diagrams of the deviations for the systems ethanol + pentane + hexane and methanol + 1-propanol + heptane, respectively. The binary interaction parameters are those used before based on the VLE (except for for methanol + heptane the one calculated from LLE is considered).

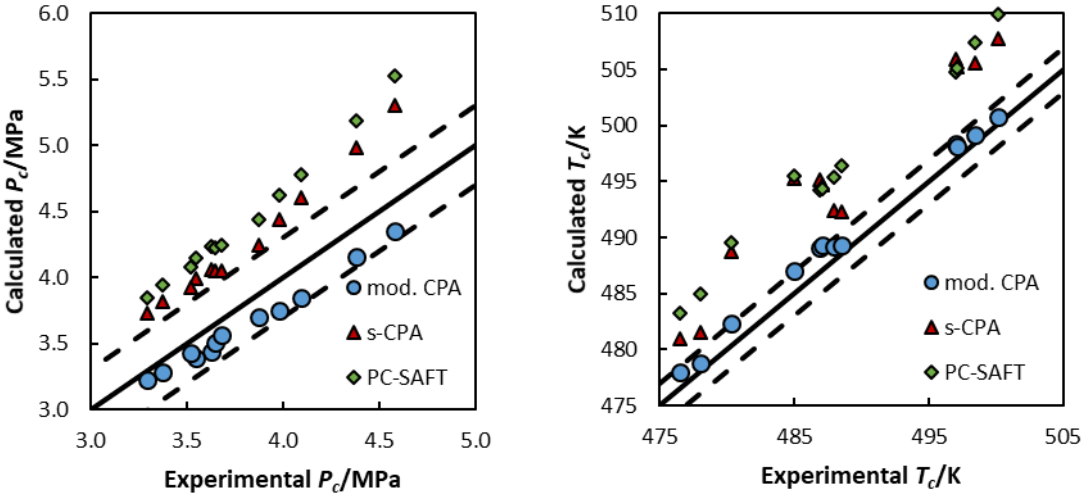

Figure 6.13 Parity diagrams for the results of the system ethanol + pentane + hexane. Dashed lines are for -0.3 MPa and +2 K respectively. Experimental data from Soo et al. [281].

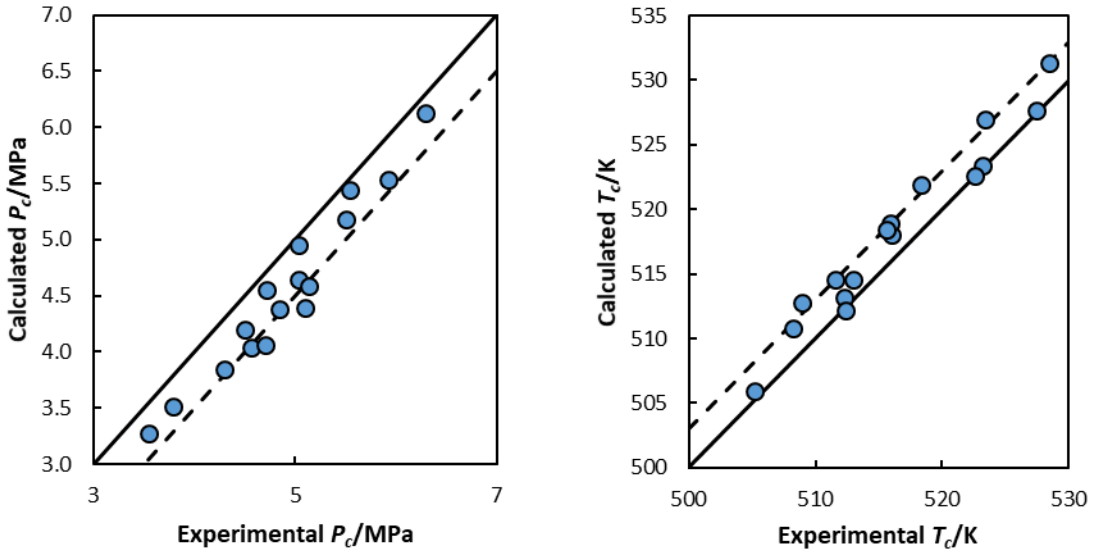

Figure 6.14 Parity diagrams for the results of the system methanol + 1-propanol + heptane. Dashed lines are for -0.5 MPa and +3 K respectively. Experimental data from Wang et al. [273].

Deviations for these systems are presented on table 6.5. For the mixture containing ethanol + pentane + hexane a comparison is made between the results of this modified version, PC-SAFT and the s-CPA, the parameters used for s-CPA are from Oliveira et al. [70] for PC-SAFT the parameters available on Multiflash [78] were used, and are presented in annex. The binary interaction parameters were calculated in the same way as those for the modified CPA and are respectively 0.056 and 0.036 for ethanol + hexane for s-CPA and SAFT, while for the mixture with pentane the values are 0.048 and 0.037. As expected, without refitting the parameter sets, both SAFT and s-CPA present far higher deviations than the modified CPA, which fits the pure component critical point.

Three other ternary systems containing alkanols and alkanes are analysed, 1-propanol/2-propanol + octane + decane and 1-propanol + heptane + cyclohexane. These results are presented in figures 6.15 to 6.17.

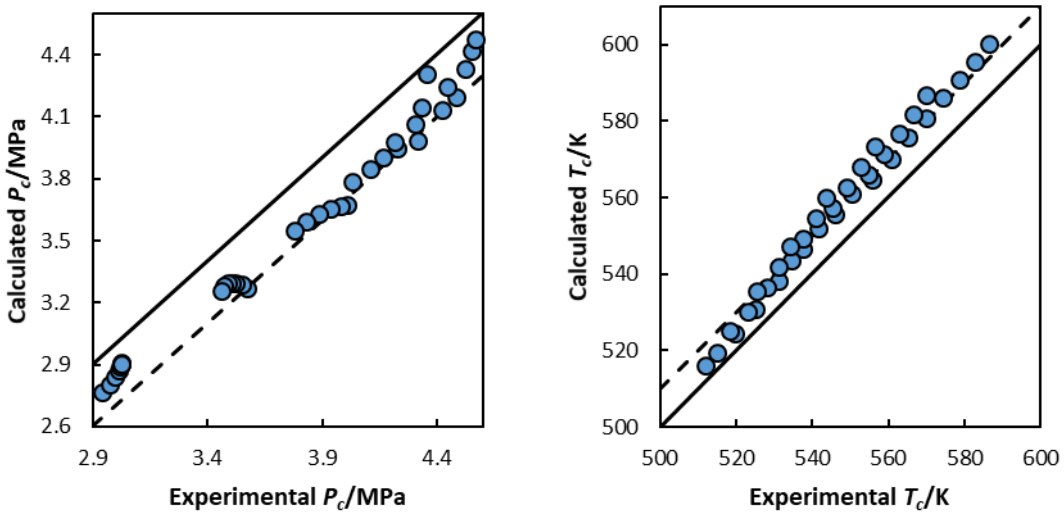

Figure 6.15 Parity diagrams for the results of the system 2-propanol + octane + decane. Dashed lines are for -0.3 MPa and +10 K respectively. Experimental data from He et al. [280].

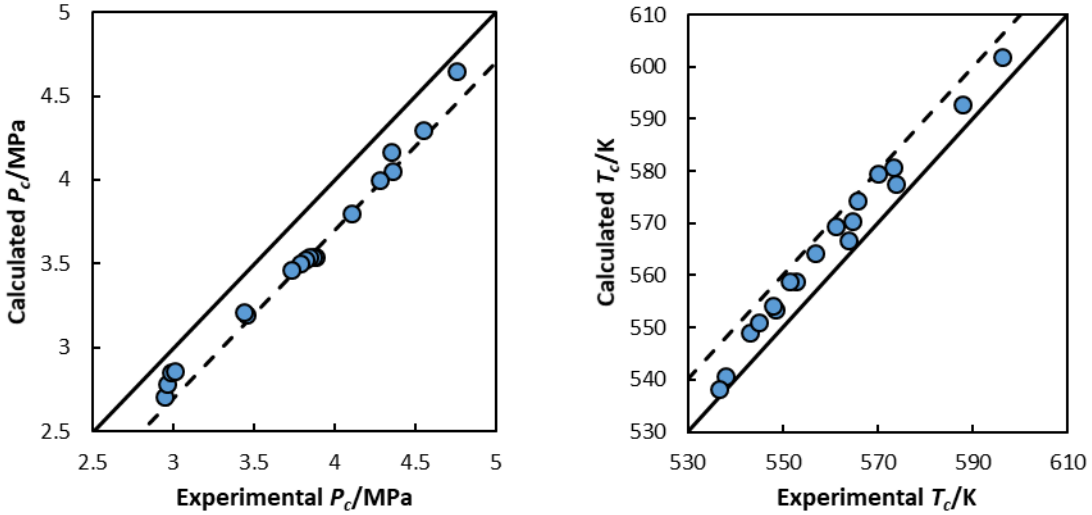

Figure 6.16 Parity diagrams for the results of the system 1-propanol + octane + decane. Dashed lines are for -0.3 MPa and +10 K respectively. Experimental from Xin et al. [282].

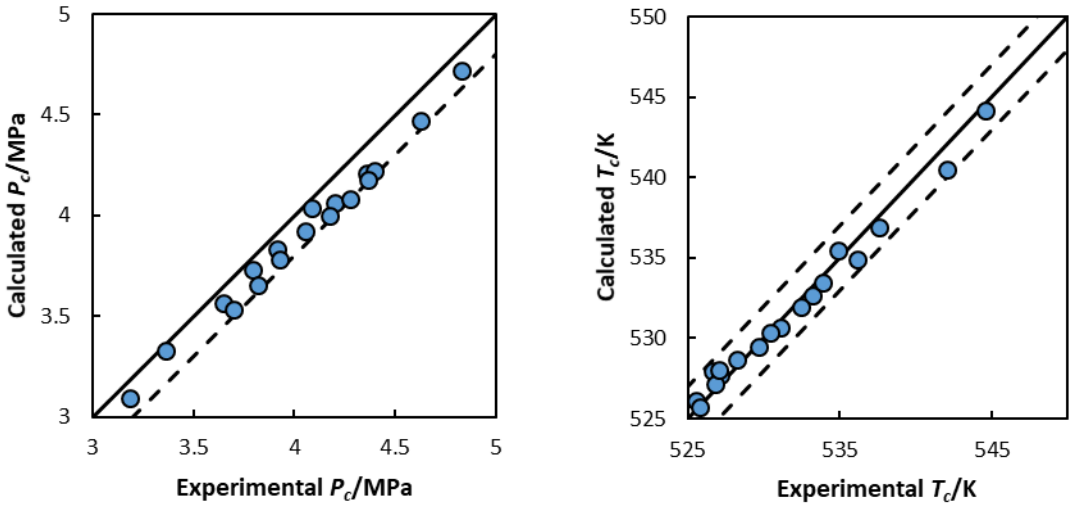

Figure 6.17 Parity diagrams for the results of the system 1-propanol + heptane + cyclohexane. Dashed lines are for -2 bar and ±2 K respectively. Experimental data from Xin et al. [282].

Two more ternary systems reported by He et al. [283] are presented in annex (2-butanol + hexane + heptane and 2-butanol + octane + decane)

Table 6.5 Average absolute deviations for P_c and T_c of ternary systems containing alkanes and alkanols.

Comp.1	Comp.2	Comp.3	%AAD *Pc*	%AAD *Tc*
ethanol	pentane	hexane	4.17	0.28
methanol	1-propanol	heptane	7.58	0.38
2-propanol	octane	decane	5.57	1.98
1-propanol	octane	decane	6.55	1.05
1-propanol	heptane	cyclohexane	3.14	0.11
2-butanol	hexane	heptane	3.04	0.47
2-butanol	octane	decane	3.46	0.70

The deviations for ternary systems present deviations similar to those of the binary systems, thus it can be considered that the predictions of the ternary systems are very successful. As in the case of the binaries, the critical temperatures are well described and most mixtures present %AAD below 1%. It is apparent, both in the binary and ternary mixtures, that in most cases the modified CPA, with the approaches proposed, tends to overestimate critical temperatures and underestimate critical pressures.

6.3.4 *Critical points for mixtures of alkane + amines*

Table 6.6 Binary interaction parameters for mixtures of alkane + amine

comp. 1	comp. 2	fitted to	k_{ij}	figures	notes
diethylamine	hexane	no k_{ij}		6.18	VLE chapter 5
dipropylamine	hexane	no k_{ij}		6.19	

Two systems were analysed for amines mixed with alkanes, diethylamine + hexane and dipropylamine + hexane. The results for these systems are presented in figures 6.18 and 6.19. The results for the first system are predictive, this approach was applied for VLE systems between 293.15 and 353.15 K with accurate results, showing a slight deviation on the pure amine vapour pressure for some temperatures.

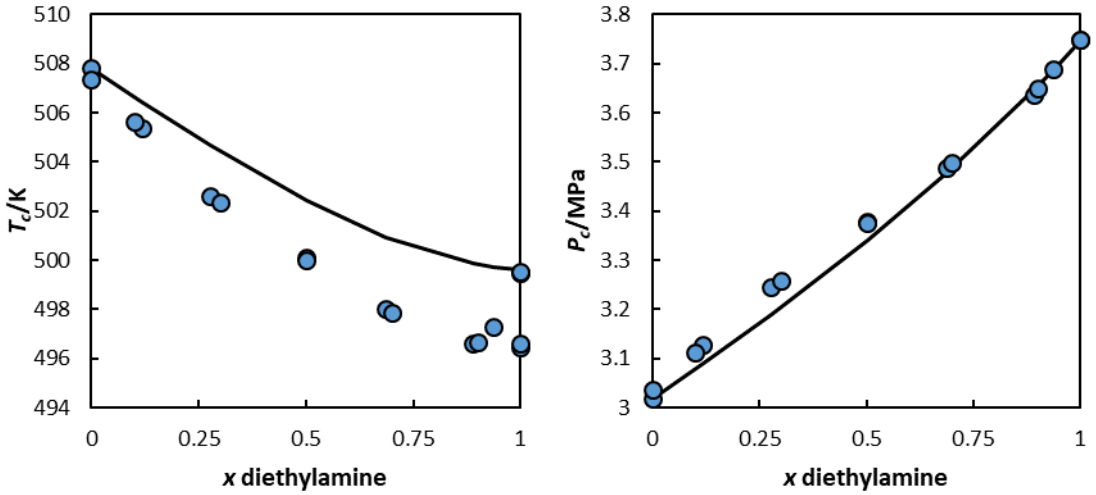

Figure 6.18 T_c and P_c results for diethylamine + hexane. Experimental data from Mandlekar et al. [284] and Kreglewski et al. [285] and the TRC database [80].

A very reasonable description of critical pressures is obtained for the system containing diethylamine, this is in part due to the small gap between the critical temperatures, there is however a notorious difference in the description of critical temperatures for the mixture with the minima close to 90% amine not being verified. However it is important to note that a large range of critical temperatures is available for diethylamine. As is presented in the figure some of this pure T_c data values are close to the temperature of this minima, presenting a relevant uncertainty in terms of this behaviour.

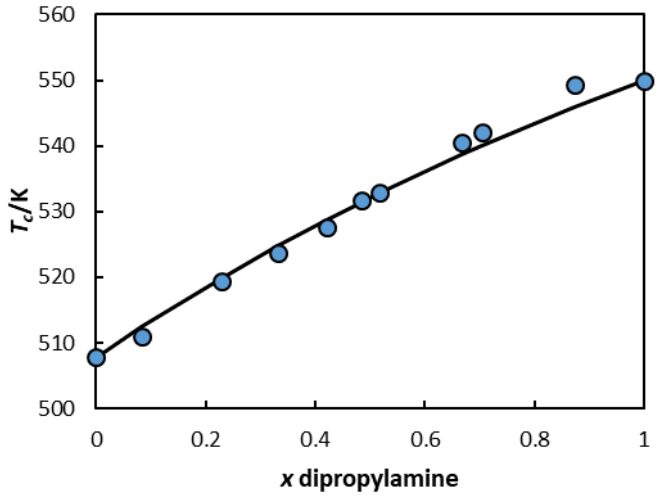

Figure 6.19 Results for T_c of dipropylamine + hexane. Experimental data from Toczylkin and Young [286].

For dipropylamine, some discrepancies are also verified for the data, with both pure critical points seemingly out of the curve of the mixture data.

6.3.5 *Critical point of methanol + methane and water + hexane (mixtures with some compositions where no critical point is observed)*

Table 6.7 Binary interaction parameters for mixtures of methanol + methane and water + hexane

comp. 1	comp. 2	fitted to	k_{ij}	figures	notes
methanol	methane	Gas solubility	$0.074+2.18\times10^{-4}T$	6.20	Fitted in chapter 4
methanol	methane	Critical data	0.069	6.20	
water	hexane	LLE	0.180	6.21	LLE Chapter 4
water	hexane	Critical data	0.075	6.21	

Two systems were studied in this section. Methanol + methane and water + hexane. It is important to note that in these systems there are compositions for which there are no critical point. For the first system, the k_{ij} obtained previously from the respective gas solubility data was applied. The results are presented in figure 6.20.

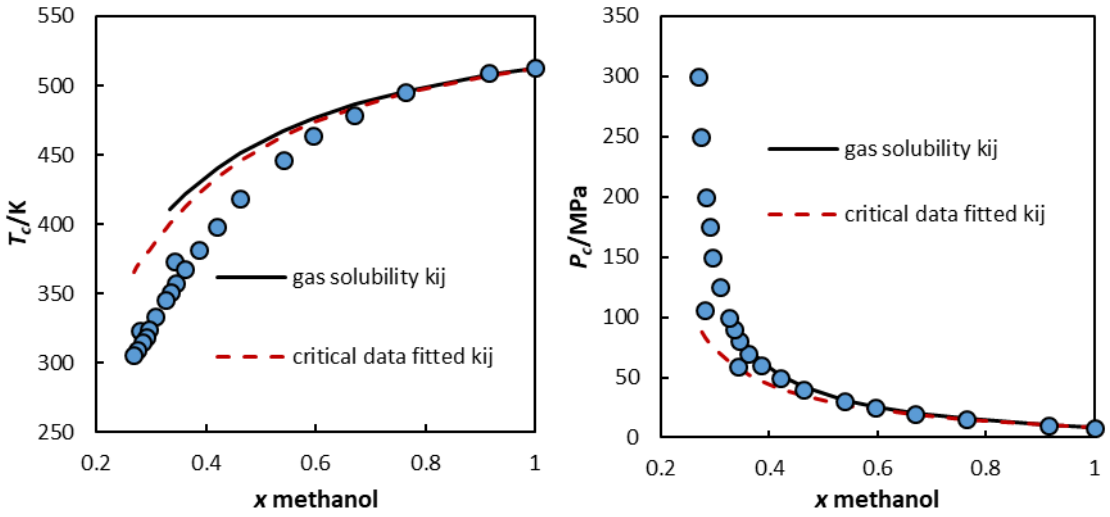

Figure 6.20 Results for T_c and P_c of methanol + methane. Experimental data from Brunner et al. [287] and Francesconi et al. [288].

Using the approach described above, the results obtained overestimate the range of composition for which it is not possible to obtain critical data, this is in part due to the k_{ij} used. The T_c is largely overestimated for higher methane concentrations while P_c is reasonably described for a large range of composition (%AAD is 4.63 between 0.334 and 0.915 x_c of methanol). Fitting a k_{ij} so that the whole experimental composition range presents critical points, but for a composition of methanol 5% below the last experimental point, no critical point is observed, results in the second set. Both sets present a reasonable estimation of critical pressures, within experimental uncertainties. While this second set improves slightly the description of critical temperatures.

Results for water + hexane are presented in figure 6.21. Two sets of binary interaction parameter were used. The first was obtained from the LLE analysed in chapter 4, while the second was fitted to the critical temperatures for fractions of water between 0.95 and 1. Figure 6.21 presents these results. Using the LLE fitted binary interaction parameter, the model predicts critical points for most of the composition range. However, their values present high deviations. Fitting the critical data, while improving the accuracy for the higher water compositions, leads to the model only predicting critical points up to a water mole fraction of approximately 0.93.

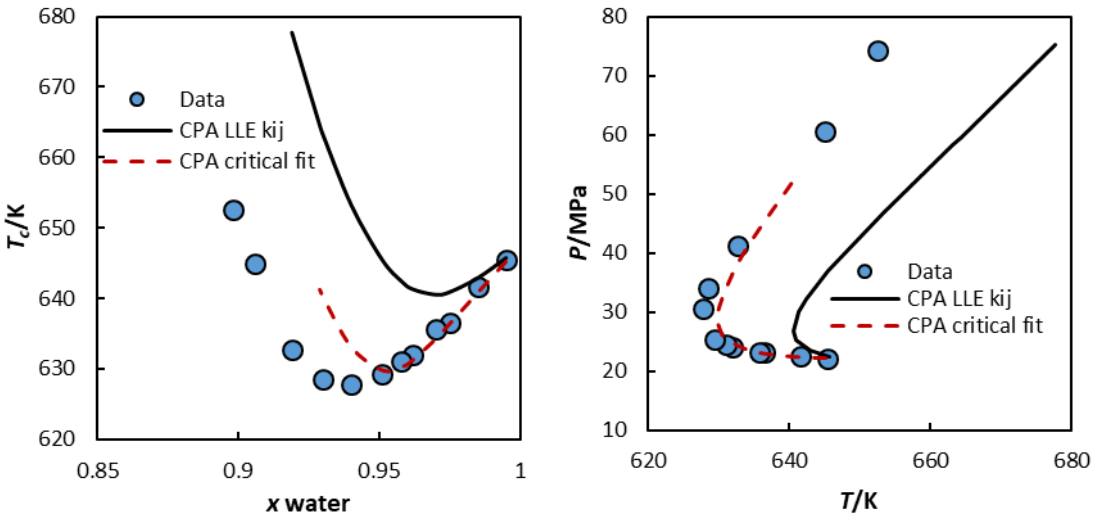

Figure 6.21 Detail of the results for T_c and P_c of water + hexane for high water compositions. Experimental data are from Tsonopoulos and Wilson [197].

6.3.6 Critical points of solvating mixtures

On chapter 4, it was shown that the method proposed by Folas et al. [136] to describe solvation also works with the modified CPA proposed in this thesis. This approach is expanded here to the study of mixture critical points containing at least one solvating component and one associative compound. Most of the binary interaction parameters were obtained from the VLE of the systems at near atmospheric conditions (whenever this is not the case it is noted in the text). The binary interaction parameters are presented in table 6.8.

As a first step and having previously studied the LLE of water + aromatics, it is of interest to evaluate if the obtained binary interaction parameters are able to describe mixture critical points. Figure 6.22 presents the results for water + benzene.

Table 6.8 Binary interaction parameters for solvating mixtures

comp. 1	comp. 2	fitted to	k_{ij}	β_{ij}	figures	notes
water	benzene	LLE	0.170	0.010	6.22	LLE chapter 4
methanol	benzene	VLE (1 bar)	0.034	no β_{ij}	6.23	VLE in annex
ethanol	benzene	VLE (1 bar)	0.042	no β_{ij}	6.23	
1-propanol	benzene	VLE (1 bar)	0.039	no β_{ij}	6.23	
2-propanol	benzene	VLE (313 K)	0.043	no β_{ij}	6.23	
1-butanol	benzene	VLE (1 bar)	0.032	no β_{ij}	6.23	
diethylamine	benzene	VLE (1 bar)	-0.028	no β_{ij}	6.24	VLE chapter 5
water	acetone	VLE (473 K)	-0.100	0.020	6.25	VLE in annex
ethanol	acetone	VLE (1 bar)	0.041	0.018	6.25	
ethanol	2-butanone	VLE (1 bar)	0.028	0.014	6.26	
2-propanol	2-butanone	VLE (1 bar)	0.022	0.005	6.26	
water	THF	VLE (1 bar)	-0.003	0.029	6.27	
1-butanol	diethyl ether	VLE (four Temp.)	no k_{ij}	no β_{ij}	6.27	
methanol	MTBE	VLE (1 bar)	0.013	0.018	6.28	
ethanol	MTBE	VLE (1 bar)	0.005	0.008	6.28	
1-propanol	MTBE	VLE (1 bar)	0.014	0.008	6.28	
heptane	MTBE	VLE (1 bar)	0.020	no βij	annexes	VLE in annex used in ternary fig. 6.29

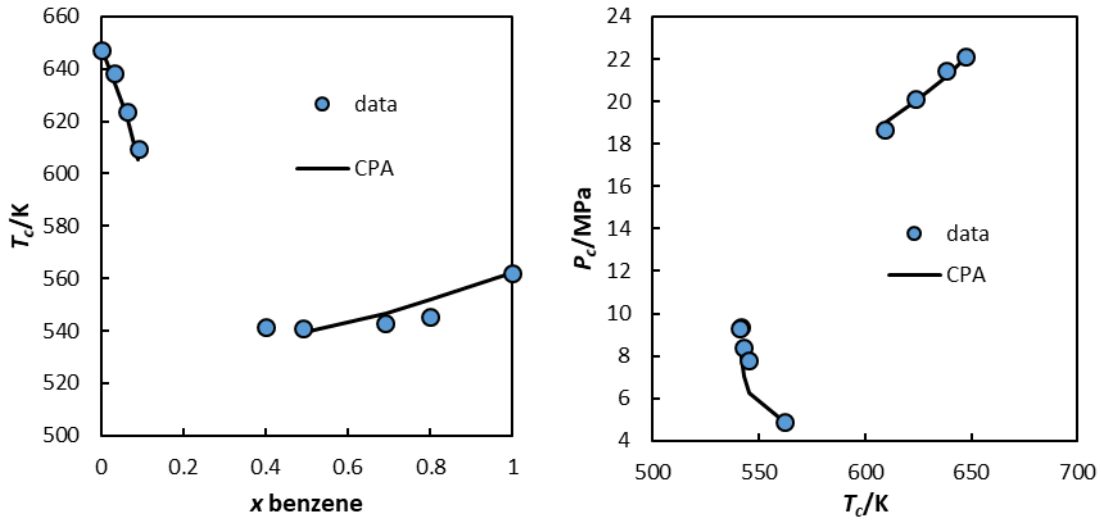

Figure 6.22 Results for the mixture critical points of water + benzene. Data from Hicks and Young [275].

The results show that the solvation approach used was able to accurately capture the dependence on composition of the critical temperature, for this system. A good description of

the relation between the critical pressure and critical temperature is also observed, which is similar, if not better, than for previously studied systems.

Following the study of water + benzene we looked at the description of aromatics + alkanols systems. However, for these systems, as with s-CPA, it is possible to describe VLE accurately without the use of a β_{ij}. This is also true for critical points. Thus, only k_{ij} was applied for these mixtures. Figure 6.23 presents the results for binary systems of benzene with five different alkanols.

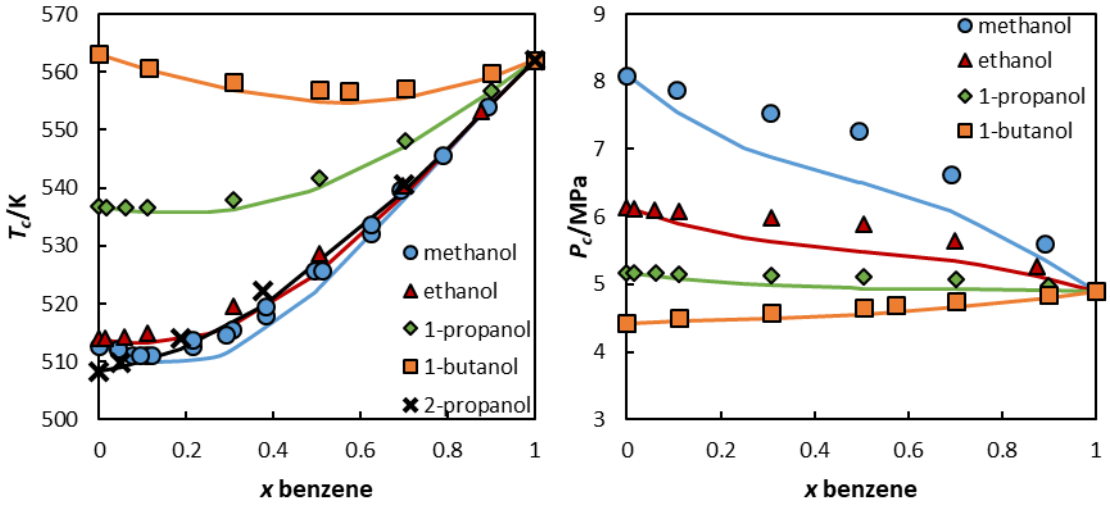

Figure 6.23 Results for the mixture critical points of alkanols + benzene. Data from Hicks and Young [275].

Without a β_{ij} value it is still possible to obtain a reasonable description for the critical temperatures. However, for the critical pressures, the deviations are significant for the systems with smaller alkanols. Such a behavior was previously observed for the mixtures of alkanols + alkanes. In the right figure 2-propanol is not presented, due to lack of experimental P_c data. The predictions for this property are, however, presented in the annexes.

The description of diethylamine + benzene is presented in figure 6.24.

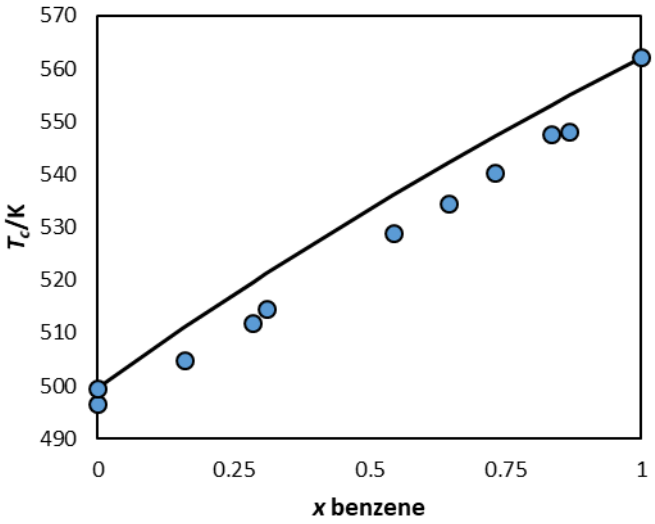

Figure 6.24 Critical temperature of diethylamine + benzene mixtures. Data from Multiflash [78] (pure compound) and Toczylkin and Young [286].

As can be seen in the figure the pure critical temperature data employed in CPA is slightly higher than that obtained by Toczylkin and Young [286]. Despite this fact the composition dependency is similar to what was previously observed for other systems.

The description of ketones is not straightforward using CPA. While for some applications they may be considered non-associative, solvating compounds, for others an associative scheme (usually 2B) is applied. In this work, the first of these approaches is considered. Figure 6.25 presents the results for the mixture acetone + water and acetone + ethanol.

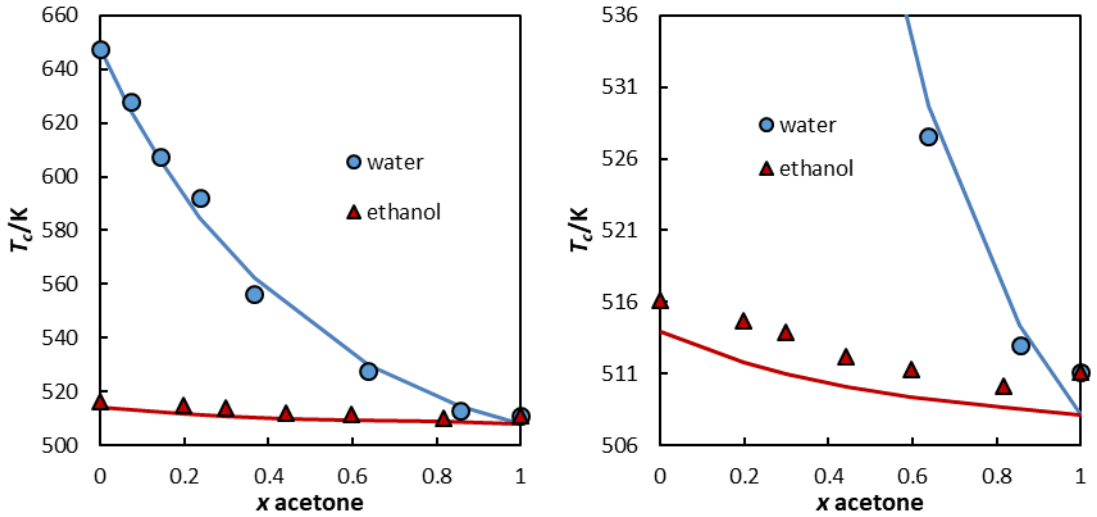

Figure 6.25 Critical temperature results for water + acetone and ethanol + acetone, binary interaction parameters obtained at 473.15 K for the first mixture and at 1 atm for the second (Figure on the right is a close-up of the one on the left). Experimental data from Marshall et al. [276].

The pure critical temperatures used in this work, taken from Multiflash [78] are slightly lower than those from Marshall et al. [276]. This can be observed on the right of figure 6.25, which is a close up of the plot on the left.

The analysis of critical data from the DIPPR [79] and TRC databases [80] corroborates the use of the critical data from Multiflash [78]. Nevertheless, the obtained trend agrees with the experimental data, which are probably overestimated, when compared to more recent values for the pure component critical data, as those available in the TRC database [80].

For 2-butanone two mixtures were analyzed, with ethanol and with 2-propanol, showing very good results, as presented in figure 6.26.

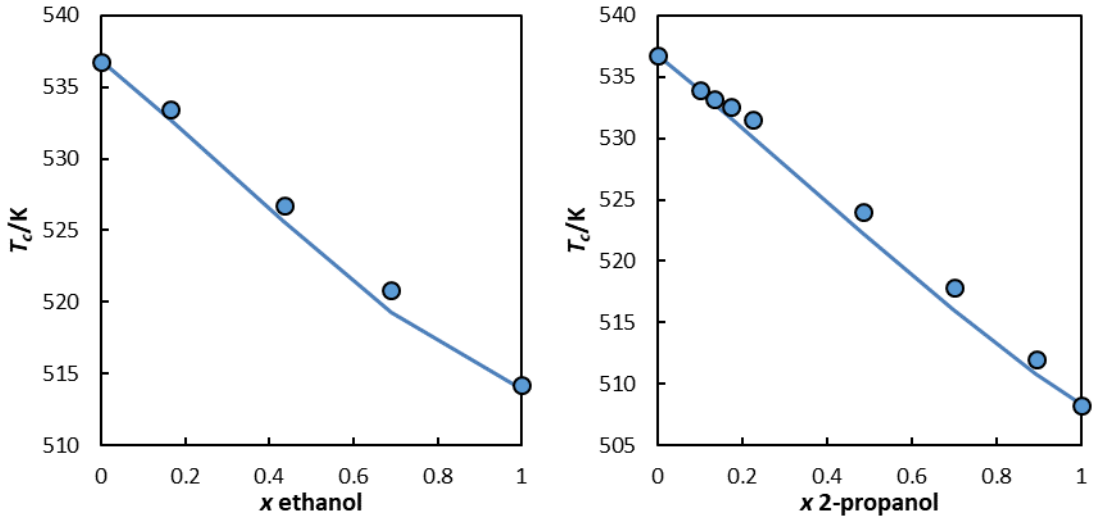

Figure 6.26 Critical temperature results for ethanol + 2-butanone (left) and 2-propanol + 2-butanone (right) mixtures. Experimental data from Nazmutdinov et al. [272].

For the mixtures containing ketones the critical temperature trends are well described. Thus, it seems reasonable to consider ketones as solvating compounds for estimating critical points. The predictions of the critical pressure for these mixtures are presented in annex.

Critical data concerning the mixtures diethyl ether + 1-butanol and THF + water are also available. The solvating approach is also able to describe the critical properties accurately for these compounds as presented in Figure 6.27.

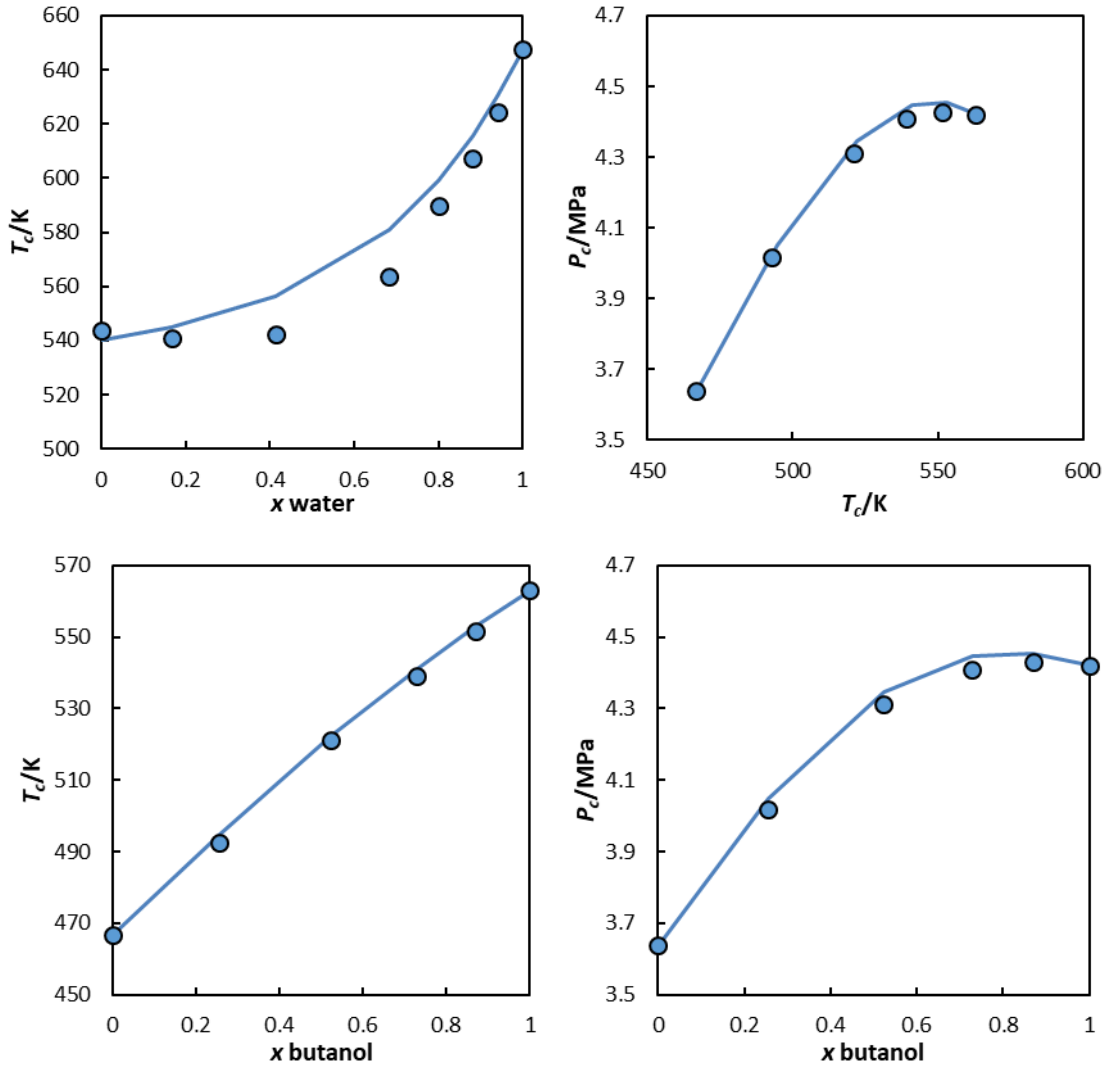

Figure 6.27 Critical temperature description for water + THF (top left) and Critical results for 1-butanol + diethyl ether. Experimental data from Kay and Donham [289] and Marshall et al. [276].

Accurate descriptions of the experimental data are obtained for the 1-butanol + diethyl, while for water + THF some deviations are observed for the critical temperature at intermediate compositions. No data was available for the critical pressures of this mixture. However, from the study of the systems where both T_c and P_c data were available, the introduction of solvation seemingly improves the description of the critical pressures. This is notorious in the next mixtures, were critical temperature also presents relevant deviations, while critical pressure is well described. However, this was only verified for these next mixtures and for water + benzene and thus should be investigated further.

For methyl tert-butyl ether (MTBE) Han et al. [290] and Wang et al. [273] have studied the critical points of three binary and two ternary systems, containing at least one associative compound. The results for the binary systems are presented in figure 6.28.

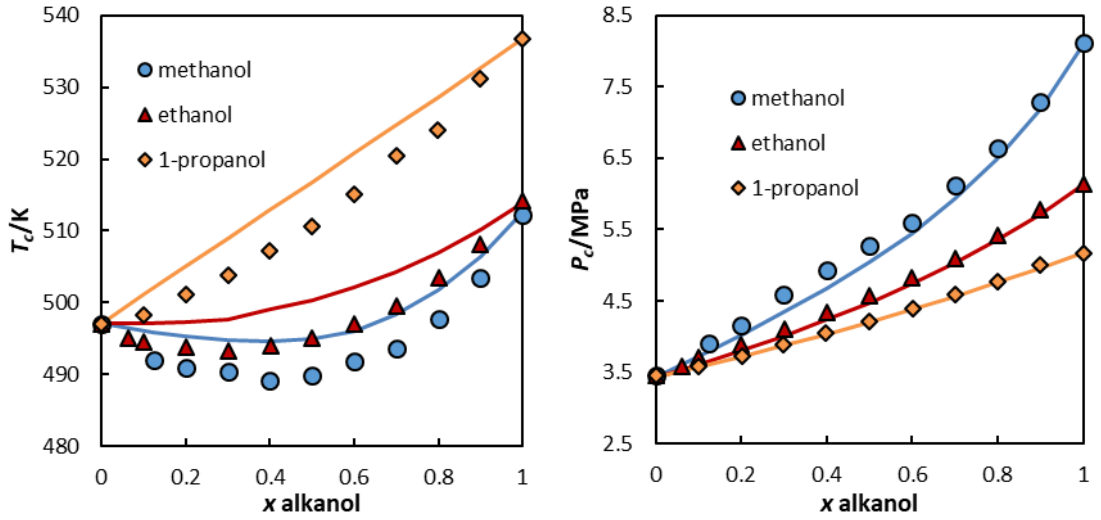

Figure 6.28 Critical results for MTBE + 1-alkanol. Experimental data is from Han et al. [290].

As previously discussed, these results present higher deviations in the critical temperatures than for the case of alkanes + alkanols. However, the deviations for the critical pressure are smaller. This may be due to the introduction of a β_{ij}. Every system in analysis where this parameter was used and compared against P_c data presents a better description of the P_c dependency with composition than for most of the non solvating systems. Nevertheless, the number of systems analyzed where this was verified is not enough to extrapolate this afirmation to other solvating mixtures.

As mentioned before, data is available for two ternary systems, MTBE + methanol + 1-propanol and MTBE + heptane + ethanol. The average absolute deviations obtained for the first of these mixtures are of 0.83% and 3.12% for T_c and P_c respectively. For the second mixture these are of 0.71% and 3.97%. The parity diagrams are presented in figure 6.29.

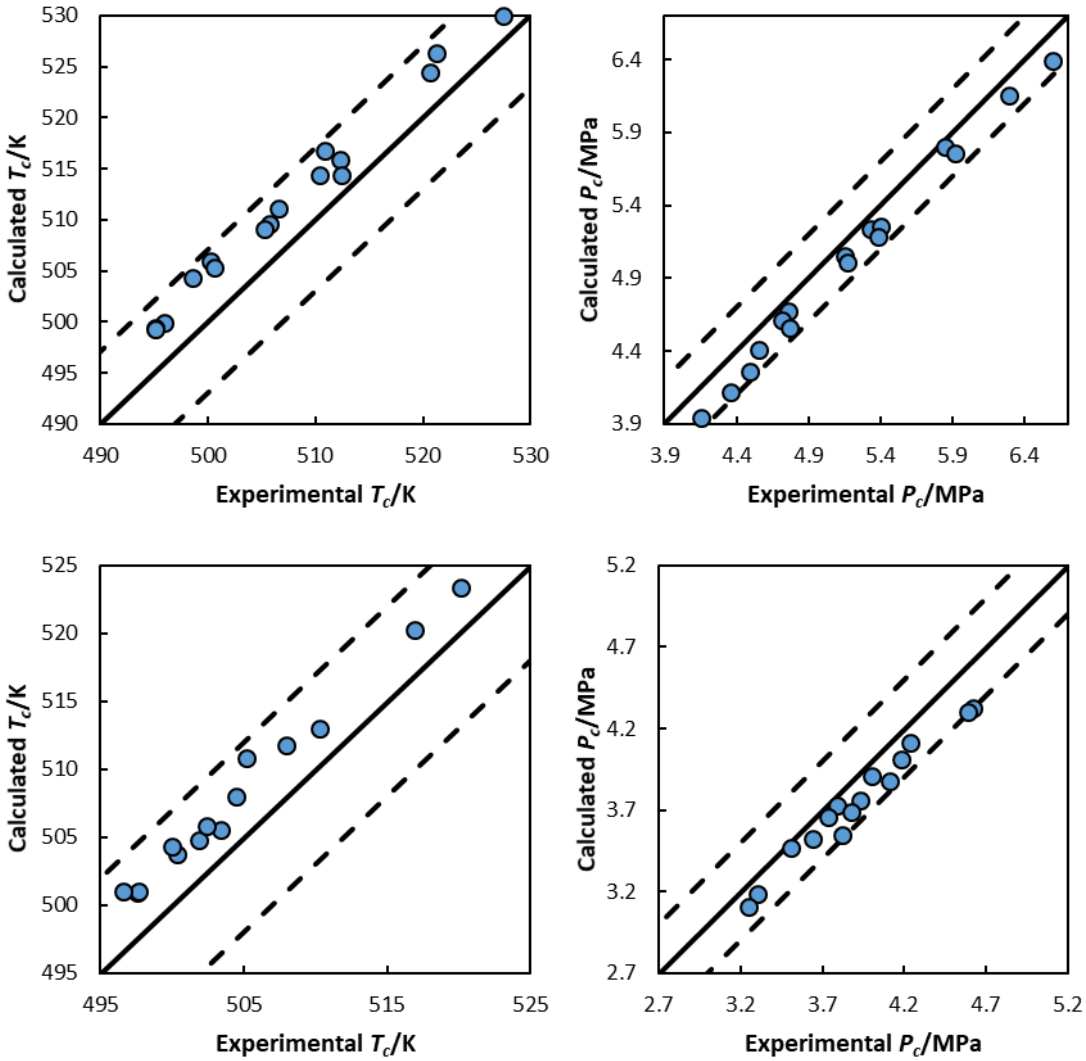

Figure 6.29 Parity diagrams for T_c and P_c of MTBE + ethanol + heptane (bottom) and for MTBE + methanol + 1-propanol (Top). The dashed lines correspond to ± 7 K and ± 0.3 MPa. Experimental data are from Wang et al. [273].

These results present deviations similar to those of the binary systems and are in reasonable agreement with the experimental data.

6.4 Conclusions

This chapter presented an evaluation of the modified CPA model presented earlier in this thesis to estimate critical properties of binary and ternary mixtures containing associating components.

The modified version of CPA was tested for the description of critical data of mixtures. The obtained results are accurate when both mixture compounds are associating compounds, as is the case of mixtures containing two primary alkanols or water + primary alkanol.

In the case of systems containing methanol and an alkane T_c results are very good, even when using an LLE fitted k_{ij}. The prediction of P_c is however slightly inferior, to that of s-CPA, due to the heavier weight of the cubic term in the present version. The association term of this version, near the critical temperature, tends to present values closer to 0 than s-CPA. Thus, the behaviour of a mixture of an associating compound + non-associating compound is closer to that of SRK, while in s-CPA the association contribution is still able to improve the description of P_c.

In most other systems of alkane + alkanol using a linearly temperature dependent k_{ij} results in an under prediction of T_c. In most cases it seems better to use a binary interaction parameter at near atmospheric conditions/ room temperature conditions. While doing this, in some cases, does not enable a good description of VLE in the whole range of temperatures, it is seemingly an accurate enough approach to describe critical temperatures.

Good descriptions are also obtained for the ternary systems containing one alkanol and two hydrocarbons. The case of the ternary containing 2-propanol is a particular case where the description presents higher inaccuracies. However, there are already relevant uncertainties in the data for the constituent binary systems, as well as, the value of the association volume being potentially too small. The results for the mixture containing ethanol + pentane + hexane were compared to those of similar equations of state, where the critical point of the pure compound is not fitted. As was expected these equations present systematically higher deviations on these properties if their parameters are not readjusted taking into account critical data.

The description of the mixtures methanol + methane and water + hexane is reasonable up to certain compositions. These mixtures are more complex, as there are certain compositions where no critical point is verified. Using the previously applied binary interaction parameters for these mixtures, the range of compositions where critical points were observed was smaller than that of the experimental data. This was improved by changing the binary interaction parameter in the mixture of methanol + methane. For the mixture water + hexane, this would lead to high deviations on the properties and thus, it was interesting to, instead, fit the critical data close to pure water, enabling a reasonable description of T_c and P_c for fraction of water from 0.93 to 1 .

The results for systems containing solvating compounds present a similar accuracy in the description of the experimental data to the previous systems. However, it is notorious that for the systems where P_c data was avalible, and β_{ij} was applied, the description of the critical

pressure was improved. However this also lead, in some cases, to a decrease on the accuracy of the critical temperatures.

In most of the systems analyzed the binary interaction parameters were either fitted to LLE data or to VLE at atmospheric conditions, which provides a considerable predictive character to these modelling results.

7 A tentative group contribution method for multifunctional molecules

7.1 Abstract

To reduce the need to parameterize the association term of every new compound, a group contribution method is proposed and tested in this chapter. This method is based on the results previously reported with the transferability approach from the previous chapters and ideas from other group contribution methods from the literature.

To evaluate the performance of the new method, the results are compared with those presented before using the transferability approach. In addition to the compounds studied in previous chapters, the new modified CPA is also applied to heavier 1-alkanols, cycloalkanols and three secondary amines not previously studied. VLE, LLE, SLE and critical mixture data for mixtures containing these compounds are also analysed.

7.2 Introduction

As presented in the introduction, the use of group contribution methods to parameterize equations of state improves the predictive features of the models.

The present CPA model uses a cubic term that is based on the components critical pressure and temperature (which in themselves can be obtained by group contribution methods) and on a single saturation property. However, association parameters have to be adjusted beforehand, or the transferability approach proposed before needs to be used. Despite the good results with the transferability approach, this methodology seems to present some problems for lighter compounds (the case of the small association volume for 2-propanol, mentioned in chapter 6, is an example) and thus requires different (specific) values for the smaller compounds of each family. This, allied to the expectation that such a simplistic approach would perform poorly when confronted with different associative groups in the same molecule, lead to the development of a group contribution approach.

This chapter focus on alkanols, diols and amines. No studies were conducted for thiols, as not enough reliable data were found to perform such analysis. In addition to the compounds previously studied, the group contribution method is also applied to heavier 1-alkanols with an even number of carbons (1-dodecanol to 1-eicosanol), two cyclic alkanols (cyclopentanol and cyclohexanol) and three more secondary amines (dibutylamine, diisopropylamine and ethylmethylamine).

Important applications for these compounds include the use of cyclohexanol as an intermediary in the production of nylon [291], and applications of cyclopentanol for cosmetics

and pharmaceuticals [292]. Various high chain alkanols have also applications in the cosmetics industry, including 1-dodecanol, which has an important role in the formulation of detergents, lubricating oils and pharmaceuticals [292]. Applications of diisopropylamine include uses in the rubber industry, production of polyester fibers and herbicides [293].

7.3 Group contribution method

The method proposed here is for the association term only. It retains the use of a constant energy of association for groups of the same type (ex: two secondary amine groups will always have the same energy of association, which is nevertheless different from that of primary amines). The method is generally based on the one proposed by Vijande and co-workers [36] with modifications to cope with branching and having multiple associative groups in the molecule. Equation 7.1 presents the main equation for this methodology:

$$\beta_{ki} = \beta_i + \sum_{j \neq i}^{n_{groups}} \frac{\Delta\beta_{ij}}{(\Gamma_{ij} d_{ij})^2} \tag{7.1}$$

where β_{ki} is the volume of association of group *k* of type *i*, β_i is the standard volume of association for groups of type *i*, $\Delta\beta_{ij}$ is the contribution to the association volume from the interaction of groups *i* and *j*. The distance between the groups is accounted as the shortest number of chemical bonds between each group in d_{ij} (ex: number of bonds between CH_3 and OH in methanol is one, while in 2-propanol is two). To account for branching and the existence of multiple association groups, a shielding factor (Γ_{ij}) is introduced:

$$\Gamma_{ij} = \left(1 + n_{ramifications\, i-j} - \varsigma_j\right); if\left(n_{ramifications\, i-j} - \varsigma_{ij}\right) < 0 \rightarrow \Gamma_{ij} = 0.5 \tag{7.2}$$

with, $n_{ramifications\, i-j}$ as the number of ramifications found between group *i* and *j*, ς_j is a binary variable which returns one if group *j* is associative and zero if this is not verified.

The first set of group parameters where obtained considering some objectives and constraints. The differences to the association volumes of methanol, ethanol and the three previously tested amines should be minimal, while the branched compounds, of the same family, with the same molecular weight, were considered as having a smaller volume of association than their linear counterpart. The volume of association should also be always positive. Some modifications to ensure this last constraint may be needed when more groups are added for secondary amines. In a first approximation it was considered that for linear alkanols the standard value was that of the transferability approach.

The parameters for both the standard association volume (β_i), considering the above mentioned restrictions, as well as the contributions from group-group interactions ($\Delta\beta_{ij}$) are presented in Table 7.1.

Table 7.1 Parameters tested for the group contribution method

Associative group i	*OH*	*NH*
$\beta_i \times 10^4$	6.472	2.547
$\beta_{i\text{-}CH2} \times 10^4$	0.000	0.000
$\beta_{i\text{-}CH3} \times 10^4$	22.500	40.706
$\beta_{i\text{-}CH} \times 10^4$	-3.064	-1.260
$\beta_{i\text{-}C} \times 10^4$	-3.47178	yet to be studied
$\beta_{i\text{-}OH} \times 10^4$	45.000	yet to be studied

7.4 Results and discussion

7.4.1 Pure compound properties

Using the group contribution method proposed above, the pure properties for primary alkanols (from 1-propanol to 1-hexanol) were recalculated, as well as those for secondary alkanols. As the standard value for the β_i of alkanols was considered to be the same as that obtained in the transferability approach for linear alkanols, testing the results up to 1-hexanol should provide enough information to compare the two approaches. With the increase in the chain length for alkanols, the volume of association obtained through the group contribution method will tend to that of the transferability approach. Figure 7.1 presents a comparison on the results for C_p.

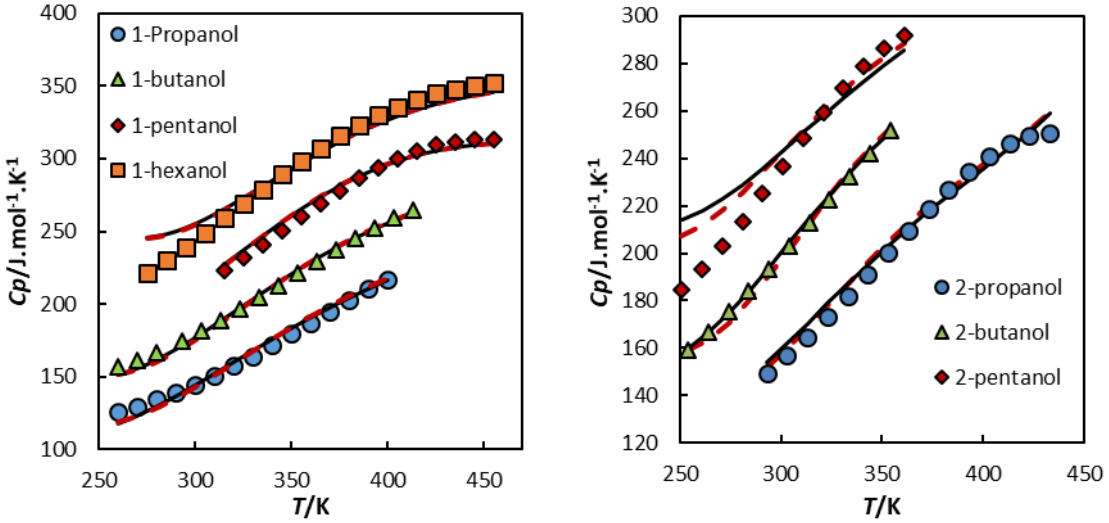

Figure 7.1 Liquid *Cp* results for primary (left) and secondary alkanols (right). Full lines are results applying the group contribution method, while dashed lines are with the transferability approach.

The differences on the isobaric liquid heat capacity of primary alkanols between the two methods are rather small and negligible, for secondary alkanols these differences are more relevant, but, with the exception of 2-pentanol, these are not too detrimental. For 2-pentanol the incorrect effect produced by the alpha function at low temperatures is increased with the new set of parameters. C_p is the pure property most affected by these modifications. Figure 7.2 presents differences for two of the other properties in study, H^{vap} and $\rho_{liq.}$, for diols.

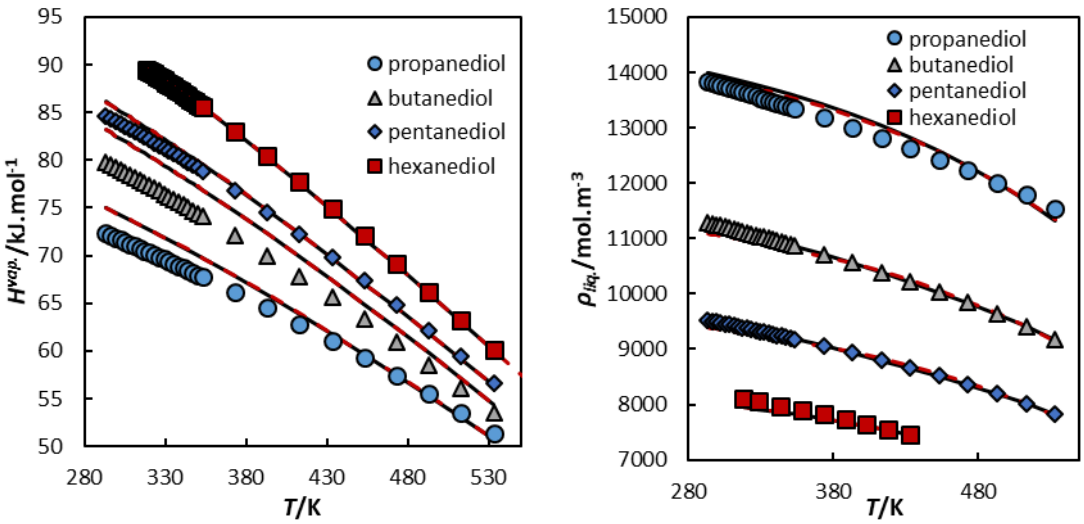

Figure 7.2 Heat of vaporization (left) and liquid density (right) results for primary diols. Full lines are results applying the group contribution method, while dashed lines are applying the transferability approach.

Looking at the present results, in terms of pure compounds properties, there is not a large difference between the parameters obtained by the two methods for C_p, H^{vap} and ρ_{liq}. In terms of the saturation pressure, the group contribution method tends to present slightly lower deviations, however both sets of results are well within the experimental uncertainty. For the three amines previously analysed the volume of association with the group contribution method are very similar to those proposed in chapter 5 and thus are not compared.

A few more compounds were studied with the group contribution method, including cyclic alkanols and three more secondary amines (diisopropylamine, ethylmethylamine and dibutylamine). The results for primary alkanols were also expanded to five more compounds (1-dodecanol, 1-tetradecanol, 1-hexadecanol, 1-octadecanol and 1-eicosanol), however the volume of association for these compounds are very close to what would be obtained with the transferability approach, and so, such analysis serves mainly the purpose of verifying if both methods work reasonably well for larger chains. The vapour pressure values used for the parameterization of these compounds were taken from the DIPPR [294] and TRC [80] databases. Figure 7.3 presents results for liquid density and liquid C_p of heavy alkanols.

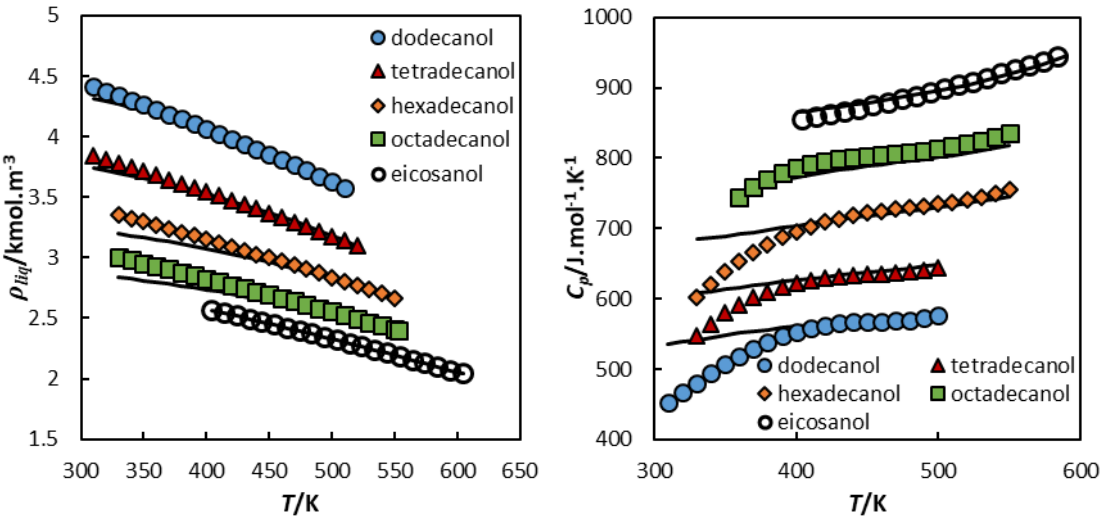

Figure 7.3 Liquid density (left) and liquid C_p (right) results for heavy alkanols. Data was obtained from the DIPPR correlations. [294]

Good results are obtained for the density of these compounds. As expected, there is an increase in deviations for lighter alkanols. However, these deviations are still reasonable within the temperature range in analysis. For the isobaric heat capacity the results are not well described at low temperatures. The lower vapour pressures and higher uncertainties for that property in these compounds, as well as the limitations of using an unconstrained alpha function are some of the possible reasons for this behaviour. Still, for higher temperatures the values and temperature dependences obtained are very reasonable. Results for the heat of vaporization are presented in figure 7.4.

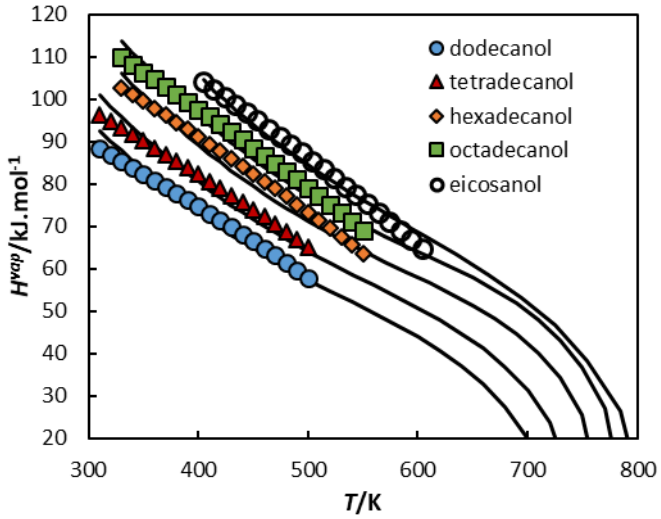

Figure 7.4 Heat of vaporization results for heavy alkanols. Data was obtained from the DIPPR correlations. [294]

As in the case of the liquid heat capacity, the results for the heat of vaporization present some deviations for lower temperatures. However, the temperature dependency at higher temperatures is very reasonable and captures the data very well.

The next set of results are related to the description of pure compound properties of cyclic alkanols and secondary amines. Figure 7.5 presents the results for liquid density and heat of vaporization of these compounds.

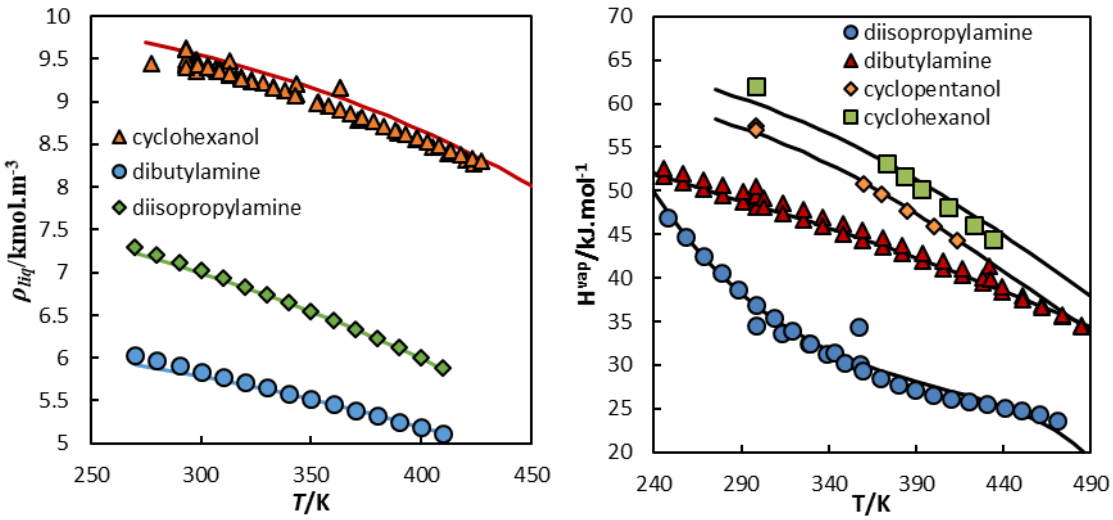

Figure 7.5 Liquid density (left) and heat of vaporization (right) results for cycloalkanols and secondary amines. Data from the DIPPR [294] and TRC [80] databases.

Two cycloalkanols and three secondary amines are analysed. However, due to the lack of experimental data for many of the properties, not all results are presented. Liquid density is well described for the two amines in analysis, while for cyclohexanol it tends to be slightly overestimated. For cyclopentanol some liquid density data is available in the literature, however only for a small temperature range, which is also far away from the 0.7 T_r, leading to a large extrapolation for the calculation of the volume shift. For the temperature range in analysis, the heat of vaporization is accurately described. Figure 7.6 presents the results for C_p.

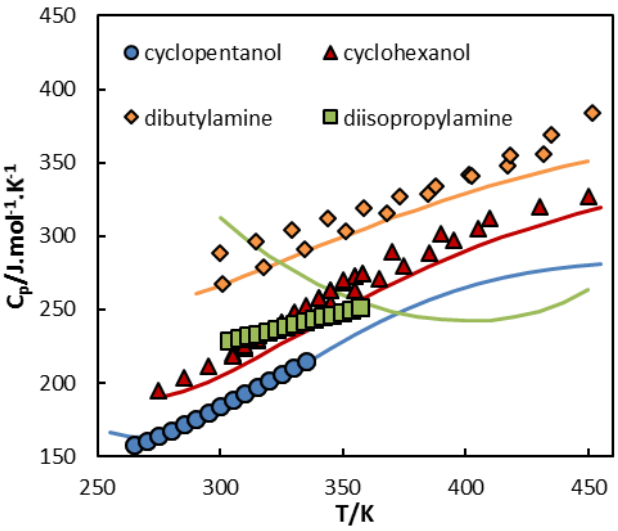

Figure 7.6 Heat capacity results for cycloalkanols and secondary amines. Data from the DIPPR [294] and TRC [80] databases.

For these compounds the heat capacity presents a correct trend, except for diisopropylamine, with slight underestimations for dibutylamine and cyclohexanol. The higher uncertainties for the vapour pressure of diisopropylamine, are more likely at the basis of the incorrect description of its heat capacity.

The pure compound properties are well described for the compounds studied. It becomes then important to analyse how the group contribution method deals with mixtures. It is important to note that no data was available for the pure critical properties of ethylmethylamine. The most common group contribution methods for critical properties [173] presented different results for the same properties on the previously studied secondary amines and thus were not considered. In approximation, these values were interpolated from the critical data on linear secondary amines from dimethylamine to dibutylamine, considering logarithmic trends for both properties. The critical data for the compounds studied in this chapter are presented in annex (Table A 18), as well as their origin.

7.4.2 Mixtures, phase behaviour and properties

The results of this section are divided in two parts. The first will deal with a comparison of VLE and critical points of mixtures using the transferability approach and the new group contribution method, while the second will analyse VLE, LLE, SLE and critical points of mixtures for a few new compounds not investigated before.

The compounds for which the parameters were most modified were the light primary alkanols, (except methanol and ethanol), light diols (except MEG), and branched alkanols and diols.

Figure 7.7 presents VLE results containing some of these compounds, in this case 2-propanol, 1,3-propanediol and tert-butanol.

Table 7.2 Binary interaction parameters obtained with both methods for previously studied mixtures.

comp. 1	comp. 2	k_{ij} transf. app.	k_{ij} GC method	Figure	Notes
1,3-propanediol	2-propanol	-0.015	0.000	7.7	
ethanol	tert-butanol	-0.024	-0.024	7.7	
water	1-propanol	$-2.93\times10^{-4}T+0.125$	$-2.70\times10^{-4}T+0.119$	7.8	
hexane	1-propanol	0.041	0.040	7.9	VLE in annex
hexane	1-butanol	0.027	0.025	7.9	
hexane	1-pentanol	0.031	0.030	7.9	
ethanol	2-propanol	-0.009	-0.009	7.10	

The compounds for which the parameters were most modified were the light primary alkanols, except methanol and ethanol, light diols, except MEG, and branched alkanols and diols. Figure 7.7 presents VLE systems containing some of these compounds, in the case 2-propanol, 1,3-propanediol and tert-butanol.

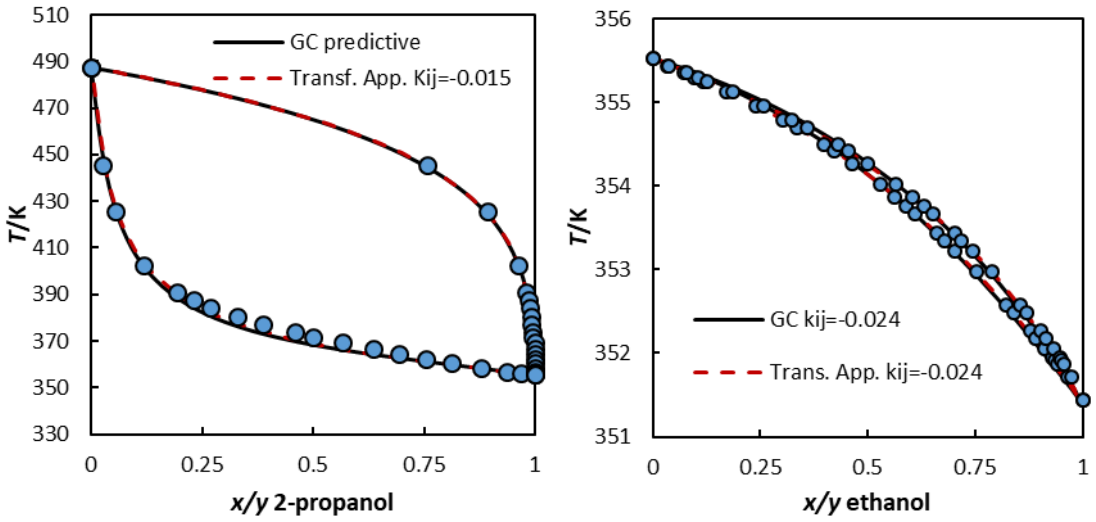

Figure 7.7 Results for the VLE of 1,3-propanediol + 2-propanol 1 atm (left) [178] and tert-butanol + ethanol at 1 atm (right) [80].

For these two systems the results are very similar with both approaches. In the case of 1,3-propanediol + 2-propanol, the group contribution approach is predictive presenting a slight advantage over the transferability approach, however for the system with tert-butanol, both need similar binary interaction parameters.

Other systems of interest are the VLE with water. The deviations for saturation pressures with both methodologies for 1-propanol or 2-propanol with water are presented in table 7.2. The

binary interaction parameters for these systems are: water + 1-propanol k_{ij} = -2.70x10^{-4}*T* +0.119 and water + 2-propanol k_{ij} = -2.08x10^{-4}*T* +0.064.

Table 7.3 Bubble and dew pressure deviations (%) for water + 1-propanol and water + 2-propanol

water + 1-propanol					**water + 2-propanol**				
	Transf. App.		GC method			Transf. App.		GC method	
***T*/K**	*Pbub*	*Pdew*	*Pbub*	*Pdew*	***T*/K**	*Pbub*	*Pdew*	*Pbub*	*Pdew*
273 [295]	2.42	-	2.64	-	**308 [296]**	3.13	1.56	4.85	2.17
279 [295]	5.25	-	5.29	-	**318 [296]**	1.9	1.08	3.99	1.93
313 [297]	1.4	1.06	1.95	1.33	**338 [296]**	0.8	0.51	3.00	1.60
403 [298]	1.41	0.76	1.24	0.90	**348 [296]**	0.92	0.53	2.69	1.50
413 [298]	1.59	1.27	0.97	1.15	**423[b] [299]**	3.76	3.07	2.74	2.75
423 [298]	2.3	0.97	1.63	0.45	**473[b] [299]**	2.03	1.61	2.14	1.12
					523[a] [299]	0.52	0.5	1.64	1.37
					548[a] [299]	2.19	0.91	0.73	1.10

For the two mixtures in analysis in table 7.2 the group contribution method seems to present some advantages when dealing with higher temperatures, while the transferability approach presents better results at lower temperatures. The results are however good and reasonably similar in both cases.

When the new parameters for the mixture water + 1-propanol are applied to calculate mixture critical points, the results for both methods are very similar, as can be observed in figure 7.8.

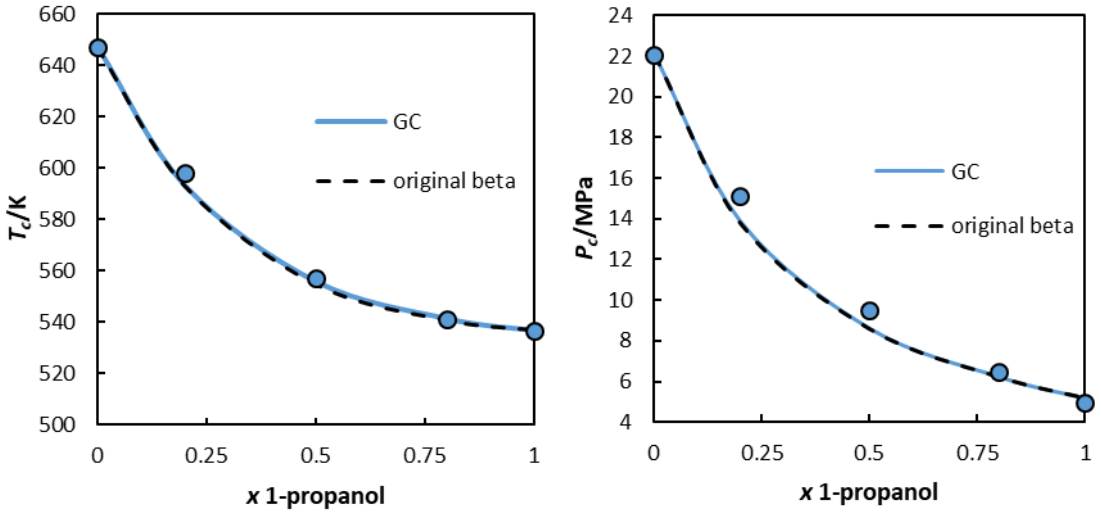

Figure 7.8 Results for T_c (left) and P_c (right) in relation to the predicted critical compositions of water for water + 1-propanol. Experimental data from Hicks and Young [275], Marshall and Bazaev et al. [277].

For mixture critical points for alkanols + alkanes, the group contribution method also presents similar results to those of the transferability approach, presenting slight improvements for smaller alkanols as is the case of 1-propanol., The results for T_c of mixtures of *n*-hexane with some primary alkanols are presented in figure 7.9. The analysis of the same mixtures at atmospheric conditions (used to obtain the interaction parameters for these critical point calculations) are presented in the annexes of chapter 7.

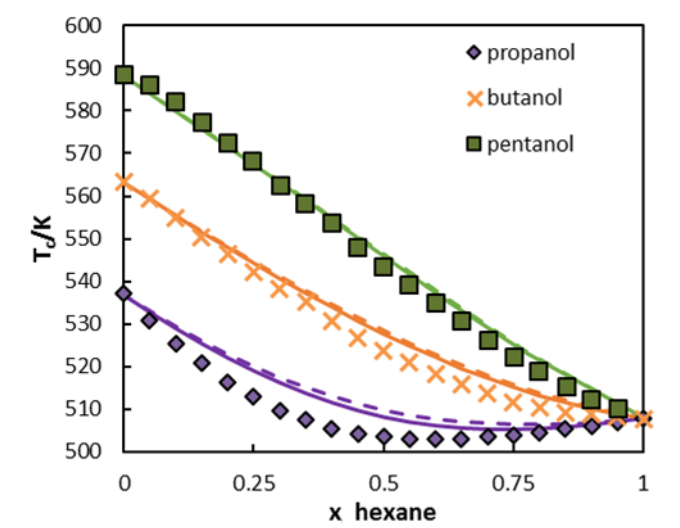

Figure 7.9 Critical temperatures for hexane + alkanol mixtures using $k_{ij's}$ obtained from atmospheric VLE data. Full lines are results using the GC method, dashed lines are with the transferability approach. Data from Gil et al. [197] and LagaLázaro [204].

One of the mixtures which presented some higher deviations while using the transferability approach was ethanol + 2-propanol. This is now improved when applying the GC method.

Nevertheless, there is still a high uncertainty in the experimental data. These results are presented in figure 7.10.

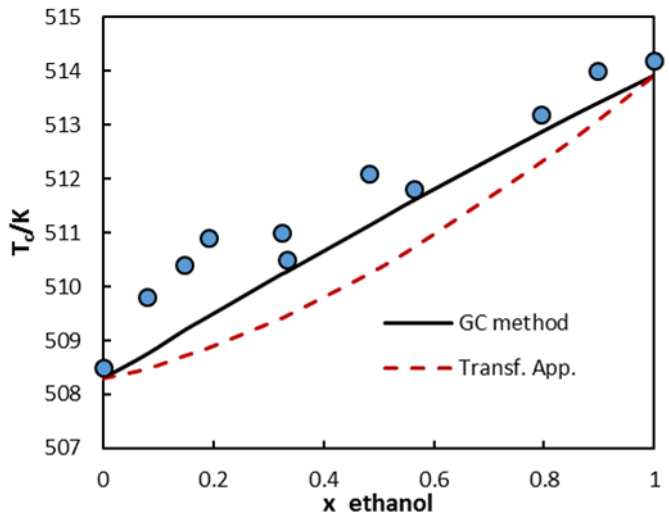

Figure 7.10 Critical temperatures for ethanol + 2-propanol, using a k_{ij}' obtained from VLE data (at 1.013 bar). Full lines are results using the GC method, dashed lines are with the transferability approach. Data from Nazmutdinov et al. [198].

For the compounds studied so far it seems that the group contribution method can be applied instead of the transferability approach, without decreasing the quality of the results and even improving some of those. It is thus important to verify if the present approach describes well mixtures for heavy alkanols and other molecules, which were not previously analysed.

For the heavy alkanols an analysis is conducted on the description of VLE with undecane and of SLE with other alkanols. Figure 7.11 presents the VLE for 1-dodecanol + undecane and 1-tetradecanol + undecane. Results for mixtures of lighter alkanols with undecane, as well as, SLE results for other systems not considered here are presented in the annexes.

Table 7.4 Binary interaction parameters for mixtures containing heavy alkanols.

comp. 1	comp. 2	k_{ij} GC method	Figure
undecane	1-tetradecanol	0.010	7.11
undecane	1-dodecanol	0.004	7.11
1-dodecanol	1-tetradecanol	-0.004	7.12
1-octadecanol	1-tetradecanol	-0.004	7.13
1-octadecanol	1-dodecanol	-0.017	7.14

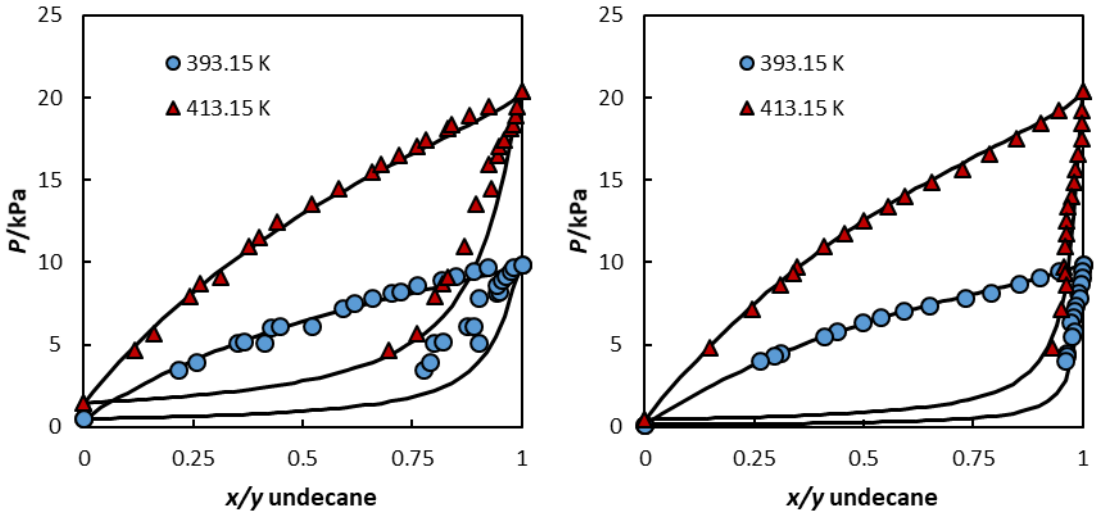

Figure 7.11 VLE results for undecane + 1-dodecanol (left) and undecane + 1-tetradecanol (right). k_{ij} values are 0.004 and 0.010 respectively. Data from Schmelzer et al. [227].

Due to the high carbon number of these alkanols, the association will not significantly affect their description as much as for lighter alkanols, and since the number of carbons on the alkane and on the alkanol are similar, it is possible to describe these systems with small interaction parameters.

Figure 7.12 presents the results for the SLE of 1-decanol + 1-tetradecanol. The boiling temperatures and heats of fusion applied for this and the other SLE systems are presented in the annexes (Table A 19).

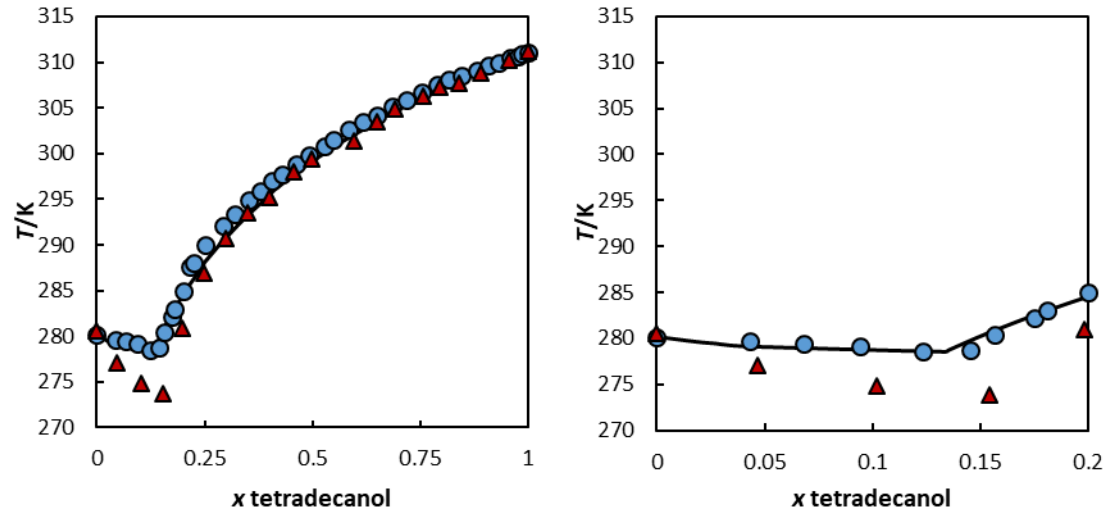

Figure 7.12 SLE results for 1-decanol + 1-tetradecanol. Circles are data from Domańska and Gonzalez [301], and triangles from Carareto et al. [302].

The results for this system are well within the uncertainty considering the two sets of data in study. The analysis of the data from the same authors for 1-octanol + tetradecanol yields similar results, presented in figure 7.13.

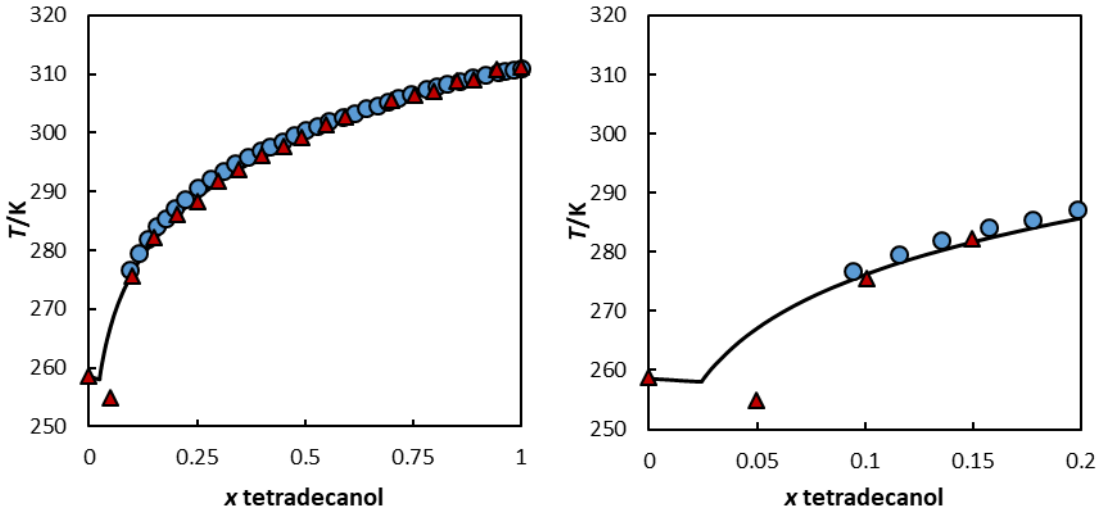

Figure 7.13 SLE results for 1-octanol + 1-tetradecanol. Circles are data from Domańska and Gonzalez [301], triangles are data from Carareto et al. [302].

For both of these mixtures the model describes well the data by Domańska and Gonzalez [228], which presents a higher eutectic temperature. For the system octadecanol + dodecanol, presented in figure 7.14, the model describes accurately the data by Carareto et al. [229]. It is also important to note that for most of these systems the binary interaction parameters, while negative are in modulus inferior to 0.01, 1-octadecanol + 1-dodecanol being one of the few exceptions.

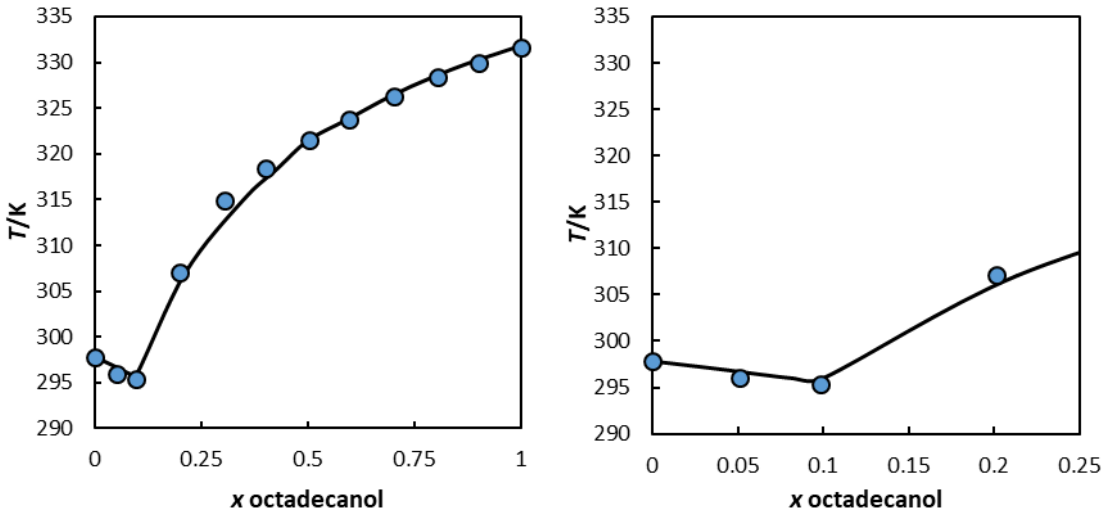

Figure 7.14 SLE results for 1-octadecanol + 1-dodecanol. Data from Carareto et al. [302]

To test the description of mixtures containing the secondary amines in analysis VLE, LLE and mixture critical data were considered. Three VLE systems are presented in figures 7.15 and 7.16: hexane + ethylmethylamine, hexane + diisopropylamine and 2-propanol + diisopropylamine.

Table 7.5 presents the binary interaction parameters for mixtures with these three secondary amines.

Table 7.5 Binary interaction parameters for mixtures containing secondary amines.

comp. 1	comp. 2	k_{ij} GC method	Figure
n-hexane	ethylmethylamine	0.032	7.15
hexane	diisopropylamine	0.000	7.16, 7.17
2-propanol	diisopropylamine	-0.012	7.16
pentane	dibutylamine	0.000	7.17
hexane	dibutylamine	0.000	7.17
octane	dibutylamine	0.000	7.17
benzene	dibutylamine	0.000	7.17
benzene	diisopropylamine	0.000	7.17
water	dibutylamine	$1.82 \times 10^{-4}T - 0.114$	7.18
water	diisopropylamine	$1.06 \times 10^{-3}T - 0.416$	7.18

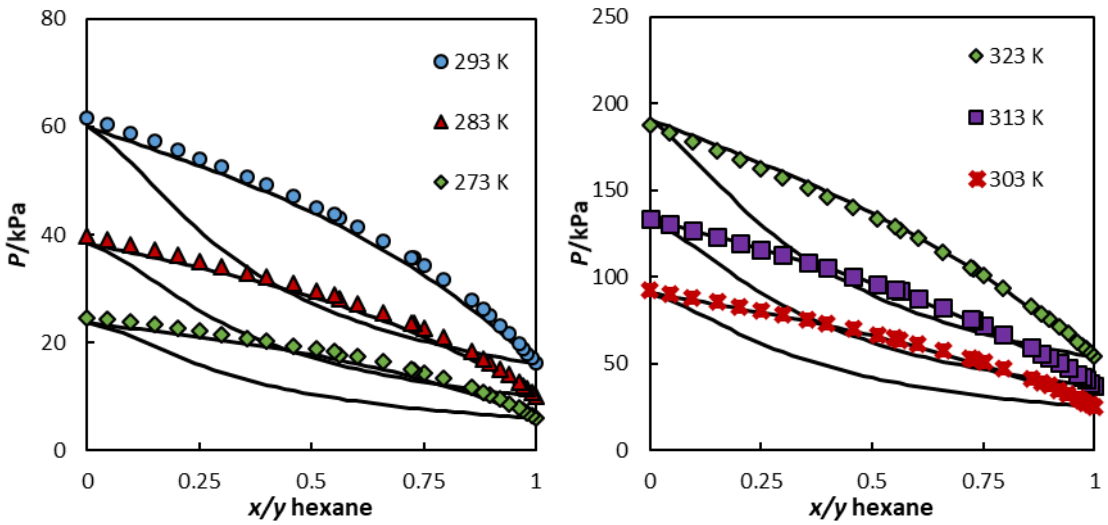

Figure 7.15 VLE description of n-hexane + ethylmethylamine at six different temperatures. Data from Wolff and Schiller [303].

As previously discussed, the pure critical data for ethylmethylamine was interpolated, as no experimental data was found in the literature and common group-contribution methods were found to be unreliable. Despite this, and knowing that the modified CPA is highly dependent on the accuracy of the critical parameters and the vapour pressure curve, the results for the mixture with hexane present a good description using a constant binary interaction parameter.

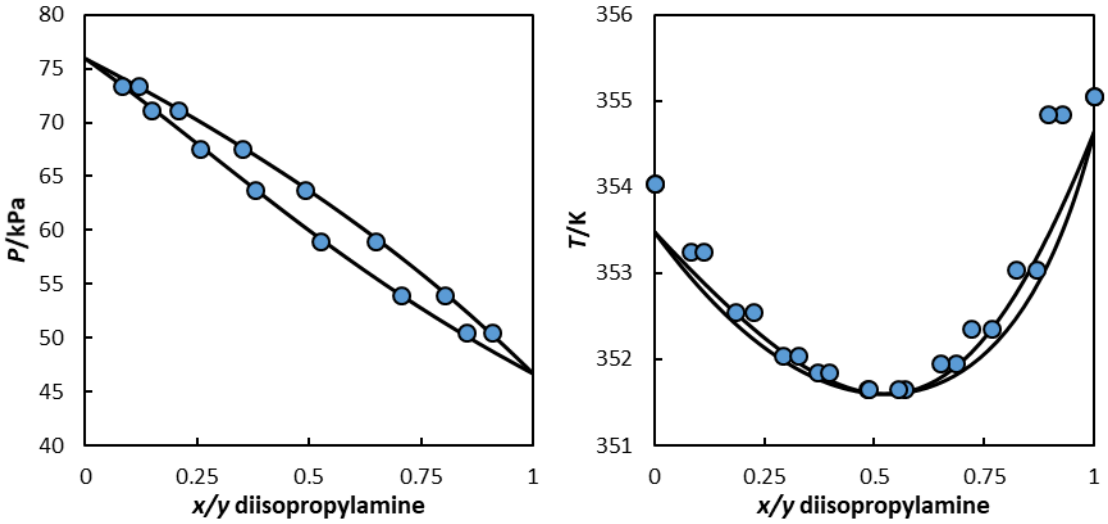

Figure 7.16 VLE prediction (k_{ij}=0.0) of n-hexane + diisopropylamine at 333.15 K (left) and correlation of diisopropylamine + 2-propanol (right, k_{ij}=-0.012, 94 kPa). Data from Humphrey and Winkle [231] and Sunder and Prasad [232].

In the above mixture containing 2-propanol, deviations on both pure compound saturation temperatures are observed. However these deviations are within the range of data available in the literature and are in both cases inferior to 0.2% of the data from Sunder and Prasad [232]. In the case of diisopropylamine + n-hexane it was possible to predict the equilibria with good accuracy. This, and the lack of available data for subcritical equilibria for systems containing these amines, lead to tests concerning mixture critical properties considering no binary interaction parameters. The results for these tests are presented in figure 7.17.

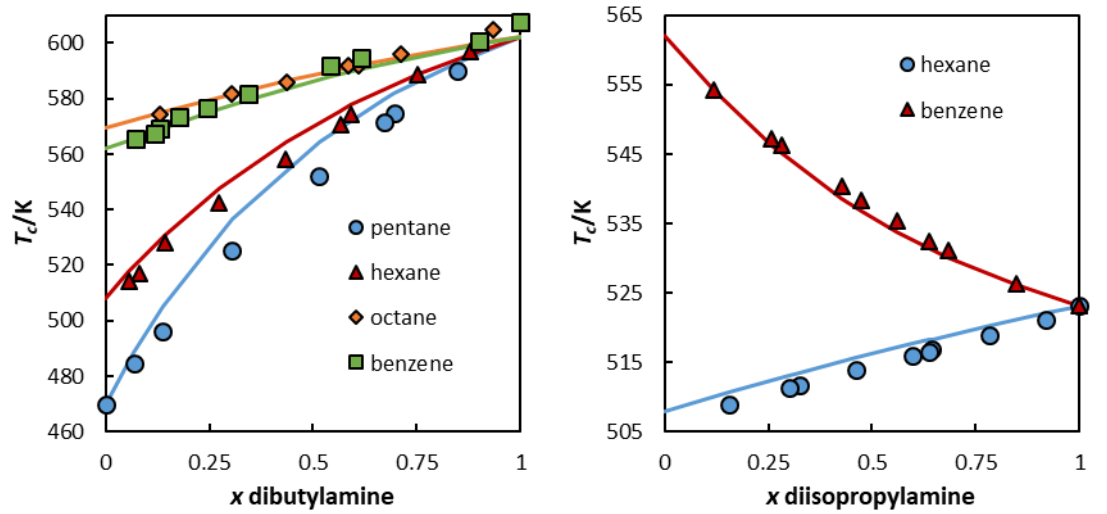

Figure 7.17 Predictions (k_{ij}=0.0) of mixture critical temperatures for binaries containing dibutylamine (left) and diisopropylamine (right) and hydrocarbons. Data from Toczylkin and Young [212].

Despite the higher uncertainties, lack of binary interaction parameters and differences in pure critical properties between the experimental data presented (for the pure critical data) and the

more recent data used to parametrize CPA, the model was capable of an accurate description of these mixture critical properties.

As in the case of dipropylamine + water presented in chapter 5, to model the LLE of secondary amines with water we need a temperature dependent binary interaction parameter to describe one of the phases, the model, with the presented parameter set, was unable to describe both phases simultaneously. Some of these LLE results are presented in figure 7.18. The binary interaction parameters with water were k_{ij} = 1.82x10^{-4}*T* -0.114 for dibutylamine and k_{ij} = 1.06x10^{-3}*T* -0.416 for dipropylamine.

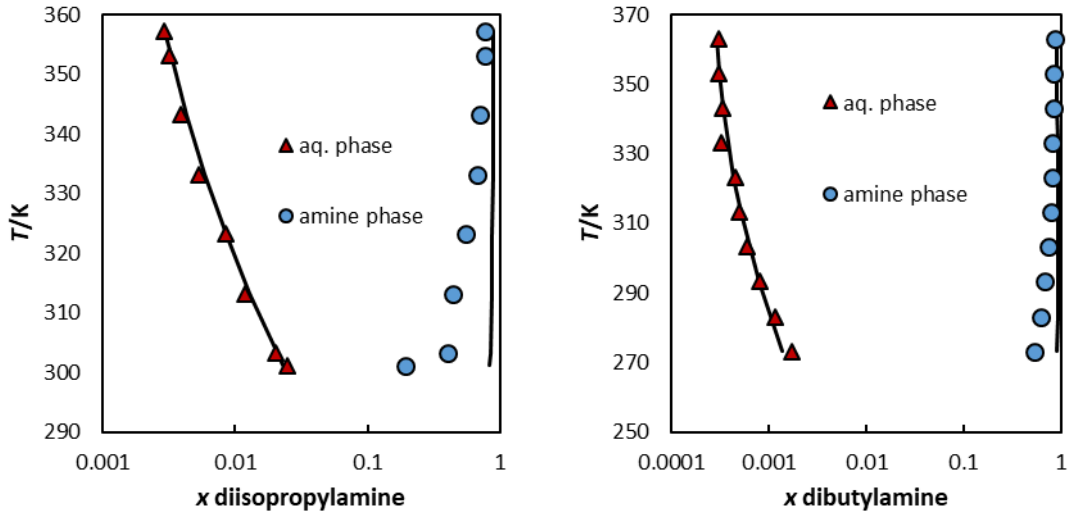

Figure 7.18 Results for the LLE of diisopropylamine (left) and dibutylamine (right) with water. Data from Stephenson [256].

Accurate descriptions of the experimental data are obtained for the aqueous phase, while the lower critical point is highly underestimated.

For systems containing cycloalkanols, the study included VLE and LLE, including some ternary mixtures. The first mixture studied was that of water + cyclohexanol, presented in figure 7.19.

. Table 7.6 presents the binary interaction parameters for mixtures containing cyclic alkanols.

Table 7.6 Binary interaction parameters used for binary and ternary mixtures containing cyclic alkanols.

comp. 1	comp. 2	k_{ij} GC method	Figure	Notes
water	cyclohexanol	0.028	7.19	
water	cyclohexanol	0.005	7.19	
cyclohexane	cyclohexanol	0.031	7.20, 7.23	
cyclohexene	cyclohexanol	0.023	7.20, 7.23	
o-xylene	cyclohexanol	0.023	7.20, 7.23	
nonane	cyclohexanol	0.023	7.20, 7.23	
heptane	cyclohexanol	0.018	7.21	
cyclopentane	cyclohexanol	0.030	7.22	
cyclohexane	cyclopentanol	0.021	7.22	
o-xylene	nonane	0.000	7.23	
water	cyclohexane	0.225	7.23	
water	cyclohexene	0.028	7.23	β_{ij}=0.010

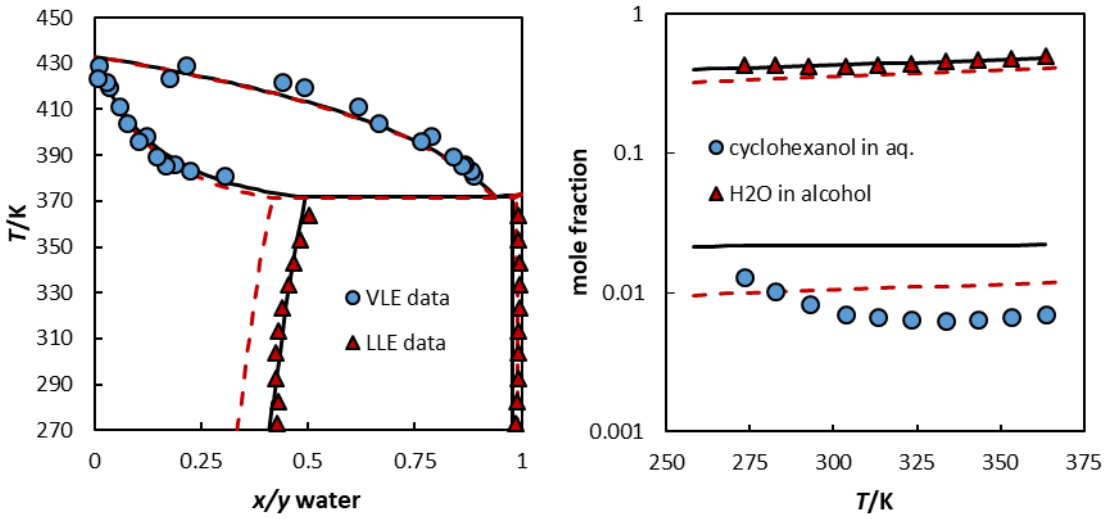

Figure 7.19 VLE and LLE of water + cyclohexanol. Dashed lines are VLE optimized k_{ij} (0.028), full lines were optimized to the amine phase LLE (k_{ij} =0.005). Data from Steyer and Sundmacher [218] and Stephenson and Stuart [234].

Contrary to what was observed for previous systems, the curvature for the solubility of cyclohexanol in water does not approach a solubility minimum. This is also true for water + cycloalkenes, as presented in the annexes for the system water + cyclohexene. The performance of the model to describe the solubility of hydrocarbons in water, seemingly decreases with cyclization, while increasing with insaturations, as for aromatics the tendency, while not completely capturing the solubility minima, is closer to the experimental behaviour. The same is visible for the mixture of water with cyclopentanol presented in the annexes.

The vapour liquid equilibria of cyclohexanol with cyclohexane, cyclohexene, o-xylene and n-nonane are presented in figure 7.20.

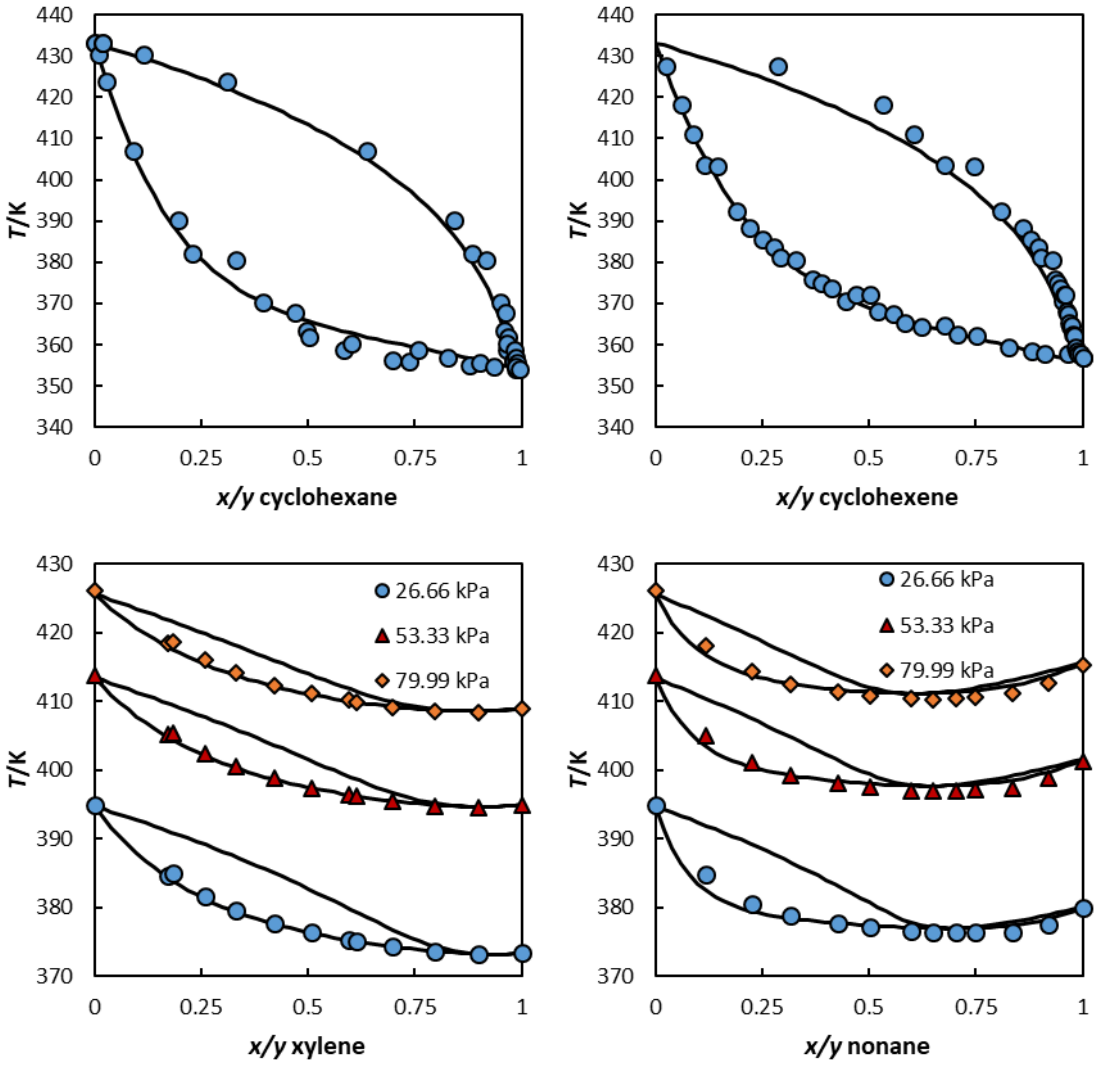

Figure 7.20 VLE for cyclohexanol with cyclohexane (top left), with cyclohexene (top right), both at 1 bar and with o-xylene (bottom left) or n-nonane (bottom right). Data from Steyer and Sundmacher [291] and Siimer et al. [306]

The four systems presented above are accurately described with acceptable values for the binary interaction parameters. For the mixture with n-nonane the temperature of the azeotropic composition is slightly overestimated at all pressures. This is even more visible in the mixture of cyclohexanol with n-heptane presented in figure 7.21.

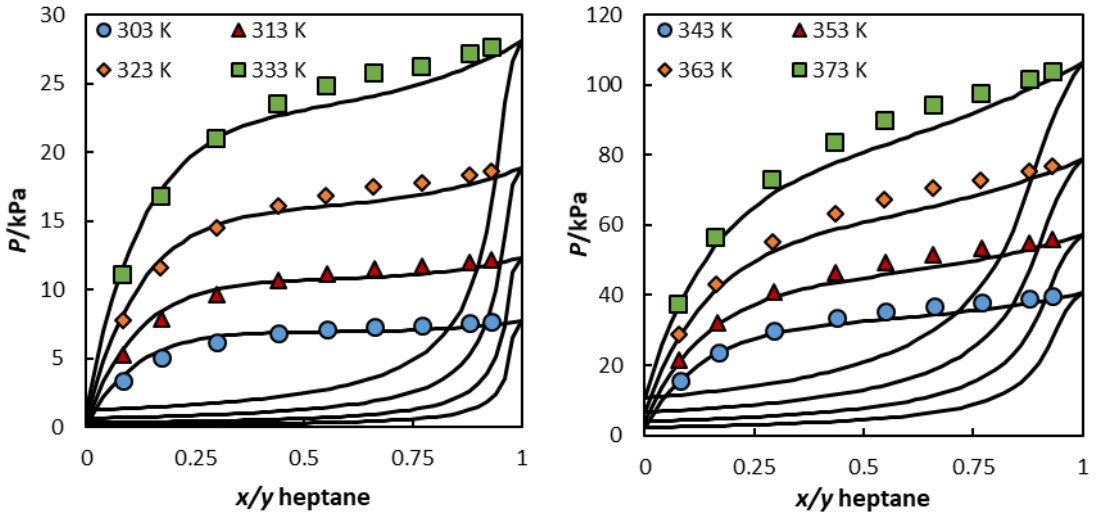

Figure 7.21 VLE for cyclohexanol with heptane (k_{ij}=0.018). Data from Sipowska and Wieczorek [307].

As can be observed for this system, the bubble pressures are not well described for high concentrations of heptane. This might be associated with the contribution of the association term being too small. This is also observed when studying cyclohexanol + cyclopentane and cyclopentanol + cyclohexane, in figure 7.22. Thus, in future improved versions of this group contribution method this issue should be addressed, while also expanding the study to more families of compounds.

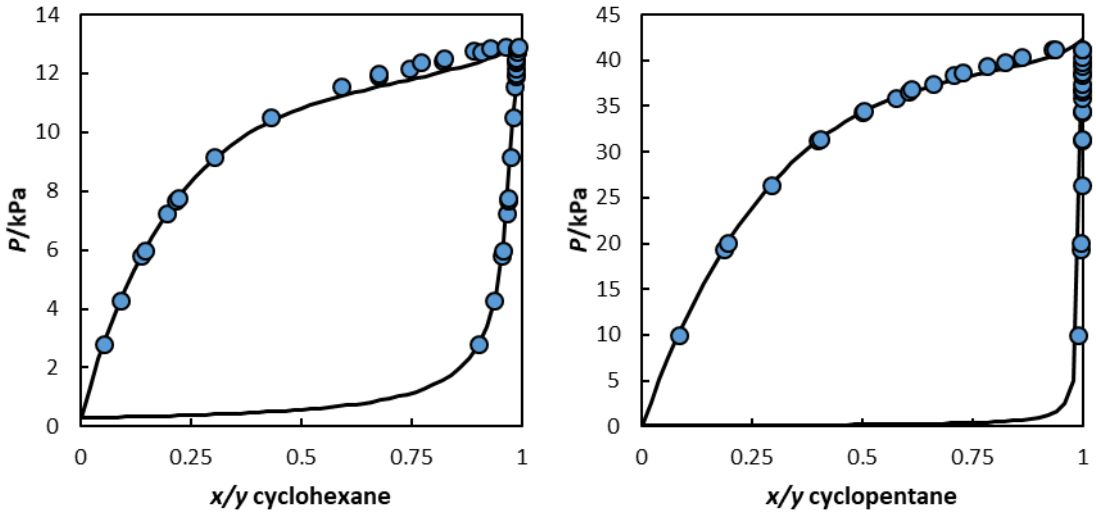

Figure 7.22 VLE for and cyclopentanol + cyclohexane (left) and cyclohexanol + cyclopentane (right). Data from Benson et al. [308].

Having studied the binary mixtures of cyclohexanol with o-xylene and n-nonane, and considering a k_{ij}=0 for the binary o-xylene + n-nonane, the corresponding ternary system was analysed. The average deviations for the bubble and dew temperatures for these system at the

pressures of 79.99, 53.33 and 26.66 kPa are 0.05% and 0.07% respectively. For $x_{nonane} \approx x_{o\text{-}xylene}$ the results are presented in figure 7.23.

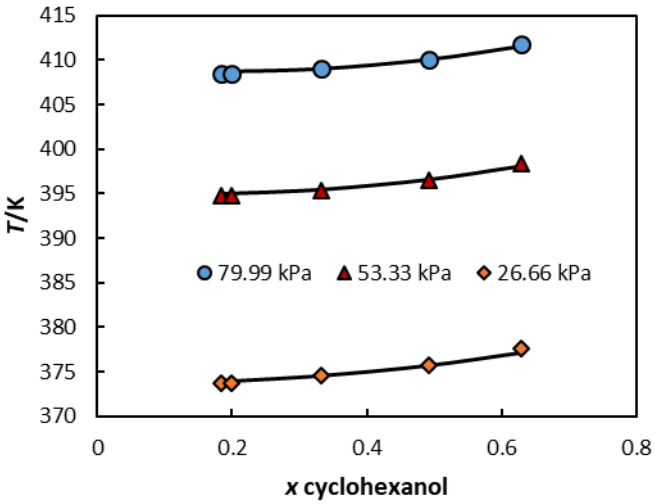

Figure 7.23 VLE for cyclohexanol + n-nonane + o-xylene for $x_{nonane} \approx x_{o\text{-}xylene}$. Data from Siimer et al. [306]

Two ternary LLE systems were also analysed, water + cyclohexanol + cyclohexane and water + cyclohexanol + cyclohexene. These systems have been studied in terms of the partition coefficients $x_{compound\ in\ HC.}/x_{compound\ in\ aq.}$, based on the data from Steyer and Sundmacher [218], Wang et al. [238] and Pei et al. [239]. The results for these system at 303 K are presented in figure 7.24, using the VLE optimized binary interaction parameters for cylohexanol + water. Results at other temperatures are presented in the annexes.

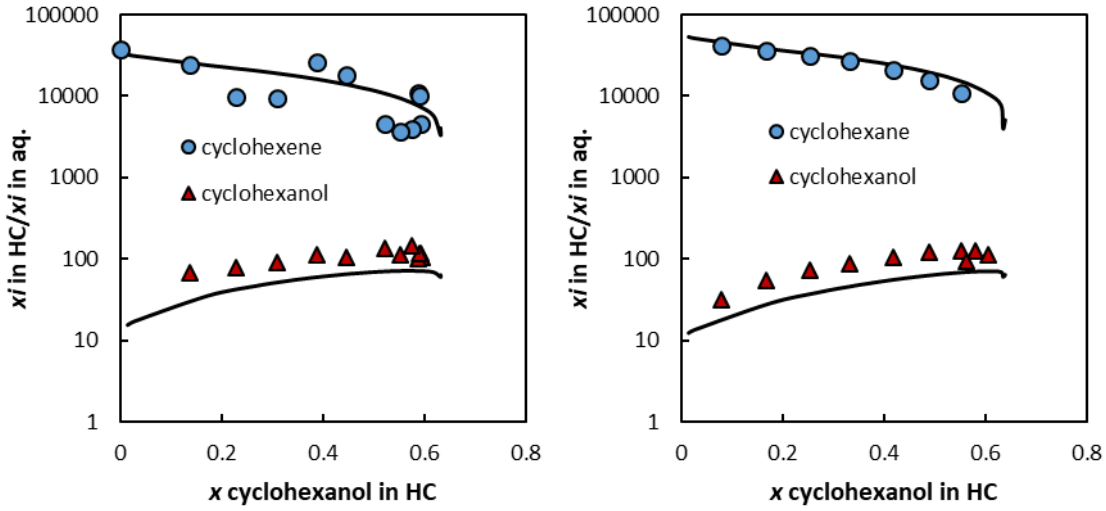

Figure 7.24 Partition coefficients for cyclohexanol + cyclohexene + water (left) and cyclohexanol + cyclohexane + water (right) at 323 K. Data from Wang et al. [309] and Pei et al. [310]

The VLE optimized binary interaction parameters for cylohexanol + water presented large advantages for these systems and are the ones presented in figure 7.24. The descriptions obtained are very good for these systems, considering the experimental data uncertainties.

7.5 Conclusions

The application of a new group contribution method was tested in alternative to the transferability approach applied in previous chapters. For the previously tested compounds both methods present similar results, with the group contribution method presenting some advantages for lighter alkanols. For the new compounds in study the method is able to accurately describe most of the properties in analysis, with C_p presenting some higher deviations, mainly due to the low vapour pressures of these compounds, the uncertainty on these data and the use of the extended Mathias –Copeman alpha function

The approach for linear alkanols seems to work very well, with an expected decrease in the accuracy of densities for heavier alkanols. Some deviations are observed in C_p and H^{vap} for these compounds, most likely due to the polynomial nature of the alpha function. As will be focused on the future work section, a more fundamental investigation on the behaviour of the alpha function and setting some restrictions in the fitting of its parameters is one of the most important topics for future developments of this modified CPA model.

The results obtained with the new sets for amines are in line with those from chapter 5. The lack of pure data for ethylmethylamine while detrimental and decreasing our understanding to judge about the quality of the parameters, still enabled the description of vapour liquid data for one system with reasonable accuracy.

The negative value applied for the interaction between the CH and OH groups is seemingly too high, leading to small association volumes for the cyclic alkanols, which are unable to completely describe vapour liquid equilibria with alkanes. Future work on this area should include an improvement of this parameter, while taking into account its influence in other molecules beside secondary and cyclic alkanols.

This group contribution method is thus a very interesting alternative to the transferability approach and should be extended further and tested as a predictive tool for more complex mixtures.

Final remarks and future work

In this work, a large group of compounds with a single functional group have been analysed, as well as multifunctional molecules with a single type of group. The main objective of the project behind this thesis is the description of multifunctional molecules. Thus, the expansion of the approaches here presented to molecules with two or more different types of groups is one of the most important steps for future work.

Another very important study lies with a more fundamental study of the performance of the alpha function. The present alpha function has diverse problems that have been described in over this thesis. Thus, studying an alternative alpha function with a maximum of three adjustable parameters is of high importance, as it could potentially overcome the weaknesses of the current alpha function, while the reducing the number of parameters. This can potentially decrease the overall performance of the model, but will surely make it more predictive and robust.

A Peng-Robinson version of the model has been prepared and in the future similar studies should be conducted using this version. It is important to look at how the PR term will influence the density description for compounds with association.

In the beginning of the project, one of the main topics was the change of main parameterization property. Using vapor pressure is not viable for a large group of compounds of interest, especially when looking at multifunctional molecules. Originally, Isobaric liquid heat capacity seemed to be one of the best properties to use in the parameterization of the alpha function, due to its ease of measurement and good results when applying this modified CPA approach. However, these results are highly dependent on the quality of the ideal gas heat capacity, which is seemingly not as accurate as desirable for complex compounds, when applying the usual calculation methodologies. There are alternative forms of calculation for the residual heat capacity. However, when not dependent on the ideal gas heat capacity, most of these functions are dependent on the vapor pressure or heat of vaporization curves, which defeats the purpose of adding to or substituting the vapor pressure by heat capacity in the parameterization process. The same issues hold true for the isochoric heat capacity.

Between the remaining derivative properties, speed of sound would be a perfect choice due to its ease of measurement and high accuracy. However, CPA, and most SAFT variants, are unable to obtain a good description of speed of sound simultaneously with the usual parameterization properties.

Usually with CPA the choice of combination rules is between CR-2 (depending on the author this rule may be called CR-1) and CR-4 (also known as the Elliot combining rule or ECR). Each of these rules is usually better for different types of equilibria. In this work the CR-2 has been the

only combining rule applied and in the future, the use of, at least, ECR should also be considered.

References

[1] G.K. Folas, G.M. Kontogeorgis, M.L. Michelsen, E.H. Stenby, E. Solbraa, Liquid−Liquid Equilibria for Binary and Ternary Systems Containing Glycols, Aromatic Hydrocarbons, and Water: Experimental Measurements and Modeling with the CPA EoS, J. Chem. Eng. Data. 51 (2006) 977–983. doi:10.1021/je050485c.

[2] H. Renon, J.M. Prausnitz, Local compositions in thermodynamic excess functions for liquid mixtures, AIChE J. 14 (1968) 135–144. doi:10.1002/aic.690140124.

[3] D.S. Abrams, J.M. Prausnitz, Statistical thermodynamics of liquid mixtures: A new expression for the excess Gibbs energy of partly or completely miscible systems, AIChE J. 21 (1975) 116–128. doi:10.1002/aic.690210115.

[4] G.M. Kontogeorgis, P.M. Vlamos, An interpretation of the behavior of EoS/G(E) models for asymmetric systems, Chem. Eng. Sci. 55 (2000) 2351–2358. doi:10.1016/S0009-2509(99)00472-8.

[5] G.M. Kontogeorgis, E.C. Voutsas, I. V. Yakoumis, D.P. Tassios, An Equation of State for Associating Fluids, Ind. Eng. Chem. Res. 35 (1996) 4310–4318. doi:10.1021/ie9600203.

[6] M.B. Oliveira, V. Ribeiro, A.J. Queimada, J. a. P. Coutinho, Modeling phase equilibria relevant to biodiesel production : A comparison of gE models , cubic EoS, EoS-gE and association EoS, Ind. Eng. Chem. Res. 50 (2011) 2348–2358. doi:10.1021/ie1013585.

[7] E. Hendriks, G.M. Kontogeorgis, R. Dohrn, J.C. De Hemptinne, I.G. Economou, L.F. Ẑilnik, V. Vesovic, Industrial requirements for thermodynamics and transport properties, Ind. Eng. Chem. Res. 49 (2010) 11131–11141. doi:10.1021/ie101231b.

[8] G.M. Kontogeorgis, G.K. Folas, Thermodynamic Models for Industrial Applications, John Wiley & Sons, Ltd, Chichester, UK, 2010. doi:10.1002/9780470747537.

[9] A.J. de Villiers, C.E. Schwarz, A.J. Burger, G.M. Kontogeorgis, Evaluation of the PC-SAFT, SAFT and CPA equations of state in predicting derivative properties of selected non-polar and hydrogen-bonding compounds, Fluid Phase Equilib. 338 (2013) 1–15. doi:10.1016/j.fluid.2012.09.035.

[10] M.B. Oliveira, L. F., C. J.A.P., L.F. Vega, Simultaneous description of second order thermodynamic derivative properties by soft-SAFT: evaluation and improvements (in preparation), n.d.

[11] J.O. Valderrama, The State of the Cubic Equations of State, Ind. Eng. Chem. Res. 42 (2003) 1603–1618. doi:10.1021/ie020447b.

[12] J.A. White, S. Zhang, Renormalization theory of nonuniversal thermal properties of fluids, J. Chem. Phys. 103 (1995) 1922–1928. doi:10.1063/1.469716.

[13] J.A. White, S. Zhang, Renormalization group theory for fluids, J. Chem. Phys. 99 (1993) 2012–2019. doi:10.1063/1.465263.

[14] J. Janeček, P. Paricaud, M. Dicko, C. Coquelet, A generalized Kiselev crossover approach applied to Soave-Redlich-Kwong equation of state, Fluid Phase Equilib. 401 (2015) 16–26. doi:10.1016/j.fluid.2015.04.024.

[15] S. Tang, J. V Sengers, Z.Y. Chen, Nonasymptotic critical thermodynamical behavior of fluids, Phys. A Stat. Mech. Its Appl. 179 (1991) 344–377. doi:10.1016/0378-4371(91)90084-P.

[16] Z.Y. Chen, A. Abbaci, S. Tang, J. V. Sengers, Global thermodynamic behavior of fluids in the critical region, Phys. Rev. A. 42 (1990) 4470–4484. doi:10.1103/PhysRevA.42.4470.

[17] F. Llovell, J.C. P??mies, L.F. Vega, Thermodynamic properties of Lennard-Jones chain molecules: Renormalization-group corrections to a modified statistical associating fluid theory, J. Chem. Phys. 121 (2004) 10715–10724. doi:10.1063/1.1809112.

[18] F. Llovell, L.F. Vega, Global Fluid Phase Equilibria and Critical Phenomena of Selected Mixtures Using the Crossover Soft-SAFT Equation, J. Phys. Chem. B. 110 (2006) 1350–1362. doi:10.1021/jp0551465.

[19] A. Fredenslund, R.L. Jones, J.M. Prausnitz, Group-contribution estimation of activity coefficients in nonideal liquid mixtures, AIChE J. 21 (1975) 1086–1099. doi:10.1002/aic.690210607.

[20] J. Vidal, Mixing rules and excess properties in cubic equations of state, Chem. Eng. Sci. 33 (1978) 787–791. doi:10.1016/0009-2509(78)80059-1.

[21] M.J. Huron, J. Vidal, New mixing rules in simple equations of state for representing vapour-liquid equilibria of strongly non-ideal mixtures, Fluid Phase Equilib. 3 (1979) 255–271. doi:10.1016/0378-3812(79)80001-1.

[22] S. Dahl, M.L. Michelsen, High-pressure vapor-liquid equilibrium with a UNIFAC-based equation of state, AIChE J. 36 (1990) 1829–1836. doi:10.1002/aic.690361207.
[23] H.P. Gros, S. Bottini, E. a. Brignole, Group contribution equation of state for associating mixtures, Fluid Phase Equilib. 116 (1996) 537–544. doi:10.1016/0378-3812(95)02928-1.
[24] E.A. Müller, K.E. Gubbins, Molecular-based equations of state for associating fluids: A review of SAFT and related approaches, Ind. Eng. Chem. Res. 40 (2001) 2193–2211. doi:10.1021/ie000773w.
[25] I.G. Economou, C. Tsonopoulos, Associating models and mixing rules in equations of state for water/hydrocarbon mixtures, Chem. Eng. Sci. 52 (1997) 511–525. doi:10.1016/S0009-2509(96)00441-1.
[26] J. Gross, G. Sadowski, Perturbed-Chain SAFT: An Equation of State Based on a Perturbation Theory for Chain Molecules, Ind. Eng. Chem. Res. 40 (2001) 1244–1260. doi:10.1021/ie0003887.
[27] L.M.C. Pereira, V. Martins, K. Adi, M.B. Oliveira, A.M.A. Dias, F. Llovell, L.F. Vega, P.J. Carvalho, J.A.P. Coutinho, High pressure solubility of CH 4 , N 2 O and N 2 in 1-butyl-3-methylimidazolium dicyanamide : Solubilities , selectivities and soft-SAFT modeling, J. Supercrit. Fluids. 110 (2016) 56–64. doi:10.1016/j.supflu.2015.12.006.
[28] P.V.A. Pontes, E.A. Crespo, M.A.R. Martins, L.P. Silva, C.M.S.S. Neves, G.J. Maximo, M.D. Hubinger, E.A.C. Batista, S.P. Pinho, J.A.P. Coutinho, G. Sadowski, C. Held, Measurement and PC-SAFT modeling of solid-liquid equilibrium of deep eutectic solvents of quaternary ammonium chlorides and carboxylic acids, Fluid Phase Equilib. 448 (2017) 69–80. doi:10.1016/j.fluid.2017.04.007.
[29] S. Tamouza, J.P. Passarello, P. Tobaly, J.C. De Hemptinne, Group contribution method with SAFT EOS applied to vapor liquid equilibria of various hydrocarbon series, Fluid Phase Equilib. 222–223 (2004) 67–76. doi:10.1016/j.fluid.2004.06.038.
[30] J. Vijande, M.M. Piñeiro, D. Bessières, H. Saint-Guirons, J.L. Legido, Description of PVT behaviour of hydrofluoroethers using the PC-SAFT EOS, Phys. Chem. Chem. Phys. 6 (2004) 766–770. doi:10.1039/B312223A.
[31] F.S. Emami, A. Vahid, J.R. Elliott, F. Feyzi, Group Contribution Prediction of Vapor Pressure with SAFT , Perturbed-Chain Statistical Associating Fluid Theory , and Elliott - Suresh - Donohue Equations of State, Ind. Eng. Chem. Res. (2008) 8401–8411. doi:10.1021/ie800329r.
[32] A. Tihic, G.M. Kontogeorgis, N. von Solms, M.L. Michelsen, L. Constantinou, A Predictive Group-Contribution Simplified PC-SAFT Equation of State: Application to Polymer Systems, Ind. Eng. Chem. Res. 47 (2008) 5092–5101. doi:10.1021/ie0710768.
[33] F.T. Peters, F.S. Laube, G. Sadowski, Development of a group contribution method for polymers within the PC-SAFT model, Fluid Phase Equilib. 324 (2012) 70–79. doi:10.1016/j.fluid.2012.03.009.
[34] Y. Peng, K.D. Goff, M.C. dos Ramos, C. McCabe, Developing a predictive group-contribution-based SAFT-VR equation of state, Fluid Phase Equilib. 277 (2009) 131–144. doi:10.1016/j.fluid.2008.11.008.
[35] A. Lymperiadis, C.S. Adjiman, A. Galindo, G. Jackson, A group contribution method for associating chain molecules based on the statistical associating fluid theory (SAFT-γ), J. Chem. Phys. 127 (2007) 234903. doi:10.1063/1.2813894.
[36] J. Vijande, M.M. Piñeiro, J.L. Legido, Group-contribution method with proximity effect for PC-SAFT molecular parameters. 2. application to association parameters: Primary alcohols and amines, Ind. Eng. Chem. Res. 53 (2014) 909–919. doi:10.1021/ie4023786.
[37] S. Pereda, J.A. Awan, A.H. Mohammadi, A. Valtz, C. Coquelet, E.A. Brignole, D. Richon, Solubility of hydrocarbons in water: Experimental measurements and modeling using a group contribution with association equation of state (GCA-EoS), Fluid Phase Equilib. 275 (2009) 52–59. doi:10.1016/j.fluid.2008.09.008.
[38] R. O'Lenick, X.J. Li, Y.C. Chiew, Correlation functions of hard-sphere chain mixtures: integral equation theory and simulation results, Mol. Phys. 86 (1995) 1123–1135. doi:10.1080/00268979500102621.
[39] S. Tamouza, J.P. Passarello, P. Tobaly, J.C. De Hemptinne, Application to binary mixtures of a group contribution SAFT EOS (GC-SAFT), Fluid Phase Equilib. 228–229 (2005) 409–419. doi:10.1016/j.fluid.2004.10.003.
[40] T.X. Nguyen Thi, S. Tamouza, P. Tobaly, J.-P. Passarello, J.-C. de Hemptinne, Application of group contribution SAFT equation of state (GC-SAFT) to model phase behaviour of light and heavy esters, Fluid Phase Equilib. 238 (2005) 254–261. doi:10.1016/j.fluid.2005.10.009.

[41] D. NguyenHuynh, J.P. Passarello, P. Tobaly, J.C. de Hemptinne, Application of GC-SAFT EOS to polar systems using a segment approach, Fluid Phase Equilib. 264 (2008) 62–75. doi:10.1016/j.fluid.2007.10.019.
[42] D. Nguyen-Huynh, J.-P. Passarello, P. Tobaly, J.-C. de Hemptinne, Modeling Phase Equilibria of Asymmetric Mixtures Using a Group-Contribution SAFT (GC-SAFT) with a k ij Correlation Method Based on London's Theory. 1. Application to CO 2 + n -Alkane, Methane + n -Alkane, and Ethane + n -Alkane Systems, Ind. Eng. Chem. Res. 47 (2008) 8847–8858. doi:10.1021/ie071643r.
[43] D. Nguyen-Huynh, T.K.S. Tran, S. Tamouza, J.P. Passarello, P. Tobaly, J.C. De Hemptinne, Modeling phase equilibria of asymmetric mixtures using a group-contribution SAFT (GC-SAFT) with a kij correlation method based on London's theory. 2. Application to binary mixtures containing aromatic hydrocarbons, n-alkanes, CO2, N2, and H2S, Ind. Eng. Chem. Res. 47 (2008) 8859–8868. doi:10.1021/ie071644j.
[44] G.M. Nguyen, T.-B.; de Hemptinne, J.-C.; Creton, B.; Kontogeorgis, GC-PPC-SAFT Equation of Sate for VLE and LLE of Hydrocarbons and Oxygenated Compounds. Sensitivity Analysis., Ind. Eng. Chem. Res. 52 (2013) 7014–7029. doi:10.1021/ie3028069.
[45] T.B. Nguyen, J.C. De Hemptinne, B. Creton, G.M. Kontogeorgis, Improving GC-PPC-SAFT equation of state for LLE of hydrocarbons and oxygenated compounds with water, Fluid Phase Equilib. 372 (2014) 113–125. doi:10.1016/j.fluid.2014.03.028.
[46] S. Ahmed, N. Ferrando, J.-C. de Hemptinne, J.-P. Simonin, O. Bernard, O. Baudouin, A New PC-SAFT Model for Pure Water, Water–Hydrocarbons, and Water–Oxygenates Systems and Subsequent Modeling of VLE, VLLE, and LLE, J. Chem. Eng. Data. (2016) acs.jced.6b00565. doi:10.1021/acs.jced.6b00565.
[47] T.-K.-H. Trinh, J.-P. Passarello, J.-C. de Hemptinne, R. Lugo, Use of a non additive GC-PPC-SAFT equation of state to model hydrogen solubility in oxygenated organic compounds, Fluid Phase Equilib. 429 (2016) 177–195. doi:10.1016/j.fluid.2016.08.003.
[48] C. Le Thi, S. Tamouza, J.-P. Passarello, P. Tobaly, J.-C. de Hemptinne, Modeling Phase Equilibrium of H 2 + n -Alkane and CO 2 + n -Alkane Binary Mixtures Using a Group Contribution Statistical Association Fluid Theory Equation of State (GC−SAFT−EOS) with a k i j Group Contribution Method, Ind. Eng. Chem. Res. 45 (2006) 6803–6810. doi:10.1021/ie060424n.
[49] J. Vijande, M.M. Piñeiro, J.L. Legido, D. Bessières, Group-contribution method for the molecular parameters of the pc-saft equation of state taking into account the proximity effect. application to nonassociated compounds, Ind. Eng. Chem. Res. 49 (2010) 9394–9406. doi:10.1021/ie1002813.
[50] A. Gil-Villegas, A. Galindo, P.J. Whitehead, S.J. Mills, G. Jackson, A.N. Burgess, Statistical associating fluid theory for chain molecules with attractive potentials of variable range, J. Chem. Phys. 106 (1997) 4168–4186. doi:10.1063/1.473101.
[51] a Galindo, L. a Davies, a Gil-Villegas, G. Jackson, The thermodynamics of mixtures and the corresponding mixing rules in the SAFT-VR approach for potentials of variable range, Mol. Phys. 93 (1998) 241–252. doi:10.1080/002689798169249.
[52] N.F. Carnahan, Equation of State for Nonattracting Rigid Spheres, J. Chem. Phys. 51 (1969) 635. doi:10.1063/1.1672048.
[53] A. Lymperiadis, C.S. Adjiman, G. Jackson, A. Galindo, A generalisation of the SAFT- group contribution method for groups comprising multiple spherical segments, Fluid Phase Equilib. 274 (2008) 85–104. doi:10.1016/j.fluid.2008.08.005.
[54] V. Papaioannou, T. Lafitte, C. Avendaño, C.S. Adjiman, G. Jackson, E. a. Müller, A. Galindo, Group contribution methodology based on the statistical associating fluid theory for heteronuclear molecules formed from Mie segments, J. Chem. Phys. 140 (2014) 1–30. doi:10.1063/1.4851455.
[55] J.R. Elliott, R.N. Natarajan, Extension of the Elliott-Suresh-Donohue Equation of State to Polymer Solutions, Ind. Eng. Chem. Res. 41 (2002) 1043–1050. doi:10.1021/ie010346y.
[56] K.L. Hoy, Solubility parameter as a design parameter for water-borne polymers and coatings, J. Coat. Fabr. 19 (1989) 53–67. doi:10.1177/152808378901900106.
[57] L. Constantinou, R. Gani, New group contribution method for estimating properties of pure compounds, AIChE J. 40 (1994) 1697–1710. doi:10.1002/aic.690401011.
[58] B.H. Patel, H. Docherty, S. Varga, a. Galindo *, G.C. Maitland, Generalized equation of state for square-well potentials of variable range, Mol. Phys. 103 (2005) 129–139. doi:10.1080/00268970412331303990.
[59] F.T. Peters, F.S. Laube, G. Sadowski, PC-SAFT based group contribution method for binary interaction parameters of polymer/solvent systems, Fluid Phase Equilib. 358 (2013) 137–150.

doi:10.1016/j.fluid.2013.05.033.
[60] A.F. Ghobadi, J.R. Elliott, Adapting SAFT-γ perturbation theory to site-based molecular dynamics simulation. I. Homogeneous fluids, J. Chem. Phys. 139 (2013). doi:10.1063/1.4838457.
[61] R.W. Zwanzig, High-Temperature Equation of State by a Perturbation Method. I. Nonpolar Gases, J. Chem. Phys. 22 (1954) 1420–1426. doi:10.1063/1.1740409.
[62] Y.T. Pavlyukhin, Thermodynamic perturbation theory of simple liquids: Monte Carlo simulation of a hard sphere system and the Helmholtz free energy of SW fluids, J. Struct. Chem. 53 (2012) 476–486. doi:10.1134/S0022476612030092.
[63] A.F. Ghobadi, J.R. Elliott, Adapting SAFT-γ perturbation theory to site-based molecular dynamics simulation. III. Molecules with partial charges at bulk phases, confined geometries and interfaces, J. Chem. Phys. 141 (2014) 94708. doi:10.1063/1.4893966.
[64] B.C.J. Segura, W.G.C. and K.P. Shukla, Associating fluids with four bonding sites against a hard wall: density functional theory, Mol. Phys. 90 (1997) 759–772. doi:10.1080/002689797172110.
[65] A. Bymaster, W.G. Chapman, An iSAFT density functional theory for associating polyatomic molecules, J. Phys. Chem. B. 114 (2010) 12298–12307. doi:10.1021/jp102677m.
[66] T. Lafitte, A. Apostolakou, C. Avendaño, A. Galindo, C.S. Adjiman, E.A. Müller, G. Jackson, Accurate statistical associating fluid theory for chain molecules formed from Mie segments, J. Chem. Phys. 139 (2013) 154504. doi:10.1063/1.4819786.
[67] S. Dufal, T. Lafitte, A.J. Haslam, A. Galindo, G.N.I. Clark, C. Vega, G. Jackson, The A in SAFT: developing the contribution of association to the Helmholtz free energy within a Wertheim TPT1 treatment of generic Mie fluids, Mol. Phys. 113 (2015) 948–984. doi:10.1080/00268976.2015.1029027.
[68] A.M. Palma, M.B. Oliveira, A.J. Queimada, J.A.P. Coutinho, Evaluating Cubic Plus Association Equation of State Predictive Capacities: A Study on the Transferability of the Hydroxyl Group Associative Parameters, Ind. Eng. Chem. Res. 56 (2017) 7086–7099. doi:10.1021/acs.iecr.7b00760.
[69] A.M. Palma, M.B. Oliveira, A.J. Queimada, J.A.P. Coutinho, Re-evaluating the CPA EoS for improving critical points and derivative properties description, Fluid Phase Equilib. 436 (2017) 85–97. doi:10.1016/j.fluid.2017.01.002.
[70] M.B. Oliveira, I.M. Marrucho, J.A.P. Coutinho, A.J. Queimada, Surface tensions of chain molecules through a combination of the gradient theory with the CPA EoS, Fluid Phase Equilib. 267 (2008) 83–91. doi:10.1016/j.fluid.2011.01.015.
[71] A.J. Queimada, F.L. Mota, S.P. Pinho, E. a. Macedo, Solubilities of biologically active phenolic compounds: Measurements and modeling, J. Phys. Chem. B. 113 (2009) 3469–3476. doi:10.1021/jp808683y.
[72] F.L. Mota, A.J. Queimada, S.P. Pinho, E. a. Macedo, Aqueous solubility of some natural phenolic compounds, Ind. Eng. Chem. Res. 47 (2008) 5182–5189. doi:10.1021/ie071452o.
[73] G.M. Kontogeorgis, I.V. Yakoumis, H. Meijer, E. Hendriks, T. Moorwood, Multicomponent phase equilibrium calculations for water–methanol–alkane mixtures, Fluid Phase Equilib. 160 (1999) 201–209. doi:10.1016/S0378-3812(99)00060-6.
[74] M.A. Mahabadian, A. Chapoy, R. Burgass, B. Tohidi, Development of a multiphase flash in presence of hydrates: Experimental measurements and validation with the CPA equation of state, Fluid Phase Equilib. 414 (2016) 117–132. doi:10.1016/j.fluid.2016.01.009.
[75] M. Hajiw, A. Chapoy, C. Coquelet, Hydrocarbons - water phase equilibria using the CPA equation of state with a group contribution method, Can. J. Chem. Eng. 93 (2015) 432–442. doi:10.1002/cjce.22093.
[76] M. Hajiw, A. Chapoy, C. Coquelet, G. Lauermann, Prediction of methanol content in natural gas with the GC-PR-CPA model, J. Nat. Gas Sci. Eng. 27 (2015) 745–750. doi:10.1016/j.jngse.2015.09.021.
[77] J.-N. Jaubert, F. Mutelet, VLE predictions with the Peng–Robinson equation of state and temperature dependent kij calculated through a group contribution method, Fluid Phase Equilib. 224 (2004) 285–304. doi:10.1016/j.fluid.2004.06.059.
[78] MULTIFLASH version 4.4, KBC Process Technology, London, United Kingdom, (n.d.).
[79] Design Institute for Physical Properties,DIPPR DIADEM Database, version 10.0, Brigham Young University, Provoh (Utah), USA, (n.d.).
[80] Thermodynamics Research Center (TRC), ThermoData Engine, version 9.0, National Institute of Standards and Technology, Boulder, Colorado, USA, (n.d.).
[81] F. a. Sánchez, S. Pereda, E. a. Brignole, GCA-EoS: A SAFT group contribution model-Extension to mixtures containing aromatic hydrocarbons and associating compounds, Fluid Phase Equilib.

306 (2011) 112–123. doi:10.1016/j.fluid.2011.03.024.
[82] T.M. Soria, a. E. Andreatta, S. Pereda, S.B. Bottini, Thermodynamic modeling of phase equilibria in biorefineries, Fluid Phase Equilib. 302 (2011) 1–9. doi:10.1016/j.fluid.2010.10.029.
[83] M.G. Prieto, F.A. Sánchez, S. Pereda, Multiphase Equilibria Modeling with GCA-EoS. Part I: Carbon Dioxide with the Homologous Series of Alkanes up to 36 Carbons, Ind. Eng. Chem. Res. 54 (2015) 12415–12427. doi:10.1021/acs.iecr.5b03269.
[84] V. Papaioannou, C.S. Adjiman, G. Jackson, A. Galindo, Simultaneous prediction of vapour–liquid and liquid–liquid equilibria (VLE and LLE) of aqueous mixtures with the SAFT-γ group contribution approach, Fluid Phase Equilib. 306 (2011) 82–96. doi:10.1016/j.fluid.2011.02.016.
[85] T.M. Soria, F. a. S??nchez, S. Pereda, S.B. Bottini, Modeling alcohol+water+hydrocarbon mixtures with the group contribution with association equation of state GCA-EoS, Fluid Phase Equilib. 296 (2010) 116–124. doi:10.1016/j.fluid.2010.02.040.
[86] M. Góral, B. Wiśniewska-Gocłowska, A. Mączyński, Recommended liquid-liquid equilibrium data. Part 4. 1-alkanol-water systems, J. Phys. Chem. Ref. Data. 35 (2006) 1391–1414. doi:10.1063/1.2203354.
[87] T.H. Cho, K. Ochi, K. Kojima, No Title, Kagaku Kogaku Robonshu. 10 (1984) 181–183 (Cited in DETHERM).
[88] S.P. Tunik, T.M. Lesteva, V.I. Chernaya, No Title, Depos. Doc. VINITI 435-77. (1977) 1–12 (cited in DETHERM).
[89] C.G. Pereira, N. Ferrando, R. Lugo, P. Mougin, J.C. de Hemptinne, Predictive evaluation of phase equilibria in biofuel systems using molecular thermodynamic models, J. Supercrit. Fluids. 118 (2016) 64–78. doi:10.1016/j.supflu.2016.07.025.
[90] A. Chremos, E. Forte, V. Papaioannou, A. Galindo, G. Jackson, C.S. Adjiman, Modelling the phase and chemical equilibria of aqueous solutions of alkanolamines and carbon dioxide using the SAFT-γ SW group contribution approach, Fluid Phase Equilib. 407 (2016) 280–297. doi:10.1016/j.fluid.2015.07.052.
[91] R.C. Phutela, Z.S. Kooner, D. V Fenby, Vapour Pressure Study of Deuterium Exchange Reactions in Water-Ethanol Systems : Equilibrium Constant Determination, (1979).
[92] D.T. Vu, C.T. Lira, N.S. Asthana, A.K. Kolah, D.J. Miller, Vapor - Liquid equilibria in the systems ethyl lactate + ethanol and ethyl lactate + water, J. Chem. Eng. Data. 51 (2006) 1220–1225. doi:10.1021/je050537y.
[93] N.H. Dong, de H. Jean-Charles, L. Rafael, P. Jean-Philippe, T. Pascal, Simultaneous liquid-liquid and vapour-liquid equilibria predictions of selected oxygenated aromatic molecules in mixtures with alkanes, alcohols, water, using the polar GC-PC-SAFT, Chem. Eng. Res. Des. 92 (2014) 1912–1935. doi:10.1016/j.cherd.2014.05.018.
[94] S. Espinosa, S. Díaz, T. Fornari, Extension of the group contribution associating equation of state to mixtures containing phenol, aromatic acid and aromatic ether compounds, Fluid Phase Equilib. 231 (2005) 197–210. doi:10.1016/j.fluid.2005.02.007.
[95] F. Galivel-Solastiouk, S. Laugier, D. Richon, Vapor-liquid equilibrium data for the propane-methanol and propane-methanol-carbon dioxide system, Fluid Phase Equilib. 28 (1986) 73–85. doi:10.1016/0378-3812(86)85069-5.
[96] X. Courtial, C. Bin Soo, C. Coquelet, P. Paricaud, D. Ramjugernath, D. Richon, Vapor-liquid equilibrium in the n-butane + methanol system, measurement and modeling from 323.2 to 443.2 K, Fluid Phase Equilib. 277 (2009) 152–161. doi:10.1016/j.fluid.2008.12.001.
[97] A. Tihic, N. von Solms, M.L. Michelsen, G.M. Kontogeorgis, L. Constantinou, Application of sPC-SAFT and group contribution sPC-SAFT to polymer systems-Capabilities and limitations, Fluid Phase Equilib. 281 (2009) 70–77. doi:10.1016/j.fluid.2009.04.002.
[98] Y. Peng, K.D. Goff, M.C. Dos Ramos, C. McCabe, Predicting the phase behavior of polymer systems with the GC-SAFT-VR approach, Ind. Eng. Chem. Res. 49 (2010) 1378–1394. doi:10.1021/ie900795x.
[99] O. Lobanova, A. Mejía, G. Jackson, E.A. Müller, SAFT- γ force field for the simulation of molecular fluids 6: Binary and ternary mixtures comprising water, carbon dioxide, and n -alkanes, J. Chem. Thermodyn. 93 (2016) 320–336. doi:10.1016/j.jct.2015.10.011.
[100] S.S. Ashrafmansouri, S. Raeissi, Modeling gas solubility in ionic liquids with the SAFT-gamma group contribution method, J. Supercrit. Fluids. 63 (2012) 81–91. doi:DOI 10.1016/j.supflu.2011.12.014.
[101] V. Papaioannou, F. Calado, T. Lafitte, S. Dufal, M. Sadeqzadeh, G. Jackson, C.S. Adjiman, A. Galindo, Application of the SAFT-γ Mie group contribution equation of state to fluids of relevance to the oil and gas industry, Fluid Phase Equilib. 416 (2016) 104–119.

doi:10.1016/j.fluid.2015.12.041.
[102] A.I. Papadopoulos, S. Badr, A. Chremos, E. Forte, T. Zarogiannis, P. Seferlis, S. Papadokonstantakis, A. Galindo, G. Jackson, C.S. Adjiman, Computer-aided molecular design and selection of CO2 capture solvents based on thermodynamics, reactivity and sustainability, Mol. Syst. Des. Eng. 3 (2016) 1645–1669. doi:10.1039/C6ME00049E.
[103] J.D. Haley, C. McCabe, Predicting the phase behavior of fatty acid methyl esters and their mixtures using the GC-SAFT-VR approach, Fluid Phase Equilib. 411 (2016) 43–52. doi:10.1016/j.fluid.2015.11.012.
[104] D. NguyenHuynh, J.-P. Passarello, J.-C. de Hemptinne, F. Volle, P. Tobaly, Simultaneous modeling of VLE, LLE and VLLE of CO2 and 1, 2, 3 and 4 alkanol containing mixtures using GC-PPC-SAFT EOS, J. Supercrit. Fluids. 95 (2014) 146–157. doi:10.1016/j.supflu.2014.07.022.
[105] J. Rozmus, J.C. De Hemptinne, N. Ferrando, P. Mougin, Long chain multifunctional molecules with GC-PPC-SAFT: Limits of data and model, Fluid Phase Equilib. 329 (2012) 78–85. doi:10.1016/j.fluid.2012.06.004.
[106] J.W. Kang, J. Abildskov, R. Gani, J. Cobas, Estimation of mixture properties from first- and second-order group contributions with the UNIFAC model, Ind. Eng. Chem. Res. 41 (2002) 3260–3273. doi:10.1021/ie010861w.
[107] H. Lubarsky, I. Polishuk, D. Nguyenhuynh, The group contribution method (GC) versus the critical point-based approach (CP): Predicting thermodynamic properties of weakly- and non-associated oxygenated compounds by GC-PPC-SAFT and CP-PC-SAFT, J. Supercrit. Fluids. 110 (2016) 11–21. doi:10.1016/j.supflu.2015.12.007.
[108] G.M.C. Silva, P. Morgado, J.D. Haley, V.M.T. Montoya, C. McCabe, L.F.G. Martins, E.J.M. Filipe, Vapor pressure and liquid density of fluorinated alcohols: Experimental, simulation and GC-SAFT-VR predictions, Fluid Phase Equilib. 425 (2016) 297–304. doi:10.1016/j.fluid.2016.06.011.
[109] M. Straka, A. Van Genderen, V. Ru, Heat Capacities in the Solid and in the Liquid Phase of Isomeric Pentanols, J. Chem. Eng. Data. 52 (2007) 794–802. doi:10.1021/je060411g.
[110] M. Zábranský, Heat Capacity of Liquids: Critical Review and Recommended Values. Supplement I, J. Phys. Chem. Ref. Data. 30 (2001) 1199–1689. doi:10.1063/1.1407866.
[111] M. Zábranský, Z. Kolská, V. Růžička, E.S. Domalski, Heat Capacity of Liquids: Critical Review and Recommended Values. Supplement II, J. Phys. Chem. Ref. Data. 39 (2010) 13103. doi:10.1063/1.3182831.
[112] E.W. Lemmon, M.L. Hubert, M.O. McLinden, NIST standard reference database 23: Reference fluid thermodynamic and transport properties - REFPROP, version 9.0, Natl. Inst. Stand. Technol. Stand. Ref. Data Program, Gaithersbg. (2010).
[113] S. Dufal, V. Papaioannou, M. Sadeqzadeh, T. Pogiatzis, A. Chremos, C.S. Adjiman, G. Jackson, A. Galindo, Prediction of thermodynamic properties and phase behavior of fluids and mixtures with the SAFT-γ mie group-contribution equation of state, J. Chem. Eng. Data. 59 (2014) 3272–3288. doi:10.1021/je500248h.
[114] M. Sadeqzadeh, V. Papaioannou, S. Dufal, C.S. Adjiman, G. Jackson, A. Galindo, The development of unlike induced association-site models to study the phase behaviour of aqueous mixtures comprising acetone, alkanes and alkyl carboxylic acids with the SAFT-γ Mie group contribution methodology, Fluid Phase Equilib. 407 (2016) 39–57. doi:10.1016/j.fluid.2015.07.047.
[115] C. Avendaño, T. Lafitte, C.S. Adjiman, A. Galindo, E.A. Müller, G. Jackson, SAFT-γ Force Field for the Simulation of Molecular Fluids: 2. Coarse-Grained Models of Greenhouse Gases, Refrigerants, and Long Alkanes, J. Phys. Chem. B. 117 (2013) 2717–2733. doi:10.1021/jp306442b.
[116] C. Avendaño, T. Lafitte, A. Galindo, C.S. Adjiman, G. Jackson, E.A. Müller, SAFT-γ Force Field for the Simulation of Molecular Fluids. 1. A Single-Site Coarse Grained Model of Carbon Dioxide, J. Phys. Chem. B. 115 (2011) 11154–11169. doi:10.1021/jp204908d.
[117] O. Lobanova, C. Avendaño, T. Lafitte, E. a. Müller, G. Jackson, SAFT-γ force field for the simulation of molecular fluids: 4. A single-site coarse-grained model of water applicable over a wide temperature range, Mol. Phys. 113 (2015) 1228–1249. doi:10.1080/00268976.2015.1004804.
[118] G.M. Kontogeorgis, P. Coutsikos, Thirty Years with EoS/GE Models - What have we learned?, Ind. Eng. Chem. Res. 51 (2012) 4119–4142. doi:10.1021/ie2015119.
[119] M.S. Wertheim, Fluids with highly directional attractive forces.1. Statistical thermodynamics, J. Stat. Phys. 35 (1984) 19–34. doi:10.1007/bf01017362.

[120] M.S. Wertheim, Fluids with highly directional attractive forces. II. Thermodynamic perturbation theory and integral equations, J. Stat. Phys. 35 (1984) 35–47. doi:10.1007/BF01017363.
[121] M.S. Wertheim, Fluids with Highly Directional Attractive Forces . IV . Equilibrium Polymerization, 42 (1986) 477–492. doi:10.1007/BF01127722.
[122] M.S. Wertheim, Fluids with highly directional attractive forces. III. Multiple attraction sites, J. Stat. Phys. 42 (1986) 459–476. doi:10.1007/BF01127721.
[123] S.H. Huang, M. Radosz, Equation of state for small, large, polydisperse and associating molecules, Ind. Eng. Chem. Res. 29 (1990) 2284–2294. doi:10.1021/ie00107a014.
[124] W.G. Chapman, K.E. Gubbins, G. Jackson, M. Radosz, New reference equation of state for associating liquids, Ind. Eng. Chem. Res. 29 (1990) 1709–1721. doi:10.1021/ie00104a021.
[125] M.B. Oliveira, J.A.P. Coutinho, A.J. Queimada, Mutual solubilities of hydrocarbons and water with the CPA EoS, Fluid Phase Equilib. 258 (2007) 58–66. doi:10.1016/j.fluid.2007.05.023.
[126] M.B. Oliveira, F.R. Varanda, I.M. Marrucho, A.J. Queimada, J.A.P. Coutinho, Prediction of Water Solubility in Biodiesel with the CPA Equation of State Prediction of Water Solubility in Biodiesel with the CPA Equation of State, Ind. Eng. Chem. Res. 47 (2008) 4278–4285. doi:10.1021/ie800018x.
[127] M.B. Oliveira, A.R.R. Teles, A.J. Queimada, J.A.P. Coutinho, Phase equilibria of glycerol containing systems and their description with the Cubic-Plus-Association (CPA) Equation of State, Fluid Phase Equilib. 280 (2009) 22–29. doi:10.1016/j.fluid.2009.03.011.
[128] M.B. Oliveira, A.J. Queimada, G.M. Kontogeorgis, J.A.P. Coutinho, Evaluation of the CO2 behavior in binary mixtures with alkanes, alcohols, acids and esters using the Cubic-Plus-Association Equation of State, J. Supercrit. Fluids. 55 (2011) 876–892. doi:10.1016/j.supflu.2010.09.036.
[129] G.M. Kontogeorgis, M.L. Michelsen, G.K. Folas, S. Derawi, N. Von Solms, E.H. Stenby, Ten Years with the CPA (Cubic-Plus-Association) equation of state. Part 2. Cross-Associating and Multicomponent Systems, Ind. Eng. Chem. Res. 45 (2006) 4855–4868. doi:10.1021/ie051305v.
[130] E.C. Voutsas, I. V Yakoumis, D.P. Tassios, Prediction of phase equilibria in water/alcohol/alkane systems, Fluid Phase Equilib. 158–160 (1999) 151–163. doi:10.1016/S0378-3812(99)00131-4.
[131] G.K. Folas, J. Gabrielsen, M.L. Michelsen, E.H. Stenby, G.M. Kontogeorgis, Application of the Cubic-Plus-Association (CPA) Equation of State to Cross-Associating Systems, Ind. Eng. Chem. Res. 44 (2005) 3823–3833. doi:10.1021/ie048832j.
[132] M. Kaarsholm, S.O. Derawi, M.L. Michelsen, G.M. Kontogeorgis, Extension of the cubic-plus-association (CPA) equation of state to amines, Ind. Eng. Chem. Res. 44 (2005) 4406–4413. doi:10.1021/ie0490029.
[133] E.C. Voutsas, G.M. Kontogeorgis, I. V Yakoumis, D.P. Tassios, Correlation of liquid-liquid equilibria for alcohol/hydrocarbon mixtures using the CPA equation of state, Fluid Phase Equilib. 132 (1997) 61–75. doi:10.1016/S0378-3812(96)03153-6.
[134] I. V. Yakoumis, G.M. Kontogeorgis, E.C. Voutsas, D.P. Tassios, Vapor-liquid equilibria for alcohol/hydrocarbon systems using the CPA Equation of state, Fluid Phase Equilib. 130 (1997) 31–47. doi:10.1016/S0378-3812(96)03200-1.
[135] G.K. Folas, G.M. Kontogeorgis, M.L. Michelsen, E.H. Stenby, Application of the cubic-plus-association equation of state to mixtures with polar chemicals and high pressures, Ind. Eng. Chem. Res. 45 (2006) 1516–1526. doi:10.1021/ie0509241.
[136] G.K. Folas, G.M. Kontogeorgis, M.L. Michelsen, E.H. Stenby, Application of the cubic-plus-association (CPA) equation of state to complex mixtures with aromatic hydrocarbons, Ind. Eng. Chem. Res. 45 (2006) 1527–1538. doi:10.1021/ie050976q.
[137] M.P. Breil, G.M. Kontogeorgis, Thermodynamics of triethylene glycol and tetraethylene glycol containing systems described by the cubic-plus-association equation of state, Ind. Eng. Chem. Res. 48 (2009) 5472–5480. doi:10.1021/ie801412y.
[138] S.O. Derawi, G.M. Kontogeorgis, M.L. Michelsen, E.H. Stenby, Extension of the cubic-plus-association equation of state to glycol-water cross-associating systems, Ind. Eng. Chem. Res. 42 (2003) 1470–1477. doi:10.1021/ie0206103.
[139] S.O. Derawi, G.M. Kontogeorgis, E.H. Stenby, T. Haugum, A.O. Fredheim, Liquid−Liquid Equilibria for Glycols + Hydrocarbons: Data and Correlation, J. Chem. Eng. Data. 47 (2002) 169–173. doi:10.1021/je010199a.
[140] S.O. Derawi, M.L. Michelsen, G.M. Kontogeorgis, E.H. Stenby, Application of the CPA equation of state to glycol/hydrocarbons liquid–liquid equilibria, Fluid Phase Equilib. 209 (2003) 163–184. doi:10.1016/S0378-3812(03)00056-6.
[141] G.K. Folas, O.J. Berg, E. Solbraa, A.O. Fredheim, G.M. Kontogeorgis, M.L. Michelsen, E.H.

Stenby, High-pressure vapor–liquid equilibria of systems containing ethylene glycol, water and methane, Fluid Phase Equilib. 251 (2007) 52–58. doi:10.1016/j.fluid.2006.11.001.
[142] N. Muro-Suñé, G.M. Kontogeorgis, N. Von Solms, M.L. Michelsen, Phase equilibrium modelling for mixtures with acetic acid using an association equation of state, Ind. Eng. Chem. Res. 47 (2008) 5660–5668. doi:10.1021/ie071205k.
[143] M.B. Oliveira, M.G. Freire, I.M. Marrucho, G.M. Kontogeorgis, A.J. Queimada, J.A.P. Coutinho, Modeling the liquid-liquid equilibria of water + fluorocarbons with the cubic-plus-association equation of state, Ind. Eng. Chem. Res. 46 (2007) 1415–1420. doi:10.1021/ie061147n.
[144] A.S. Avlund, G.M. Kontogeorgis, M.L. Michelsen, Modeling Systems Containing Alkanolamines with the CPA Equation of State Modeling Systems Containing Alkanolamines with the CPA Equation of State, Ind. Eng. Chem. Res. 47 (2008) 7441–7446. doi:10.1021/ie800040g.
[145] Y. Le Guennec, S. Lasala, R. Privat, J.N. Jaubert, A consistency test for alpha-functions of cubic equations of state, Fluid Phase Equilib. 427 (2016) 513–538. doi:10.1016/j.fluid.2016.07.026.
[146] G. Soave, Equilibrium constants from a modified Redlich-Kwong equation of state, Chem. Eng. Sci. 27 (1972) 1197–1203. doi:10.1016/0009-2509(72)80096-4.
[147] M.L. Michelsen, Robust and Efficient Procedures for Association Models, Ind. Eng. Chem. Res. 45 (2006) 8449–8453. doi:10.1021/ie060029x.
[148] P.M. Mathias, T.W. Copeman, Extension of the Peng-Robinson equation of state to complex mixtures: Evaluation of the various forms of the local composition concept, Fluid Phase Equilib. 13 (1983) 91–108. doi:10.1016/0378-3812(83)80084-3.
[149] M.S. Graboski, T.E. Daubert, A Modified Soave Equation of State for Phase Equilibrium Calculations. 1. Hydrocarbon Systems, Ind. Eng. Chem. Process Des. Dev. 17 (1978) 443–448. doi:10.1021/i260068a009.
[150] J.R. Elliott, S.J. Suresh, M.D. Donohue, A Simple Equation of State for Nonspherical and Associating Molecules, Ind. Eng. Chem. Res. 32 (1990) 1476–1485. doi:10.1016/j.rmed.2009.03.007.
[151] A. Péneloux, E. Rauzy, R. Fréze, A consistent correction for Redlich-Kwong-Soave volumes, Fluid Phase Equilib. 8 (1982) 7–23. doi:10.1016/0378-3812(82)80002-2.
[152] J.-N. Jaubert, R. Privat, Y.L.E. Guennec, L. Coniglio, Note on the properties altered by application of a Péneloux–type volume translation to an equation of state, Fluid Phase Equilib. 419 (2016) 88–95. doi:10.1016/j.fluid.2016.03.012.
[153] G.M. Kontogeorgis, M.L. Michelsen, G.K. Folas, S. Derawi, N. Von Solms, E.H. Stenby, Ten Years with the CPA (Cubic-Plus-Association) equation of state. Part 1. Pure compounds and self-associating systems, Ind. Eng. Chem. Res. 45 (2006) 4855–4868. doi:10.1021/ie051305v.
[154] I. Polishuk, Generalization of SAFT+Cubic equation of state for predicting and correlating thermodynamic properties of heavy organic substances, J. Supercrit. Fluids. 67 (2012) 94–107. doi:10.1016/j.supflu.2012.02.009.
[155] I. Polishuk, Standardized critical point-based numerical solution of statistical association fluid theory parameters: The perturbed chain-statistical association fluid theory equation of state revisited, Ind. Eng. Chem. Res. 53 (2014) 14127–14141. doi:10.1021/ie502633e.
[156] A.P.C.M. Vinhal, W. Yan, G.M. Kontogeorgis, Evaluation of equations of state for simultaneous representation of phase equilibrium and critical phenomena, Fluid Phase Equilib. 437 (2017) 140–154. doi:10.1016/j.fluid.2017.01.011.
[157] A. Nath, E. Bender, On the thermodynamics of associated solutions. I. an analytical method for determining the enthalpy and entropy of association and equilibrium constant for pure liquid substances, Fluid Phase Equilib. 7 (1981) 275–287. doi:10.1016/0378-3812(81)80012-X.
[158] R. Privat, J.-N. Jaubert, Y. Le Guennec, Incorporation of a volume translation in an equation of state for fluid mixtures: which combining rule? which effect on properties of mixing?, Fluid Phase Equilib. 427 (2016) 414–420. doi:10.1016/j.fluid.2016.07.035.
[159] H. Baled, R.M. Enick, Y. Wu, M.A. Mchugh, W. Burgess, D. Tapriyal, B.D. Morreale, Prediction of hydrocarbon densities at extreme conditions using volume-translated SRK and PR equations of state fit to high temperature , high pressure PVT data, Fluid Phase Equilib. 317 (2012) 65–76. doi:10.1016/j.fluid.2011.12.027.
[160] I. Polishuk, The Journal of Supercritical Fluids Till which pressures the fluid phase EOS models might stay reliable ?, J. Supercrit. Fluids. 58 (2011) 204–215. doi:10.1016/j.supflu.2011.05.014.
[161] M.J. Dávila, R. Alcalde, M. Atilhan, S. Aparicio, PRhoT measurements and derived properties of liquid 1-alkanols, J. Chem. Thermodyn. 47 (2012) 241–259. doi:10.1016/j.jct.2012.08.014.
[162] W.D. Hill, M. Van Winkle, VAPOR-LIQUID EQUILIBRIA in METHANOL BINARY SYSTEMS. Methanol-Propanol, Methanol-Butanol, and Methanol-Pentanol., Ind. Eng. Chem. 44

(1952) 205–210. doi:10.1021/ie50505a056.
[163] L.R. Hellwig, M. Van Winkle, Vapor-Liquid Equilibria for Ethyl Alcohol Binary Systems, Ind. Eng. Chem. 45 (1953) 624–629. doi:10.1021/ie50519a044.
[164] A. Arce, A. Blanco, A. Soto, J. Tojo, Isobaric Vapor-Liquid Equilibria of Methanol + 1-Octanol and Ethanol + 1-Octanol Mixtures, J. Chem. Eng. Data. 40 (1995) 1011–1014. doi:10.1021/je00020a063.
[165] G. Hradetzky, D. a. Lempe, Phase equilibria in binary and higher systems methanol + hydrocarbon(s), Fluid Phase Equilib. 69 (1991) 285–301. doi:10.1016/0378-3812(91)90040-E.
[166] H. Matsuda, K. Ochi, Liquid-liquid equilibrium data for binary alcohol + n-alkane (C 10-C16) systems: Methanol + decane, ethanol + tetradecane, and ethanol + hexadecane, Fluid Phase Equilib. 224 (2004) 31–37. doi:10.1016/j.fluid.2004.05.006.
[167] R.L. Rowley, W.V. Wilding, A. Congote, N.F. Giles, A Systems Approach for Improved Accuracy of Thermophysical Properties in the DIPPR 801 Database: 1, n -Alkanediols as a Case Study, J. Chem. Eng. Data. 59 (2014) 1031–1037. doi:10.1021/je400747s.
[168] M. Plass, A. Kolbe, Intramolecular Hydrogen Bond Interaction in Selected Diols, Z. Phys. Chem. 217 (2003) 1085–1096. doi:10.1524/zpch.217.9.1085.20405.
[169] M.B. Oliveira, F. Llovell, J. a. P. Coutinho, L.F. Vega, New Procedure for Enhancing the Transferability of Statistical Associating Fluid Theory (SAFT) Molecular Parameters: The Role of Derivative Properties, Ind. Eng. Chem. Res. 55 (2016) 10011–10024. doi:10.1021/acs.iecr.6b02205.
[170] J.G. Bleazard, T.F. Sun, R.D. Johnson, R.M. DiGuilio, a. S. Teja, Transport properties of seven alkanediols, Fluid Phase Equilib. 117 (1996) 386–393. doi:10.1016/0378-3812(95)02976-1.
[171] P. Góralski, M. Tkaczyk, Heat Capacities of Some Liquid a , ω -Alkanediols within the Temperature Range between (293 . 15 and 353 . 15) K, J. Chem. Eng. Data. 111 (2008) 1932–1934. doi:10.1021/je800356x.
[172] T.-S. Yeh, Y.-P. Chang, T.-M. Su, I. Chao, Global Conformational Analysis of 1,2-Ethanediol, J. Phys. Chem. 98 (1994) 8921–8929. doi:10.1021/j100087a018.
[173] K.G. Joback, R.C. Reid, Estimation of Pure-Component Properties From Group-Contributions, Chem. Eng. Commun. 57 (1987) 233–243. doi:10.1080/00986448708960487.
[174] D.N. Rihani, L.K. Doraiswamy, Estimation of heat capacity of organic compounds from group contributions, Ind. Eng. Chem. Fundam. 4 (1965) 17–21. doi:10.1021/i160013a003.
[175] E. Sheikholeslamzadeh, S. Rohani, Vapour-liquid and vapour-liquid-liquid equilibrium modeling for binary, ternary, and quaternary systems of solvents, Fluid Phase Equilib. 333 (2012) 97–105. doi:10.1016/j.fluid.2012.07.016.
[176] J. Li, C. Chen, J. Wang, Vapor – liquid equilibrium data and their correlation for binary systems consisting of ethanol , 2-propanol , 1 , 2-ethanediol and methyl benzoate, 169 (2000) 75–84. doi:10.1016/S0378-3812(99)00340-4.
[177] J.D. Olson, Thermodynamics of Hydrogen-Bonding Mixtures 3.: GE, HE, SE, and VE of Ethylene Glycol plus 1,3-Propylene Glycol, 116 (1996) 414–420. doi:10.1016/0378-3812(95)02913-3.
[178] Y.-F. Lin, C.-H. Tu, Isobaric vapor–liquid equilibria for the binary and ternary mixtures of 2-propanol, water, and 1,3-propanediol at P=101.3kPa: Effect of the 1,3-propanediol addition, Fluid Phase Equilib. 368 (2014) 104–111. doi:10.1016/j.fluid.2014.02.006.
[179] C. Yang, Y. Sun, Z. Qin, Y. Feng, P. Zhang, X. Feng, Isobaric Vapor-Liquid Equilibrium for Four Binary Systems of Ethane-1,2-diol, Butaned-1,4-diol, 2-(2-Hydroxyethoxy)ethan-1-ol, and 2-[2-(2-Hydroxyethoxy)ethoxy]ethanol at 10.0 kPa, 20.0 kPa, and 40.0 kPa, J. Chem. Eng. Data. 59 (2014) 1273–1280. doi:10.1021/je401020e.
[180] I. Mokbel, T. Sawaya, M.L. Zanota, R.A. Naccoul, J. Jose, C. De Bellefon, Vapor-liquid equilibria of glycerol, 1,3-propanediol, glycerol + water, and glycerol + 1,3-propanediol, J. Chem. Eng. Data. 57 (2012) 284–289. doi:10.1021/je200766t.
[181] M. Riaz, M.A. Yussuf, G.M. Kontogeorgis, E.H. Stenby, W. Yan, E. Solbraa, Distribution of MEG and methanol in well-defined hydrocarbon and water systems: Experimental measurement and modeling using the CPA EoS, Fluid Phase Equilib. 337 (2013) 298–310. doi:10.1016/j.fluid.2012.09.009.
[182] F.-Y. Jou, F.D. Otto, A.E. Mather, Solubility of methane in glycols at elevated pressures, Can. J. Chem. Eng. 72 (1994) 130–133. doi:10.1002/cjce.5450720120.
[183] F.-Y. JOU, R.D. DESHMUKH, F.D. OTTO, A.E. MATHER, VAPOR-LIQUID EQUILIBRIA OF H 2 S AND C0 2 AND ETHYLENE GLYCOL AT ELEVATED PRESSURES, Chem. Eng. Commun. 87 (1990) 223–231. doi:10.1080/00986449008940694.

[184] D. Zheng, W. Ma, R. Wei, T. Guo, Solubility study of methane , carbon dioxide and nitrogen in ethylene glycol at elevated temperatures and pressures, Fluid Phase Equilib. 155 (1999) 277–286. doi:10.1016/S0378-3812(98)00469-5.
[185] W. Afzal, M.P. Breil, I. Tsivintzelis, A.H. Mohammadi, G.M. Kontogeorgis, D. Richon, Experimental study and phase equilibrium modeling of systems containing acid gas and glycol, Fluid Phase Equilib. 318 (2012) 40–50. doi:10.1016/j.fluid.2011.12.025.
[186] F.-Y. Jou, K. a. G. Schmidt, A.E. Mather, Vapor–liquid equilibrium in the system ethane+ethylene glycol, Fluid Phase Equilib. 240 (2006) 220–223. doi:10.1016/j.fluid.2005.12.032.
[187] F.-Y. Jou, F.D. Otto, A.E. Mather, The solubility of propane in 1,2-ethanediol at elevated pressures, J. Chem. Thermodyn. 25 (1993) 37–40. doi:10.1006/jcht.1993.1004.
[188] M. Riaz, G.M. Kontogeorgis, E.H. Stenby, W. Yan, T. Haugum, K.O. Christensen, E. Solbraa, T. V. Løkken, Mutual solubility of MEG, water and reservoir fluid: Experimental measurements and modeling using the CPA equation of state, Fluid Phase Equilib. 300 (2011) 172–181. doi:10.1016/j.fluid.2010.10.006.
[189] A.R. Bazaev, I.M. Abdulagatov, A.A. Bazaev, A.A. Abdurashidova, A.E. Ramazanova, Isochoric heat-capacity measurements for pure methanol in the near-critical and supercritical regions, J. Supercrit. Fluids. 41 (2007) 217–226. doi:10.1007/s10765-007-0164-4.
[190] M. Frost, G.M. Kontogeorgis, E.H. Stenby, M.A. Yussuf, T. Haugum, K.O. Christensen, E. Solbraa, T. V. Løkken, Liquid-liquid equilibria for reservoir fluids+monoethylene glycol and reservoir fluids+monoethylene glycol+water: Experimental measurements and modeling using the CPA EoS, Fluid Phase Equilib. 340 (2013) 1–6. doi:10.1016/j.fluid.2012.11.028.
[191] M. Riaz, G.M. Kontogeorgis, E.H. Stenby, W. Yan, T. Haugum, K.O. Christensen, T. V Lokken, E. Solbraa, Measurement of Liquid-Liquid Equilibria for Condensate plus Glycol and Condensate plus Glycol plus Water Systems, J. Chem. Eng. Data. 56 (2011) 4342–4351. doi:Doi 10.1021/Je200158c.
[192] M. Frost, G.M. Kontogeorgis, N. von Solms, T. Haugum, E. Solbraa, Phase equilibrium of North Sea oils with polar chemicals: Experiments and CPA modeling, Fluid Phase Equilib. 424 (2016) 122–136. doi:10.1016/j.fluid.2015.11.030.
[193] I.M. Abdulagatov, V.I. Dvoryanchikov, A.N. Kamalov, Measurements of the heat capacities at constant volume of H2O and (H2O+KNO3), J. Chem. Thermodyn. 29 (1997) 1387–1407. doi:10.1006/jcht.1997.0248.
[194] C.T.A. Chen, High-pressure specific heat capacities of pure water and seawater, J. Chem. Eng. Data. 32 (1987) 469–472. doi:10.1021/je00050a026.
[195] H. Segura, T. Kraska, A. Mejía, J. Wisniak, I. Polishuk, Unnoticed Pitfalls of Soave-Type Alpha Functions in Cubic Equations of State, Ind. Eng. Chem. Res. 42 (2003) 5662–5673. doi:10.1021/ie020828p.
[196] U.K. Deiters, K.M. De Reuck, Guidelines for publication of equations of state - I. Pure fluids, Chem. Eng. J. 69 (1998) 69–81. doi:10.1016/S1385-8947(97)00070-3.
[197] C. Tsonopoulos, G.M. Wilson, High-temperature mutual solubilities of hydrocarbons and water. Part I: Benzene, cyclohexane and n-hexane, AIChE J. 29 (1983) 990–999. doi:10.1002/aic.690290618.
[198] C. Marche, C. Ferronato, J. Jose, Solubilities of n -Alkanes (C 6 to C 8) in Water from 30 °C to 180 °C, J. Chem. Eng. Data. 48 (2003) 967–971. doi:10.1021/je025659u.
[199] J.L. Heidman, C. Tsonopoulos, C.J. Brady, G.M. Wilson, High- Temperature Mutual Solubilities of Hydrocarbons and Water, AIChE J. 31 (1985) 376–384.
[200] F. Jou, A.E. Mather, Vapor−Liquid−Liquid Locus of the System Pentane + Water, J. Chem. Eng. Data. 45 (2000) 728–729. doi:10.1021/je000065h.
[201] I.G. Economou, J.L. Heidman, C. Tsonopoulos, G.M. Wilson, Mutual solubilities of hydrocarbons and water: III. 1-hexene; 1-octene; C10-C12 hydrocarbons, AIChE J. 43 (1997) 535–546. doi:10.1002/aic.690430226.
[202] P. Schatzberg, Solubilities of Water in Several normal alkanes from C7 to C16, J. Phys. Chem. 67 (1963) 776–779. doi:10.1021/j100798a014.
[203] K. Noda, K. Sato, K. Nagatsuka, K. Ishida, Ternary Liquid-Liquid Equilibria for the systems of Aqueous Methanol Solutions And Propane or n-Butane, J. Chem. Eng. Japan. 8 (1975) 492–493. doi:10.1252/jcej.8.492.
[204] A. Mączyński, B. Wiśniewska-Gocłowska, M. Góral, Recommended Liquid–Liquid Equilibrium Data. Part 1. Binary Alkane–Water Systems, J. Phys. Chem. Ref. Data. 33 (2004) 549–577. doi:10.1063/1.1643922.

[205] C. Tsonopoulos, Thermodynamic analysis of the mutual solubilities of normal alkanes and water, Fluid Phase Equilib. 156 (1999) 21–33. doi:10.1016/S0378-3812(99)00021-7.
[206] M. Góral, B. Wiśniewska-Gocłowska, A. MącZyński, Recommended liquid-liquid equilibrium data. Part 3. Alkylbenzene-water systems, J. Phys. Chem. Ref. Data. 33 (2004) 1159–1188. doi:10.1063/1.1797038.
[207] D.J. Miller, S.B. Hawthorne, Solubility of Liquid Organics of Environmental Interest in Subcritical (Hot / Liquid) Water from 298 K to 473 K, J. Chem. Eng. Data. 45 (2000) 78–81. doi:10.1021/je990190x.
[208] F. Jou, A.E. Mather, Liquid - Liquid Equilibria for Binary Mixtures of Water + Benzene , Water + Toluene , and Water + p -Xylene from 273 K to 458 K, J. Chem. Eng. Data. 48 (2003) 750–752. doi:10.1021/je034033g.
[209] Z. Shen, Q. Wang, B. Shen, C. Chen, Z. Xiong, Liquid-Liquid Equilibrium for Ternary Systems Water + Acetic Acid + m-Xylene and Water + Acetic Acid + o-Xylene at (303.2 to 343.2) K, J. Chem. Eng. Data. 60 (2015) 2567–2574. doi:10.1021/acs.jced.5b00043.
[210] W.A. Pryor, R.E. Jentoft, Solubility of m- and p-Xylene in Water and in Aqueous Ammonia from O° to 300° C., J. Chem. Eng. Data. 6 (1961) 36–37. doi:10.1021/je60009a011.
[211] J. Lohmann, R. Joh, J. Gmehling, Solid−Liquid Equilibria of Viscous Binary Mixtures with Alcohols, J. Chem. Eng. Data. 42 (1997) 1170–1175. doi:10.1021/je9700683.
[212] D. Hessel, G. Geiseler, Pressure dependence of the heteroazeotropic system n-butanol + water, Z. Phys. Chem. 229 (1965) 199–209.
[213] A. Dallos, J. Liszi, (Liquid + liquid) equilibria of (octan-1-ol + water) at temperatures from 288.15 K to 323.15 K, J. Chem. Thermodyn. 27 (1995) 447–448. doi:10.1006/jcht.1995.0046.
[214] E.C. Voutsas, C. Pamouktsis, D. Argyris, G.D. Pappa, Measurements and thermodynamic modeling of the ethanol-water system with emphasis to the azeotropic region, Fluid Phase Equilib. 308 (2011) 135–141. doi:10.1016/j.fluid.2011.06.009.
[215] E. Vercher, F.J. Rojo, A. Martínez-Andreu, Isobaric vapor-liquid equilibria for 1-propanol + water + calcium nitrate, J. Chem. Eng. Data. 44 (1999) 1216–1221. doi:10.1021/je990069q.
[216] J. Soujanya, B. Satyavathi, T.E. Vittal Prasad, Experimental (vapour + liquid) equilibrium data of (methanol + water), (water + glycerol) and (methanol + glycerol) systems at atmospheric and sub-atmospheric pressures, J. Chem. Thermodyn. 42 (2010) 621–624. doi:10.1016/j.jct.2009.11.020.
[217] M.D. Bermejo, A. Martín, L.J. Florusse, C.J. Peters, M.J. Cocero, Bubble points of the systems isopropanol–water, isopropanol–water–sodium acetate and isopropanol–water–sodium oleate at high pressure, Fluid Phase Equilib. 244 (2006) 78–85. doi:10.1016/j.fluid.2006.03.021.
[218] N. Kamihama, H. Matsuda, K. Kurihara, K. Tochigi, S. Oba, Isobaric Vapor–Liquid Equilibria for Ethanol + Water + Ethylene Glycol and Its Constituent Three Binary Systems, J. Chem. Eng. Data. 57 (2012) 339–344. doi:10.1021/je2008704.
[219] M.T. Sanz, B. Blanco, S. Beltrán, J.L. Cabezas, Vapor Liquid Equilibria of Binary and Ternary Systems with Water , 1,3-Propanediol , and Glycerol, J. Chem. Eng. Data. 46 (2001) 635–639.
[220] J. Kiepe, S. Horstmann, K. Fischer, J. Gmehling, Experimental Determination and Prediction of Gas Solubility Data for Methane + Water Solutions Containing Different Monovalent Electrolytes, Ind. Eng. Chem. Res. 42 (2003) 5392–5398. doi:10.1021/ie030386x.
[221] M. Rigby, J.M. Prausnitz, Solubility of water in compressed nitrogen, argon, and methane, J. Phys. Chem. 72 (1968) 330–334. doi:10.1021/j100847a064.
[222] K. Lekvam, P.R. Bishnoi, Dissolution of methane in water at low temperatures and intermediate pressures, Fluid Phase Equilib. 131 (1997) 297–309. doi:10.1016/S0378-3812(96)03229-3.
[223] A.H. Mohammadi, A. Chapoy, B. Tohidi, D. Richon, Measurements and Thermodynamic Modeling of Vapor−Liquid Equilibria in Ethane−Water Systems from 274.26 to 343.08 K, Ind. Eng. Chem. Res. 43 (2004) 5418–5424. doi:10.1021/ie049747e.
[224] A.D. King, C.R. Coan, Solubility of water in compressed carbon dioxide, nitrous oxide, and ethane. Evidence for hydration of carbon dioxide and nitrous oxide in the gas phase, J. Am. Chem. Soc. 93 (1971) 1857–1862. doi:10.1021/ja00737a004.
[225] A. Chapoy, S. Mokraoui, A. Valtz, D. Richon, A.H. Mohammadi, B. Tohidi, Solubility measurement and modeling for the system propane-water from 277.62 to 368.16 K, Fluid Phase Equilib. 226 (2004) 213–220. doi:10.1016/j.fluid.2004.08.040.
[226] R. Kobayashi, D. Katz, Vapor-Liquid Equilibria For Binary Hydrocarbon-Water Systems, Ind. Eng. Chem. 45 (1953) 440–446. doi:10.1021/ie50518a051.
[227] M.B. King, A. Mubarak, J.D. Kim, T.R. Bott, The mutual solubilities of water with supercritical and liquid carbon dioxides, J. Supercrit. Fluids. 5 (1992) 296–302. doi:10.1016/0896-8446(92)90021-B.

[228] S.-X. Hou, G.C. Maitland, J.P.M. Trusler, Measurement and modeling of the phase behavior of the (carbon dioxide+water) mixture at temperatures from 298.15K to 448.15K, J. Supercrit. Fluids. 73 (2013) 87–96. doi:10.1016/j.supflu.2012.11.011.
[229] N. Kamihama, H. Matsuda, K. Kurihara, K. Tochigi, S. Oba, Isobaric Vapor–Liquid Equilibria for Ethanol + Water + Ethylene Glycol and Its Constituent Three Binary Systems, J. Chem. Eng. Data. 57 (2012) 339–344. doi:10.1021/je2008704.
[230] R. Burgass, A. Reid, A. Chapoy, B. Tohidi, Glycols Partitioning at High Pressures, in: GPA Conf., San Antonio, 2017.
[231] M. Riaz, M.A. Yussuf, M. Frost, G.M. Kontogeorgis, E.H. Stenby, W. Yan, E. Solbraa, Distribution of gas hydrate inhibitor monoethylene glycol in condensate and water systems: Experimental measurement and thermodynamic modeling using the cubic-plus-association equation of state, Energy and Fuels. 28 (2014). doi:10.1021/ef500367e.
[232] M. Frost, G.M. Kontogeorgis, N. von Solms, E. Solbraa, Modeling of phase equilibrium of North Sea oils with water and MEG, Fluid Phase Equilib. 424 (2016) 79–89. doi:10.1016/j.fluid.2015.10.014.
[233] K.S. Pedersen, J. Milter, C.P. Rasmussen, Mutual solubility of water and a reservoir fluid at high temperatures and pressures, Fluid Phase Equilib. 189 (2001) 85–97. doi:10.1016/S0378-3812(01)00562-3.
[234] W. Yan, G.M. Kontogeorgis, E.H. Stenby, Application of the CPA equation of state to reservoir fluids in presence of water and polar chemicals, Fluid Phase Equilib. 276 (2009) 75–85. doi:10.1016/j.fluid.2008.10.007.
[235] K.S. Pedersen, M.L. Michelsen, A.O. Fredheim, Phase equilibrium calculations for unprocessed well streams containing hydrate inhibitors, Fluid Phase Equilib. 126 (1996) 13–28. doi:10.1016/S0378-3812(96)03142-1.
[236] N. Rossihol, Equilibres de phases à basse température de mélanges d'hydrocarbures légers, deméthanol et d'eau: mesure et modélisation, PhD. Thesis, Université Lyon I Claude Bernard, Lyon, 1995.
[237] http://www.h2o2.com, consulted on 20/09/2017, (n.d.).
[238] www.basf.com, consulted on 20/09/2017, (n.d.).
[239] J.A. Awan, K. Thomsen, C. Coquelet, P.L. Fosbol, D. Richon, Vapor-Liquid Equilibrium Measurements and Modeling of the Propyl Mercaptan plus Methane plus Water System, J. Chem. Eng. Data. 55 (2010) 842–846. doi:10.1021/je900441f.
[240] J.A. Awan, G.M. Kontogeorgis, I. Tsivintzelis, C. Coquelet, Vapor-liquid-liquid equilibrium measurements and modeling of ethanethiol + methane + water, 1-propanethiol + methane + water and 1-butanethiol + methane + water ternary systems at 303, 335, and 365 K and pressure up to 9 MPa, Ind. Eng. Chem. Res. 52 (2013) 14698–14705. doi:10.1021/ie400779m.
[241] M. Kaarsholm, S.O. Derawi, M.L. Michelsen, G.M. Kontogeorgis, Extension of the cubic-plus-association (CPA) equation of state to amines, Ind. Eng. Chem. Res. 44 (2005) 4406–4413. doi:10.1021/ie0490029.
[242] J. Rozmus, J.C. de Hemptinne, P. Mougin, Application of GC-PPC-SAFT EoS to amine mixtures with a predictive approach, Fluid Phase Equilib. 303 (2011) 15–30. doi:10.1016/j.fluid.2010.12.009.
[243] M.C. Dos Ramos, J.D. Haley, J.R. Westwood, C. McCabe, Extending the GC-SAFT-VR approach to associating functional groups: Alcohols, aldehydes, amines and carboxylic acids, Fluid Phase Equilib. 306 (2011) 97–111. doi:10.1016/j.fluid.2011.03.026.
[244] G. Das, M.C. Dos Ramos, C. McCabe, Accurately modeling benzene and alkylbenzenes using a group contribution based SAFT approach, Fluid Phase Equilib. 362 (2014) 242–251. doi:10.1016/j.fluid.2013.10.016.
[245] J.A. Awan, I. Tsivintzelis, M.P. Breil, C. Coquelet, D. Richon, G.M. Kontogeorgis, Phase Equilibria of Mixtures Containing Organic Sulfur Species (OSS) and Water/Hydrocarbons: VLE Measurements and Modeling Using the Cubic-Plus-Association Equation of State, Ind. Eng. Chem. Res. 49 (2010) 12718–12725. doi:10.1021/ie101470b.
[246] H. Wolff, R. Wuertz, Hydrogen bonding and vapor pressure isotope effect of dimethylamine, J. Phys. Chem. 74 (1970) 1600–1606. doi:10.1021/j100702a032.
[247] J.L. Humphrey, M. Van Winkle, Vapor-liquid equilibrium at 60.degree. for n-hexane-alkyl amines and 1-hexene-alkyl amines, J. Chem. Eng. Data. 12 (1967) 526–531. doi:10.1021/je60035a018.
[248] T.M. Letcher, J.W. Bayles, Thermodynamics of Some Binary liquid Mixtures Containing Aliphatic Amines, J. Chem. Eng. Data. 16 (1971) 266–271. doi:10.1021/je60050a026.

[249] R. Srivastava, B.D. Smith, Total-Pressure Vapor-Liquid Equilibrium Data for Binary Systems of Diethylamine with Acetone, Acetonitrile, and Methanol, J. Chem. Eng. Data. 30 (1985) 308–313. doi:10.1021/je00041a022.
[250] R.R. Davison, Vapor-liquid equilibriums of water-diisopropylamine and water-di-n-propylamine, J. Chem. Eng. Data. 13 (1968) 348–351. doi:10.1021/je60038a013.
[251] C. Yang, Z. Qin, Y. Xu, H. Zeng, F. Sun, P. Zhang, Y. Feng, Isobaric vapor-liquid equilibrium for the binary systems of methanol, diethylamine, and N, N-diethylethanolamine at p = (60.0 and 101.3) kPa, J. Chem. Eng. Data. 58 (2013) 482–487. doi:10.1021/je301219c.
[252] C. Yang, P. Zhang, Z. Qin, Y. Feng, H. Zeng, F. Sun, Isobaric vapor-liquid equilibrium for the binary systems (Diethylamine + Ethanol), (Ethanol + N, N -Diethylethanolamine), and (Diethylamine + N, N -Diethylethanolamine) at p = (80.0 and 40.0) kPa, J. Chem. Eng. Data. 59 (2014) 750–756. doi:10.1021/je4008712.
[253] S. Held, Diplomarbeit, TH Leuna-Merseburg, (1976).
[254] S. Villa, R. Garriga, P. Pérez, M. Gracia, J.A. González, I.G. de la Fuente, J.C. Cobos, Thermodynamics of mixtures with strongly negative deviations from Raoult's law, Fluid Phase Equilib. 231 (2005) 211–220. doi:10.1016/j.fluid.2005.01.013.
[255] M. Kato, H. Tanaka, Vapor—Liquid Equilibrium Determination with a Flow-type Ebuliiometer for Six Binary Systems Made of Alcohol and Amine, J. Chem. Eng. Data. 34 (1989) 203–206. doi:10.1021/je00056a017.
[256] R.M. Stephenson, Mutual Solubility of Water and Aliphatic Amines, J. Chem. Eng. Data. 38 (1993) 625–629. doi:10.1021/je00012a039.
[257] H. Wolff, J. Szydlowski, L. Dill-Staffenberger, Vapor-liquid equilibria of deuteroisomeric methanethiols and their mixtures with n-hexane, J. Chem. Thermodyn. 12 (1980) 641–652. doi:10.1016/0021-9614(80)90086-5.
[258] N.F. Giles, G.M. Wilson, Phase equilibria on seven binary mixtures, J. Chem. Eng. Data. 45 (2000) 146–153. doi:10.1021/je990221o.
[259] N.F. Giles, L.C. Wilson, G.M. Wilson, W.V. Wilding, Phase Equilibria on Eight Binary Mixtures, J. Chem. Eng. Data. 42 (1997) 1067–1074. doi:10.1021/je970028z.
[260] R.L. Denyer, F.A. Fidler, R.A. Lowry, Azeotrope Formation between Thiols and Hydrocarbons, Ind. Eng. Chem. 41 (1949) 2727–2737. doi:10.1021/ie50480a018.
[261] http://www.supercriticalfluid.org, consulted on 02/10/2017, (n.d.).
[262] J. Cai, D. Qiu, L. Zhang, Y. Hu, Vapor-liquid critical properties of multi-component fluid mixture, Fluid Phase Equilib. 241 (2006) 229–235. doi:10.1016/j.fluid.2005.11.003.
[263] J. Cai, J.M. Prausnitz, Thermodynamics for fluid mixtures near to and far from the vapor-liquid critical point, Fluid Phase Equilib. 219 (2004) 205–217. doi:10.1016/j.fluid.2004.01.033.
[264] A.J. Shen, Q. Liu, Y.Y. Duan, Z. Yang, Crossover VTSRK equation of state for selected alkane + alkane and CO2 + alkane binary mixtures, Fluid Phase Equilib. 408 (2016) 180–189. doi:10.1016/j.fluid.2015.08.033.
[265] H. Behnejad, H. Cheshmpak, A. Jamali, The Extended Crossover Peng–Robinson Equation of State for Describing the Thermodynamic Properties of Pure Fluids, J. Stat. Phys. 158 (2015) 372–385. doi:10.1007/s10955-014-1134-4.
[266] C.P. Hicks, C.L. Young, Theoretical prediction of phase behaviour at high temperatures and pressures for non-polar mixtures. Part 1.—Computer solution techniques and stability tests, J. Chem. Soc., Faraday Trans. 2. 73 (1977) 597–612. doi:10.1039/F29777300597.
[267] I. Cibulka, Estimation of excess volume and density of ternary liquid mixtures of non-electrolytes from binary data, Collect. Czechoslov. Chem. Commun. 47 (1982) 1414–1419. doi:10.1135/cccc19821414.
[268] R.A. Heidemann, A.M. Khalil, The calculation of critical points, AIChE J. 26 (1980) 769–779. doi:10.1002/aic.690260510.
[269] M.L. Michelsen, Calculation of critical points and phase boundaries in the critical region, Fluid Phase Equilib. 16 (1984) 57–76. doi:10.1016/0378-3812(84)85021-9.
[270] H. Hoteit, E. Santiso, A. Firoozabadi, An efficient and robust algorithm for the calculation of gas-liquid critical point of multicomponent petroleum fluids, Fluid Phase Equilib. 241 (2006) 186–195. doi:10.1016/j.fluid.2005.12.019.
[271] L. Gil, S.T. Blanco, C. Rivas, E. Laga, J. Fernández, M. Artal, I. Velasco, Experimental determination of the critical loci for { n -C 6 H 14 or CO 2 + alkan-1-ol } mixtures . Evaluation of their critical and subcritical behavior using PC-SAFT EoS, J. Supercrit. Fluids. 71 (2012) 26–44. doi:10.1016/j.supflu.2012.07.008.
[272] A.G. Nazmutdinov, E. V. Alekina, T.N. Nesterova, Concentration dependences of the critical

temperatures of binary mixtures of nonaqueous components, Russ. J. Phys. Chem. A. 82 (2008) 1857–1862. doi:10.1134/S0036024408110125.
[273] L. Wang, K. Han, S. Xia, P. Ma, F. Yan, Measurement and correlation of critical properties for binary mixtures and ternary mixtures containing gasoline additives, J. Chem. Thermodyn. 74 (2014) 161–168. doi:http://dx.doi.org/10.1016/j.jct.2014.01.025.
[274] Z. J., P. Oracz, S. Warycha, Total vapour pressure measurements and excess Gibbs energies for the binary systems methanol + ethanol, ethanol + 2-propanol, benzene + cyclohexane, benzene + carbon tetrachloride and benzene + ethanol at 303.15 and 313.15 K, Fluid Phase Equilib. 58 (1990) 191–209. doi:10.1016/0378-3812(90)87014-G.
[275] C.P. Hicks, C.L. Young, The Gas-Liquid Critical Properties of Binary Mixtures, Chem. Rev. 75 (1975) 119–175. doi:10.1021/cr60294a001.
[276] W.L. Marshall, E. V. Jones, Liquid-vapor critical temperatures of several aqueous-organic and organic-organic solution systems, J. Inorg. Nucl. Chem. 36 (1974) 2319–2323. doi:10.1016/0022-1902(74)80276-9.
[277] E.A. Bazaev, A.R. Bazaev, A.A. Abdurashidova, An experimental investigation of the critical state of aqueous solutions of aliphatic alcohols, High Temp. 47 (2009) 195–200. doi:10.1134/S0018151X09020072.
[278] E. LagaLázaro, Determinación de Puntos Críticos y Propiedades PVT de Fluidos, TAD report, Unpublished Results, Department of Organic Chemistry and Physical Chemistry, University of Zaragoza, Spain, 2009.
[279] D.W. Morton, M.P.W. Lui, C.L. Young, The (gas + liquid) critical properties and phase behaviour of some binary alkanol (C 2 – C 5) + alkane (C 5 – C 12 Þ mixtures, 35 (2003) 1737–1749. doi:10.1016/S0021-9614(03)00151-4.
[280] M. He, N. Xin, Y. Liu, Y. Zhang, Determination of critical properties for binary and ternary mixtures containing short chain alcohols and alkanes using a flow view-type apparatus, J. Supercrit. Fluids. 104 (2016) 19–28. doi:10.1016/j.supflu.2015.10.010.
[281] C. Soo, P. Théveneau, C. Coquelet, D. Ramjugernath, D. Richon, Determination of critical properties of pure and multi-component mixtures using a “ dynamic – synthetic ” apparatus, J. Supercrit. Fluids. 55 (2010) 545–553. doi:10.1016/j.supflu.2010.10.022.
[282] N. Xin, Y. Liu, X. Guo, X. Liu, Y. Zhang, M. He, Determination of critical properties for binary and ternary mixtures containing propanol and alkanes using a flow view-type apparatus, J. Supercrit. Fluids. 108 (2016) 35–44. doi:10.1016/j.supflu.2015.10.010.
[283] M. He, N. Xin, C. Wang, Y. Liu, Y. Zhang, X. Liu, Experimental determination of critical data of multi-component mixtures containing potential gasoline additives 2-butanol by a flow-type apparatus, J. Chem. Thermodyn. 101 (2016) 35–43. doi:10.1016/j.jct.2016.05.010.
[284] A. V. Mandlekar, W.B. Kay, R.L. Smith, A.S. Teja, Phase equilibria in the n-hexane + diethylamine system, Fluid Phase Equilib. 23 (1985) 79–88. doi:10.1016/0378-3812(85)85029-9.
[285] A. Kreglewski, W.B. Kay, Critical constants of conformal mixtures, J. Phys. Chem. 73 (1969) 3359–3366. doi:10.1021/j100844a035.
[286] L.S. Toczylkin, C.L. Young, Gas-liquid critical temperatures of mixtures containing electron donors II. Amine mixtures, J. Chem. Thermodyn. 12 (1980) 365–370. doi:10.1016/0021-9614(80)90149-4.
[287] E. Brunner, W. Hultenschmidt, G. Schlichtharle, Fluid mixtures at high pressures IV . Isothermal phase equilibria in binary mixtures consisting of (methanol + hydrogen or nitrogen or methane or carbon monoxide or carbon dioxide), J. Chem. Thermodyn. 19 (1987) 273–291. doi:10.1016/0021-9614(87)90135-2.
[288] A.Z. Francesconi, H. Lentz, E.U. Franck, Phase Equillbrla and PVT Data for the Methane-Methanol System to 300 MPa and 240 °C, J. Phys. Chem. 85 (1981) 3303–3307. doi:10.1021/j150622a019.
[289] W.B. Kay, W.E. Donham, Liquid-vapour equilibria in the iso-butanol—n-butanol, methanol—n-butanol and diethyl ether—n-butanol systems, Chem. Eng. Sci. 4 (1955) 1–16. doi:10.1016/0009-2509(55)85001-4.
[290] K. Han, S. Xia, P. Ma, F. Yan, T. Liu, Measurement of critical temperatures and critical pressures for binary mixtures of methyl tert-butyl ether (MTBE)+alcohol and MTBE+alkane, J. Chem. Thermodyn. 62 (2013) 111–117. doi:10.1016/j.jct.2013.03.002.
[291] F. Steyer, K. Sundmacher, VLE and LLE data for the system cyclohexane + cyclohexene + water 4 + cyclohexanol, J. Chem. Eng. Data. 49 (2004) 1675–1681. doi:10.1021/je049902w.
[292] https://pubchem.ncbi.nlm.nih.gov , Consulted on 29/09/2017, (n.d.).
[293] http://www.eastman.com , Consulted on 29/09/2017, (n.d.).

[294] Design Institute for Physical Properties,DIPPR DIADEM Database, version 1.2, Brigham Young University, Provoh (Utah), USA, (2001).
[295] E.B. Munday, J.C. Mullins, D.D. Edie, Vapor Pressure Data for Toluene, I-Pentanol, I-Butanol, Water, and I-Propanol and for the Water and I-Propanol System from 273.15 to 323.15 K, J. Chem. Eng. Data. 25 (1980) 191–194. doi:10.1021/je60086a006.
[296] E. Sada, Tetsuo Morisue, Isothermal Vapor-Liquid Equilibrium of Isopropanol-Water System, (1952) 191–195.
[297] J.D. Raal, A.M. Motchelaho, Y. Perumal, X. Courtial, D. Ramjugernath, P–x data for binary systems using a novel static total pressure apparatus, Fluid Phase Equilib. 310 (2011) 156–165. doi:10.1016/j.fluid.2011.08.009.
[298] A.F. Cristino, S. Rosa, P. Morgado, A. Galindo, E.J.M. Filipe, A.M.F. Palavra, C.A. Nieto de Castro, High-temperature vapour–liquid equilibrium for the (water+alcohol) systems and modelling with SAFT-VR: 2. Water-1-propanol, J. Chem. Thermodyn. 60 (2013) 15–18. doi:10.1016/j.jct.2012.12.019.
[299] F. Barr-David, B.F. Dodge, Vapor-Liquid Equilibrium at High Pressures. The Systems Ethanol - Water and 2-Propanol - Water, J. Chem. Eng. Data. 4 (1959) 107–121. doi:10.1021/je60002a003.
[300] J. Schmelzer, I. Lieberwirth, M. Krug, R. Pfestorf, Vapour-liquid equilibria and heats of mixing in alkane-alcohol(1) systems. I. Vapour-liquid equilibria in 1-alcohol-undecane systems, Fluid Phase Equilib. 11 (1983) 187–200. doi:10.1016/0378-3812(83)80058-2.
[301] U. Domańska, J.A. Gonzalez, Solid-liquid equilibria for systems containing long-chain 1-alkanols III. Experimental data for 1-tetradecanol, 1-hexadecanol, 1-octadecanol or 1-icosanol + 1-butanol, 1-hexanol, 1-octanol or 1-decanol mixtures. Characterization in terms of DISQUAC, Fluid Phase Equilib. 129 (1997) 139–163. doi:10.1016/S0378-3812(96)03150-0.
[302] N.D.D. Carareto, M.C. Costa, M.P. Rolemberg, M.A. Krähenbühl, A.J.A. Meirelles, The solid–liquid phase diagrams of binary mixtures of even saturated fatty alcohols, Fluid Phase Equilib. 303 (2011) 191.e1-191.e8. doi:10.1016/j.fluid.2011.01.028.
[303] H. Wolff, O. Schiller, The vapour pressure behaviour and the association of N-methylethylamine, diethylamine and their N-deuterioanalogues in mixtures with n-hexane, Fluid Phase Equilib. 22 (1985) 185–207. doi:10.1016/0378-3812(85)85019-6.
[304] M.S. Sunder, D.H.L. Prasad, Vapor-liquid equilibrium and excess gibbs energies of hexane + N,N-dimethyl formamide, 2-methylpropan-2-ol + 2-aminophenol, N,N-dimethyl formamide, and 2-propanol + diisopropyl amine at 94.4 kPa, J. Chem. Eng. Data. 52 (2007) 2050–2052. doi:10.1021/je7001336.
[305] R. Stephenson, J. Stuart, Mutual Binary Solubilities: Water-Alcohols and Water-Esters, J. Chem. Eng. Data. 31 (1986) 56–70. doi:10.1021/je00043a019.
[306] E. Siimer, H. Kirss, M. Kuus, L. Kudryavtseva, Isobaric Vapor−Liquid Equilibrium for the Ternary System o -Xylene + Nonane + Cyclohexanol, J. Chem. Eng. Data. 47 (2002) 52–55. doi:10.1021/je0101404.
[307] J.T. Sipowska, S.A. Wieczorek, Vapour pressures and excess Gibbs free energies of (cyclohexanol + n-heptane) between 303.147 and 373.278 K, J. Chem. Thermodyn. 16 (1984) 693–699. doi:10.1016/0021-9614(84)90051-X.
[308] G.C. Benson, G.C. Benson, S.C. Anand, O. Kiyohara, Thermodynamic properties of some cycloalkane-cycloalkanol systems at 298. 15.deg.K. II, J. Chem. Eng. Data. 19 (1974) 258–261. doi:10.1021/je60062a027.
[309] B. Wang, X. Ge, H. Zheng, T. Qiu, Y. Wu, Liquid - Liquid Equilibrium for the System Water + Cyclohexene + Cyclohexanol over the Temperature Range of (303 . 2 to 403 . 2) K, (2010) 2529–2531.
[310] Y. Pei, Q. Wang, X. Gong, F. Lei, B. Shen, Distribution of cyclohexanol and cyclohexanone between water and cyclohexane, Fluid Phase Equilib. 394 (2015) 129–139. doi:10.1016/j.fluid.2015.02.029.

Estes anexos só estão disponíveis para consulta através do CD-ROM.
Queira por favor dirigir-se ao balcão de atendimento da Biblioteca.

Serviços de Biblioteca, Informação Documental e Museologia
Universidade de Aveiro